EPRI. *Proceedings: Fourth International Conference on Cold Fusion Volume 3: Nuclear Measurements Papers, TR-104188-V3*. 1994. Lahaina, Maui, Hawaii: Electric Power Research Institute.

This book is available here:

http://my.epri.com/portal/server.pt?Abstract_id=TR-104188-V3

Product ID: TR-104188-V3   **Sector Name:** Nuclear

Date Published: 7/28/1994   **Document Type:** Technical Report

File size: 18.87 MB   **File Type:** Adobe PDF (.pdf)

Full list price: No Charge
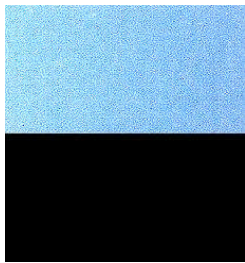
This Product is publicly available

The LENR-CANR version of the book (this file) is 10 MB, and it is in "text under image" or "searchable" Acrobat format.

EPRI

Electric Power
Research Institute

Proceedings: Fourth International Conference on Cold Fusion Volume 3: Nuclear Measurements Papers

Proceedings: Fourth International Conference on Cold Fusion

Volume 3: Nuclear and Measurements Papers

TR-104188-V3

Proceedings, July 1994

December 6-9, 1993
Lahaina, Maui, Hawaii

Conference Co-chairmen

T.O. Passell
Electric Power Research Institute

M.C.H. McKubre
SRI International

DISCLAIMER OF WARRANTIES AND LIMITATION OF LIABILITIES

ORDERING INFORMATION

FOREWORD

These four volumes include the full text or, in five cases, just the visual materials of papers presented at the Fourth International Conference on Cold Fusion. This meeting was the latest in a series of conferences devoted to a new area of scientific endeavor, variously called, "Deuterated Metals Research", "Anomalous Nuclear Phenomena in Solids", and "Research on New Hydrogen Energy". The first three conferences were held in Salt Lake City, Utah, (U.S.A)., Como, (Italy), and Nagoya, (Japan), in March, 1990, June, 1991, and October 1992, respectively. The authors and participants in this fourth conference should be thanked for four days of stimulating presentations and discussions. A conscious effort was made to maintain a high standard of scientific content and avoid exaggerated claims propagated by various public media. It is gratifying that this effort was largely successful without the need for extraordinary measures.

A number of new experimental approaches were evident compared with the Nagoya meeting. Use of ceramic proton conductors at high temperature was one such. Another was the use of ultrasonic cavitation in heavy water to load palladium and titanium foils with deuterium. Many theoretical papers were given, with some progress evident toward explaining some of these puzzling experimental observations. However, the wide range of theoretical models and speculations shows that the field remains in an exploratory phase, at least for the majority of theorists.

The use of concurrent sessions for the first time caused some attendees to miss hearing significant papers. It is hoped that this compendium of papers will serve to redress that shortcoming. Proceedings, including only those papers passing a rigorous peer review, will appear later as a publication of the American Nuclear Society's Fusion Technology Journal, thanks to the initiative of Editor George Miley.

242 persons from 12 countries registered and attended the conference. The hotel facility and the weather were such as to allow concentration on the technical meetings without serious distraction. Attendees included 124 from the United States, 62 from Japan, 19 from Italy, 11 from Russia, 10 from France, 5 from Canada, 4 from China, 2 from Switzerland, 2 from Germany, and 1 each from Spain, India, and England. A large number of interested persons from the former Soviet Union and eastern Europe were unable to attend but sent several papers that are included in these volumes.

Some 156 abstracts were originally submitted of which 125 papers appear in these proceedings. Since some of the enclosed material is in an unfinished state, the authors would appreciate being contacted by those who desire to reference the work reported here. The papers are divided so that Volume 1 contains all the papers received from authors who participated in the four plenary sessions, Volume 2 includes contributed papers on calorimetry and materials, Volume 3 has contributions on nuclear particle detection and measurement, and Volume 4 contains the papers contributed on theory and special topics. The papers are ordered in the same order of abstracts in the two volumes distributed at the meeting, with a few minor exceptions.

Thanks are due to the International Advisory and the Organizing Committees for their supportive efforts in arranging a successful meeting on such a controversial, yet potentially significant and hence absorbing, topic. Persons particularly active in arranging the agenda were M.C.H. McKubre, S. Crouch-Baker, D. Rolison, T. Claytor, H. Ikegami, and P. Hagelstein. I also wish to thank the following persons who ably served as session chairmen or co-chairmen during the meeting: M. Srinivasan, S. Smedley, P. Hagelstein, F. Tanzella, A. Miller, D. Rolison, S. Crouch-Baker, M. McKubre, K. Kunimatsu, E. Storms, F. Will, T. Claytor, F. Scaramuzzi, H. Ikegami, J. Bockris, G. Miley, B. Liaw, A. Takahashi, J. Cobble and M. Rabinowitz.

Supporting the logistical and physical arrangements were EPRI and the Office of Naval Research (ONR), represented by L. Nelson and R. Nowak respectively. Cosponsoring the meeting in addition to EPRI and ONR, was Comitato Nationale per la Ricerca e per lo Sviluppo dell'Energia Nucleare e delle Energie Alternative (ENEA), represented by Franco Scaramuzzi. My sincere gratitude goes out to these persons and organizations. Many other organizations implicitly supported the meeting by funding the travel of a number of attendees. Notable among these were ENECO with 21, NEDO with 26, and IMRA with 10 attendees respectively.

The search for a definitive signature of some nuclear reaction correlated with the production of excess heat in the palladium-deuterium system was advanced by the presentations of D. Gozzi, G. Gigli, and M. Miles and their respective coworkers who reported measuring He^4 in the vapor phase of both closed and open electrochemical cells. However, the concentrations observed were at levels well below the atmospheric concentration of He^4 (5.2 ppmv) and hence are not robustly above criticism as possible atmospheric air contamination. On the other hand, the tritium results of F. Will and coworkers appear robust, with great care taken to establish reliable backgrounds and checking for contamination. I also found the tritium results of T. Claytor and coworkers convincing.

M. Fleischmann, S. Pons, and coworkers provided two papers elaborating the excess heat phenemena: one of the more intriguing results was the excess heat observed well after complete cessation of current flow due to evaporative loss of electrolyte in "boil-off" experiments of the kind first described at the Nagoya meeting.

Several papers using gas loading of palladium claimed evidence of nuclear reaction products. Y. Iwamura and coworkers appear to have replicated the experiment reported by E. Yamaguchi and his NTT coworkers at Nagoya, but emphasizing neutrons and a mass 5 peak in the mass spectrum tentatively assigned to the TD molecule.

The paper chosen by M. Fleischmann in the final panel session as the most outstanding of the conference was by D. Cravens, who on a very modest budget, had discovered many of the better methods for loading palladium with deuterium to high levels and getting the excess heat phenomenon.

Insight into the loading of hydrogen and deuterium into metals was provided by four excellent papers by R. Huggins, R. Oriani, K. Kunimatsu and coworkers, and F. Cellani and coworkers, respectively.

Particularly insightful papers on the theoretical side were presented by R. Bush, S. Chubb, P. Hagelstein, G. Hale, S. Ichimaru, Y. Kim, X. Li, G. Preparata, M. Rabinowitz, A. Takahashi, and J. Vigier .

A thoughtful paper by J. Schwinger was read by E. Mallove at a special evening session. Also, E. Storms gave an excellent summation of the meeting in the final panel session.

I apologize in advance for failing to mention here results from many other equally excellent and significant papers given at the conference.

I agree with and echo H. Ikegami's remarks in the preface of the Nagoya meeting proceedings, "It is my belief that cold fusion will become one of the most important subjects in science, one for which we have been working so patiently, with dedication and with courage, for future generations, for those who will live in the twenty-first century. In order to achieve our goal, our ultimate goal, we must continue and extend our interdisciplinary and international collaboration".

The International Advisory and Organizing Committees met late in the sessions to set the location of the next two meetings. For the next meeting (April 9-13, 1995) Monaco (near Nice, France) was chosen, and in 1996, Beijing, China.

International Advisory Committee

VOLUME 3

NUCLEAR MEASUREMENT PAPER

TABLE OF CONTENTS

ALKALI-HYDROGEN COLD FUSION ACCOMPANIED
WITH TRITIUM PRODUCTION ON NICKEL

R. Notoya

Catalysis Research Center

Hokkaido University

kita-11,Nishi-10,Kitaku

Sapporo,060,Japan

Abstract

It is clarified that alkali metal species,as well as
hydrogen,undergoes cold fusion in the boundary layer of
the electrode surface. The considerable amount of alkali
metal species is absorbed in the boundary layer forming
the intermetallic compound with some electrode materials,
so called the low overvoltage metals as the intermediate
of hydrogen evolution reaction as well as hydrogen atom,
in alkali metallic ions' solutions. Some behaviors of
cold fusion are easily elucidated on the basis of the
knowledge of kinetics of hydrogen evolution reaction in
alkali metallic ions' solutions. Tritium production
proves to be occurring in the same hydrogen electrode
reaction system of both light and heavy water electro-
lytes on porous nickel. But,excess heat is hardly due to
tritium production for the reason of too small rate of
the production in comparison with calcium generation from
potassium and proton.

1. Introduction

Since lithium ion's solution was used as the electrolyte
for the first study of cold fusion(1),many experiments
were carried out in solutions including alkali metallic
ions with the same aim. The mechanism of the hydrogen
evolution reaction(HER) so called on the low overvoltage
metals in alkali and neutral solutions containing various
alkali or other metallic cations has been determined by a
series of studies by use of the Galvanostatic Transient
Method(GSTM)(2),which can be expressed as:

$$M^+ \; + \; e^- \; \rightarrow \; M(I) \qquad\qquad\qquad\qquad\qquad\qquad I$$
$$M(I) \; + \; H_2O \; \rightarrow \; H(a) \; + \; OH^- \; + \; M^+ \qquad\qquad II$$
$$H(a) \; + \; H(a) \; \overset{\wedge}{\rightarrow} \; H_2 \qquad\qquad\qquad\qquad\qquad III$$
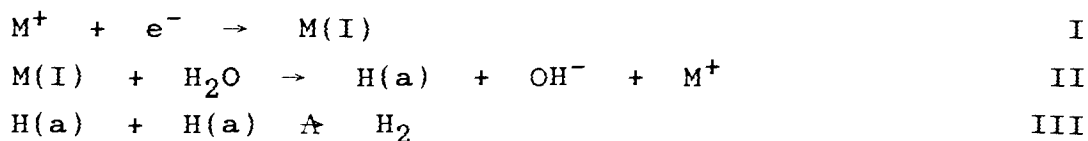
where M(I) and H(a) denote the intermetallic compound of
the alkali metal with the electrode metal and absorbed or
adsorbed hydrogen atom in or on the electrode,respective-
ly and $\overset{\wedge}{\rightarrow}$ in the last step III,rate determining. In this
background,some types of cold fusion proved to be occur-
ring. The aim of the present report is to clarify the
elementary acts causative of cold fusion.

2. HER in Alkali Ions' Solutions

GSTM of analyzing a quite initial stage of overvoltage-
time curve was proposed more than 30 years ago by
A.Matsuda(2) as an effective one to determine separately
from an overall reaction,the kinetics of the electron
transfer step which was not rate-determining. From the
results of the studies by use of GSTM(2),the electron
transfer step of HER in alkaline or neutral solution
including monoatomic metallic cation proved to be the dis-

charge of this metallic cation as shown by step I on the low overvoltage metals for HER,for example,platinum group metals, nickel,silver,gold,titanium etc.. The exchange current densities i_{10}(rates of the equilibrium state) of step I per unit true surface area cm^2 in the cases of Li^+,Na^+ and Cs^+ in 1 mole ion/l solutions on Pt are found to be 2.0·,1.5· and 1.3· 10^{-2} amp/cm^2, and those on Ni, 9.0·,6.5· and 6.8·10^{-3} amp/cm^2, respectively. For comparison,the exchange current densities i_0 of the overall reaction on Pt and Ni are found to be 3.1·10^{-4} and 6.0·10^{-6} amp/cm^2 in all ions' solutions.

3. Intermetallic Compounds of Alkali Metals and Electrode Materials

The next stage of overvoltage-time curve also can be analyzed by use of GSTM of determining pseudo-capacity due to the accumulation and the decomposition of M(I) near the electrode surface(3). In the course of build up of overvoltage the intermediates continue to increase till the overall reaction reaches to the steady state. In the course of decay of overvoltage after the lapse of time τ_1, the time constant of the discharge step,the intermediate species are consumed through the elementary steps II and III which follow the discharge step,as the discharge step is kept in equilibrium in this stage of the decay process. Fig.1 shows a typical example of the oscillogram of potential-time curve, observed on evaporated platinum film electrode in Na_2SO_4 acidified with sulfuric acid(pH= 2.83). As seen from Fig.1,a long plateau appears on the decay curve at E_{nhe}=-0.7~0.8 volt, which may be due to the decomposition of alkali-intermediate.

Fig.2 shows relations between pseudo-capacity and E_{nhe} obtained on Pt in Na_2SO_4 solutions of Na^+ ion concentration of 1 mole/l, but various pH's. As seen from Fig.2, practically the same peak appears at $E_{nhe} \approx -0.8$ volt in both cases of the acidic and alkaline solutions. It is concluded from the result that the major intermediate is formed with a certain component of the intermetallic compound of sodium atom and Pt.

The amounts of Na(I) obtained by integrating the both curves in Fig.2 are plotted against E_{nhe}, which coincide with one another, as shown in Fig.3. The amount of sodium atom composing the intermetallic compound is saturated at $E_{nhe} = -0.9$ volt which is corresponding to 6~7 monolayers on the surface, but taking into account the composition of the intermetallic compound and the presence of the diffusion layer of sodium atom in platinum, sodium atom may be penetrating into the depth of 100~1000 monolayers from the surface of the electrode. The similar relation obtained in the case of nickel electrode in Na_2SO_4 is shown in Fig.4.

The X-ray diffraction pattern of the Pt-cathode surface insitu was observed during electrolysis in sodium or cesium ions' solution. On the pattern, a few weak circles were found, which were corresponding to neither Pt nor Na(or Cs) lattice.

4. Cooling Effect on Excess Heat

It has been reported in previous work(4) that the large excess heat(200~360% for the input power) was observed, reproducibly. But, it was often observed that the decrease of excess heat was caused by the omission of

cooling a cell. Such a cooling effect on excess heat is explained in terms of the differences in the activation energies of steps I,II and III. The activation energy of step I in all cases of Li^+,Na^+ and Cs^+ on Ni was found to be ca. 3 Kcal/mol(2), while those of the overall HER and the self-diffusion of potassium on(and in) Ni were found to be 8~14 Kcal/mol and 9.8 Kcal/mol in the range of temperature 0~60°C, respectively(5). It can be under- standable by reason of the differences in the activation energies of the steps that a rise of the temperature in cell increases the rates of steps II and III more greatly than that of step I, should result in the decreases in the density of M(I) in electrode and then in the rate of cold fusion occurring among intermediates.

5. Tritium Production During Electrolysis of Light and Heavy Water Solutions of Potassium Carbonate

As shown in the preceding paper(4), an unexpected amount(ca.4ppm) of calcium was detected in light water electrolyte of potassium ion after electrolysis, repro- ducibly. With the aim of seeking the other evidences of cold fusion,the amount of tritium in light and heavy water electrolytes was measured by means of Liquid Scin- tillation Analyzer. The experimental procedure is the nearly same as in the previous work(4),except for the main part of the cell vessel made of quartz glass and the cell not cooled directly by any air or water stream.

Fig.4 shows the relations between ^3t amounts expressed by Bq/20ml·24hr in electrolyte of 20ml used for electroly- sis, during 24 hours and the electrolytic current I or the input power W_{input} which was observed on the porous Ni cathode(1.0x0.5 cm size,0.1 cm thickness),in 0.5 mole

K_2CO_3 light water electrolyte. In the series of the experiments, excess heat was, roughly speaking, kept constant, i.e. 68~82 %. It is found from Fig.4 that the amount of ^3t produced during electrolysis is increasing with both increase of current and input power. But, if there are very large differences in excess heat, the amount of produced ^3t was found to be proportional to the excess heat.

The amount of ^3t produced by electrolysis in heavy water solution of 0.5 mole/l K_2CO_3 was measured to be 10~100 times more than that in light water's. It seems that ^3t is mainly produced not by D+D(1) and D+D+D(6) reactions but by others, taking into account the small effect of D-content of electrolyte on the rate of ^3t production.

Light water used in the present work is containing a small amount of deuterium even less than 0.015%. But, Srinivasan made a similar experiment of electrolysis in true light water and also detected ^3t(7) in electrolyte after electrolysis. It suggested the above idea.

References

1. M.Fleischmann, and S.Pons. "Electrochemically Induced Nuclear Fusion of Deuterium." J.Electroanal.Chem., Vol. 261, 301(1989).

2. R.Notoya, and A.Matsuda. "Hydrogen Overvoltage on Platinum in Aqueous Sodium Hydroxide, Part III Intermediates." J.Res.Inst.Catal., Vol.14,198(1966); see also "Kinetic Study of Electron Transfer Step of Hydrogen Evolution Reaction on Metals in Aqueous Media." Paper No. 515,presented at 34th Meeting of International Society of

Electrochemistry,Erlangen,Germany(September 1983) and
R.Notoya."Galvanostatic Transient Method for the Study of
Electrocatalysis." Elektokhimiya, Vol.29,53(1993).

3. A.Matsuda."On the Differential Capacities of Iron and
Nickel Hydrogen Electrodes observed by Past and Jofa."
J.Res.Inst.Catal., Vol.8,151(1960).

4. R.Notoya."Cold Fusion by Electrolysis in a Light
Water-Potassium Carbonate Solution with a Nickel Elec-
trode." Fusion Technol., Vol.24,202(1993).

5. Ed.Japan Chemical Soc., Chemical Handbook, Fundamental
Edition. Vol.2, Table 6~48, Maruzen Inc,Tokyo,1984;and
Ed.A.J.Bard, Encyclopedia of Electrochem. of the Ele-
ments. Vol.9 Part2, Marcel Deker Inc, New York and Basel,
529(1973).

6. A.Takahashi et al.."Excess Heat and Nuclear Products
by D_2O/Pd Electrolysis and Multibody Fusion." Inter
J.Appl.Electromagnet.Mat., Vol.3,221(1992).

7. M.Srinivasan et al.."Tritium and Excess Heat Genera-
tion during Electrolysis of Aqueous Solutions of Alkali
Salts with Nickel Cathode." Frontiers of Cold Fusion,
Proc. ICCF-3, Nagoya, p.123(1992).
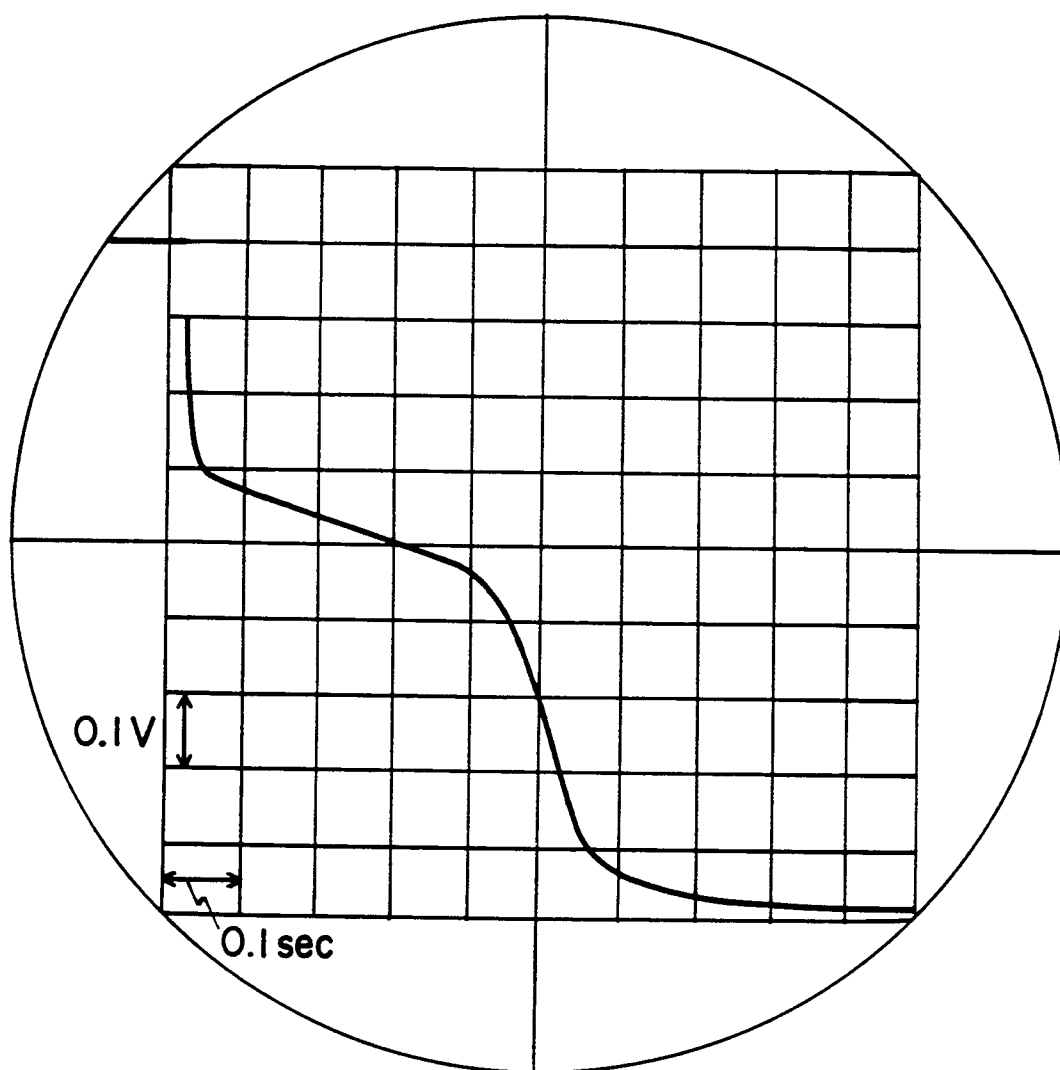
Fig.1 Potential-time variation after switching off a
polarizing current on Pt in Na_2SO_4, pH=2.83.
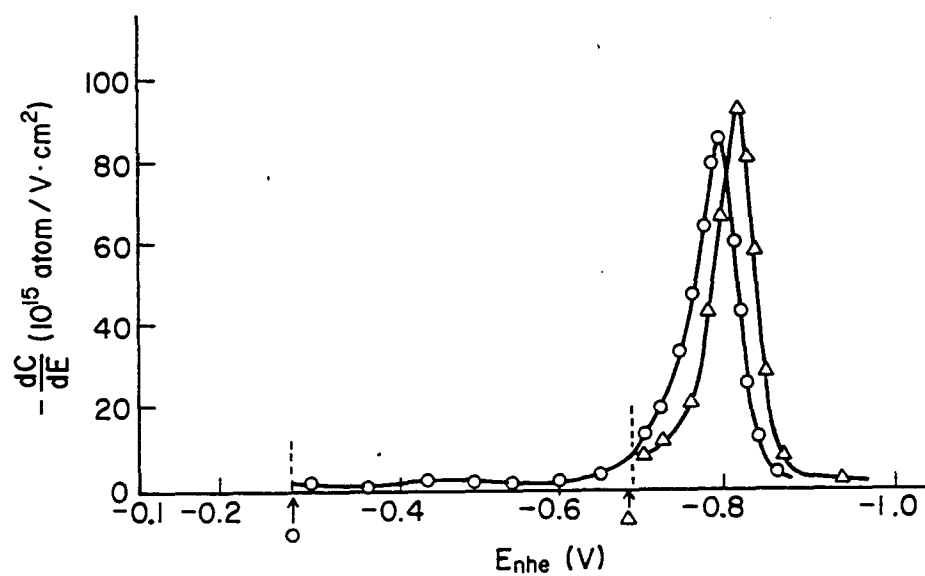
Fig.2 -dC/dt vs.E_{nhe} in the decay processes; in $[Na^+]=$ 1mole/1, Na_2SO_4 solutions, pH=4.7($\bigcirc$) and pH=11.38($\triangle$).
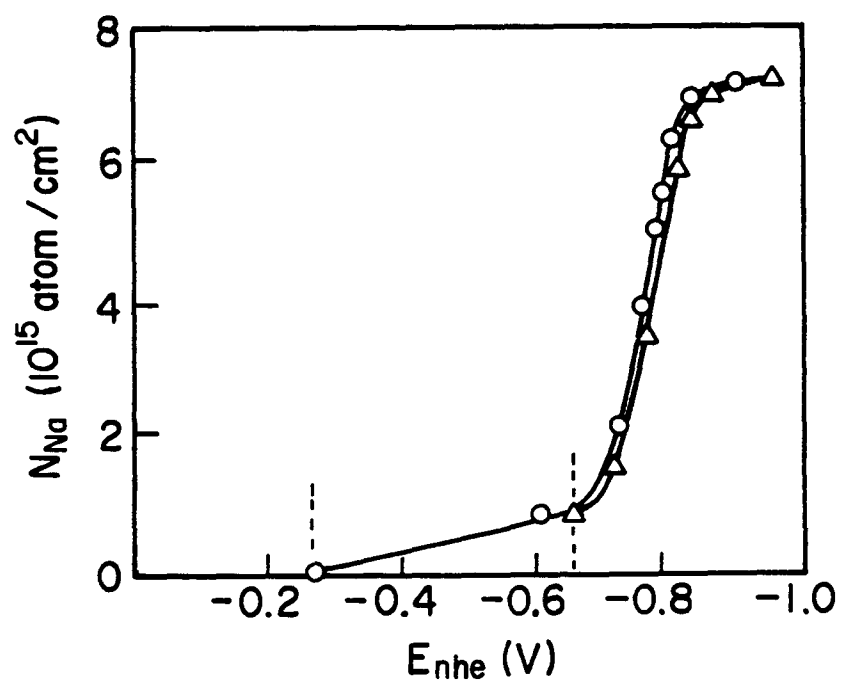
Fig.3 Amount of Na atom on unit true surface area cm^2 of electrode vs. E_{nhe} on Pt; in $[Na^+]$1mole/1,Na_2SO_4 solutions,pH=4.7($\bigcirc$) and pH=11.38($\triangle$).
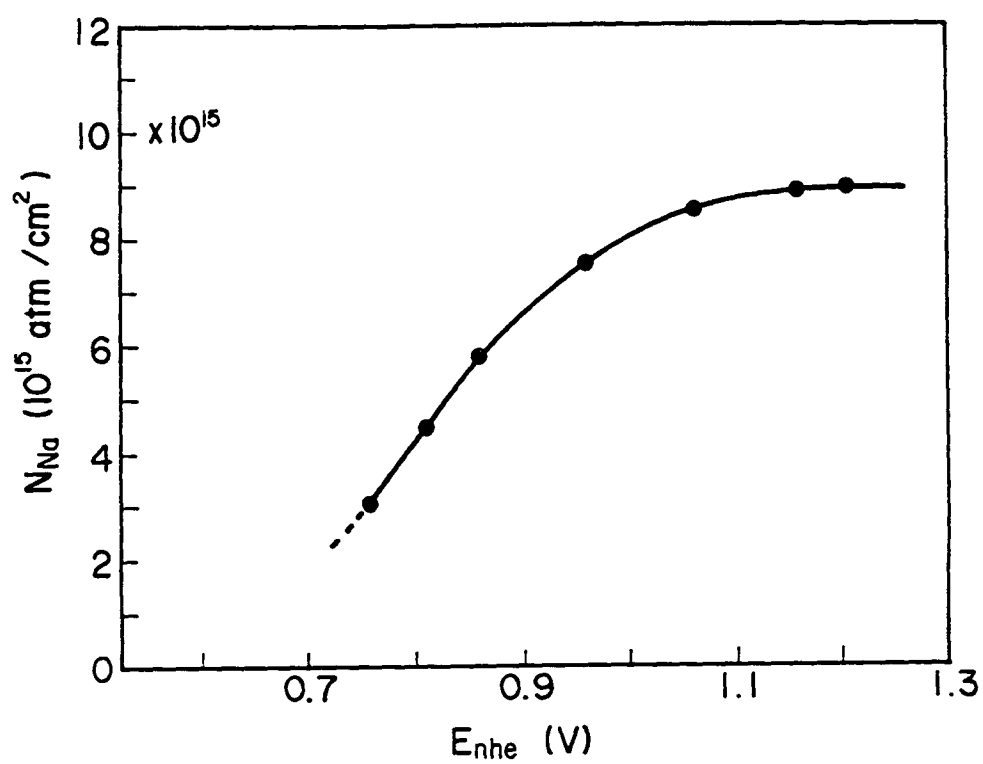
Fig.4. Amount of Na atom on unit true surface area cm^2 of electrode vs. E_{nhe} on Ni;in 1mole/l NaOH solution, pH=13.75.
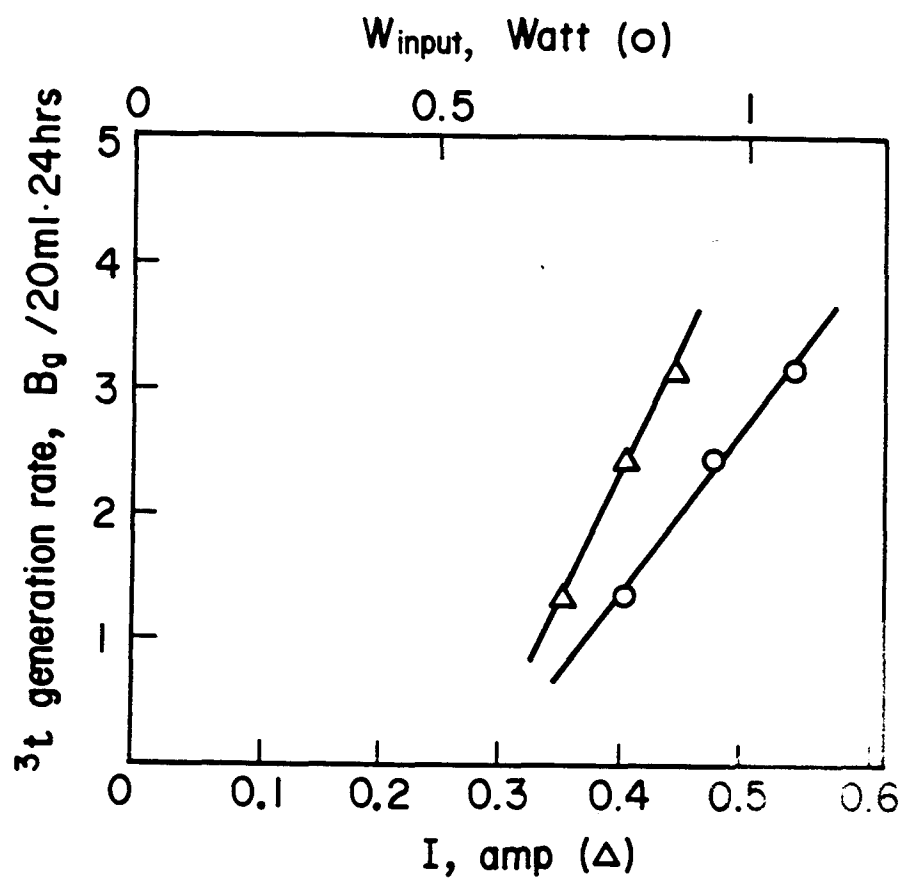
Fig.5 Relations between amount of ^{3}t in 20ml electrolyte during 24 hours electrolysis,Bq/20lm·24hr and current, I($\triangle$) and input power,W_{input}($\bigcirc$) observed in 0.5mole/l K_2CO_3 on porous nickel electrode.

1. Dr.Reiko Notoya is Research Associate in Catalysis
Research Center, Hokkaido University in Sapporo, Japan.
The Center is responsible for research on electrochemical
kinetics and different types of energy conversion.

2. Dr.Notoya received a B.S.degree in Chemistry from
Hokkaido University and a Dr. of Science in Electrochem-
istry from Hokkaido University.

"Evidence for Electrolytically Induced Transmutation and Radioactivity Correlated with Excess Heat in Electrolytic Cells With Light Water Rubidium Salt Electrolytes"

R. Bush and R. Eagleton

Physics Department, California State Polytechnic University*
and
ENECO**

Abstract

Two separate mass spectrometric analyses, SIMS and ICPMS of 1.0 amu discrimination preceded by an ion-exchange column separation of strontium and rubidium, performed by two independent laboratories on the pre-run and post-run cathode material from a light water based rubidium carbonate cell and a rubidium hydroxide cell provide strong evidence for the electrolytically induced transmutation of rubidium to strontium originally hypothesized by Bush in connection with his CAF hypothesis ("Cold Alkali Fusion"). The SIMS analysis showed that the abundance ratio of Sr86 to Sr 88shifted from the normal abundance ratio of about 0.12 in the prerun cathode sample to essentially the same value, 2.6, as the natural abundance ratio of Rb85 to Rb87, where the latter are the respective parent isotopes hypothesized by Bush. Proof that this shift by a factor of about 22 from the natural abundance ratio for the strontium isotopes could not have been a spurious SIMS result due to rubidium hydride formation was demonstrated by additional mass spectroscopy, ICPMS, preceded by an ion-exchange column separation of the strontium and the rubidium. In the ICPMS tests, the postrun cathode material from both cells demonstrated a shift in the strontium isotope abundance ratio by an amount that is more than 600 standard deviations away from the normal ratio (prerun sample). In addition, for a third rubidium carbonate cell, strong preliminary evidence is presented for electrolytically induced radioactivity. The experimental work provides strong initial support for Bush's LANT hypothesis ("Lattice Assisted Nuclear Transmutation").

Introduction

Analyses of the pre-run electrode material and post-run electrodes from two light water based rubidium salt electrolytic cells, cell 53 (rubidium carbonate) and cell 56 (rubidium hydroxide) having nickel mesh cathodes by two independent laboratories provide strong initial evidence in support of Bush's CAF Hypothesis[1,6] ("Cold Alkali Fusion") that strontium is being produced from rubidium via a cold nuclear reaction in which a proton is being added to Rb^{85} (Rb^{87}) to produce Sr^{86}(Sr^{88}). The postrun cathode material of cell 53 was analyzed via SIMS, while that for cell 53 and cell 56 was analyzed via Inductively Coupled Mass Spectrometry (1 amu discrimination) following an ion exchange column enhancement of the strontium relative to the rubidium[1,2,6] at WCAS (" West Coast Analytical Service, Inc. ") of Santa Fe Springs, CA. For an additional rubidium carbonate cell, cell 71, there is initial evidence for electrolytically induced radioactivity. A scintillation tube combined with a multi-channel analyzer was employed to establish a radioactive decay curve corresponding to an average half-life of about 3.8 days. This result combined with the earlier mass spectrometric evience and its correlation with the excesss heats measured

via calorimetry provides support for Bush's LANT ("Lattice Assisted Nuclear Transmutation") hypothesis[3] according to which a cold nucleosynthetic chain extending beyond strontium production is revealed for the light water rubidium electrolytic cells.

Cell Design and Calorimetry

The cell and calorimeter design employed for the present series of experiments were of two types: (1) Cells 53 and 56 were essentially the same as that reported in Ref. 2. which was a modified Fleishmann-Pons (Ref. 4) electrolytic cell with the following principal modifications: (a) the use of a *platinum black recombiner* in the cell to allow for *closed-cell operation*, (b) a *magnetic stirrer* that provided for more uniform electrolyte mixing, and (c) *Teffon* coating of all nonelectrode materials to reduce electrolyte contamination. Cell 71 was of a single wall construction and is described in another paper (ref. 4).

The electrolytic cells, as shown in Fig. 1, consisted of double wall pyrex vessels surrounded by a one inch thick layer of styrofoam. Cell temperature was regulated by controlling the temperature of the bath water which flowed through the jacket surrounding the cell. Data on cell temperatures, current, and voltage were monitored and logged by a MacIntosh IIx computer equipped with National Instrument's LabView software. Four type K thermocouples were used with each cell: one at the bath inlet port, one at the bath outlet port, and two within the electrolytic cell. The thermocouple voltages were converted to temperature by use of AD595AQ/9217 integrated circuit chips. This system permitted steady state temperature measurements with standard deviations of about 0.05 °C. Corrections for thermocouple temperature offsets were made within the software. Current and voltage signals were logged from Fluke 45 dual display multimeters which were equipped with IEEE bus.

Pertinent details for the cells of interest in this report are as follows:

Cell #	Cathode	Anode	I ma/cm^2	Electrolyte
53	Nickel Sponge, 45 cm^2	Pt	1.0	0.57M Rb$_2$CO$_3$ 50ml
56	Nickel Sponge, 45 cm^2	Pt	1.0	0.57M RbOH 45ml
71	Nickel Sponge, 55cm^2	Pt	1.0	0.57M Rb$_2$CO$_3$ 65ml

Here the charging current density for the cells is given in the column headed by "I ma/cm^2". Anodic calibration was used for all cells.

The cells were calibrated by determining the steady-state temperature difference across the cell walls as a function of the electrical power supplied to the cell while running anodically. Since the thermal power out of the cell must equal the electrical power into the cell when it is in steady-state, one can use the calibration curve to determine the thermal power out of the cell for a given average temperature drop across the cell wall. The average temperature drop across the cell wall is found by taking the average of the inlet and outlet bath temperatures and subtracting this from the average of the two cell thermocouples. Excess power production was obtained by subtracting the electrical power supplied to the cell from the thermal power flowing from the cell.

SIMS Results for Postrun Cathode of Cell 53

A SIMS analysis for the pre- and post-run cathode material of cell #53 showed strong lines at mass numbers 86 and 88 that were not present in the pre-run spectrum[1,2,6]. Figures 2 through 5 portray the four mass spectrograms, respectively: Postrun cathode material: 0-100 amu, Prerun: 0-100 amu, Postrun: 100-200 amu, and Prerun: 0-100 amu. Appendix A provides an interpretation of these from the standpoint of hpothetical strontium production. An interesting finding from the standpoint of the CAF Hypothesis[1,3,6] is the fact that, within experimental error, the ratio of the line height for mass number 86 to that for 88 was the same as that for the ratio of the rubidium signals at masses 85 and 87. (The SIMS tests were performed under the auspices of a wellknown U.S. National Laboratory, which because of the present political atmosphere for cold fusion work, prefers not to have their name revealed at this time.)

A disadvantage of these SIMS tests was that the mass spectrometer employed was unable to discriminate between rubidium hydride and strontium; i.e. $Rb^{85}H$ would be indistinguishable from Sr^{86}. So, even though there was strong evidence pointing to the noninvolvement of rubidium hydride, such as the instability of the latter and the fact that the rubidium oxide lines, which should have been higher than those for RbH because of the greater stability of RbO, were shorter than those for the putative RbH, it was decided to pursue additional tests in which a chemical separation of the rubidium and strontium would first be performed prior to the mass spectrometric analysis. These analyses were carried out by West Coast Analytical Services, Inc., of Santa Fe Springs, CA.

Ion Column Exchange Separation of the Rubidium and Strontium Followed by ICPMS ("Inductively-Coupled Plasma Mass Spectroscopy") (Cells 53, 56)

Since, at least in priciple, criticism could be levelled at the SIMS results by suggesting the formation of RbH to account for an apparent strong enhancement of Sr86 to Sr88 it was decided to have an ICPMS ("Indictively Coupled Plasma Mass Spectrometry") analysis performed at an independent laboratory, West Coast Analytical Service, Inc.[1,2](Hereafter: WCAS) of Santa Fe Springs, CA. Two pages of their final report is included as Appendix B. Because the mass discrimination of the spectrometer was limited to one amu, they first performed an ion-exchange column separation to concentrate the divalent strontium relative to the monovalent rubidium, which was washed selectively out of the column.

A summary of the WCAS results is included in the Table of Fig. 6. Previously WCAS had found that the virgin cathode material gave readings for the relative percentages of the two strontium isotopes of interest essentially the same as that of the Strontium Standard average given in the data table of Fig. 6 as follows: Sr 86: (10.51 ± 0.04)% and Sr 88: (89.49 ± 0.04)%. This gives a ratio of Sr 88 to Sr 86 for the standard (and vigin cathode material) of (8.515 ± 0.004) to which the ratios for the postrun cathode material will next be compared. From the data summary in Fig. 6 the following results are seen for the post-run cathode material of cell 53 (Sample A#53) for the test date of (4/9/93): Sr 86: (22.20 ± 0.05)% and Sr 88 (77.80 ± 0.05)%. The ratio of Sr 88 to Sr 86 is thus (3.504 ± 0.002), which is lower than the ratio for the virgin material by about 716 standard deviations as seen by the following: (8.515 - 3.504)/ (0.007) = 715.8. Since the ratio was reduced from that of the standard (virgin cathode material), this provides good evidence for an enhancement of Sr 86 relative to Sr 88 for the postrun cathode of cell 53, a light water based rubidium carbonate cell. For cell 56

(light water based rubidium hydroxide), which had evidenced about five times as much excess heat as cell 53 based upon calorimetry, the data table of Fig. 6 gives results for the analysis of sample #56PR on (4/9/93) as follows: Sr 86: <u>(26.80 ± 0.05)%</u> and Sr 88 <u>(73.20 ± 0.05)%</u>. The following ratio of Sr 88 to Sr 86 for these numbers implies an even greater electrolytically induced enhancement of Sr 86 relative to Sr 88, which could be anticipated based upon the greater excess heat exhibited by cell 56: <u>(2.731 ± 0.003)</u> Again, as dramatic evidence for this enhancement of Sr 86 relative ro Sr 88 this ratio is less than the standard by about <u>826 standard deviations</u> as seen by the following: (8.515 - 2.731)/ (0.007) = 826.3. Thus these ICPMS results of WCAS obtained by first achieving a chromatographic concentration of the strontium relative to the rubidium provide strong independent support for the SIMS results.

Support for the LANT Hypothesis

According to Bush's LANT hypothesis[3] ("Lattice Assisted Nuclear Transmutation") strontium production would not necessarily be the end of the transmutation line. Rather, the Sr atoms formed in the lattice would themselves now become targets for the lattice assisted addition of a proton. This would produce an entire cold nucleosynthetic series, the Rubidium Series[3], shown in Fig .7 taken from reference 3. A comparison of the SIMS spectrographs of the cathode material of Cell 53 (rubidium carbonate) before and after running provides evidence for the synthesis of such nuclides as shown in the Table of Fig. 8 entitled "Isotope Production via Cold Nucleosynthesis: Rubidium Series[3]." In this respect it is interesting to note from the Table in Fig. 8 that the total excess heat produced in connection with this synthesis should be $(3.8 ± 0.4) \times 10^{19}$ MeV, whereas the actual excess heat for cell 53 as determined from calorimetry[3] was approximately $(4.0 ± 0.8) \times 10^{19}$ MeV. This is rather good agreement and provides initial support for the LANT hypothesis.

Evidence for Electrolytically Induced Radioactivity

Fig. 9 displays a radioactive decay curve obtained employing the postrun cathode material of cell 71, a light water rubidium carbonate cell (0.57 M) with nickel mesh cathode and platinum anode that ran for approximately two months. Nine days elapsed betwen the end of electrolysis and the beginning of radiation monitoring with the sample in a lead bunker to reduce background levels. Counting was carried out with a Bicron 1.5 inch diameter NaI scintillation detector encased in a thickness of about one-eighth inch of aluminum. The signal from the scintillation detector was fed into a mulitichannel analyzer employing an 811-3 multichannel analyzer PC board and software by Nucleus, Inc. of Oak Ridge, Tennessee. The counts shown were each taken over a twenty four hour period to even out diurnal background fluctuations and each represents the sum of the counts in the lowest twenty two channels, channel 19 through channel 40, with channel 40 corresponding to an energy of about 20 keV. The first two points of the decay curve in Fig. 9 correspond to two consecutive 24 hour background counts taken in the lead bunker, and were each about 5 million counts. However, once the sample was in place, it was deemed important to monitor the postrun cathode without moving it between the twenty four hour counts. The monitoring for radioactivity continued for about one month as shown, and at which time the count appears to be approaching the background asymptotically. Fig. 10 displays a semi-log plot of count versus time in days yielding a half-life of about 3.8 days. In that regard Bush points out that it is interesting that a simple unweighted average of the half-lives for the short-lived radionuclides deduced by Bush from his LANT Hypothesis[3] (See Fig. 8) for

his hypothesized Rubidium Series[3] (Fig. 7) and from the SIMS analysis for cell 53 (rubidium carbonate) yields an average half-life of 3.5 days: (From Fig. 8) Tc-96 (4.35 D), Ru-97 (2.90 D), Pd-100 (4.0 D), and In-111 (2.8 D). Also, possibly related to this is the fact that a "down" data point on the decay curve, meaning one that was lower than the previous twenty four hour count , was usually followed by one or more points where the count stayed the same, or increased. Whether this is indicative that a larger standard devistion (error bar) on the order of ±3,000,000 counts in a 24 hour period is more appropriate than the ±1,000 count error bar used, or whether this represents an additional phenomenon of interest such as the emergence of tritium from the sample is not clear at this stage.. At any rate, Bush notes that if he employs just the "down" (decreasing count) data points that the half-life of the decay curve is equal to the 3.5 days indicated above, and this is displayed in the semi-log plot of Fig. 11. (Fig. 12 portrays a plot of average half-life versus channel number based upon the first twenty days of counting, and is consistent with the average half-life for the sum of the twenty four hour counts for the first twenty two channels of about 3.8 days.) So far as we know, this data constitutes the first reported results for radioactivity associated with measurement for cathode material removed from the electrolytic cell. We had previously reported[5] x-ray detection in the case of an LiOH cell with a nickel mesh cathode measured while the cell was running, and for an LiOD cell with a palladium cathode measured following the end of electrolysis but measured with the electrode in place in the cell.

Conclusions

With the corroborative independent mass spectrographic results of the two separate laboratories the evidence supporting the electrolytically induced transmuation of rubidium to strontium, as evidenced by the shift in the abundance ratio or Sr-86 to Sr-88, must be considered very strong. These results add support to Bush's CAF and LANT hypotheses. Note that any strontium contamination would only tend to shift this ratio back to the natural abundance ratio for the two strontium isotopes. If these results can be corroborated by independent observers, they should stand as one of the high water marks of cold fusion research. The evidence for electrolytically induced radioactivity in a rubidium cell as monitored outside the cell by a scintillation counter after the discontinuation of electrolysis represents another breakthrough if it can be independently verified.

Acknowledgments

References
1. R. Bush, "A Light Water Excess Heat Reaction Suggests that 'Cold Fusion' May Be 'Alkali-Hydrogen Fusion' ", Fusion Technol., 22, 301 (1992).
2. R. Bush and R. Eagleton, "The Transmission Resonance Model for Cold Fusion in Light Water: I. Correlation of Isotopic and Elemental Evidence with Excess Power", Proc. 3-ICCF, 409,(1993).

3. R. Bush, "Towards a Nuclear Physics of Condensed Matter", accepted for Fusion Technol., under revision, est. issue: March '94.
4. R. Bush and R. Eagleton, "Calorimetric Studies For Several Light Water Electrolytic Cells With Nickel Fibrex Cathodes and Electrolytes With Alkali Salts of Potassium, Rubidium, and Cesium", submitted to Proc.4-ICCF (1994).
5. R. Bush and R. Eagleton, "Experimental Studies Supporting the Transmission Resonance Model for Cold Fusion in Light Water: II. Correlation of X-Ray Emission with Excess Power", Proc. 3-ICCF, 409 (1993).
6. R. Bush, "Will the Light Water excess Heat Effect Lead to a Unification with Cold Fusion?", Twenty First Century Science and Technology, Fall 1993, p. 75.

*3801 West Temple Avenue, Pomona, CA 91768.
**University of Utah Research Park, 391-B Chipeta Way, Salt Lake City, Utah 84108.

APPENDIX A: Interpretation of the SIMS Mass Spectrograms

The mass spectrograms of Fig. 2 and Fig. 3 were carried out by SIMS analysis, respectively, for the postrun cathode material and for the prerun cathode. (Earlier mass spectrometry established an upper limit on the strontium in the post-run solution from cell 53 of 5 ppb.) Note the following from Fig. 3 (Prerun):

Fig. 3 (Prerun): Mass 86: The height of this signal is about 3.6 cm corresponding on the log-scale to an ordinate of 190 counts.
3.5 cm signal height: 150 counts

    Nickel 58: 10.0 cm signal height: 1,250,000 counts

Fig. 2 (Postrun): Note that the signal height discrimination for this spectrogram is greater than that for the one of Fig. 3. Thus, the spectrogram of Fig 3 is associated with only a 50 V offset, whereas that of Fig. 2 is associated with a 125 V offset. Thus, in comparing signal heights from Fig. 2 to those on Fig. 3 we must multiply the numbers of counts in Fig. 2 by the ratio of the Nickel 58 signal in Fig. 3 to that in Fig. 2:

    Mass 86: 3.25 signal height: 36 counts

    Mass 88: 2.6 cm signal height: 16 counts

    Nickel 58: 9.5 cm signal height: 31,000 counts

Ratio of Nickel 58 signal in Fig.3 to that in Fig.2:   (1,250,000/ 31,000)= 40.32.

    Corrected counts from Fig.2 to compare with those in Fig.3:

        Mass 86: 36 x 40.32 = 1, 452 counts

        Mass 88: 16 x 40.32 = 645

Ratio of Sr-86 to Sr-88: (Corrected for background in Fig.3):

$$(1,452 - 190) / (645 - 150) = \underline{2.55}. \qquad (1)$$

Note that the ratio of the natural abundances of Sr-86 and Sr-88 is approximately:

$$\underline{0.12} \qquad (2)$$

Thus, we have an isotopic abundance ratio shift by a factor of

$$\underline{2.55/ \, 0.12 = 21}. \qquad (3)$$

Note, also, that the ratio of the natural abundances of Rb-85 and Rb-86 is about

$$\underline{2.59}. \qquad (4)$$

The fact that the ratio in (1) so closely matches that in (4) is strong support for Bush's hypothesis that the strontium arises from the rubidium via the addition of a proton at the surface of the nickel.

Finally, how do we know that masses 86 amd 88 in B correspond to strontium and not, say, to rubidium hydride. Quite aside from the well-known instability of rubidium hydride is the fact that a second mass spectrometric study in which the rubidium and strontium are first chemicaly separated via an ion exchange column shows a strong enhancement of Sr-86 over Sr-88 both for the post-run cathode material of cell 53 and for a new light water rubidium hydroxide (0.57 M) cell (cell 56).

APPENDIX B (WCAS)
WEST COAST ANALYTICAL SERVICE, INC.

C.S.P.U. **Job # 23653**
Dr. Robert T. Bush **April 22, 1993**

LABORATORY REPORT

Text

Strontium Isotope Ratio Determination

Summary

The results obtained and listed in Table 1 (fig. 6) show that the method works as designed, using single and mixed standards. For sample A#53, some enhancement was determined, particularly on 4-9-93 when sequence 2 was performed, Sr86 = 22.2±0.05. Sequence 2 has been producing the most consistent results. Sample #56PR demonstrated verifiable enhancement, Sr86 = 26.8±0.05.

WEST COAST ANALYTICAL SERVICE, INC.

C.S.P.U.   Job # 23653
Dr. Robert T. Bush   April 22, 1993

LABORATORY REPORT

On 4-14-93, we decided to run A#53W1 from the first sequence just to have similar batch results as obtained for #56PR. The strontium standard looks great; not much strontium detected in the sample. (Pages 50 and 9)

The next experiment was designed to improve the chromatography. The amount of rubidium in solution exceeds the capacity of one column, so two columns were hooked together and a series of solutions run through them. The results for the standard are very consistent with single column values; however, for a real sample such as A#53, the strontium is still coming out early in W1 instead of DP-2 where we would like it to. (See pages 51 and 52, also results pages 10 and 11, 4-15-93.)

To demonstrate adequate resolution of the mass spectrometer, an experiment was devised on 4-16-93 (page 53). The idea is to use the scanning mode on the ICPMS instead of the peak jumping mode used when measuring isotope ratios. In the scanning mode, the resolution between peaks would be more obvious because many more data points are taken as the mass spec scans through the mass ranges. This test was run twice because the detector tripped off due to the high rubidium counts. For the second scan, the autotrip function was overridden. Page 12 shows the trip results while page 13 shows the scan with the trip switched off. The results are most vividly shown in the two mass spectra, page 14 and 15. Page 14 shows excellent base-line resolution and demonstrates the difference in magnitude of the rubidium/strontium concentrations.

Page 15 shows what would happen to the spectrum and the results if no chromatography was used on the samples to reduce the rubidium levels. Notice peak saturation for both rubidium isotopes as indicated by pitch-fork shaped peaks. Also notice the peak widths and how they spread out into the mass 84 and 87 to some extent.

Page 16 is a mass spectrum of the peak jumping mode, and it shows the resolution, peak width also.

Experimental

Rubidium carbonate impregnated nickel matte electrodes from WCAS Job number 22542 were subjected to ultrasonic cleaning and acid etching to solubilize any strontium isotopes present so isotope ratio measurements using ICPMS could be made. Results are summarized in Table 1. Total Strontium levels were calculated and are reported in Table 1.

Ion Chromatography/cation exchange was used to separate the nonovalent rubidium from the divalent strontium. Ten milliliter fractions were collected from the end of the column and analyzed in batches by ICPMS.

A two-step sample preparation scheme was used. The first step was eight hours of sonication in 2mH HCl. The second step was 24 hours of sonication in 10% HCl, followed by 4 days of room temperature etching with the end point being a light green color from the nickel matrix. Each of the two samples was then washed with DI water three times and set aside to dry. The solutions of 10% HCl were then brought to approximately thirty milliliters (see page 43).

The first analytical sequence (Ion Chromatography, fraction collection, Isotope ratio ICPMS) of the two samples and a strontium only standard is recorded on pages 44 & 45. The actual instrument printouts are on unruled paper, pages 1-3. The results indicate possible enhancement for A#53 and substantial enhancement for #56, data Table 1, 4-8-93.

The second analytical sequence (pages 46 & 47, results pages 4-6) is from sending the fractions collected in sequence one, back through the column to try to get better separation between the rubidium and strontium. The results indicate enhancement for both samples. See results Table 1 data for 4-9-93.

The third sequence came out of our concern for demonstrating that the rubidium levels in the samples were not artificially enhancing the strontium isotopes, resulting in false ratios. (Pages 48 & 49 on 4-13-93 and pages 7 & 8 from printouts contain test information.) The conclusion is that the chromatography is providing enough separation and the resolution of the mass spectrometer is such that <u>no</u> artificial ratio enhancement is being induced by the high rubidium levels. Isotope ratio values are listed in Table 1 for 4-13-93.

Figure 1

Diagram labels: To Bubbler, T cell, T cell, (+), (-), T in, Coolant In, Recombiner, Baffle, Heat Sink, T out, Nickle Fibrex Cathode, Stir bar, Coolant Out
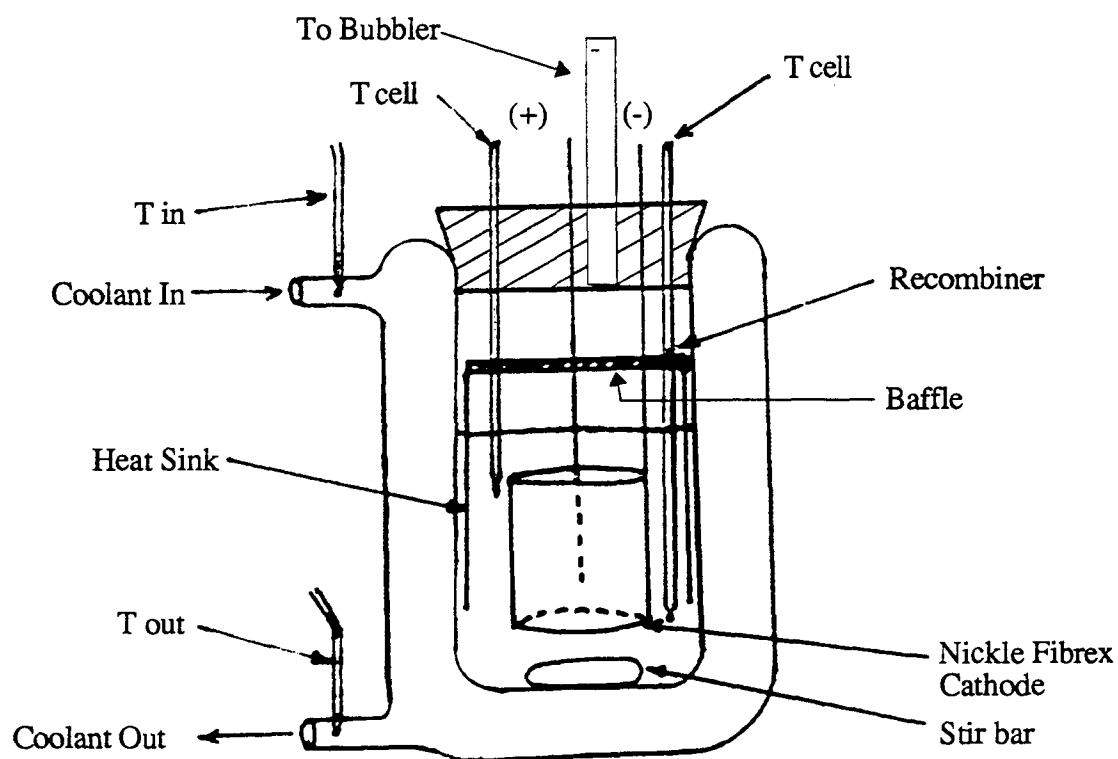
PRINCIPAL FEATURES

- CLOSED CELL OPERATION
- MECHANICALLY STIRRED ELECTROLYTE
- RECOMBINER BAFFLE & HEAT SINK
- TEFLON CELL
- PLATINUM ANODE
- NICKEL FIBREX CATHODE
- NANOPURE H_2O BASE ELECTROLYTE
- CONSTANT COOLANT FLOW RATE
- CONSTANT CURRENT AND TEMPERATURE OPERATION

Figure 2. Cathode post-run mass spectrogram.
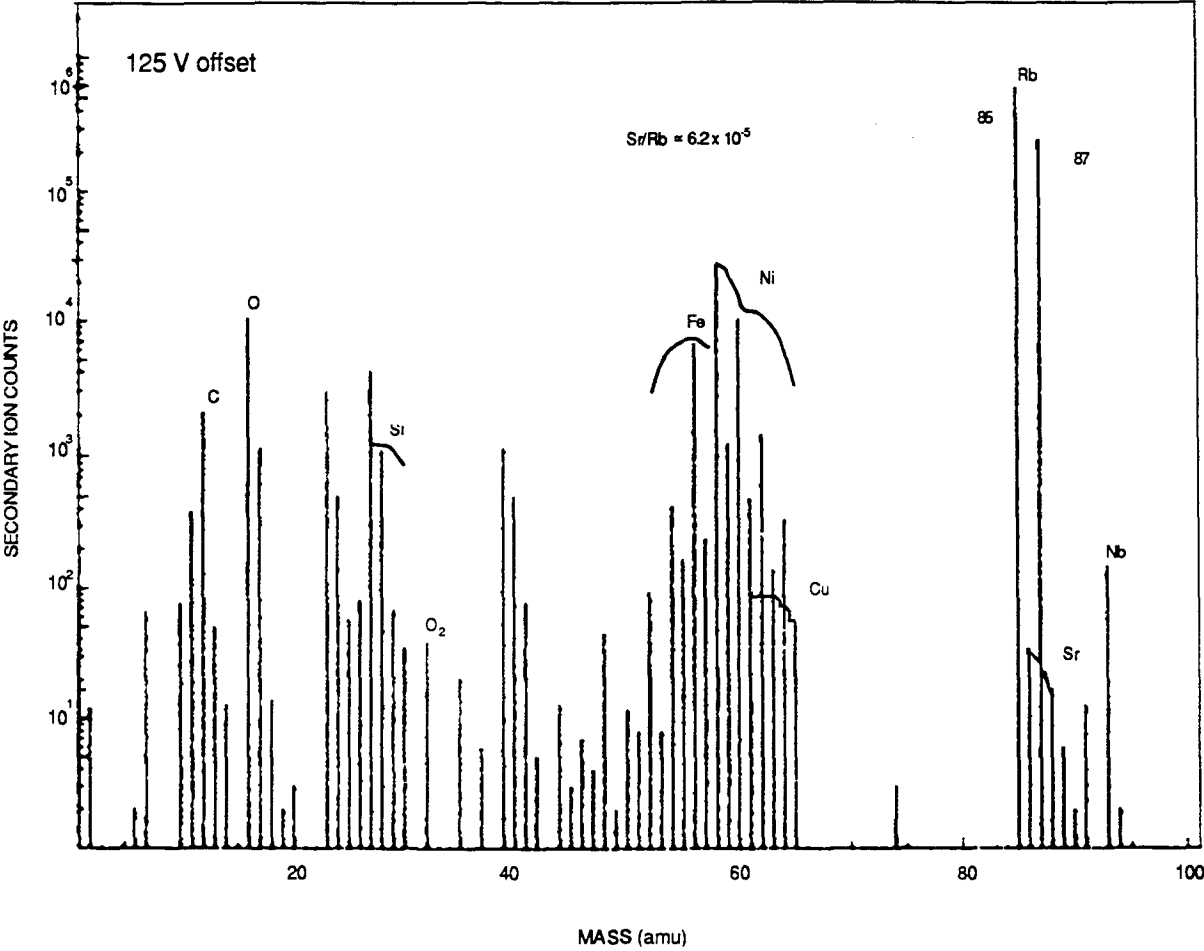
Figure 3. Cathode pre-run mass spectrogram.
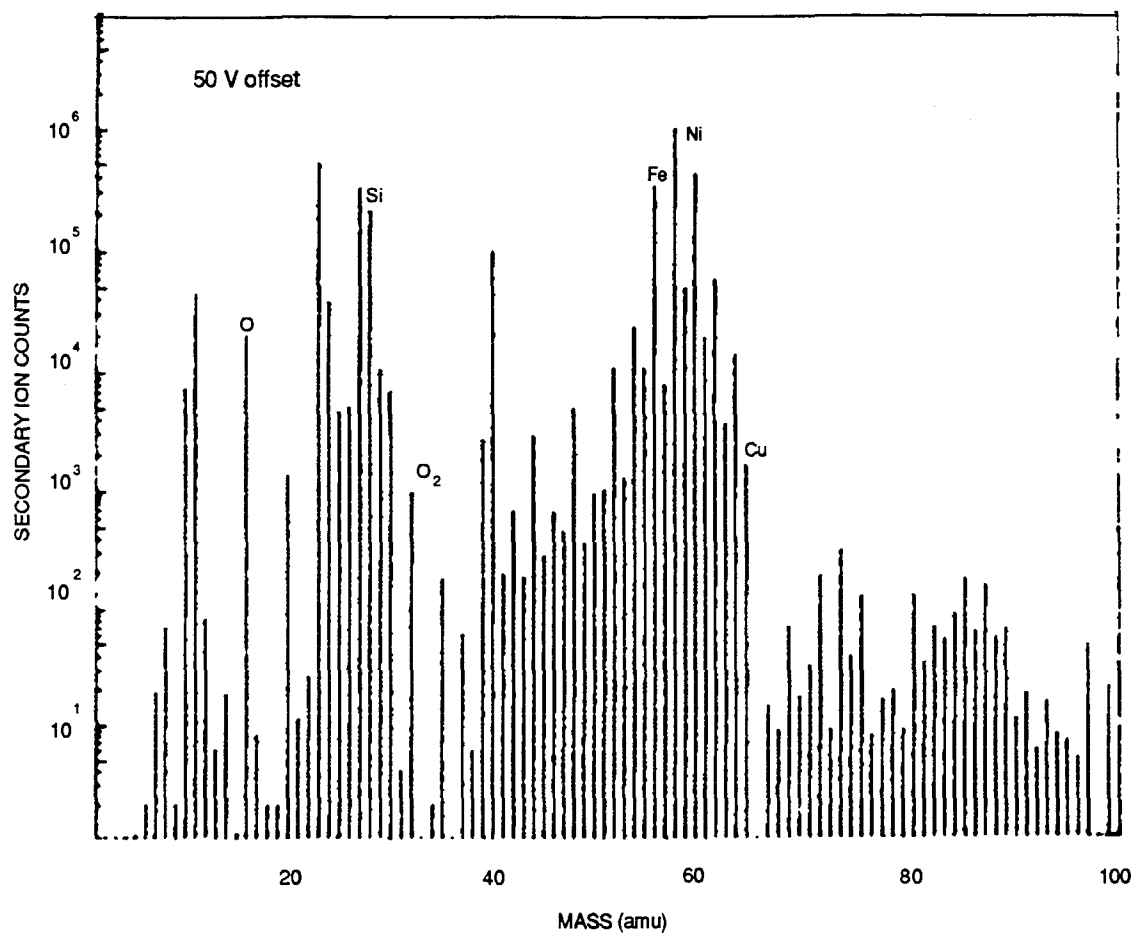
Figure 4. Cathode post-run mass spectrogram.
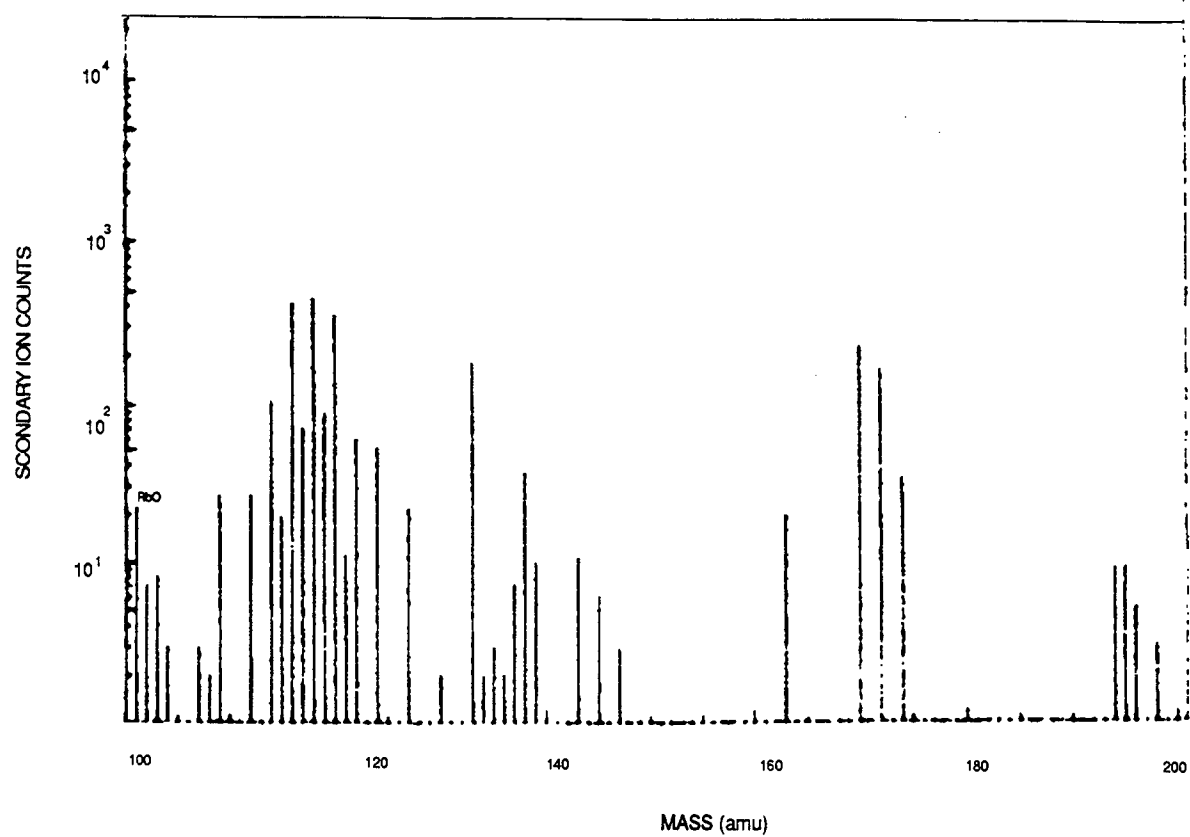
Figure 5. Cathode pre-run mass spectrogram.
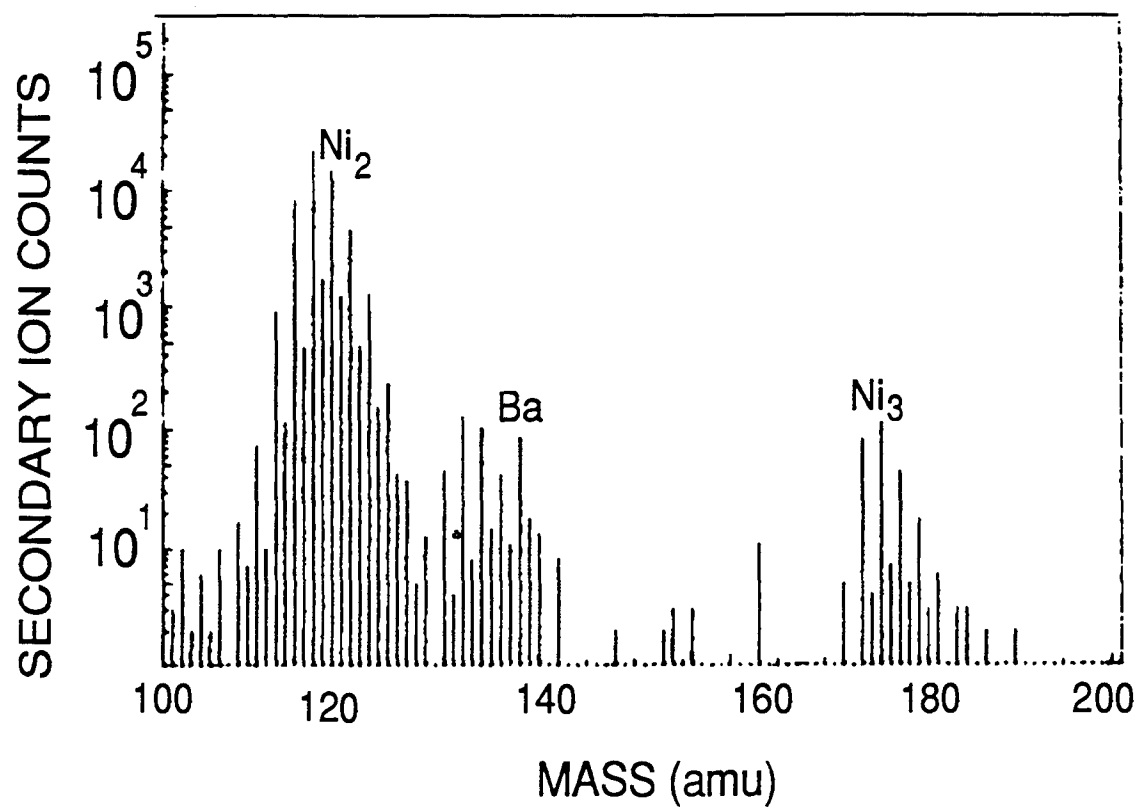
Figure 6

WEST COAST ANALYTICAL SERVICE, INC.

C.S.P.U.   Job # 23653
Dr. Robert T. Bush   April 22, 1993

LABORATORY REPORT

Table 1

Date	Sample ID	Sr 86	Sr 88	Total Strontium
4-8-93	0.01ppm Sr Std	10.48	89.52	10ppb
4-9-93	0.01ppm Sr Std	10.48	89.52	10ppb
4-13-93	0.01ppm Sr Std	10.56	89.44	10ppb
4-14-93	0.01ppm Sr Std	10.53	89.47	10ppb
		10.51±0.04	89.49±0.04	

Date	Sample ID	Sr 86	Sr 88	
4-13-93	100ppm Rb/0.01ppm Sr.	10.47	89.53	10ppb
4-15-93	100ppm Rb/0.01ppm Sr.	10.55	89.45	10ppb
		10.51±0.06	89.49±0.06	

Date	Sample ID	Sr 86	Sr 88	
4-8-93	A#53	ND	ND	ND
4-9-93	A#53	22.2	77.8	1400ppb
4-15-93	A#53	12.05	87.95	NC

Date	Sample ID	Sr 86	Sr 88	
4-8-93	#56PR	22.3	77.7	NC
4-9-93	#56PR	26.8	73.2	1500ppb

NC - not calculated

Figure 7

Isotope Production via Cold Nucleosynthesis: Rubidium Series
(Cell 53)

Mass Number (A)	Nuclides Synthesized	Net number of Nuclei Synthesized x 10^{16}	Total Energy Released (MeV x 10^{17})
86	$_{38}Sr^{86}$	1.34	1.29
87	$_{38}Sr^{87}$	19.25	33.30
88	$_{38}Sr^{88}$, $_{39}Y^{88}$(108D), $_{40}Zr^{88}$(88D)	0.52	0.55
89	$_{39}Y^{89}$	1.66	4.6
90	$_{40}Zr^{90}$	0.28	1.1
91	$_{41}Nb^{91}$	3.00	12.1
92	$_{42}Mo^{92}$	(small)	(small)
93	$_{42}Mo^{93}$	27.03	148.10
94	$_{42}Mo^{94}$	0.23	1.43
95	$_{42}Mo^{95}$	(small)	(small)
96	$_{44}Ru^{96}$, $_{43}Tc^{96}$(4.35D)	(small)	(small)
97	$_{43}Tc^{97}$, $_{44}Ru^{97}$(2.9D)	(small)	(small)
98	$_{44}Ru^{98}$	(small)	(small)
99	$_{44}Ru^{99}$, $_{45}Rh^{99}$(16.1D)	(small)	(small)
100	$_{45}Rh^{100}$, $_{46}Pd^{100}$(4D)	0.30	3.90
101	$_{44}Ru^{101}$, $_{45}Rh^{101}$(3y)	3.70	41.30
102	$_{45}Rh^{102}$, $_{46}Pd^{102}$	1.21	14.50
103	$_{45}Rh^{103}$, $_{46}Pd^{103}$(17D)	1.40	17.80
104	$_{46}Pd^{104}$	0.54	7.30
105	$_{46}Pd^{105}$, $_{47}Ag^{105}$(40D)	(small)	(small)
106	$_{46}Pd^{106}$, $_{48}Cd^{106}$	(small)	(small)
107	$_{47}Ag^{107}$	0.54	7.30
108	$_{48}Cd^{108}$	0.23	3.90
109	$_{47}Ag^{109}$, $_{48}Cd^{109}$(453D)	2.25	39.70
110	$_{48}Cd^{110}$	(small)	(small)
111	$_{48}Cd^{111}$, $_{49}In^{111}$(2.8D)	(small)	(small)
112	$_{50}Sn^{112}$	2.25	44.60

Sums: 65.73 x 10^{16} **384.17**   x

10^{16} MeV

Estimating a ten percent error, then, the total energy to produce the above based upon the LANT Model is approximately $(3.8 \pm 0.4) \times 10^{19}$ MeV versus the total excess heat

determined from calorimetry for Cell 53 of $(4.0 \pm 0.8) \times 10^{19}$ MeV.

Figure 8

Lattice-Assisted Nucleosynthesis: Rubidium Series

Figure 9

Radioactive Decay of Cell 71 Cathode

Y-axis: Decay Count (10^6/24 hrs)
X-axis: Time (Days)

Figure 10

Semi-log Plot of Decay Count vs Time

y = 3.2902 - 0.18001x   R^2 = 0.777

Half-life: T= (0.693/0.1800) = 3.8 Days

Y-axis: Ln(Decay counts 10^6/24 hr))
X-axis: Time (Days)

Figure 11

Semilog Plot: Decay Count vs. Time (Days)

$y = 3.0884 - 0.19145x$ $R^2 = 0.990$

Half-life: $T = (0.693/0.1945) = 3.6$ Days

Figure 12

Average Half-life vs Channel Number

Radioactive decay
Cell 71 postrun cathode

INVESTIGATION OF LOW LEVEL TRITIUM GENERATION IN Ni -H$_2$O ELECTROLYTIC CELLS

T. K. SANKARANARAYANAN

M. SRINIVASAN[t]

M. B. BAJPAI

D. S. GUPTA

- -

Chemical Engineering Division

[t]Neutron Physics Division

B.A.R.C — BOMBAY - INDIA

SUMMARY OF BARC TRITIUM
134 # RESULTS (NAGOYA PROCEEDINGS)

Table II. Other Excess Heat and Tritium Experiments.

Srl No.	Expt. No.	Cathode	Alkali	Solvent	Excess Power (%)	Tritium Level (Bq/ml)
1	NtPD–1	Solid Ni	K_2CO_3	25% D_2O	< 5%	88
2	NtPD–2	Por. Ni	K_2CO_3	H_2O	65%	NIL
3	NtPD–3	Solid Ni	Na_2CO_3	25% D_2O	72%	NIL
4	NtPD–4	Solid Ni	Li_2CO_3	H_2O	68%	NIL
5	TiB–1	Ti Button	Li_2CO_3	H_2O	10%	205
6	TiB–2	Ti Button	Li_2CO_3	H_2O	10%	124
7	TiF–1	Ti Foil	LiOD	D_2O	*	147
8	KSR–1	Por. Ni	K_2CO_3	H_2O	*	NIL
9	FP–1	Por. Ni	K_2CO_3	H_2O	*	310
10	OM–1	Por. Ni	K_2CO_3	25% D_2O	*	74
11	OM–3	Por. Ni	$^6Li_2CO_3$	H_2O	*	223

* Not measured

Table III. Variation of Tritium Level (Bq/ml) in
Cells B3, B4 and B5 (Porous Ni Cathode).

Cell #	B3	B4	B5
Alkali	Li_2CO_3	Li_2CO_3	Li_2CO_3
Enrichment of Lithium	54%	7% (natural)	54%
Solvent	50% D_2O	50% D_2O	100% D_2O
12th day	28.8	28.6	61.6
16th day	64.1	30.6	79.2

(Reverse electrolysis done for 4 days)

19th day	36.8 *	56.9	53.8 *
33rd day	513	69	193

* Note 'T' Level has decreased
before rising again

3-2

OM3:TRITIUM BUILD-UP:SEPT.5 TO OCT.6,92
ENRICHED Li2CO3 (54%) IN H20;POROUS Ni

TRITIUM LEVEL IN Bq/ml

3-3
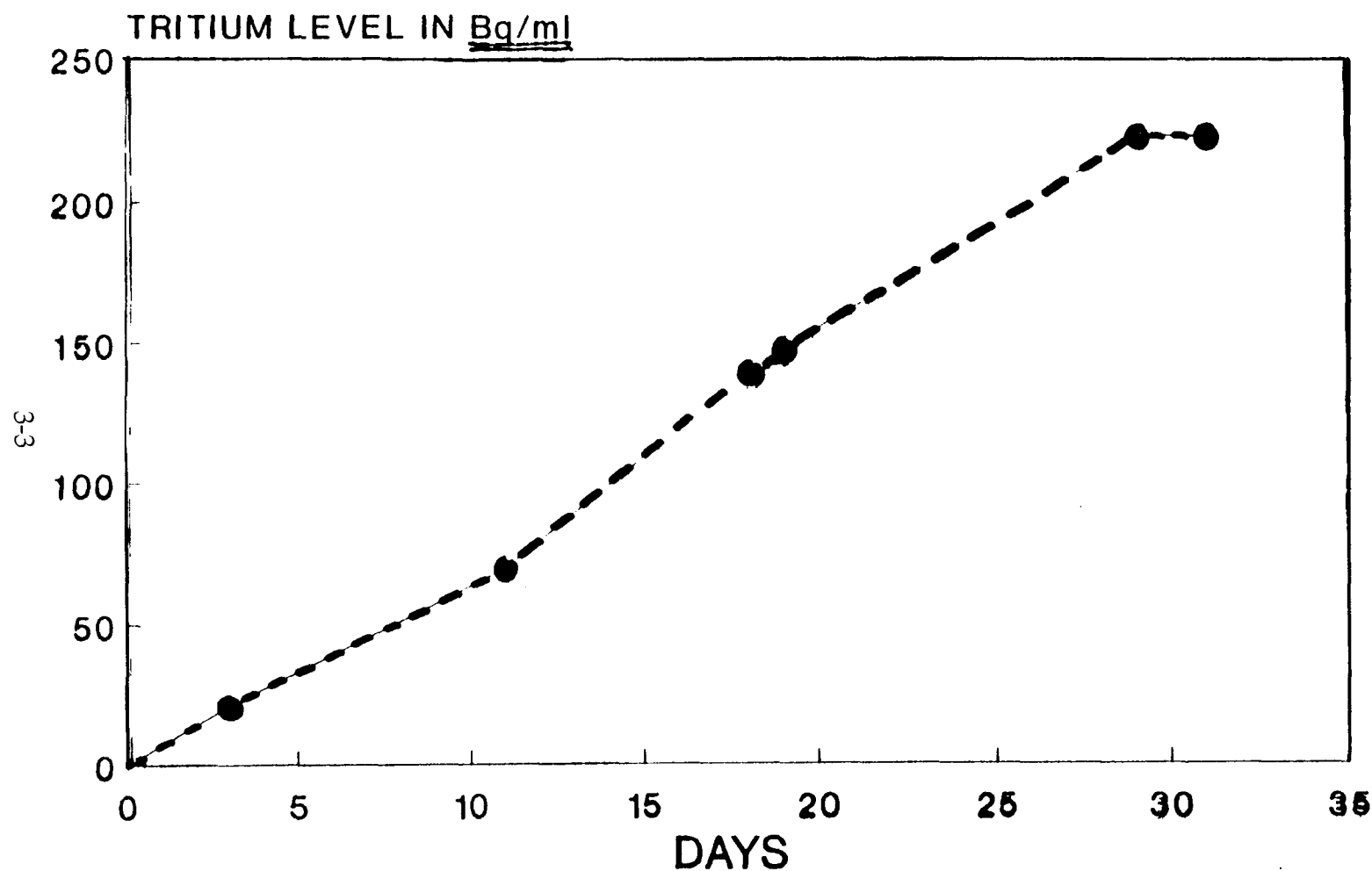
[FIG. 8 , Page 138 , Nagoya Proc.]

TRITIUM BUILD-UP IN CELL # OM-3

SINTERED POROUS Ni " (INAYAR)"

$0.1M \ Li_2CO_3$ IN H_2O

(SEPT 5th TO NOV 9th 1992)

	DAYS OF OPERATION	TRITIUM LEVEL (Bq/ml)	Recombined H_2O
5th sept 92	0	BKG COUNTS	
	3	21 ⟶	42.3 Bq/ml
	11	70	
	18	139	
	19	148	
	29	223	
6th oct 92	31	213	
	....	....	
9th oct 92 →	34	151	
	37	184	
	46	241	
	54	188	
	58	220	
9th Nov 92 →	65	166	

TRITIUM LEVEL FLUCTUATIONS
IN CELL OM-3
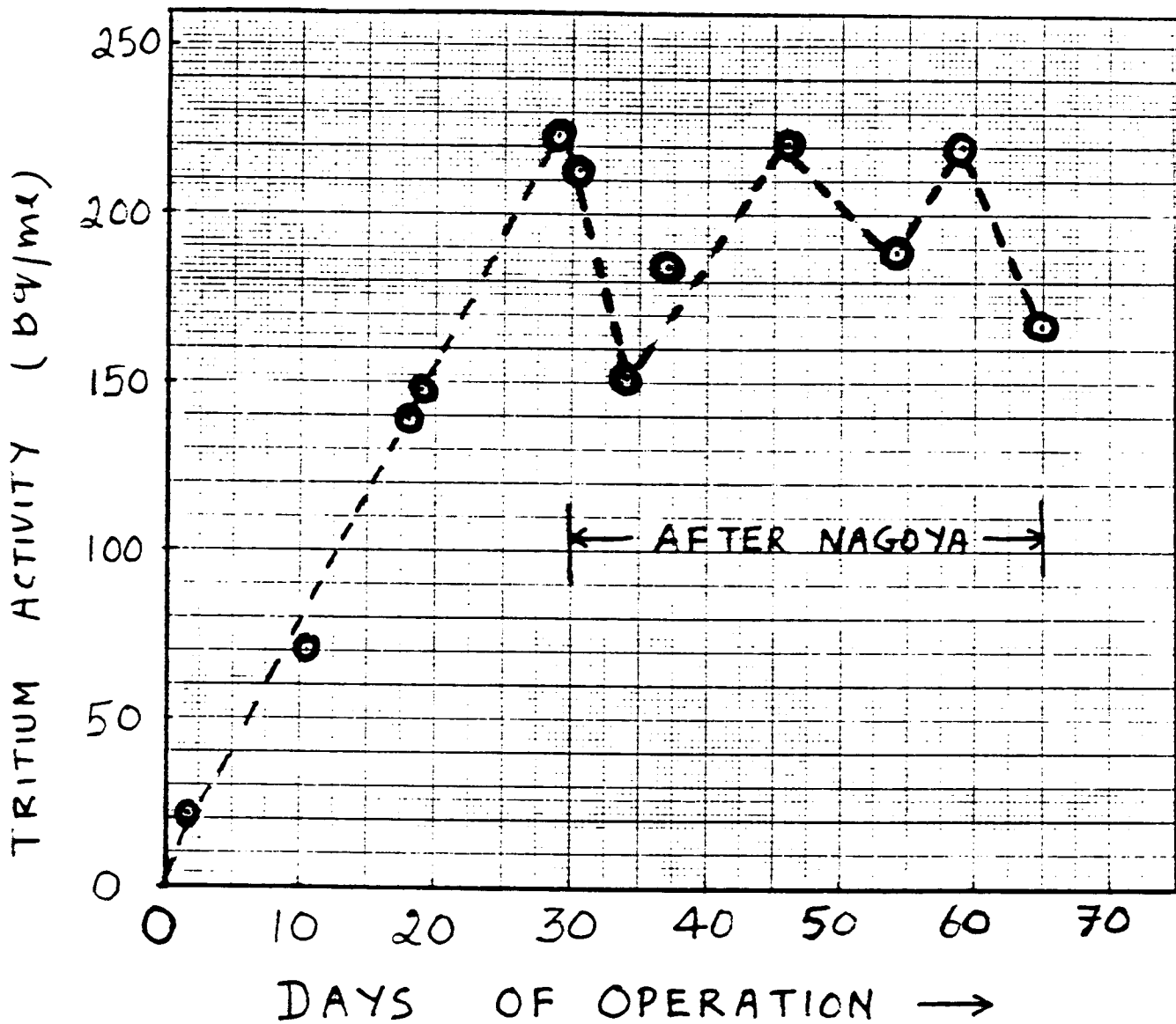
STABILITY DATA

DATE (1993)	BACKGROUND ← COUNTS PER	STANDARD (~2300 dpm/m) SOURCE COUNTS 3 MINS →
AUG 19th	75	1680
20th	84	1644
23rd	72	1566
24th	72	1539
SEP 1st	70	1539
6th	81	1533
7th	75	1629
8th	79	1560
13th	70	1539
21st	72	–
22nd	72	–
23rd	72	–
28th	73	–

EXCESS OVER BACKGROUND ⇩

AVERAGE : 3 MIN → 79.5   1605 ± 3%   1525/.

9 MIN : **238**   **4815**   4577/.

⇩

~ 110 dpm/mℓ equivalent .

CELLS OPERATED SPECIFICALLY TO STUDY TRITIUM LEVEL VARIATIONS

(JUNE – SEPTEMBER 1993)

AFTER PROCURING DEDICATED COUNTING UNIT

S.No.	CELL #	VOL.	ALKALY-SOLVENT	ELECTRODE	DAYS OF OP^N	MAX. T LEVEL
1	OM-5	100 mℓ	Li_2CO_3* H_2O	Nayar Ni	54	NIL
2	OM-6	100 mℓ	Li_2CO_3* H_2O	Totlani Ni	44	NIL
3	OM-7	100 mℓ	Li_2CO_3 25% D_2O	Nayar Ni	64	~2.6 Bq, (153 dpm/ℓ
4	OM-8	100 mℓ	Li_2CO_3 "	Bush Ni	54	NIL
5	OM-9	50 mℓ	Li_2CO_3 H_2O **	Nayar Ni	46	~3.2 Bq/ℓ (188 dpm/m
6	OM-10	20 mℓ	LiOD D_2O	Pd tube	17	NIL

* Enriched ^6Li (54%)

3-7

** Used in an earlier experiment and

TRITIUM IN CELL # OM-7 (100 ml)

POROUS Ni - Pt WIRE

ENRICHED (54%) Li_2CO_3 IN H_2O (0.1M)

(8th JULY TO 9th SEPT 1993)

DAYS OF OPERATION	RAW COUNTS PER 9 MINS (AVG. OF 3)	TYPICAL BKG - AVG COUNTS PER 9 MINS
1	260	
2 → 3 [RECOMBINED WATER]	316 @ → [360]	
12	542	
16	381	
19	310	
29	503 *	(238)
36	377	
39	376	
48	364	
54	390	
64	332	

@ corresponds to ~ 153 dpm/ml

* corresponds to ~133 dpm/ml

TRITIUM LEVEL VARIATION
IN CELL # OM-7

3-9
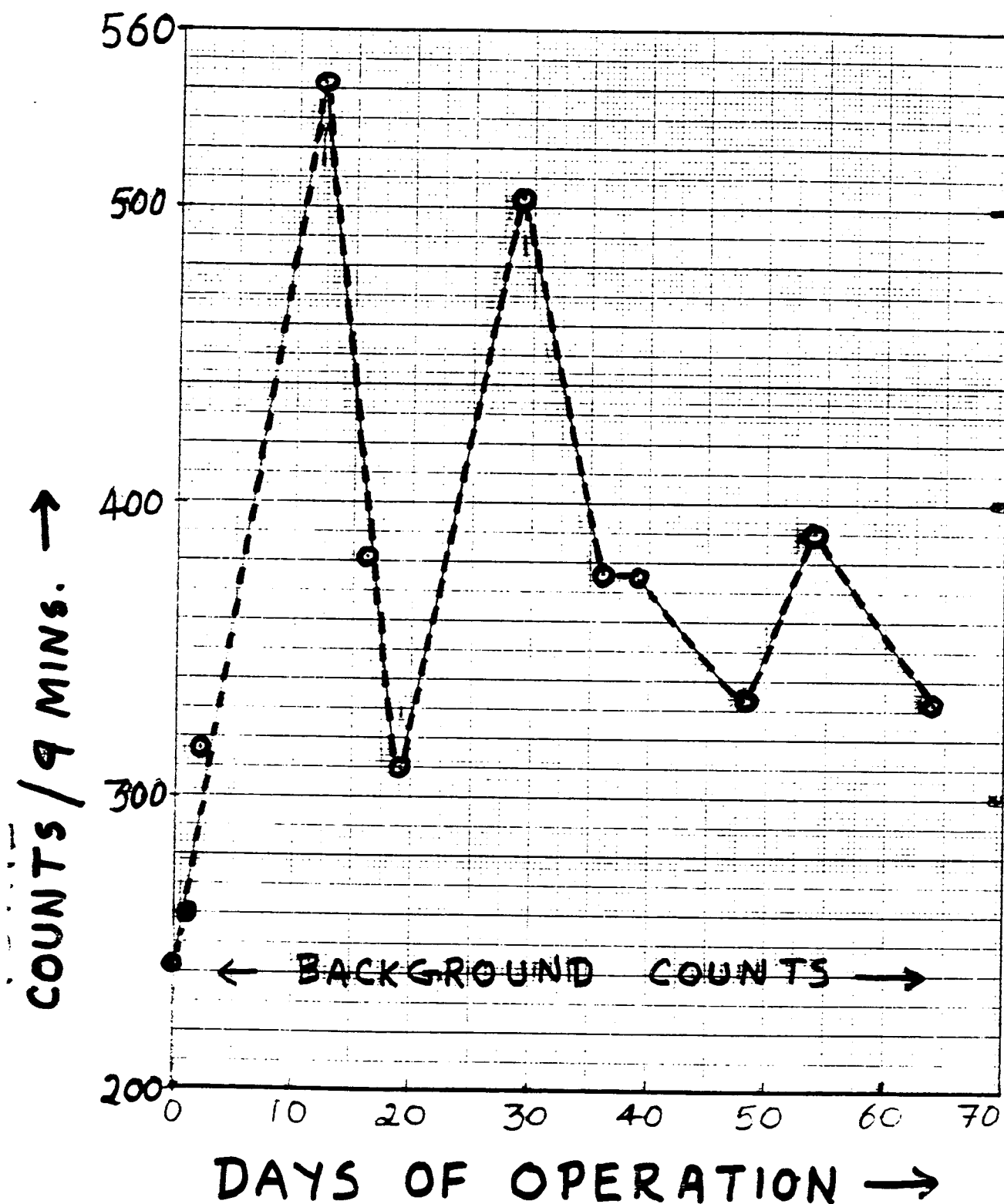
TRITIUM LEVEL VARIATION IN CELL#OM-9

SINTERED POROUS Ni — Pt WIRE

NAT. Li_2CO_3 IN H_2O (<u>USED</u> <u>EARLIER</u>)[*]

(30th JULY to 7th SEPT 1993)

DAYS OF OPERATION	COUNTS PER 9 MINS	BKG CTS PER 9 MIN
0	460[*]	
7	298	
13	252	
20	217	
26	240	
28	430	238
31	(613)[@]	
33	494	
35	484	
38	438	
41	386	
46	431	

@ corresponds to ~ <u>188</u> dpm/e

[*] Note that in this cell the electrolyte already contained some tritium ($110 \frac{dpm}{M}$

VARIATION OF TRITIUM ACTIVITY

IN CELL # OM-9
(23rd JULY TO 7th SEPT 1993)

TOTAL COUNTS PER 9 MINS →

DAYS OF OPERATION →
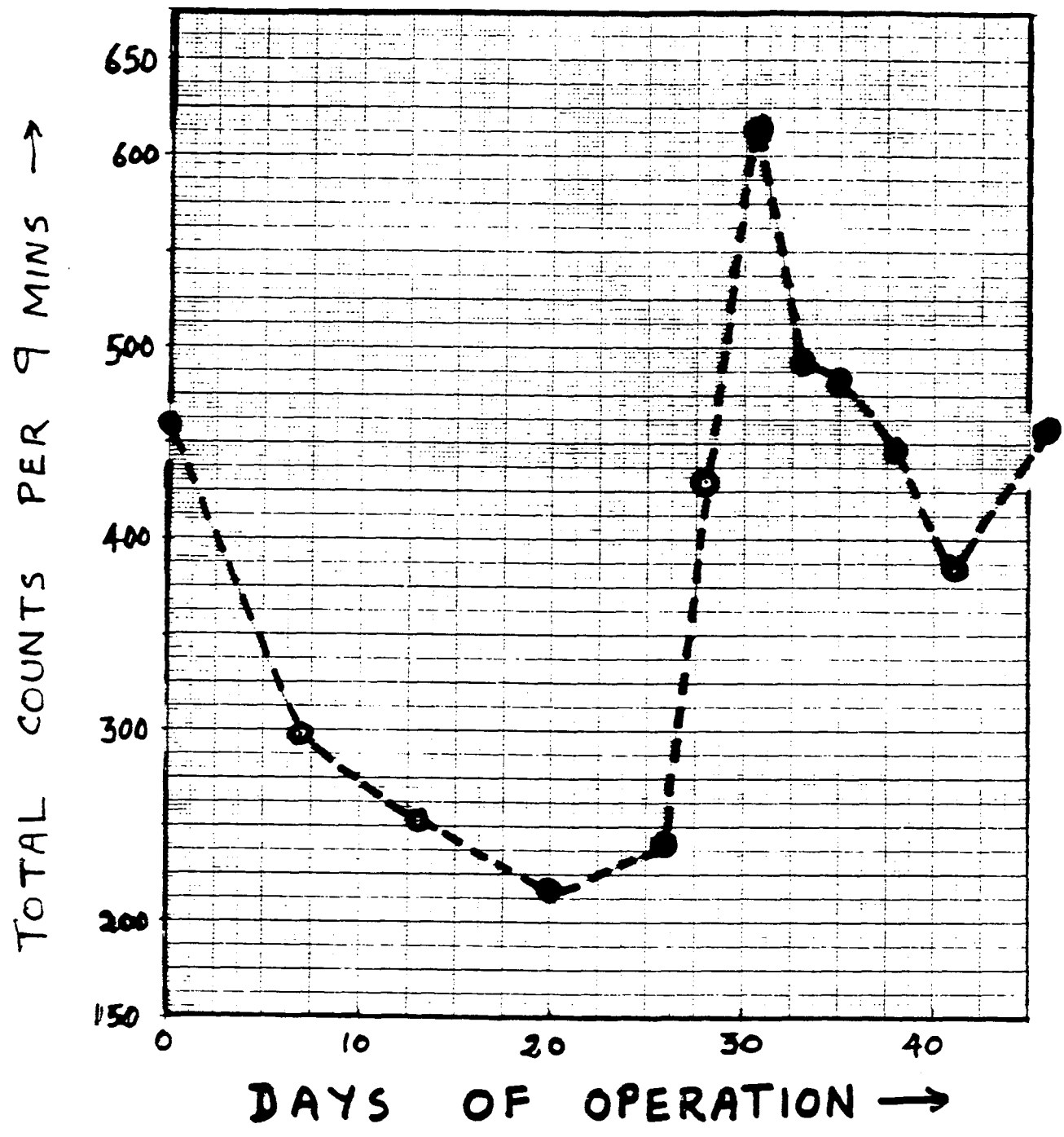
OBVIOUS QUESTIONS

CONTAMINATION ?

· Many cells show no "T"
Leaching from Ni/Glass etc

· Ni peice dissolved & counted
→ NIL

"TROMBAY AIR IS FULL OF T ?"

"Cold strip" technique routinely
used to condense & count
→ < 0.1 Bq/ml

(Health Physics dept.)

Cross Contamination during
distillation / counting ?

− samples from same cell
analysed by two different
groups −

− Also repeat samples from
same cell
⌐ Within 10% − same resul

SUMMARY AND CONCLUSIONS

- 10 out of **23** (~**40%**) Ni–H_2O cells analysed have shown tritium

- No preference seen w.r.t. electrolyte type, H_2O vs D_2O, Nat.Li vs enriched Li, type of Ni cathode etc for "T" production

- Maximum amount of "T" measured in Post Nagoya experiments ~**200** dpm/ml (3·5 Bq/m

- Electrolytic enrichment of the TRITIUM isotope cannot account for this because of low currents, above ambient temperature and addition of make up water frequently.

- Tritium activity of electrolyte seems to oscillate in an erratic saw tooth type fashion. Close examination of sampling/ distilling/ counting technique in conjunction with several auxiliary measurements strongl Suggests that "T" level actually varies — It

3-13

- While a sudden - sharp increase in
  tritium level can be understood
  as a production (burst) phase (5~10 days,
  30 days in OM-3), the decreasing phase
  (lasting again for 5~10 days; upto 27
  days in OM-9) is difficult to understand.
  Electrolysis can not account for it.
  (critics please make up your mind:
  you cant invoke contamination and
  electrolytic enrichment to explain
  this decrement!)

- We are forced to conclude that there
  is a strong as yet unidentified
  mechanism cleansing the electrolyte
  of tritium periodically. It could be
  electrochemical in nature — absorption/
  desorption — But this implies preferential
  migration - absorption of T over H - an
  idea not easily acceptable. Alternative:
  nuclear?

DEUTERIUM ABSORBABILITY AND ANOMALOUS NUCLEAR EFFECT OF YBCO HICH TEMPERATURE SUPER-CONDUCTOR

JIN Shang-xian, ZHAN Fu-xiang and LIU Yu-zhen
Graduate School, University of Science and Technology of China, P.O.Box 3908, Beijing 100039, PRC

Abstract

The experimental sutdies of YBCO−D system indicated that YBCO high temperature super-conductor (HTSC) was shown to have a similar effect on deuterium absorbability and anomalous nuclear effect like palladium[1]. We found that $Y_1Ba_2Cu_3O_{7-\delta}$ could absorb deuterium at normal temperature and forms $D_xY_1Ba_2Cu_3O_{7-\delta}$. We also found that the deuterated YBCO could produce high energy charged particles far larger than background. The influence of the absorbed deuterium on the characteristics of YBCO HTSC and the mechanism of the anomalous nuclear effect are not clear and needed to be further studied.

INTRODUCTION

It has been found[2-4] that $Y_1Ba_2Cu_3O_{7-\delta}$ high temperature super conductor has an unusual property of absorbing hydrogen. The absorption process could be expressed by a general equation:

$$(x/2)H_2 + Y_1Ba_2Cu_3O_{7-\delta} \longrightarrow H_xY_1Ba_2Cu_3O_{7-\delta}.$$
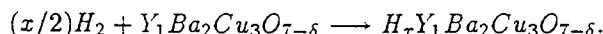
The structural analysis indicated that the absorbed hydrogen is located on the Cu−O surface[5] and the state of the hydrogen changes with temperature, etc.. As an isotope of hydrogen, deuterium should have similar effect. So we were engaged in an experimental study on absorbability of deuterium by $Y_1Ba_2Cu_3O_{7-\delta}$ HTSC at normal temperature. Here we report some experimental results on deuterium absorbability of YBCO HTSC and anomalous nuclear effect occurred during the absorbing process.

EXPERIMENTAL

In this experiment the YBCO HTSC sample was prepared by a new technology[6] that high speed direct combine of Y_2O_3, Ba_2 and CuO which were made up on 1, 2 and 3 weight. The zero resistance temperature of the sample was 90^0K. The experimental

system is sketched in Fig.1. The $Y_1Ba_2Cu_3O_{7-\delta}$ pellet or powder was put on the frame in the vacuum chamber. The CR-39 nuclear track etch detectors which are used to detect charged particles were placed around the sample. The chamber was evacuated to about 10^{-3} torr and then filled with 99.8% purity deuterium of ~ 1 atm. About 1 or 2 days after the CR-39 were taken out and etched and observed in the microscope.
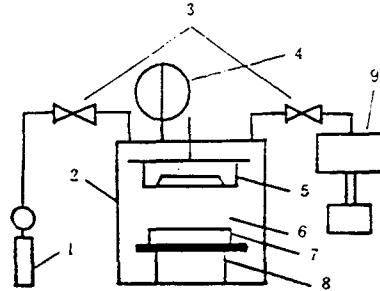
Fig.1. Experimental set up.

1. D_2 tand, 2. Vacuum chamber
3. Valves, 4. Vacuum gage
5. Au-Si surface-barrier
6. YBCO HTSC sample, 7. CR-39
8. Sample frame
9. Vacuum pump

RESULTS AND DISCUUSSION

The specific property of deuterium absorption by the YBCO HTSC in the normal temperature is shown in Fig.2. The content ratio of deuterium in $D_xY_1Ba_2Cu_3O_{7-\delta}$ was about $x\sim 0.2$. Fig.3 shows a photo of nuclear tracks on the CR-39. The net number density of the tracks after subtracting the background was $\sim 3x10^5/cm^2$. The statistical distribution of the tracks with circular surface mouth on the CR-39 which were produced by the vertically incident particles is shown in Fig.4. For comparison, the statistical distribution of the tracks with circular surface mouth on the CR-39 which were produced by the vertically incident α-particles from standard[241] Am α-source is shown in Fig.5. Comparing the Fig.4 and Fig.5, we can see that the deuterated YBCO HTSC could produce high energy charged particles with several kinds or/and with different energies. The control experiments were performed without filling deuterium and no any anomalous effects were found. Further study is needed for identifying the particles and measuring the energy distribution.

Time(day)
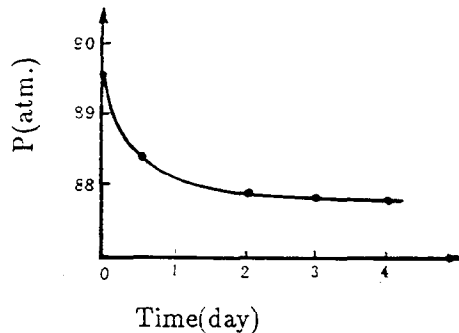
Fig.2. The specific property of deuterium absorption by an YBCO HTSC .
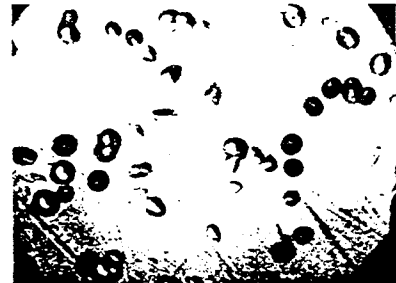
x 400

Fig.3. A photo of nuclear tracks on the CR-39 produced by $D_xY_1Ba_2O_{7-\delta}$
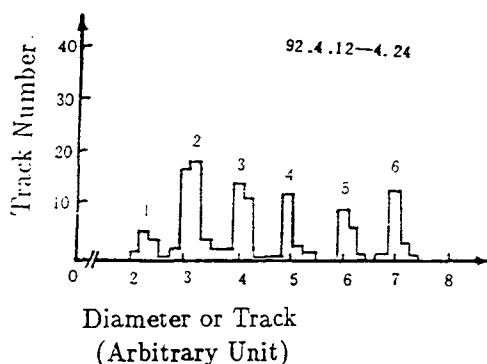
Fig.4. Statistical distribution of the
tracks with circular surface mouth
on the CR−39 produced by vertically
incident particles.
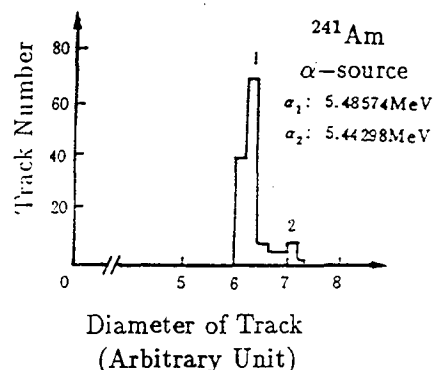
Fig.5. Statistical distribution of the
tracks with circular surface mouth
on the CR−39 produced by standard
^{241}Am α−source.

CONCLUTION

The YBCO high temperature super-conductor could absorb deuterium at normal temperature and forms $D_x Y_1 Ba_2 Cu_3 O_{7-\delta}$. The deuterated YBCO HTSC could produce high energy charged particles far larger than background. The mechanism of the anomalous nuclear effects and the influence of absorbed deuterium on the characteristics of YBCO HTSC are not clear and needed to be further investigated.

REFERENCES

1. S.X.Jin et. al., Proceedings of the II Annual Conference on Cold Fusion, Como, Italy, 145(1991).
2. J.J. Reilly et al., Rev., B36. 5694(1987).
3. C.Y.Yang et al., Phy. Rev., B36. 8798(1987).
4. T.Kato et al., Jpn. J. Appl. Phys., 27, 2564(1988).
5. H.Niki et al., Solid State Comm., Vol. 69, 547(1989).
6. W.Q.Shi et al., Proceedings of the National High Temperature Super-cnductor Meeting, Hefei, China(1991).

The influence of conductivity on neutron generation process in proton conducting solid electrolytes.

A.L. Samgin, A.N. Baraboshkin, I.V. Murigin,
S.A. Tsvetkov, V.S. Andreev, S.V. Vakarin.

Institute of High-Temperature Electrochemistry
Russian Academy of Science, Ekaterinburg, RUSSIA, 620219.

Abstract

It is mentioned, that the nature and the mechanism of conductivity and the existence of multilayered structures with different conductivity types in solids appears to be the additional critical conditions of abnormally increased rate of nuclear-electron reactions in solid state-deuterium system.

Introduction

Anomalous nuclei-electron phenomena, including cold fusion process, accompanied with neutrons or gamma-quantum generation are observed in solids, which have different conductivity nature: metals[1,2], oxide bronzes[3], KH_2PO_4-type segnetoelectrics[4], heavy ice[5], solid proton conducting electrolytes[6]. Therefore the investigations of phase transformation influence on the process of neutron generation, resulted conductivity mechanism change or even the conductivity type transformation are very important.

In this paper we tried to look over the anomalous nuclear effects from the protonic conductivity point of view. Actually all the materials from the papers listed before are protonic conductors. This papers, except the works on the base of metals, one would think with quite different materials are unificated on the base of deuteron conducting electrolytes. It's true, that heavy ice, KH_2PO_4 in paraelectric phase are low-temperature protonic conductors, with relatively small electric conductivity. In ice the proton is moving along a chain of H_2O. It is characteristic, that KH_2PO_4 – crystal is low-temperature protonic conductor, with intrinsic structures irregularities having the spasmodically conductivity change during phase transformation at definite temperatures. Oxide bronzes of transition metals are one of the type of superionic crystals with high protonic mobility and oriented movement along channels in the lattice. Finally, some high-temperature solid electrolytes possesses large deuteronic conductivity. Quick deuteronic transport at temperatures in range of 600°-900° C is possible to them, but the spasmodically conductivity change didn't observed.

Results and discussion

Among the following electrolytes the last ones with
perovskite-like structure have high protonic conductivity in
deuterium atmosphere and as for perovskite-proton conductive
electrolytes on the base of doped $SrCeO_3$. It's especially
significant, that the proton conductivity in them is not mask
over the conductivity background on the other ions. Moreover, the
proton nuclei in them is transported as an individual particle-
H^+ ion. That's so, on the base of criteria of appreciable
protonic conductivity it is possible to determine (as
experimentally revealed) the class of materials, optimal to
nuclei-electronic phenomena investigations. In this case the only
difference in above mentioned experiments will be the way of
external energy admission to deuterons. It takes place during
mechanical distortion of heavy ice, segnetoelectric-superionic
conductor phase transformation in KH_2PO_4 crystal, hydrogen gas
saturation of near-surface structures in oxide bronzes in which
the spatial conductivity channels are made by electrochemical
treatment, and during long strontium cerate electrolysis.

Let us mention, that with the criteria described above some
other conditions, which are necessary to cold fusion existence,
have a good corellation. We'll note two of them:
- first-the formation during deuterium saturation of solids with
nonlinear properties in strongly nonequilibrium conditions of
local zones with sufficiently increased deuteron to lattice atoms
ratio (at the first time this hypothesis was spoken out by Tsarev
V. et al[8]. The theoretical basis of this effect during
electrolysis and from the gas-phase saturation was made in our
previous paper[7]);
- second-the high transport speed and the oriented nuclei
movement. Since the proton conductivity is calculated from proton
concentration and proton mobilities and suggested spatial or
energy channel existence, the view on current problem seems to be
correct.

Another important feature for anomalous nuclei effect's
investigations in deuterium-solid system is the problem of making
clear the question of phase boundary and heterostructures with
different conductivity types role. In dependence of stoichiometry
composition oxide bronzes possess both metal and semiconductor
conductivity type. In paper[2] before deuterium intercalation the
stretching of sodium ions took place. Decreasing of alkali metal
concentration and the replacement of such atoms by hydrogen
isotopes near the surface resulted in the formation of thin layer
with semiconductor conductivity type. To obtain neutron
generation the removal of sodium ions took place[2]. The hypothesis
of formation of regions with dielectrical properties in Pd was
already discussed[8]. The additional factor is the electrical
current which flow throe phase boundary during electrolysis.
This peculiarities of conductivity nature may also related with
mechanism which have "a common origin" in "electromagnetic
current behavior in dense media" and in the process of "capillary
fusion" in special structures with channels[9].

In our experiments with barium and strontium cerate the
correlation between neutron generation and the sample's
conductivity was observed.

Detailed description of experimental method and apparatus was
presented in ref[6] (in paper presented on the Fourth International
Conference on Cold Fusion, December 6-9, 1993, Hyatt Regency
Maui, Lahaina, Hawaii). The sample was made as a heterostructure

from a doped strontium cerate ceramics or barium cerate ceramics disk covered with porous metallic electrodes. The cell's construction and the installation which the sample was placed on, permits to make both gas pumping out and electrolysis with increased deuterium pressure with the sample's heating or cooling in the same time (fig.1).

During definite time the sample was under electrolysis treatment at temperature 750° C after which thermocycling was made in temperature range from 800° till 400° C with electrolysis in the same time (the typical change of temperature and electrolysis current presented on fig.).

At this process some single neutron bursts which prolonged a few seconds were observed, when the electrolysis was conducted more then twenty four hours. They were detected both in process of increasing the sample's temperature and during electrolysis current rasing and at the sample's temperature decreasing.

Neutron emission only observed at temperatures related to high sample's protonic conductivity. In the case of the highest deuterium pressure in cell (3 atm.) and the sample's thermocycling without electrolysis it was founded the sample's reduction accompanied turning the sample blackening. As the result of the reduction process is change the sample's conductivity to n-type electronic conductivity. A neutron emission usually is over when reduction process is completed and it suppose to be related to type of conductivity change from electronic/cationic to pure electronic. This phenomena was observed both on barium and on strontium cerate.

Deuteron conductivity of the high temperature electrolyte based on the doped strontium cerate is changing as an exponential function. During this conductivity change initiated by temperature change of the ceramic sample with predetermined speed was discovered enough intensive neutron burst. It was correlated with strictly specified ceramic temperature which was measured by thermocouple placed near the sample at 3 mm distance. These neutron burst where reproduces in three times on the same sample during the experiments before it's degradation (fig. 3). On fig.3 it is shown the most severe first burst, every following burst had the obviously expressed damping nature as the temperature raise near the sample's surface accompanied the appearance of .neutron impulses. On the same fig. it is shown the spontaneous deuterium gas pressure change in cell. The excess of pressure and temperature are correlated in time with neutron bursts.

We compared the results of the analysis of the sample before and after saturation by deuterium during electrolysis and thermocycling in the increased temperatures. It was discovered the an existence of unmovable structure changes. The sample's degradation is reflected in the simultaneous neutron burst decreasing and further cessation it's emission.

Conclusions

Our experiments have shown the main condition of a neutron emission is an existence of ion (proton) conductivity in cerate channels. Appearance of an electron conductivity with reduction of ceramic resulted by neutron emission cessation.

Obviously the nature and mechanism of conductivity and the existence of multilayered heterostructures with different conductivity type are an additional critical condition of essential increasing of speed and the intensity of electron-

nuclei reactions in   solid state/deuterium system.

References

1. M. Fleischmann and S. Pons."Electrochemically induced nuclear fusion of deuterium". Electroanal. Chem. Vol. 261, p. 301 (1989).

2. S.E. Jones, E.P. Palmer, J.B. Czirr et al. "Observation of cold nuclear fusion in condensed matter". *Nature*. Vol.338., N 6218, p. 737 (1989).

3. K. Kaliev, A. Baraboshkin, A. Samgin et al. "Reproducible Nuclear Reactions during Interaction of Deuterium with Oxide Tungsten Bronze. Phys. Lett. A. Vol. 172, p.199 (1993); *Frontiers Science,* Series No. 4, *Tokyo Proc. of ICCF-3:* Universal Academy Press, 1992, pp. 241-244.

4. A. Lipson, D. Sakov, U. Kalinin et al. Pisma v zhyrnal tekhnicheskoi fiziki. Vol. 18, N 16, p. 52 (1992) (in Russian).

5. V. Kluev, A. Lipson, Yu. Topornov et al. Pisma v zhyrnal tekhnicheskoi fiziki. Vol. 12, p. 1333 (1986) (in Russian).

6. A. Samgin, A. Baraboshkin, V. Andreev et al. "Neutron generation in the solid protonic conductors with perovskite-type structure". Paper N2.7, presented at the ICCF-4, Hawaii (December 1993).

7. A. Samgin, V. Tsidilkovski and A. Baraboshkin. "On the possible formation of regions with high hydrogen isotope concentration at nonlinear diffusion in transition metals". Proc. All-Union Workshop "Chemistry and Technology of Hydrogen". Zarechny, USSR. November 1991, p.30; Paper presented at ICCF-3, Japan, Abst. of ICCF-3, p.39 (October 1992).

8. V. Tsarev. "Cold fusion". Uspekhi fizicheskih nauk. Vol. 160, p. 1 (1990) (in Russian); *"Cold Fusion Researches in Russia".* *Frontiers Science,* Series No. 4, *Tokyo Proc. of ICCF-3,* Universal Academy Press, 1992, p. 341-351.

9. J. Vigier. "New Hydrogen Energies in Specially Structured Dense Media: Capillary Chemistry and Capillary Fusion". *Frontiers Science.* Series No. 4, *Tokyo Proc. of ICCF-3,* Universal Academy Press, 1992, p. 325-336.
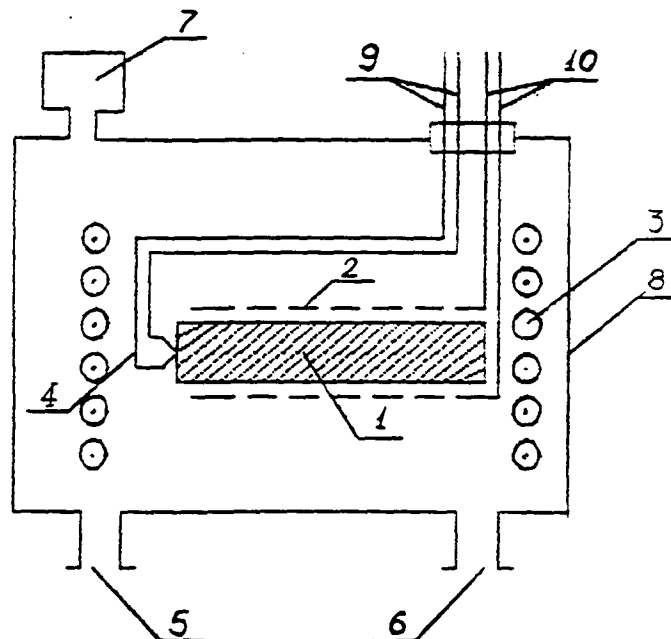
1. Working element.
2. Sample's porous cover.
3. Cylindrical heater.
4. Thermocouple.
5. ... to the vacuum pump system.
6. Deuterium flow.
7. Vacuum gage.
8. Vacuum cell.
9. ... to temperature gage.
10. Current lead to the sample.

High-temperature electrolysis cell with solid electrolytes.

fig 1
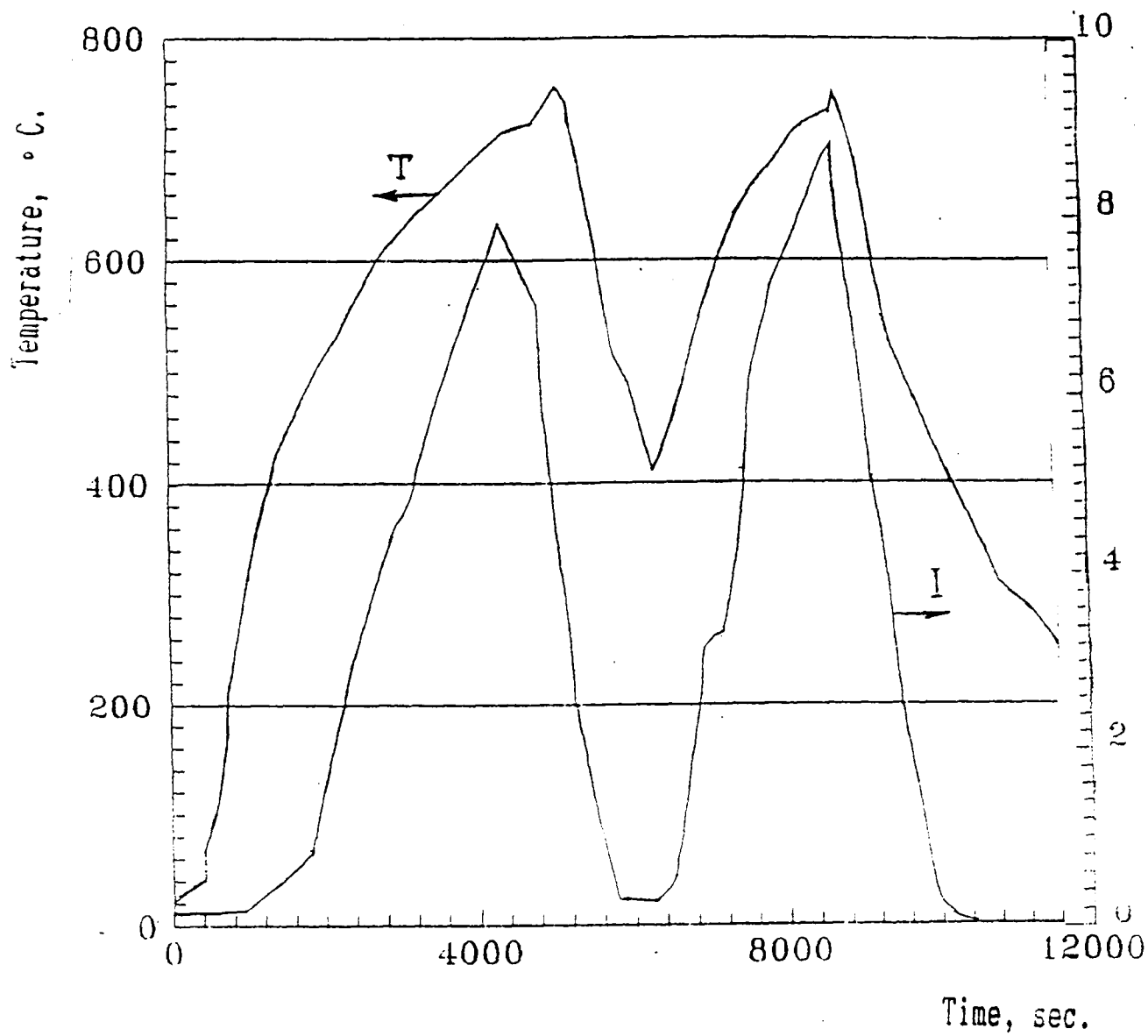
Dependence temperature and current at termocycling

Fig 2
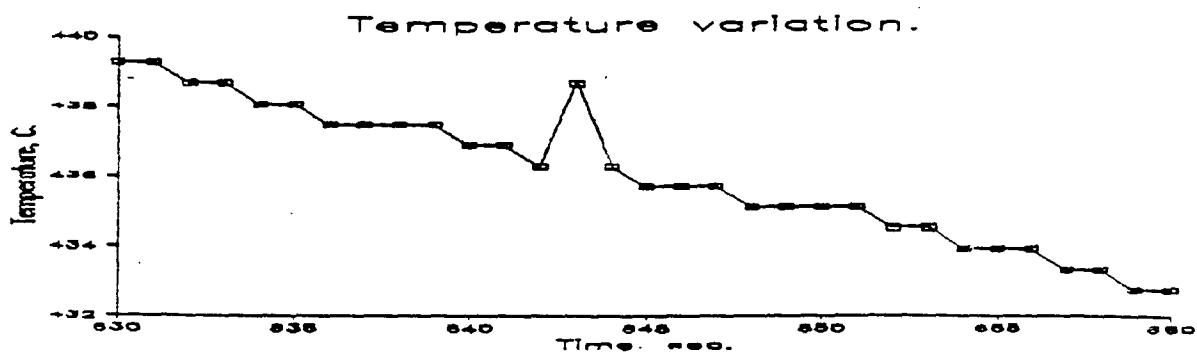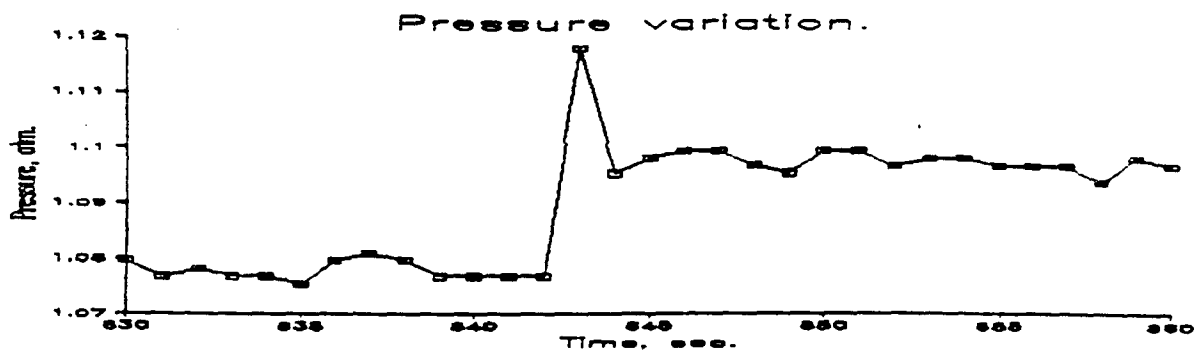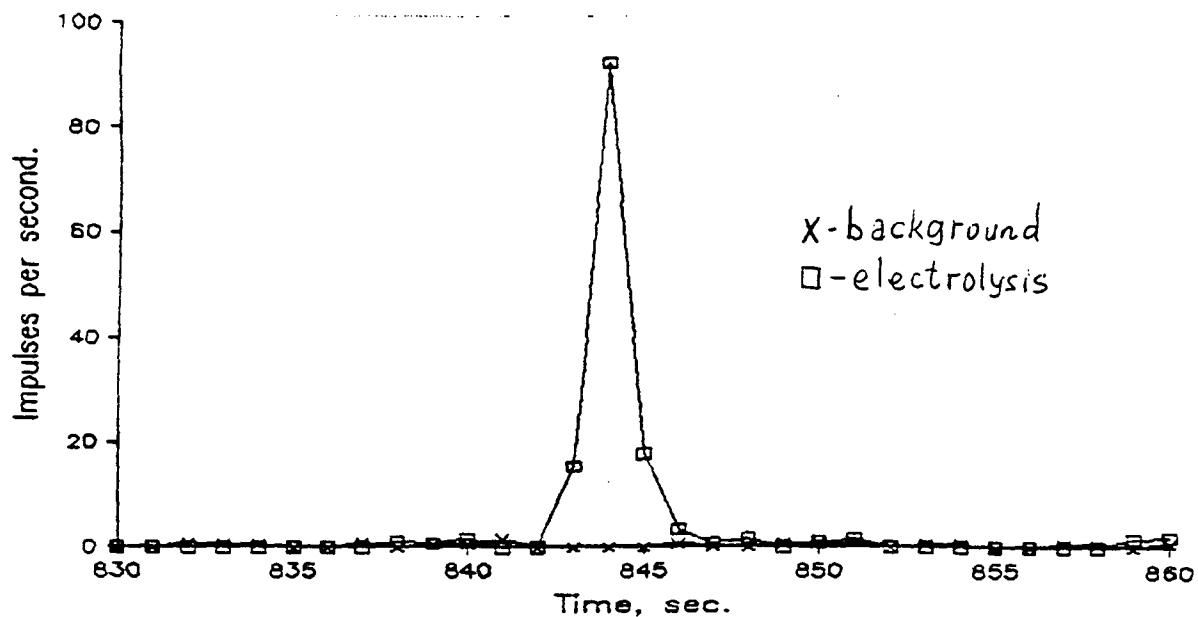
Neutron burst during solid electrolyte
thermocycling and electrolysis.

Particle Acceleration and Neutrons Emission in a Fracture Process of a Piezoelectric Material

T. SHIRAKAWA

Department of Social Information Processing,

Otsuma Women's University,

Karakida, Tama, Tokyo 206

M. FUJII, M. CHIBA, K. SUEKI, T. IKEBE,

S. YAMAOKA, H. MIURA, T. WATANABE,

T. HIROSE, H. NAKAHARA

Faculty of Science, Tokyo Metropolitan University,

Minamiohsawa, Hachioji, Tokyo 192-03

M. UTSUMI

Faculty of Engineering, Tokai University,

Kitakaname, Hiratsuka, Kanagawa, 259-12

JAPAN

Abstract

We reported neutron emission in a fracture process of a piezoelectric material $LiNbO_3$. Excess emitted neutron were observed. The emitted neutrons of fracture process in deuterium gas were confirmed by comparison with the fracture in hydrogen gas. The possibility of mechano-fusion was 92.4%.

Introduction

In a solid crushing process, chemical bonds are broken and ionic charges appear on the crushing surface. An activate state is induced by these charges. The mechanochemical reaction arise extraordinary chemical reactions. Kluev et al. and Derjaguin et al. have reported neutron

emissions from deuterated metal due to the mechanochemical process.[1),2)] Also in a crushing process of piezoelectric materials, a high voltage generate between a cleavage in piezoelectric crystal that impacted in the crushing process. Deuterium atom ionize and accelerate by the high voltage. Accelerating deuterium ion collide with another deuterium atoms. The collision of accelerated deuterium atoms occurs fusion reaction and emit neutrons. In the previous paper, we reported a neutron emission of a crushing process of lithium niobate-deuterium system.[3)] These nuclear reaction is so-called mechano-fusion. To make sure that this results was not mechanical noise effects, we examined a comparison of the neutron emission of crushing processes of lithium niobate in deuterium and in hydrogen atmosphere gases.

Experimental

We chose a single crystal of lithium niobate($LiNbO_3$) as the piezoelectric material. It has a high piezoelectric strain constant of 6.92×10^{-11} C/N(d_{15}) and a relatively low dielectric constant of $85.2(X_{11}{}^T)$. The generated voltage by forcing on the piezoelectric material is proportional to the piezoelectric strain constant and inverse proportional to the dielectric constant. A high piezoelectric constant and low dielectric constant are necessary to generate high voltage. The low conductivity ensures the charge retain after the charge unbalance of the fracturing process. The generated voltage is proportional to g (d/ε) value . Lithium niobate has one of the largest g value in inorganic materials.

The vibromill(VP-100, ITOH Co. Ltd.) was composed of a 93 cm^3 cup and a stainless steel ball (40 mm diameter) which vibrated at the frequency of 50 Hz with the vertical amplitude of 3 mm. The emitted neutrons were detected 8 ^{3}He proportional counters arrayed circularly in a cylindrical shaped paraffin block of 38 cm outer diameter and 10 cm inner diameter. The neutrons thermalized by the paraffin and reacted with 3He making a proton and a tritium with a Q value of 760 keV. The pulse heights of output signals of the ^{3}He counters were digitized by analog to digital converters. The vibromill was set in the center of the cylindrical paraffin. In order to increase the signal to noise ratio, counts between 600 and 1599 channels were selected. The detection efficiency was measured to be 2.6% by a calibrated ^{252}Cf source. The experiment was done in the low background facility at Nokogiri mountain. of The Cosmic-ray Research Institute, The University of Tokyo. It was located underground at the depth of 100 m water equivalent. The average count rate of the background neutrons were observed 5.7 counts / h during 960h.

The crushing for a sample was continued 1 hour duration. The crystal of lithium niobate was ca. 3 mm granule initially and after 15 min crushing the size was reduced to ca. 1 μm diameter. The crushing process of $D_2+LiNbO_3$, $H_2+LiNbO_3$ were carried out alternatively.

Results and discussion

Fig. 1 shows the mean value of observed neutrons of 1 hour duration and error bar from back ground, in hydrogen and in deuterium gases of the crushing process of lithium niobate. The trial number of experiments of $D_2+LiNbO_3$, $H_2+LiNbO_3$ and back ground were 24.6, 10 and 960 respectively. The counts of observed average neutrons $D_2+LiNbO_3$, $H_2+LiNbO_3$ and back ground during 1 hour were 6.4 ± 0.5, 5.7 ± 0.7 and 5.7 ± 0.08 respectively.

We observed excess neutrons emission (0.7 ± 0.5) over the background neutrons in the crushing process of $D_2+LiNbO_3$ system. On the other hand, the $H_2+LiNbO_3$ system, we did not observe excess neutrons emission over background neutrons. We also analyzed by a statistical treatment of the observed data. The comparison of statistical difference between $D_2+LiNbO_3$ and back ground emitted neutron counts were regarded as 92.4% significant. In contrast the difference of $H_2+LiNbO_3$ and back ground observed neutron counts were not regarded as 99.9% significant. These results given that excess neutrons emitted in the crushing process of $D_2+LiNbO_3$, but excess neutrons did not emitted in the crushing process of $H_2+LiNbO_3$. The mechanical noise did not disturb the experimental results.

Conclusion

We concluded that excess neutrons emitted from the crushing process of $D_2+LiNbO_3$. The excess neutrons did not observe in the crushing process of $H_2+LiNbO_3$. These results given a proof that mechano-fusion occurred in crushing process of $D_2+LiNbO_3$.

References

1). V. A. Kluev , A. G .Lipson, Yu. P. Toporov, B. Derjaguin, V. I. Lushikov, A. V. Strelkov, and E. P. Shabalin, *J. Sov. Tech. Phys. Lett.* **12**, 1333(1986).

2). B. V. Derjaguin, A. G. Lipson, V. A Kluev, D. M. Sakov and Yu. P Toporov. *Nature*, **341**, 492(1989).

3). T. Shirakawa, M. Chiba, M. Fujii, K. Sueki, S. Miyamoto, Y. Nakamitu, H. Toriumi, T. Uehara, H. Miura, T. Watanabe, K. Fukushima, T. Hirose, T. Seimiya, and H. Nakahara, *Chem. Letters* 897(1993).

Fig. 1
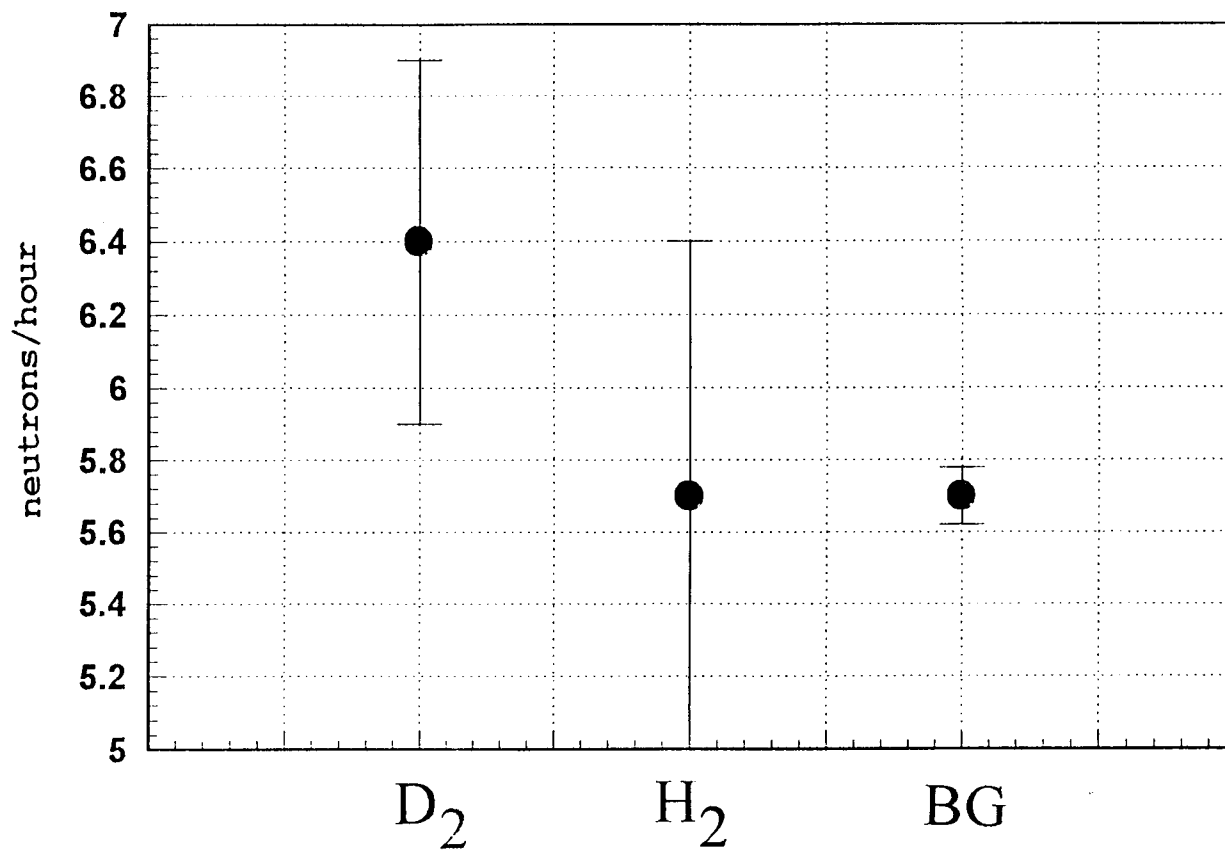
Figure caption

Figure 1. The mean value and error bar of observed neutrons of 1 hour duration. D_2 , H_2 are the observed neutrons of the fracture of lithium niobate in deuterium gas and hydrogen gas respectively. BG is the observed neutrons of back ground.

THE ANALYSIS OF THE NEUTRON EMISSION FROM THE GLOW DISCHARGE IN DEUTERIUM GAS TUBE

Z. Q. Ma, Y. T. Chen, G. S. Huang, W. Z. Yu,
D.W. Mo, and X. Z. Li
Department of Physics, Tsinghua University
Beijing 100084, CHINA

Abstract

This paper corrects an important mistake. The high energy component of the neutron emission from the glow discharge in deuterium gas tube is not as what previously reported. However, the low energy nuclear radiation might be still anomalous.

Introduction

As reported in ICCF3, the reproducible neutron emission [1,2] from the gas discharge tube with flowing deuterium was impressive. The most important feature was the neutron energy spectrum. It was found that there was a high energy component in the spectrum (3~10 MeV), and the conventional d-d neutron (2.45 MeV) was unexpectedly at the valley of the energy spectrum. In some cases, the yield of high energy component was 9 times greater than that of 2.45 MeV neutron. In order to confirm this important result, more than three sets of glow discharge tube were running in China soon after the Nagoya Conference. A national workshop was held to discuss this anomalous nuclear phenomenon. If it had been confirmed, we would have had an easily reproducible anomalous neutron emission which would have revealed the mechanism of it. Unfortunately, after the carefully study by the best experts of nuclear physics in China, none of three sets of experiments could find any high energy neutron component in the spectrum. There were neutron emissions from the glow discharge tubes at the Southwestern Institute of Nuclear Physics and Chemistry, at the Sichuan Institute of Material and Technology, and at the Tsinghua University, but the energy of these neutrons is just at the vicinity of 2.45 MeV. It seems that the overlapping of the intensive γ-ray in the ZnS detector caused the false signals which were taken as the high energy component of neutrons in the early experiments.

Experimental

Fig.1 shows one of the experimental set-ups at Tsinghua University. The liquid scintillation detector (ø5cm X 5cm, NE213 type) is used in stead of ZnS scintillation detector. Pulse shape discriminator is used to reduce the interference due to γ radiation. 5cm thick lead bricks are used for shielding. The background is reduced to a level of 0.01 signal per second. During the electrical discharge, we did see the neutron signal at a level of 2~3 counts per second. the maximum rate was 10 counts per second (Table 1). After the discharge, the liquid scintillation detector was checked again, and the signals were clearly due to fast neutron emission. [137]Cs and ^{60}Co radioactive sources were

used to calibrate the energy spectrum. The energy of these neutrons was in the range of 2.5 MeV. It is definite that there was no high energy component in the neutron energy spectrum. Fig.2 shows one of the discharge bubbles which were running with Zirconium electrodes in the deuterium gas. One of the electrodes was so hot that it was bent down by its own weight.

Having considered the efficiency (~0.15) and the correction for solid angle, we estimate that the total number of neutrons is ca. 10^3 per second (Table 2). The electrical voltage on the discharge tube was about 6.6kV, the discharge current was about 4mA, and the deuterium gas pressure was in the range of 25~5 Pascal. It is hard to calculate the theoretical value for the 2.45 MeV neutron yield based on these parameters, if the beam-target effect is assumed. Because the A.C. power supply and the transformer were used for discharge, it is very difficult to calculate the transient voltage between the electrodes and the thin film on the surface of glass bulb. According to these we could not conclude that there was any anomalous nuclear effect. However, the nature of the strong nuclear radiation at low energy region is still unclear.[3]

Improvement

To improve the experiment, a new set of glow discharge tube has been installed. (Fig.3). D.C. power supply is used instead of A.C. power supply. A new bubble-damage polymer detector (Fig.4) is used to search the anomalous neutron emission at low discharge voltage. This bubble-damage polymer detector is sensitive to neutron only, and it has no electronic noise at all. This bubble-damage polymer detector is capable of measuring the neutron energy spectrum also, if the neutron emission is strong enough. In parallel to this new neutron detector, the plastic track detectors(CR-39) are put inside the discharge tube for detecting the energetic charged particles (e.g. α, proton or triton etc.). A coil of palladium wire is immersed into the glow discharge plasma, and the electrical resistance is monitored to infer the loading ratio. Hopefully, with this new type of detector we may verify what Russian scientists have seen in their discharge tube.

Acknowledgments

References

1. H. Q. Long, et al. "The Anomalous Nuclear Effects Inducing by the Dynamic Pressure Gas Discharge in a Deuterium/Palladium System." in *Frontiers of Cold Fusion*, Edited by H. Ikegami, Universal Academy Press, Tokyo ,1993, pp.455-459.

2. H. Q. Long, et al. "Anomalous Effects in Deuterium/Metal Systems." in *Frontiers of Cold Fusion*, Edited by H. Ikegami, Universal Academy Press, Tokyo ,1993, pp.447-454.

3. H. Q. Long, et al. "New Experiment Results of Anomalous Nuclear Effects in Deuterium/Metal Systems." N 4.11 of ICCF4 notebook, volume one.
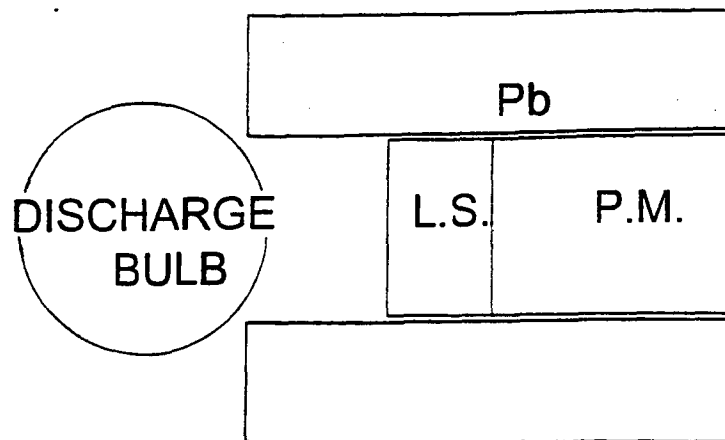
Fig.1. Schematics of Electrical Discharge Bubble
with the Liquid Scintillation Detector(L.S.)
Photo-multiplier (P.M.) and Lead Shielding (Pb)
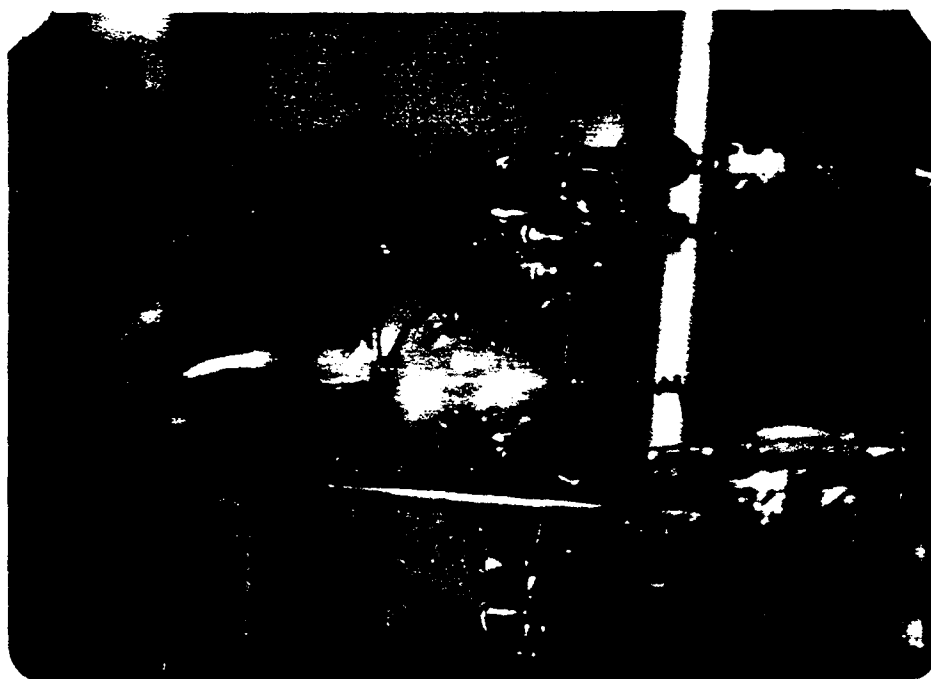
Fig.2 A Photo of Electrical Discharge Bubble
with Zirconium Electrode in Deuterium Gas
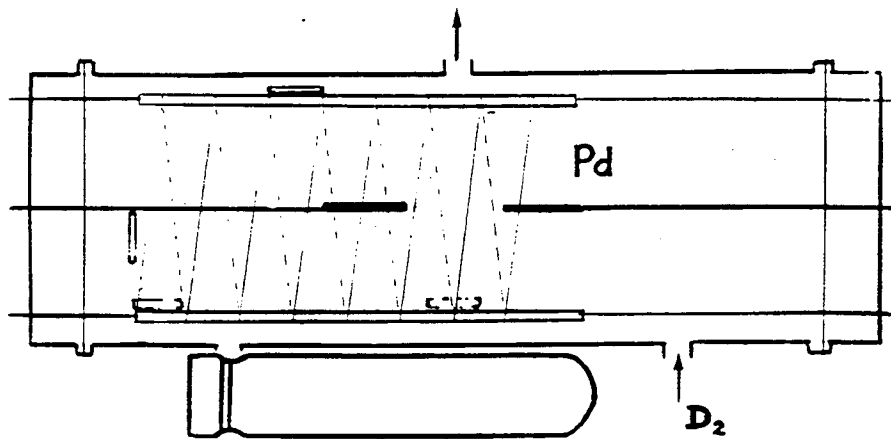
Fig.3 Schematics of New D/Pd Discharge Tube
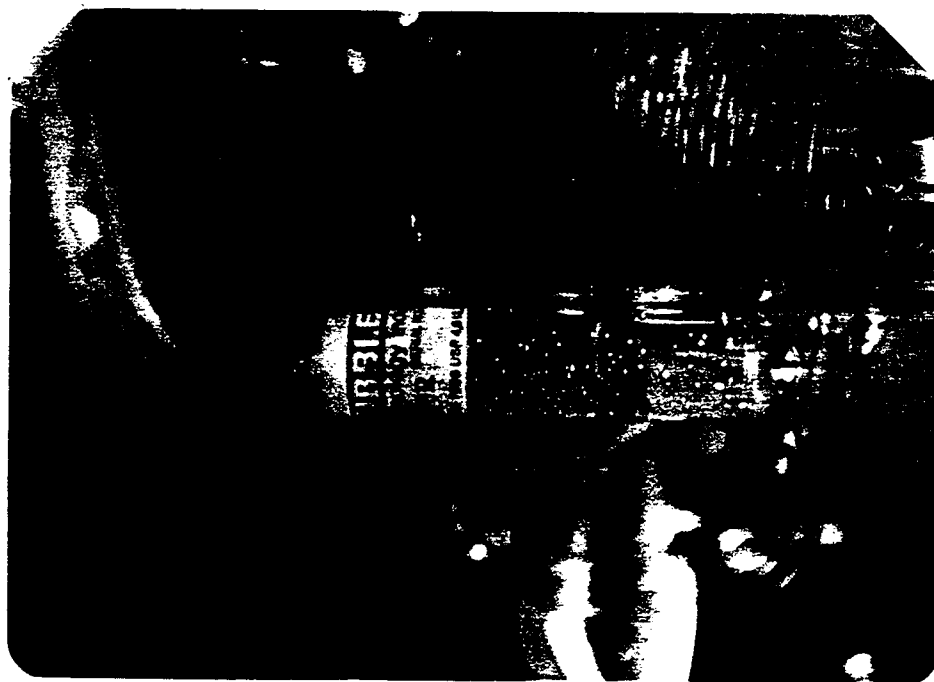
Fig.4 A Close-up Photo of the New D/Pd Discharge Tube
Showing the Bubble-Damage Detector,
and the Palladium Wire Coil

Table 1 Neutrons from D/Pd Discharge Bubble

VOLTAGE (keV)	CURRENT (mA)	PRES-SURE(Pa)	COUNTS (Sec^{-1})
4.75	5	8	0.05
5.05	7	7	2
5.9	8.5	4.5	0.3
BACKGROUND			0.04
6.6	4	2 5→5	10-2.9 -2.8-0.5 (SP1) (SP2)
6.4	7.5	6	5.5-2.4 (SP3)
6.5	THIN FILM EFFECTS ?		< 0.5

Table 2 Energy of the Neutrons from the D/Pd Discharge Bubble

COUNTS	ELEC. E. (keV)	ENERGY (MeV)	NUMBER
558	705	2.3	2.5×10^5
1211	760	2.6	5.4×10^5
522	800	2.7	2.3×10^5

EXPERIMENTAL TESTING OF THE ERZION MODEL BY REACTING OF ELECTRON FLUX ON THE TARGET

D.S.Baranov, Yu.N.Bazhutov, N.I.Khokhlov* V.P.Koretsky,
A.B.Kuznetsov, Y.B.Skuratnik*, N.N.Sukovatkin**
Scientific Research Center of
Physical Technical Problems "Erzion"
P.O.Box 134, 119633 Moscow, Russia
Fax: (095) 292-6511 Box 6935 Erzion
*Karpov Institute of Physical Chemistry
** MRTI RAN

Abstract

Nuclear transmutation was investigated in the irradiated samples of LaSm, LiSn, LaNd alloys. The electron irradiation was provided on Sr-Y radiactive source. Beta and gamma activity on LaSm target was recorded. It was demonstrated that the activity may be explained by production of Promethium isotopes. This process was predicted by the Erzion model.

Introduction
In this work it is proposed to investigate the possibilily of triggering the irradiation-induced transmutation reactions in the target material based on the Erzion model. Such transmutation is assumed to start in the field of ionizing radiation betas or gammas with energy below nuclear reactions thresholds. The radiation may to "shake off" the enions ϑ_N from nucleus-"donor" and to trigger closed cycles of convertions of these enions into erzions (neutral ϑ^0 or negative ϑ^-) and back. As the result of these convertions, the radioactive and stable isotopes may to turn out. Their appearence would be registrated by the methods of gamma – or beta – spectrometry.

1.Experimental Procedure
1.1.Targets
The experimental scheme presumes the availability of proper elements in target material and of proper target construction. The target material must consist of the elements – donors and elements-fuel. The first ones can capture the enions on their nuclei on stable state with binding energy in the order of 100 eV. There are about 30 elements-donors in nature (about 50 isotopes)[1]. The elements-donors Tin Sn, Neodymium Nd and

Samarium Sm were choosen for this experiment. The other elements-fuel can provide the closed cycles of reactions with conversion of released enions into erzions and back. There are about 30 elements-fuel [1] in nature (about 70 isotopes). The Lithium Li and Lanthanium La were selected as elements-fuel.

The mixture of elements-donors and elements-fuel have been prepared using some "soft" procedure without "shaking off" enion from donor. The alloying may be such procedure where the alloys LiSn, LaNd and LaSm with the mass relationships respectively 35/65,47/53 and 50/50 were prepared. Based on the features of radiation source the targets were fabricated in cylindrical form with diameter 40 cm and height 4-7 mm.

1.2.Irradiation
As a source of radiation, the beta-active radioisotopic sources Strontium-90,Yttrium-90 were choosen. This choice has to provided irradiation with the beta-particles energies below nuclear reactions thresholds (the maximum of spectrum energy is equal to 2.26 MeV, the average energy-0.9 MeV) and at low level power, transferred to the target (below 1 milliwatt).

In order to liberate enion, it is necessary to transmitt some energy into target material.One can estimate the value of this energy as follows.As electrolytic experiments indicated [2,3], the cold fusion reaction starts after transfering about 10 kilojoules of energy into cathode material.One may expect that this is just condition under which a such reaction can start.

The irradiation of targets was performed normally to their plane with periodically measurment of samples beta-activity. The gamma-spectroscopy can be carried out if beta-activity was registrated.The largest time exposure was equal to 35 days.

1.3.Measurements
Beta-mesurements were conducted with Geiger counter (typeСИ8Б) which registrated particles in the range 150 to 2870 keV. Gamma-spectroscopy was performed with the semiconductor silicon detector (type-80) which registrated gamma-rays in the range 200-5000 keV with energy resolution of no more than 1%.

2.Results
The measurement of beta-activity of all targets, with one exception, did not give any statistically important counts for any time exposure. The only target from LaSm showed clearly defined beta-activity after the latest exposure (35 days). The measurement gave the follows counts in a time of 10 minutes: one day after exposure-790 (integrated counts),690 (background); three days after exposure-760 (intergrated counts),660 (backround). Counts excess are equal to 100. It is almost four times greater than integrated statistical error.

The gamma-spectrum of this target was measured (fig.1) after two weeks of irradiation completition. Time of measurement was equal to 9000 seconds. Curve 2 on fig.1 represents the measured results without sample background. A "pure" target (not irradiated) identical to being analysed was applied for sample. The arrows show the energies of gamma-lines for isotopes Pm-146 and Pm-148. Two sharp lines on curve 1,fig.1, represent two lines for isotop La-138 presenting in the natural Lanthanium at the extent of 0,09%.

3.Discussions and Conclusions

As beta-measurements showed, some beta-active isotopes may appear in the sample of LaSm under investigation. The Erzion model may predict appearance of beta-active isotopes in the following reactions (half-lifes and beta-energies are defined):

La-139 $(\partial^-,\partial^\odot)$ Ba-139; 85m ; 2.3 MeV;

Sm-147 (∂^-,∂_N) Pm-146; 5.5y; 780 kev;

Sm-147 $(\partial^-,\partial^\odot)$ Pm-147; 2.6y; 224 keV;

Sm-148 (∂^-,∂_N) Pm-147; 2.6y; 224 keV;

Sm-149 (∂^-,∂_N) Pm-148; 5.4d; 2.5 MeV;

Sm-149 $(\partial^-,\partial^\odot)$ Pm-149; 53h ; 1.1 MeV.

With the most probability target activity will follow from istopes of Prometium-146, 147 and 148 as the most long-lived. Decay of Pm-147 isn't attended with gamma-particles. The lines of another two isotopes Pm-146 and Pm-148 are to be abound in the gamma-spectrum. One can see from curve 2 on fig.1 that the presense of these lines is quite possible, but effect is not achieved statistically.

Some reasons of such small effect are possible.Firstly, gamma-counts frequency 1/300 Hz is much less than frequency of beta-counts 1/6 Hz. It is responsible for low efficiency of semiconductor detector for high energy gamma-rays. We can increase considerably (three orders of magnitude) the relation effect/background if we will use the gamma-gamma cascade coincidence of the resultant isotopes. Secondly, the target absorb energy after irradiation may be estimated as 10^3 joules, about order of magnitude less than necessary (part 1.2). This fact may explain the lack of transmutation on another targets. So we may increase on three orders of magnitude the intensity of irradiation. And thirdly, we may increase the registration efficiency making the beta-spectroscopy of irradiated targets. We suppose to carry out the experiments with targets of a different compositions. For this purpuse we have prepared the following targets: BeNi, BeSn, BiNi, LiBi, LaNi, CuBe, InBe.

Referensis

1. Yu.N.Bazhutov, A.B.Kuznetsov. "Erzion-Nuclear Spectroscopy of Stable Isotopes". Preprint No 4, CSRIMash, 1992
2. P.K.Iyengar, M.Srinivasan. "Overview of BARC Studies in Cold Fusion", Invited Paper, presented at the First Annual Conference on Cold Fusion, Salt Lake City, Utah, USA (March 1990)
3. M.McKubre,S.Crouch-Baker,S.Smedley,F.Tanzella. "An Overview of Calorimetric Studies on the D/Pd System, at SRI; May 1989 to October 1993". Presented at the Russian Conference on Cold Fusion, Abrau-Durso, Russia (September 1993)
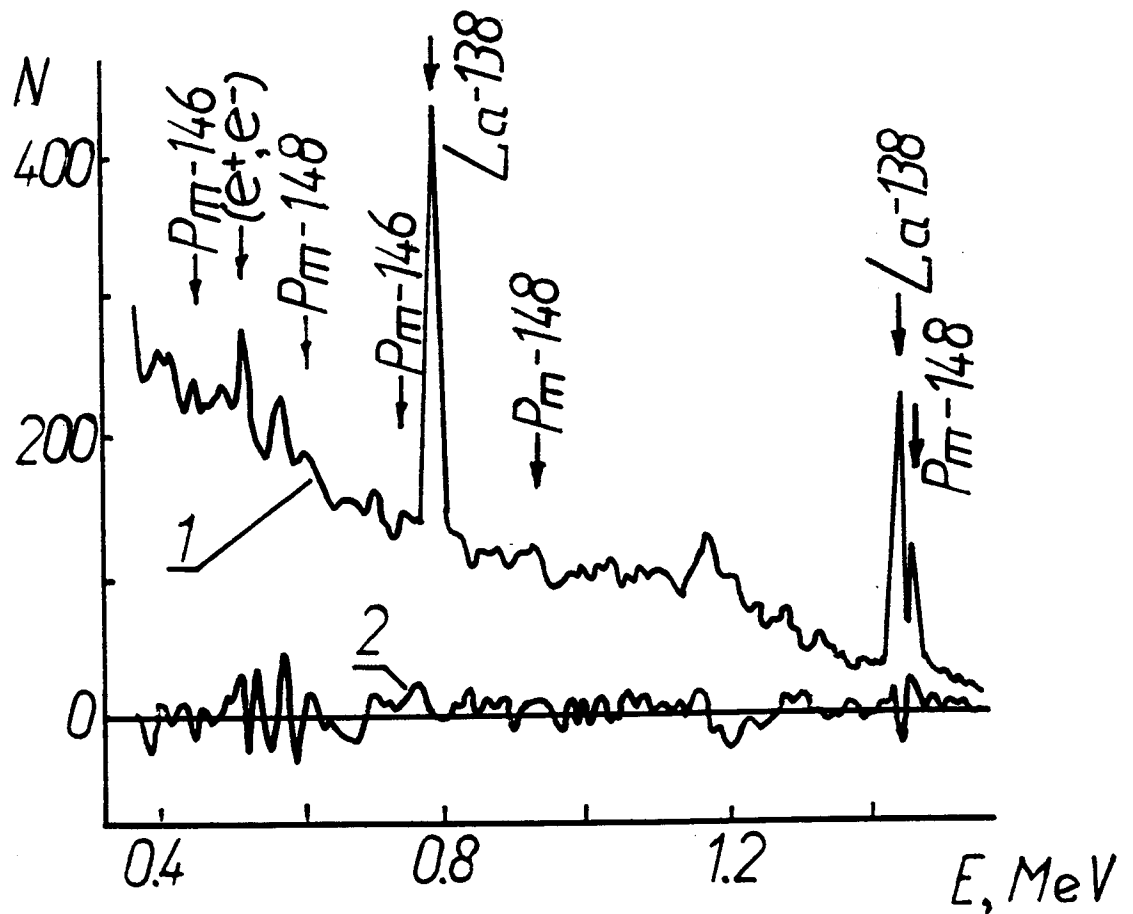
Fig.1. Gamma-spectrum of irradiated Lanthanum-Samarium target (E-gamma energy, N-counts per channel).

A STUDY
ON ANOMALOUS NUCLEAR FUSION REACTION
BY USING HV PULSE DISCHARGE

Jingtang HE   Yingping ZHANG   Guoxiao REN
Guoyi ZHU   Xiaoli DONG
Duanbao CHEN   Hongguang HAN

Institute of High Energy Physics,
Academia Sinica
P. O. Box 918, Beijing 100039,
P. R. of China

Long WANG   Sunsheng YI

Institute of Physics,
Academia Sinica
Beijing 100080, P. R. of China

Shangxian JIN

Graduate School
Academia Sinica
Beijing 100039, P. R. of China

INTRODUCTION

Since M. Fleischmann, B. S. Pons[1, 2] and S. E. Jones et al[3] reported in 1989 that nuclear fusion of deuterium (D_2) occurred at room temperature in Pd or Ti cathodes during the electrolysis of heavy water (D_2O), much efforts have been made to investigate so — called 'cold fusion' by many laboratories in the world. These experiments include several types: Electrolysis of heavy water; cold-hot cycles of deuterated palladium between liquid nitrogen temperature and room temperature; processing deuterated palladium by mechanical treatment and gas discharging of deuterated palladium[4, 5] etc. However the results are in conflict with each other[6].

As well known, there exist three reaction modes in D-D fusion:

(1) $D+D \rightarrow n$ (2. 45MeV) $+ ^3$He (0. 82MeV)

(2) $D+D \rightarrow P$ (3. 02MeV) $+T$ (1. 01MeV)

(3) $D+D \rightarrow ^4$He$+ \gamma +23$. 85MeV

From the knowlege of thermonuclear fusion, the reaction probability of mode 3 is extremely low, mode 1 and 2 have nearly the same probability. If we define

$$R = \frac{(\text{reaction rate of mode2})}{(\text{reaction rate of mode1})}$$

For normal D-D fusion $R \approx 1$

The neutrons originated from the reactions can come out from the discharge chamber and can be detected by neutron detectors. but the charged particles originated from the reactions. P, T, ^{3}He and ^{4}He can not be directly detected due to their low energies to penetrate the chamber envelope. The charged particles would collide with the material of the reactor. such as the Pd cathode. exciting the Pd nuclei. When the excited Pd deexcites, a characteristic gamma ray would be originated, for example:

$$^{108}Pd^* \rightarrow ^{108}Pd + \gamma \ (425 KeV)$$
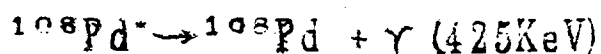
In order to investigate the anomalous nuclear effects, we have designed and performed a new type of experiment by using high voltage discharge. We simultaneously, during the HV period and out of the HV period, detected neutrons, charged particles and gamma rays.

EXPERIMENT

The arrangement of experimental set up is shown in Fig. 1. The main parts are described as following:

* Discharge chamber

The diagram is shown in Fig. 2. In order to enlarge discharge area of the anode, a thin stainless steel net was wound out of the tungsten rod. We checked the radioactive contamination of all the electrodes using the most sensitive solid state nuclear track detector CR-39. The electrodes used have no radioactive contamination.

* HV pulse generator

Module NE555 produces voltage pulses with adjustable width to trigger the thyratron ZQ1-0.1/1.3, then its output triggers hydrogen thyratron ZQM1 -130/10 which provides discharge chamber with high voltage pulse (maximum amplitude 10KV).

* γ counter

The scintillator is a NaI(Tl) with diameter of 4 cm and thickness of 4 cm. It was coupled directly with PMT(GDB-44F) via silicon oil. The spectrum of gamma counter for ^{22}Na is shown in Fig. 3a.

The energy resolution of the γ counter is 11% for 1270KeV. The effciency of the γ counter is about 2.6 ×10^{-3} for 1270 KeV.

* Neutron counter

The diagram of neutron counter is shown in Fig. 4. In the front there is a 17cm × 17cm plastic scintillator with thickness of 5 cm, then a Φ 10cm ^{6}Li glass scintillator with thickness of 0.3cm. ^{6}Li glass was directly coupled on to PMT(GDB-100) by silicon oil.

When ^{6}Li absorbed a slow neutron,
^{6}Li(n, α)T reaction will take place,
then the glass can produce light by α
and T. The light is viewed by PMT
and a neutron signal comes out which
will be recorded by MCA.

The slow neutron spectrum of ^{252}Cf
neutron source with intensity of about
$3000/4\pi \cdot$ sec is shown in Fig. 5. The
FWHM of the peak is 25%. The
effciencdy of the neutron detector is
about 3×10^{-3}.

Firstly the chamber was pumped to
2.7×10^{-2} torr, and then fill with
1 atm deuterium gas. The D_2 was absorbed
for 1 hour by the electrode Pd.
Switching on 10KV HV, the pulse
generator produced pulses of 10KV in
amplitude, $150 \mu s$ in width and 10Hz
in rate. At this time, sparks appeared
in the chamber.

The gate A was triggered by the
rising of the HV pulse and opened
until the HV pulse terminated (see Fig. 1).
The signal of gata A triggered MCAs A_1
and A_2. A_1 and A_2 recorded
simultaneously gammas and neutrons
came out from the discharging chamber
during the discharging.

There will be a gata B in the interval between HV pulses.

The gate B was triggered by the falling of the HV pulse and opened until another HV pulse rising. The width of gate B is about 0.1 set. The signal B triggered MCAs B_1 and B_2. B_1 and B_2 recorded simultaneously the gammas and neutrons which came out from the chamber.

Results are summarized as follows:

1. The spectrums of both gammas and neutrons outside the period of HV pulse detected by system B are consistent with background spectrums recorded without HV within statistic error.

2. During HV discharging, the neutron signals are comparable with background.

However, there are extra gamma rays.
Figure 6(a) is the gamma ray spectrum
detected by MCA A_1 in 8h. Figure 6(b) is
the background spectrum in 4h. From Fig.
6(a), we subtracted the background for
8h to obtain Fig. 7. In Fig. 7 it is very
clear that there exist two peaks.
According to the calibration curve of
system A_1, one peak is at 425 ± 40KeV,
another is at 870 ± 50KeV. Because the
electrodes are made of Pd, Fe and also
W, the spectrum of gamma rays might be
relevant to the following nuclear
deexcitation processes:

$$^{108}Pd^* \rightarrow ^{108}Pd + \gamma \ (E_\gamma = 425\text{KeV})$$
$$^{56}Fe^* \rightarrow ^{56}Fe + \gamma \ (E_\gamma = 854\text{KeV})$$
$$^{184}W^* \rightarrow ^{184}W + \gamma \ (E_\gamma = 110\text{KeV})$$
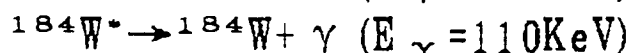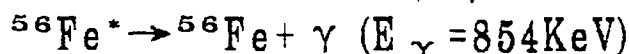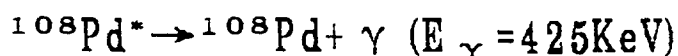
However, the energy of γ originated
from $^{184}W^*$ is too low to be seen
against noise.

Since the HV is only 10KV, the electron/deuteron with energy of 10KeV can excite only atoms, but not nuclei. So, the high energy gamma ray could be produced only from nuclear Coulomb excitation by charged particles with high energies[7]. The gamma yields are about 10^{-6} per 3.0 MeV proton absorbed in palladium[8]. Our result can probably be explained by the exciting Pd and Fe in the products from the reaction mode 2. From the present experiment, we would conclude that in HV pulse discharging experiment we only detected the characteristic gamma ray without neutrons. It seems that the reaction rate of mode 2 is much higher than mode 1 in a low energy D-D fusion under palladium environment.

Taking the acceptance into account, from our experimental results, we can deduce: $R > 10^9$.

We are going to do some experiments with different electrodes.

ACKNOWLEDGEMENT

REFERENCES

1. M. Fleischmann, B. S. Pons and M. Hawkins, J. Electroanal. Chem., 261(1989)301.
2. B. S. Pons and M. Fleischmann, Fusion Technol, 17(1990)669.
3. S. E. Jones et al., Nature 338(1989)737.
4. F. Celani et al., Report Il Nuovo Cimento Conf. Varenna 15-16 Sept. 1989.
5. E. Yamaguchi et al., Japan. J. Appl. Phys., 29(1990)L666.
6. R. W. Kuhne, Phys. Lett., A155(1991)L666.
7. K. Alder et al., Rev. Mod. Phys., 28(1956)432.
8. David C. Bailey, UTPT-89-15.
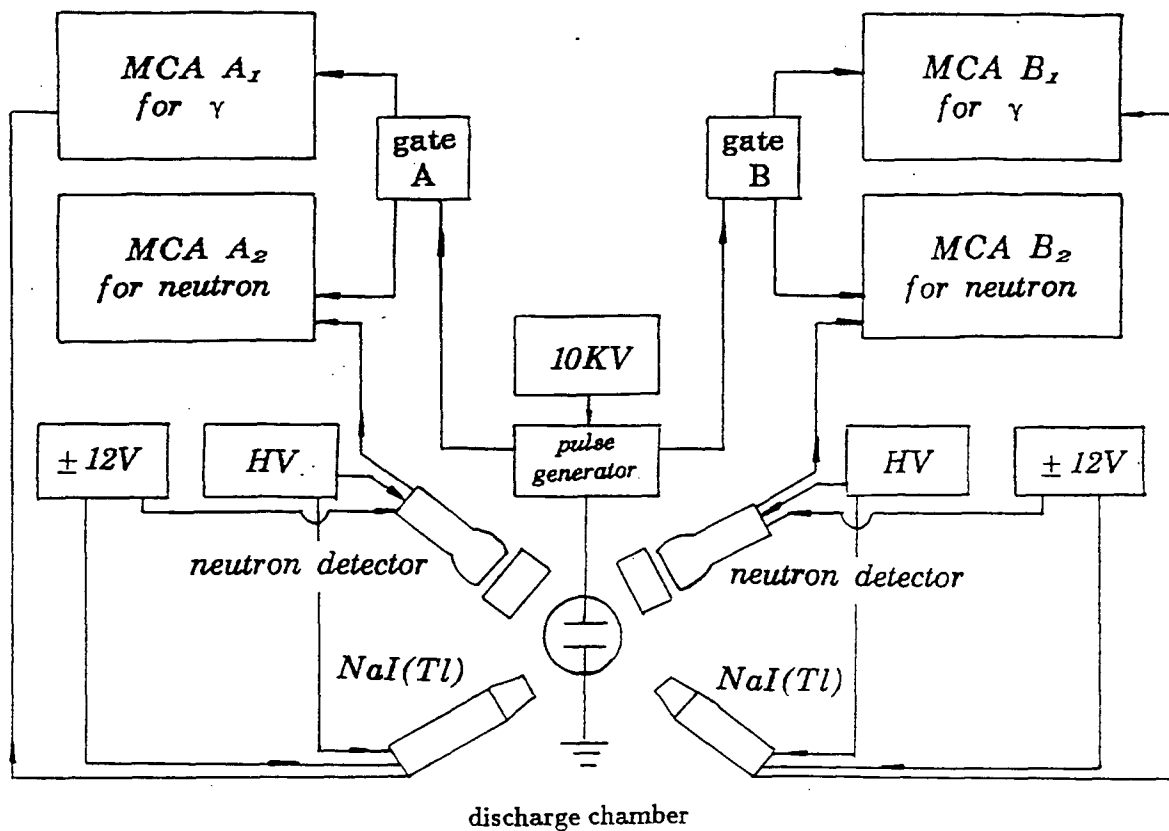
Fig. 1 Experimental arrangement and recording system.

Inlet   Outlet

Tungsten electrode
A case of cooling water

Electrical net of stainless steel
A tube of quartz
Pd electrode
A case of cooling water
Outlet

Inlet

Evacuation pipe
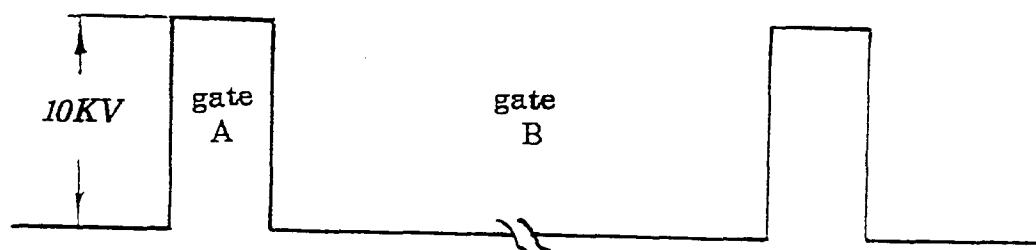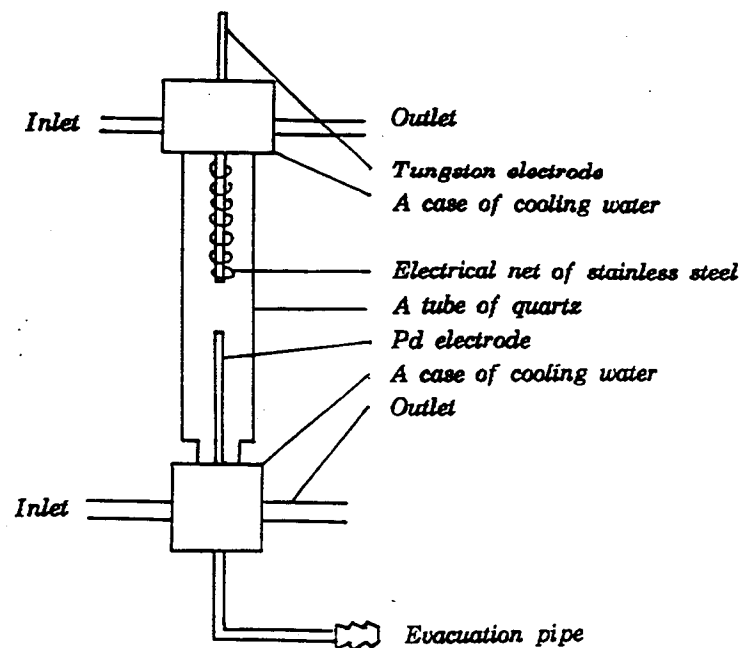
Fig.2 Diagram of discharge chamber.

spectrum of ^{22}Na
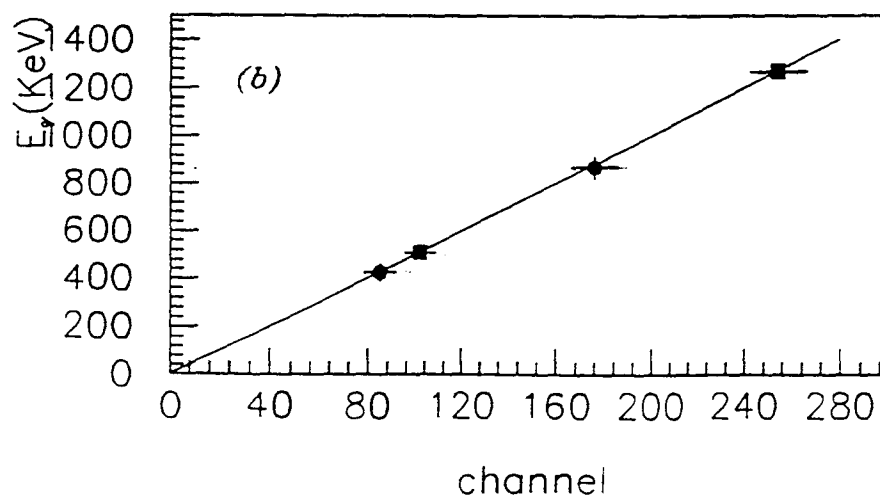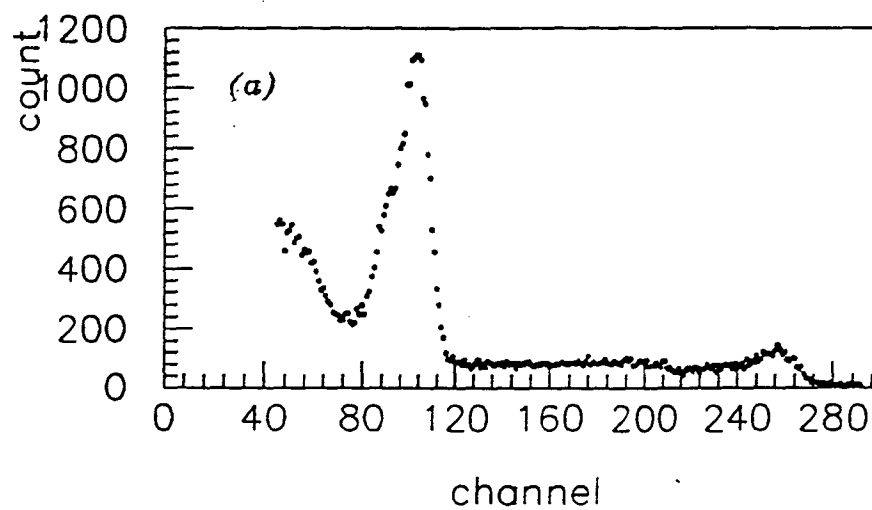
Fig.3 Calibration of NaI(Tl) gamma counter.
  a) Spectrum of source ^{22}Na.
  b) Calibration curve.
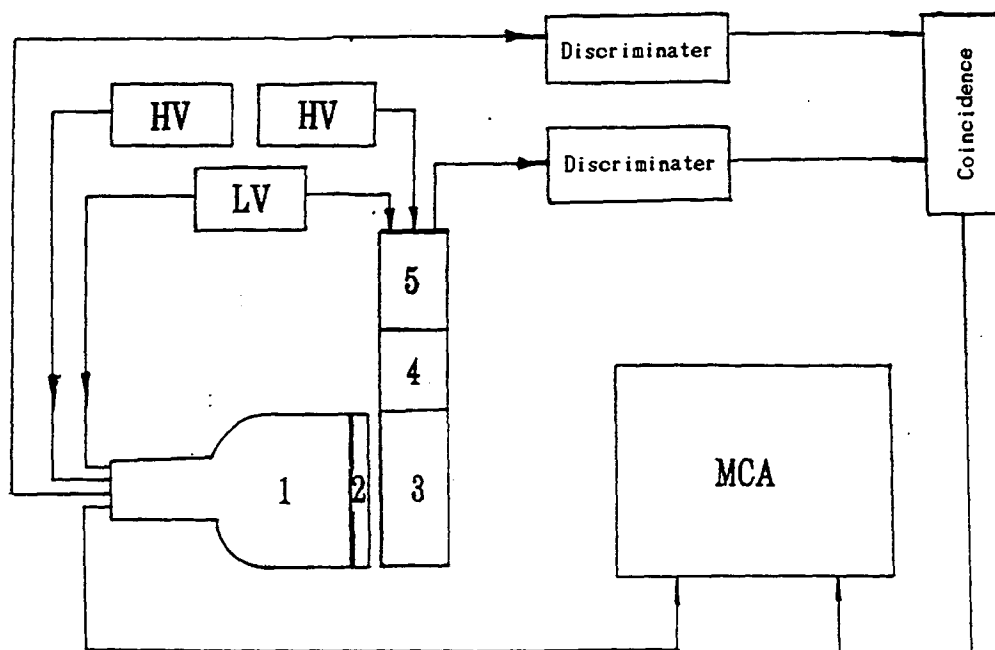
Fig.4 Neutron detector system
1—GDB-100PM   2—ϕ 100*3 Li-6 glass
3—5cm thickness of plastic scintillator
4—light guide   5—56 AVP PM
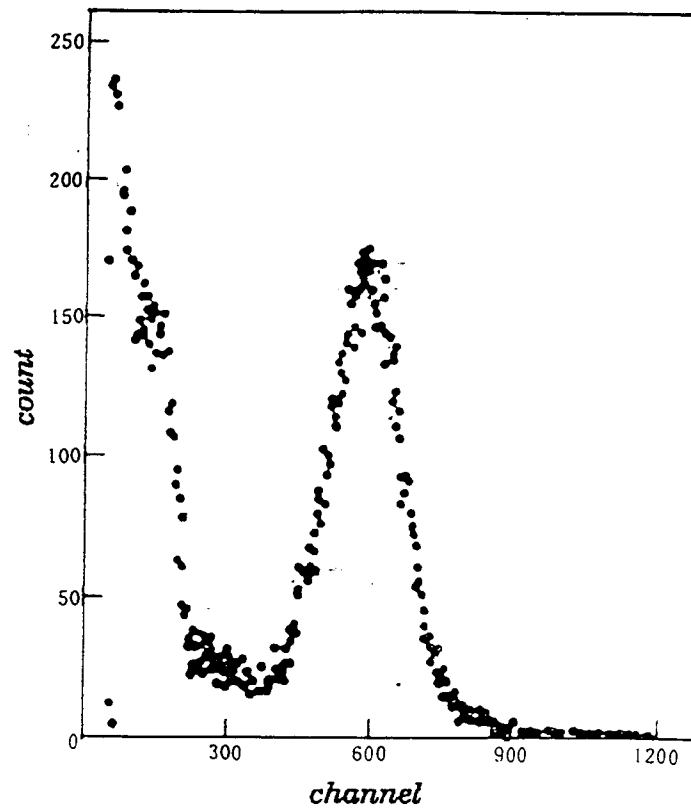
Fig.5 Slow neutron and γ-ray spectrum
from lithium glass detector
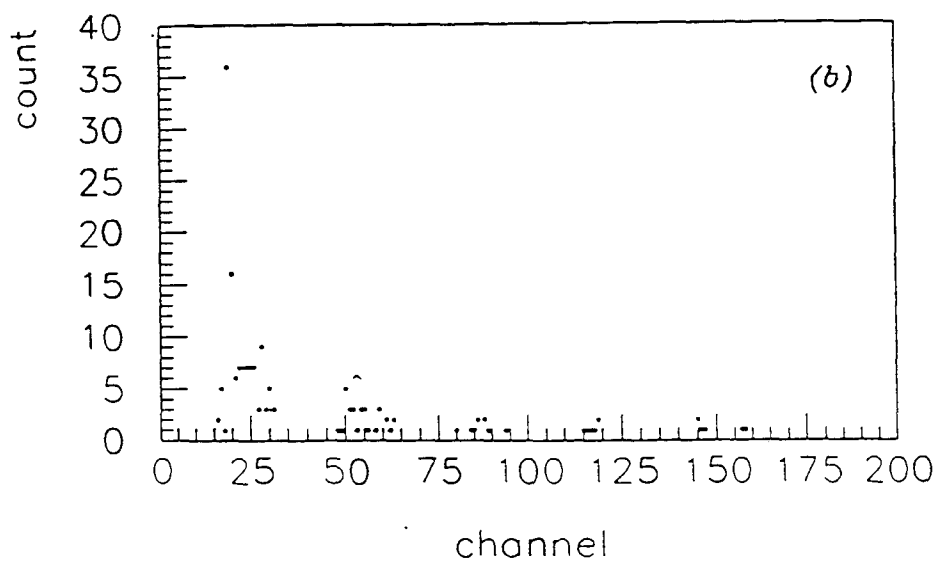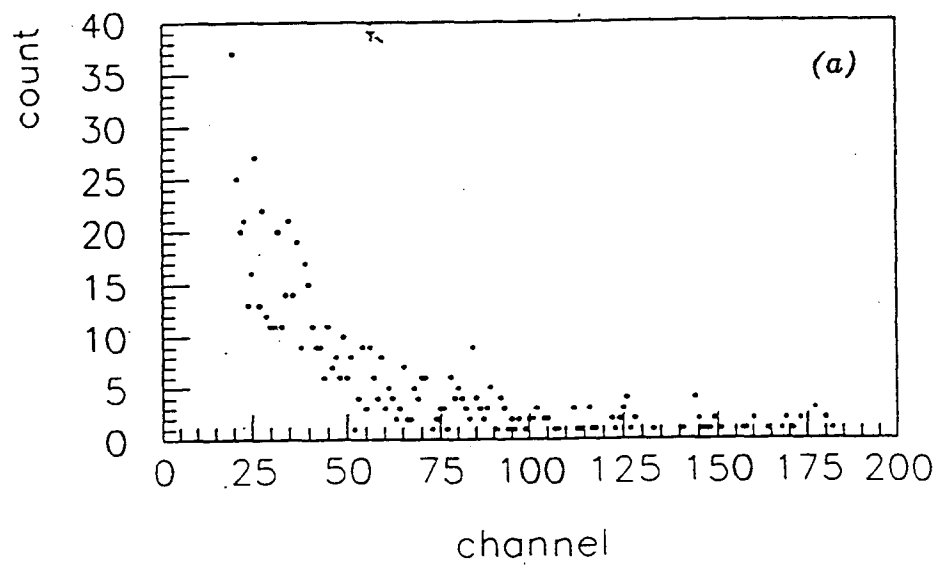
Fig 6 The gamma-rays spectrum.
   a) Spectrum during HV pulse for 8 hours.
   b) Background for 4 hours.
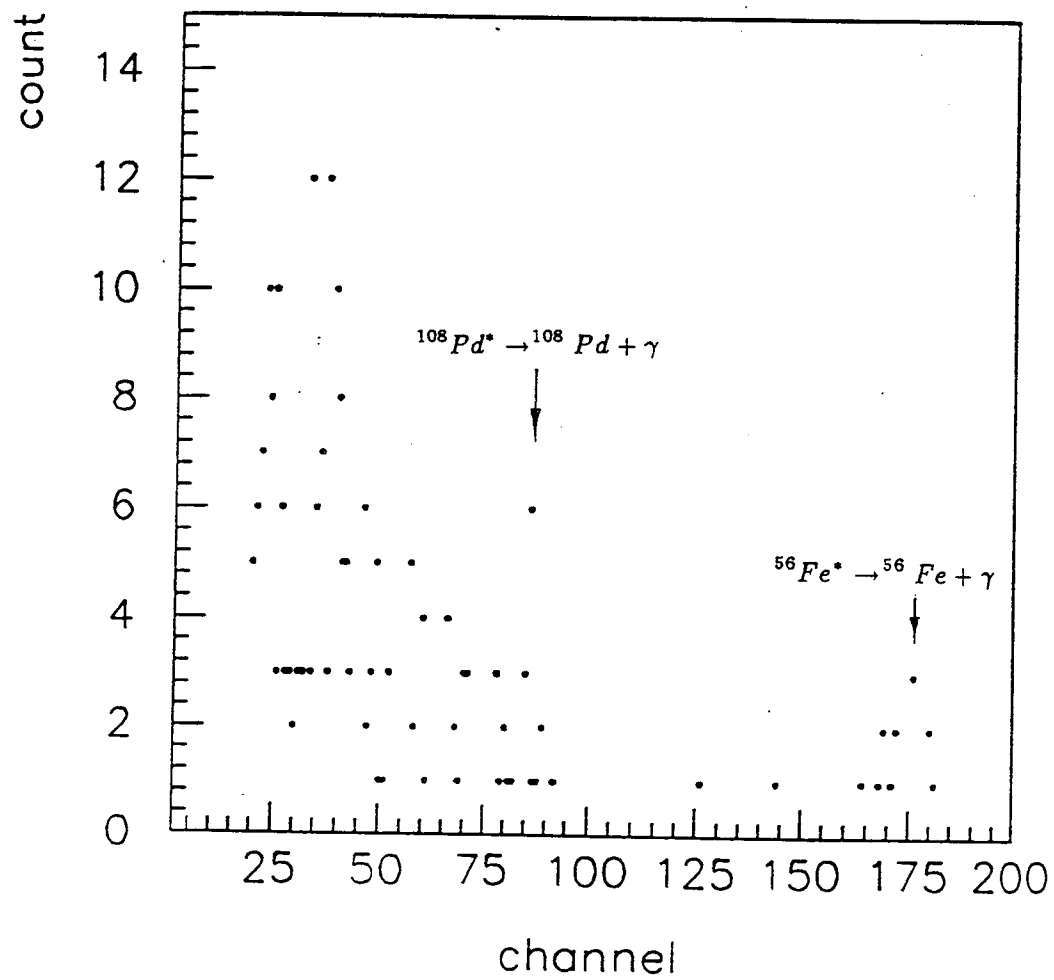
Fig.7 The net spectrum of gamma ray.

COLD FUSION EXPERIMENTS BY USING ELECTRICAL DISCHARGE IN WATER

Takaaki MATSUMOTO
Department of Nuclear Engineering
Hokkaido University
North 13, West 8, Sapporo 060, Japan

Abstract

This paper describes that cold fusion can be easily induced by electrical
discharge in water. AC shots of about 100 V were applied to wire electrodes
of palladium, platinum and nickel. Cold fusion reactions were observed by
a system of a microtelescope and VTR, and nuclear emulsions. The VTR system
has successfully recorded explosive cold fusion reactions on the surface
of the metals. With the nuclear emulsions, several traces indicating cold
fusion were found. Tiny ball lightening was observed, related to strange
traces of combined rings. Implosive cold fusion is also described.

Introduction
Many attempts have been made to induce cold fusion reactions, usually by
charging hydrogen into a metal. According to the Nattoh model(1), cold
fusion essentially requires the compression of a hydrogen-cluster into a
tiny assembly. Since electrons contained in the cluster play an important
role in the compression process, the reaction rate of cold fusion can be
extremely enhanced by electrical discharge. Here, the cold fusion reactions
can be induced not only in the metal but also on the surface of the metal.
The compression by discharge is so strong that significant reactions, such
as the production of tiny black holes, can be expected to easily occur. In
a previous paper dealing with one-point cold fusion experiments(2), a pin
electrode of platinum vertically located over a copper plate was melted
down by a couple of the electrical discharge with about 100 V in water.
Several traces indicating that cold fusion reactions occurred were record-
ed on the copper plate.

In this paper experiments using pulsed AC discharges in water were perform-
ed with wire electrodes. The cold fusion reactions induced by the dis-

charges were observed by a system utilizing a microtelescope with a video
tape recorder (VTR), and nuclear emulsions. Furthermore, implosive cold
fusion experiments were attempted, in which the wires exploded.

Experiments

Two kinds of cold fusion experiments were performed using electrical dis-
charge: cold fusion directly induced by electrical discharge and implosive
cold fusion induced by the explosions of the cold fusion reactions. The ex-
periments were made by applying AC shots (50 Hz and up to about 100 V) to
the wire electrodes in water.

The electrolyte solution consisted of ordinary water mixed with 0.6 Mol/l
potassium carbonate. Wires of palladium, platinum and nickel were used for
the electrodes. Two kinds of electrode arrangements were employed for the
direct discharging cold fusion: vertical and parallel. In the former, a pin
of the platinum wire (0.3 mm ϕ x 2 mm long) was vertically located about 2
or 3 mm distant from the wire of palladium (0.5 - 2.0 mm ϕ x about 25 mm
long). In the latter, two wires of palladium, nickel and platinum (0.3 -
2.0 mm ϕ x about 25 mm long) were located parallel to one another with a
gap of 2 - 3 mm. For the implosive cold fusion, on the other hand, a helic-
al electrode of nickel (0.5 ϕ) was placed around a pin electrode of palla-
dium (0.5 ϕ x about 3 mm long). The diameter of the helical electrode was
about 10 mm. The electrical discharge was employed with pulsed AC up to
100 V (20 - 80 msec ON and 1 - 15 sec OFF). The phase was fixed such that
the voltage at the anode started to increase positively.

Reactions were observed using a microtelescope and VTR system, and nuclear
emulsions. They were alternately located outside the bottom of a cylin-
drical glass cell (an acrylite plate 2 mm thick). The cell was located such
that the bottom was vertical. Pictures from the microtelescope (10 - 100
times amplication) were recorded on the VTR. Important pictures were then
stepwise picked up with a color copier. The nulcer emulsions were similar
to that used previously(3) (100 μm thick x 50 x 50 mm; coated on both sides).
Reference nuclear emulsions were located about 5 m from the cell in the
same room.

Results

(a) Direct Discharging Cold Fusion

Figure 1 shows a sequence of pictures taken by the VTR of the surface of
the palladium wire (2 mm ϕ) in the parallel arrangement. The time step was
33 msec. In Fig. 1(b), the surface was completely covered by tiny bubbles.
As the voltage increased, explosive reactions were induced on the surface
(Fig. 1(c) and (d)). The VTR system also recorded explosions induced in the

vertical arrangement. Here, the explosions took place on the pin electrode.
A couple of wave fronts that were reflected by the AC cycle could be clearly
seen in the pictures, and particles with high energy seem to be emitted. The
observation of the nuclear emulsions showed that the explosion was cold
fusion reactions and that a plasma state was created by the released energy.

Classification of the reactions can be done by observing the nuclear emul-
sions located outside the acrylite window. Assemblies of two and three deu-
terons were observed. The production of deuteron during cold fusion experi-
ments with ordinary water was predicted by the Nattoh model(1). A star was
also recorded on the nuclear emulsion. Similar traces were also observed in
a previous experiment(4). A star can be created in the nuclear emulsion by
a multi-body fission reaction of a highly excited compound nucleus that cap-
tures a multiple-neutron emitted from the cell. Furthermore explosive traces
that can be generated by the gravity-decay of di-neutrons were observed. Si-
milar traces were also observed in previous experiments(1). This trace is
one of the most credible piece of experimental evidence indicating that cold
fusion has taken place. When the hydrogen-cluster is compressed to induce a
cold fusion reaction, hydrogen atoms that are not directly involved in a
fusion reaction should scatter. Those traces could be clearly seen in the
trace. Simultaneous plural reactions might take place in the compressed
hydrogen-cluster. Fortunately, pictures indicating such a reaction were
taken by chance with mismade nuclear emulsions that were thinner.

Strange combined rings were first observed in this experiment (Fig. 2). These
rings can be clearly distinguished from the previous ring traces because they
were recorded only on the surface and had combined with each other. The dia-
meter of the combined rings is different in each event but samilar within the
same event. The events are densely concentrated in a narrow space between
the first and second nuclear emulsions.

(b) Implosive Cold Fusion
Implosive cold fusion experiments were attempted by applying AC shots to a
helical wire within which a strong electrical field was concentrated to the
tip of the pin electrode. A sequence of two explosions occurred. The first
explosion was directly induced by the discharge. The second explosion was
not induced by the electrical discharge, but by the first cold fusion react-
ions. Because the duration time of the discharge was 80 msec and the second
explosion occurred later than 100 msec. After the explosions, there remained
black fine materials.

(c) Observation of Ball Lightening
Phenomena of ball lightening have been observed twice during the earlier dis-
charge experiments. We have not yet succeeded in taking pictures of the
ball lightening. The first was on August 13 in 1992, observed during the dis-

charge in the vertical arrangement of a palladium wire (0.5 $\emptyset$ x about 20 mm long) and a platinum pin (0.3 $\emptyset$ x about 3 long). After hydrogens were charged into palladium with DC electrolysis for about 1 hour, AC shots of about 100 V were repeated. Tiny ball lightening was emitted from a point about 1 cm distant from the discharging point. They flew about 1 cm in the opposite direction and exploded when they stopped. The emission of ball lightening took place with a somewhat delayed time after the discharge and it was very often repeated. The second was on August 25 in 1992, observed during discharge in the parallel arrangement of wires of palladium (0.5 mm $\emptyset$ x about 25 mm long: gap was about 3 mm). After hydrogens were also charged for about 1 hour, AC shots were repeated among the electrodes. In the moment after the discharge, two bolts of tiny ball lightening were emitted upwards from the wires (their positions were not identified), and they also exploded at the end.

Discussions
In the experiments of discharge cold fusion, two kinds of the electrode arrangements were examined with an AC discharge of up to 100 V. Several pieces of experimental evidence indicating cold fusion have been obtained. The traces on the nuclear emulsions showed the production of deuterons and stars that were induced by the multi-body fission reactions. The gravity-decays of di-neutron were also recorded on the nuclear emulsions. All of those traces were already obtained in the previous experiments(1). Further-more, the tiny explosions on the surface of palladium were successfully ob-served by the VTR system. This means that cold fusion reactions can be in-duced on the metal surface by the electrical discharge, as predicted by the Nattoh model.

The strange traces of the combined rings, first observed in this experiment, suggest the production of tiny black holes. The tiny balckholes that were produced in the cell dropped down to the space between the first and second nuclear emulsions. They seem to have continued hopping there and remained the combined rings. With the observation of the tiny ball lightening during the earlier discharge experiments, the ball lightning might consist of the tiny black holes. In the natural environment, there are terrible discharges, thunderstorms. Here, large scale reactions of cold fusion should take place to generate massive black holes. It is suggested that the extraordinary be-haviors of the ball lightening could be well explained by the tiny black holes.

This experiment has verified that the electrical discharge with a moderate voltage of around 100 V can easily and credibly induce the cold fusion reactions in water.

2 mm
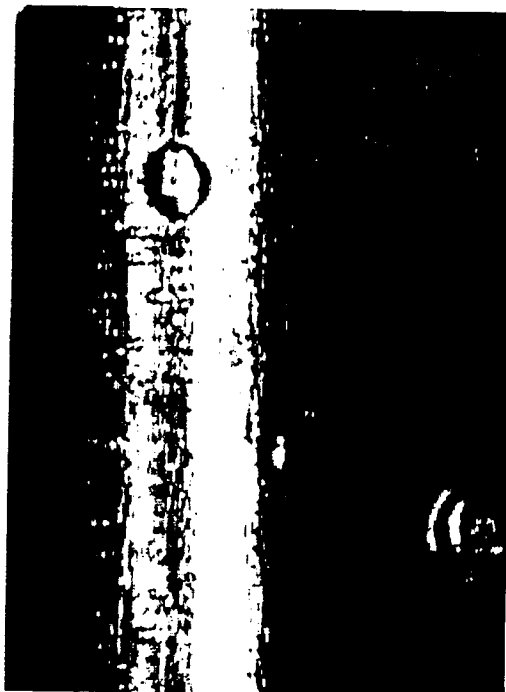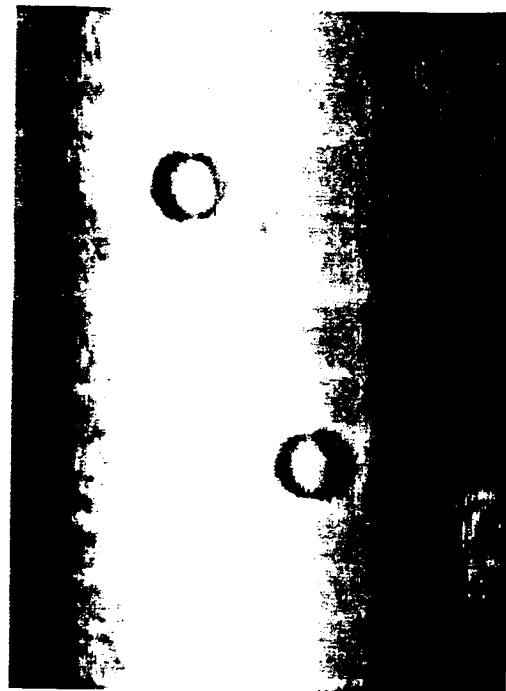
(a)   (b)

(c)   (d)

Fig. 1: Surface of the palladium rod in parallel arrangement

50 μm

Fig. 2: Combined rings on nuclear emulsion

References
1. T. Matsumoto. "Mechanisms of Cold Fusion: Comprephensive Explanations by
   the Nattoh Model." Submitted to Fusion Technology in March and distributed
   at the Hawaii conf. in December(1993).
2. T. Matsumoto. "Experiments of One-Point Cold Fusion." Fusion Technology.
   Vol.24, p.332(1993).
3. T. Matsumoto. "Observation of New Particles Emitted on Cold Fusion."
   Fusion Technology. Vol.18, p.356(1990).
4. T. Matsumoto. "Observation of Stars Produced During Cold Fusion."
   Fusion Technology. Vol.22, p.518(1992).

THE CUBIC-TETRAGONAL PHASE TRANSITION IN TiD_x (x≥1.7) AND ITS POSSIBLE RELATION TO COLD FUSION REACTIONS

J.F.Fernàndez, F.Cuevas, M.Alguerò and C.Sànchez

Dpto. Fìsica de materiales C-IV, Universidad Autònoma de Madrid

Cantoblanco, 28049 Madrid, Spain

Abstract

Samples of TiD_x (x≥1.7) have been produced with a controlled and reproducible method. Quality of the samples (powder, rod, plates) has been checked by measuring the specific heat on passing the crystallographic (cubic-tetragonal) phase transition presented by TiD_x at temperatures close to room temperature. A possible triggering effect on nuclear (D+D) fusion reactions induced by that phase transition has been investigated by measuring neutron emissions from the sample in the 1-7 Mev energy range. No clear relation between the phase transition and neutron production has been found.

Introduction

Nuclear ashes from Ti in cold fusion (electrolytic and pressurized gas) type experiments have been detected by many authors from 1989. However no clear conclusion has yet been reached on the possible triggering mechanism of nuclear fusion reactions (mainly D+D) giving place to such nuclear products (neutrons of several energies, tritium, etc.). Non equilibrium in the TiD_x lattice has been established as a necessary condition for cold fusion reactions to take place. In particular, several theoretical models and experimental results[1-2] suggest that phase transitions in TiD_x could be a convenient non-equilibrium condition under which cold fusion reactions could be triggered.

Titanium deuteride (TiD_x) shows a crystallographic phase transition (cubic to tetragonal) whenever x≥1.7. Phase transition temperature is a function of x, but it stands close to room temperature whenever x≥1.8. The exact value depending on purity and other characteristics of the TiD_x samples. However it has been shown by several authors[3-4] (and we have confirmed in our experiments) that the characteristics of the crystallographic phase transition (even its own existence) depend drastically on the experimental procedure followed in the sample preparation. In fact, several authors have published that after preparing TiD_x samples (by the pressurized gas technique) some of them presented the crystallographic transition and other did not. No reason was given for that anomaly.

In the purpose of investigating any possible relation between the crystallographic phase transition and nuclear reactions in TiD_x we firstly should make sure that all the prepared samples presented the phase transition, i.e. that all they were well reproduced . To this aim we have studied with detail the TiD_x preparation procedure when the pressurized gas (both H_2 and D_2) technique is used with Ti. The reason for the lack of reproducibility of the TiD_x properties has been unequivocally determined. As a consequence, high quality TiD_x samples

have been tested in cold fusion experiments (thermal cycles around the critical temperature of the phase transition).

Neutron detection (1-7 Mev) was used as a confident technique to prove the reality of possible nuclear reactions (D+D) in the TiD_x samples. No neutron signal greater than the background (≈ 1 n/s coming from the sample) was found to be related to the crystallographic phase transition. Additional experiments are still in course.

Sample preparation. Phase transition in TiD_x

TiD_x samples were prepared by putting metallic Ti (powder, sponge, rods) with D_2 in a 316 stainless steel reactor. A thermocouple was placed in close contact with the sample. The Ti samples were first degassed under vacuum of 10^{-3}-10^{-6}mb. at different temperatures and times in the reactor. Then the temperature was increased up to the value (stabilization temperature, T_s) where the D_2 should be let go into the reactor. Once T_s was reached D_2 was introduced into the reactor . After a certain time, dependent on T_s, the Ti samples absorb the gas. We have observed that due to the exothermic nature of the absorption process the sample temperature can be considerable increased (several hundred degrees) in an uncontrolled way. We have found that this step plays a fundamental role on determining the final quality of the TiD_x samples.

The reactor is kept at T_s during a variable time (t_s) to favour a continuos and slow additional absorption of deuterium. Finally the whole system is cooled down under controlled conditions.

The following variables of the experimental procedure have been studied with detail:

D_2 pressure: 6b.
Degassing temperature: 200°C
Degassing time: 0-17h
Stabilization temperature (T_s): 350°C, 500°C, 800°C
Stabilization time (t_s): 1-72h
Cooling rate: 0.1-15°C/min
Purity of Ti: 97%, 99.7%, 99.99%

The quality of the prepared TiD_x samples was checked by measuring their specific heat variation on crossing the phase transition critical temperature. Fig.1 shows some of the obtained results corresponding to three different samples. It can been seen that the three samples presented the expected λ-shape of c_p corresponding to a second order phase transition. However several differences between them are evident. The critical temperature goes down on going from a) to c) in Fig.1. Simultaneously the peak c_p value also decreases in the same sequence. As a consequence of both facts the λ-shape is perfectly defined in sample a) and becomes much worst on going to c). This behavior determines the quality of the samples. Sample a) is of "high quality". All the samples (both TiD_x and TiH_x) used in our cold fusion experiments were of this "high quality" type

As a result of our experiments it was concluded that the sample quality is mainly determined by the nucleation rate of the TiD_x δ-phase controlled by the sample temperature variation on passing from the β-phase to the δ-phase. A second factor which must be carefully watched is the cooling rate (CR). Rates not faster than 0.5°C/min are recommendable.

Nuclear experiments

The purpose of the nuclear experiments was to elucidate whether the crystallographic phase transition may be (or induce) a triggering agent for cold fusion nuclear reactions. Three different neutron detectors were placed close to the reactor to investigate any possible neutron emission from the samples. Characteristics of the detection system are given in Table I.

Table I
Characteristics of the neutron detector system

Neutron detector	Dimensions (cylindrical) (cm)	Distance sp-det (cm)	Efficiency % (at 2Mev)	Background (counts/sec)	Nd/Ne
NE213	3.8×3.8	3.5	25	3×10^{-3}	9×10^{-4}
BC501	13.5×13.5	3	50	2×10^{-1}	8×10^{-3}
BF$_3$	22×35	25	0.1	8×10^{-4}	2×10^{-5}

Third column of the table gives the distance from the sample to each detector and the last one (N_d/N_e) is the quotient between the emitted neutrons (N_e) and those detected (N_d). All the detector were calibrated with an Am-Be source. According to this, the smallest signal we were able to separate from the background corresponds to 1n/s emitted by the sample. All the nuclear experiments were accomplished in a thermostized room where temperature variations were less than $\pm 1°C$. The neutron-gamma discrimination for both liquid scintillators (BC501 and NE213) was checked by using the Am-Be neutron source. Rise time spectra from this calibration are shown in Fig.2. In the same figures the channel where the discrimination is placed is indicated by an arrow. In all experiments counts from the two detectors were recorded as a function of time (or temperature) with MCA's (from Camberra) used in a MCS mode. Simultaneously the energy spectrum from the NE213 was taken in all experiments. Signals from the BF$_3$ dosimeter were taken in a pen recorder and with an electronic pulse counter.

The samples were thermally cycled between temperatures around the critical one. Table II shows the characteristics of all the nuclear experiments accomplished. T_c refers to the critical temperature of the phase transition. T_{max} and T_{min} indicate the upper and lower temperature values of thermal cycles. Finally, the last part of the Table gives the detected signal averaged over different detection times (1h. and 10s.). In all cases the measured signal were below the background level.

Fig.3 and 4 show part of one of the experimental results. Fig.3a is the evolution of the sample temperature during the thermal cycles of the experiment no.8. In Fig 3b the counts per hour from the NE213 detector during the experimental time and during a blank are shown as a function of the cycling time, 3σ is indicated by a bar. Fig.4a and b are equivalent to Fig.3b but for the BC501 and BF$_3$ detectors. It is clear from the figures that no significant signal is detected by anyone of the three detectors. Therefore no correlation can be established between the phase transition and possible cold fusion nuclear reactions.

Sample characteristics				Experimental characteristics					Neutron measurements				
									NE213		BC501		BF₃
#exp	Mass (g)	x=D/Ti	T (°C)	T max (°C)	T min (°C)	HR/CR (°C/m)	duration (min)	#cycle	Ne(1h) (n/s)	Ne(10s) (n/s)	Ne(1h) (n/s)	Ne(10s) (n/s)	Ne(10s) (n/s)
1	.571	1.96	21	60	-60	3	447	4	<3.8	<440	<3.2	<160	<131
2	1.180	1.92	40	60	-60	3	447	4	<4.4	<440	<3.1	<165	<126
3	1.180	1.92	40	60	-60	3	448	4	<4.7	<450	<3.4	<165	<139
4	.571	1.96	21	60	-60	0.5	501	1	<4.0	<450	<3.0	<138	<153
5	.571	1.96	21	60	-60	0.5	500	1	<4.6	<440	<3.1	<140	<167
6	1.180	1.92	40	60	-60	0.5	500	1	<4.6	<440	<3.1	<140	<167
7	1.180	1.92	40	50	30	3	500	20	<4.5	<440	<3.0	<137	<160
8	1.180	1.92	40	60	-60	3	4374	40	<4.6	<65*	<3.0	<29*	<139

*Time interval 2 min.

CONCLUSIONS

1) The influence of the preparation method on the reproducibility and quality of the $TiH_x(D_x)$ samples has been analyzed and explained.

2) It has been defined a method to prepare in a reproducible way stoichiometric TiD_2 samples.

3) On preparing the samples it has been found that cooling rate during the β-δ phase transition is the more important factor affecting the ϵ-δ phase transition quality

4) No correlation has been found between the ϵ-δ phase transition and cold fusion reactions as indicated by the neutron measurements. Experiment to measure whether or not tritium atoms are produced during the experiments are in course.

Acknowledgements

References

1)T.Izumida et al., Fusion Technology, 18(1990)641-646
2)I. Boltyukov et al, Fusion technology, 20(1991)234-238
3)Z.M.Azarkh and P.I.Gavrilov, Soviet Physics-Crystallography, 15(1970)231-234
4)C.Korn, Physical Review B, 17(1978)1707-1720
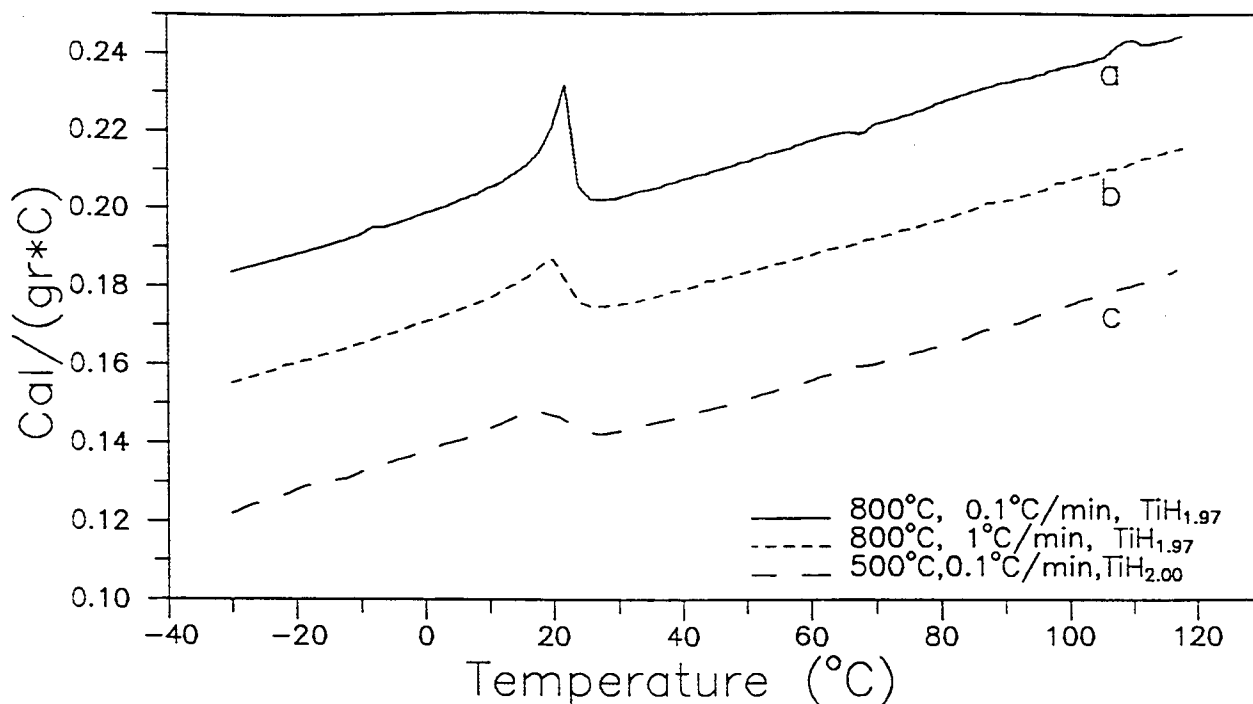
Fig.1 Specific heat of TiH$_x$ samples on crossing the cubic-tetragonal phase transition.
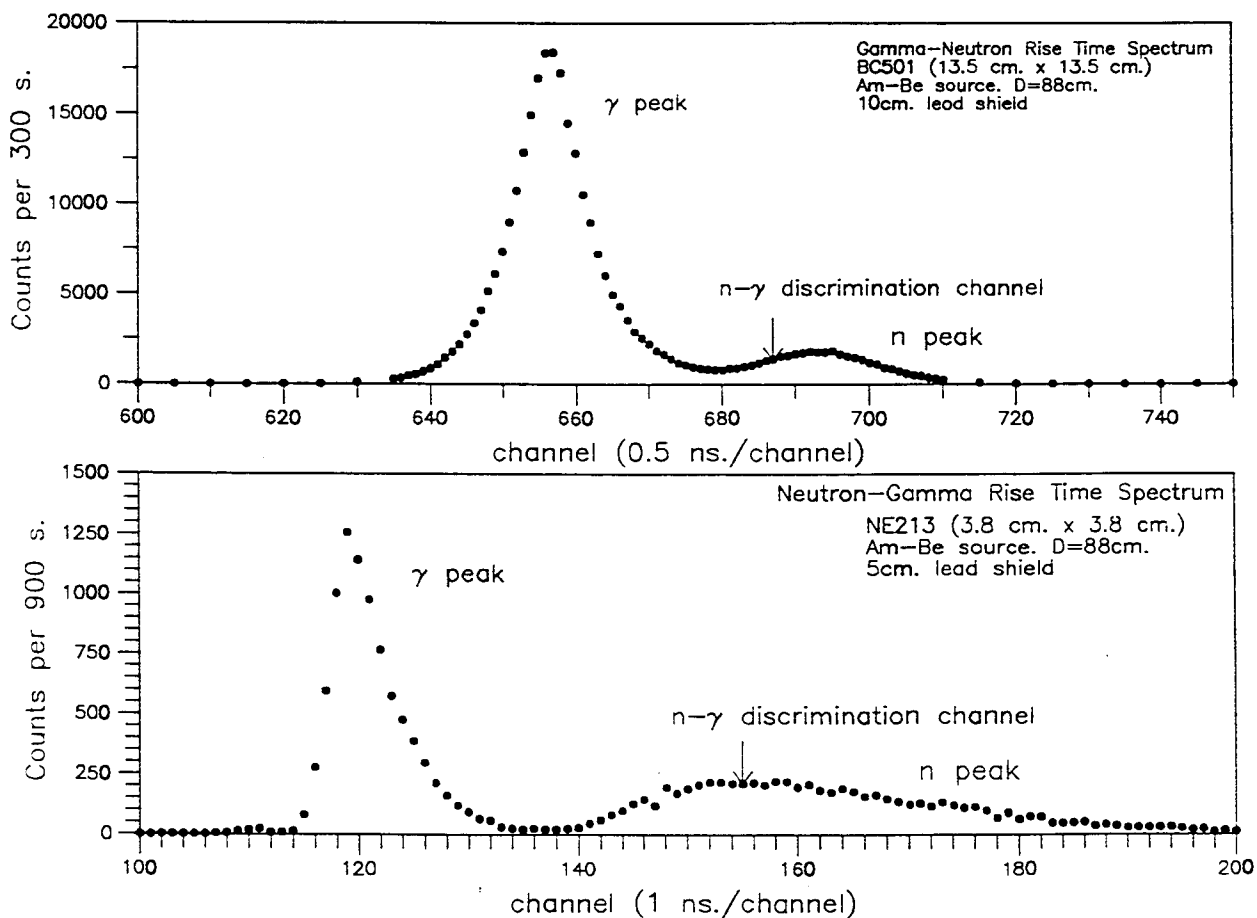
Fig.2 Rise time spectrum for both liquid scintillators obtained with an Am-Be neutron source

11-5
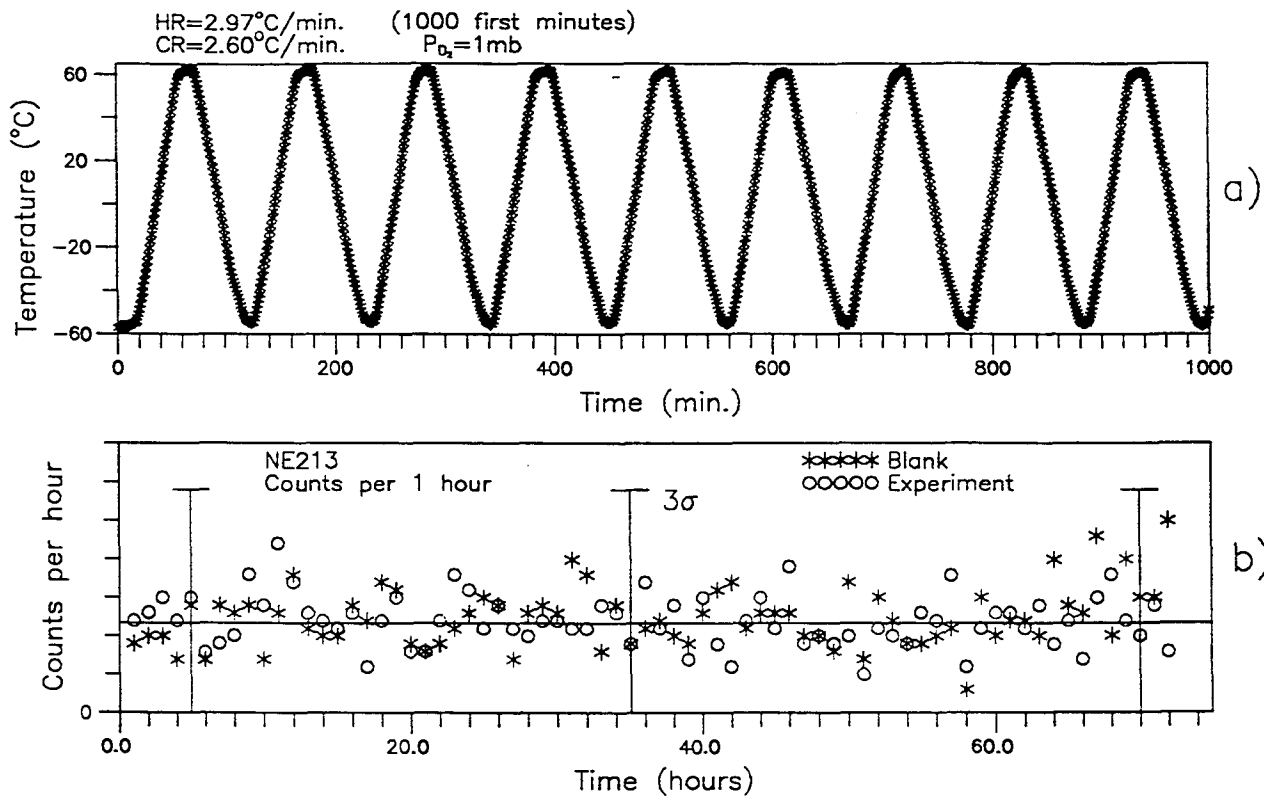
Fig.3 a)Evolution of temperature in experiment n°8
b)Neutron counts in NE213 . Same experiment
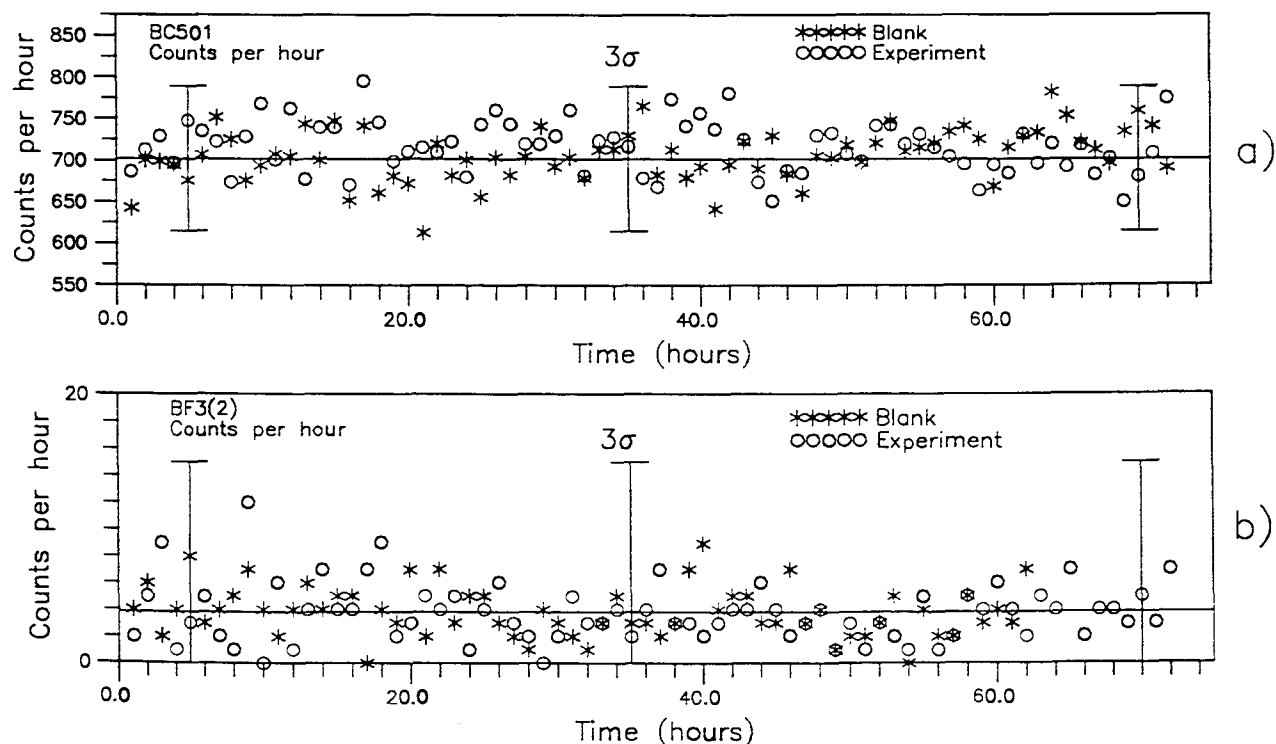
Fig.4 Evolution of the neutron counts during the
experiment n°8. a)BC501   b)BF₃

Observation of Anomalous Nuclear Effects in D_2-Pd System

Yasuhiro Iwamura, Takehiko Itoh and Ichiro Toyoda
Advanced Technology Research Center,
Mitsubishi Heavy Industries, Ltd.
1-8-1, Sachiura, Kanazawa-ku, Yokohama, 236, Japan

Abstract

Gas loading experiments have been performed with a method of heating deuterated palladium metals in a vacuum chamber to induce anomalous nuclear effects. Neutron emissions and tritium productions were observed in some cases when deuterium gas was released from the deuterated palladium samples with heating. It shows anomalous and unexpected phenomena occur in D_2-Pd system as reported in many papers on cold fusion.

1. Introduction

Research on cold fusion began in 1989 with the announcement of Dr. Fleishman and Pons[1]. Since cold fusion phenomena have possibility of being a new energy technology, considerable efforts have been paid to confirm their experimental results that nuclear reactions are electrochemically induced in D_2 -Pd system[2-4]. However, we still have much uncertainty on the nature of cold fusion phenomena.

The authors started the research on cold fusion from the begging of 1993, in order to clarify the nature of cold fusion phenomena and investigate its potentiality as a new energy source. In this paper, we performed gas loading type experiments in D_2-Pd system, and could observe neutron and tritium production several times.

2. Experimental methods

2-1 Preparation of deuterated palladium

Palladium samples loaded with deuterium gas were prepared as follows. Palladium sheets (25x25x1mm; Tanaka Kikinzoku Kogyo K.K.) were washed with acetone in a supersonic cleaning device and heated in the air at

573K for an hour to remove organic contaminants from the surface. After that, we cooled down the samples to room temperature (~ 298K) in deuterium gas. After loading (D/Pd ~ 0.66), we kept the deuterated palladium samples in liquid nitrogen temperature (77K) for several hours. Usually it takes more than a week to finish loading. We estimate a loading ratio (D/Pd) by measuring mass change of a palladium sample caused by absorption of deuterium gas. Loading ratio we obtain in 1 atm is about 0.66. The samples were bring back to room temperature environment, and then gold or aluminum thin-film was vapor deposited onto both surfaces of the deuterated palladium in order to reduce the rate of deuterium gas release. We tried many kinds of pre-treatment methods. Some samples were heated in the air at 900K for two hours and were quenched in pure water instead of cooling the samples in liquid nitrogen.

2-2 Experimental system

The sample is introduced into a vacuum chamber and set on a heater located in it. Figure 1 shows a schematic view of experimental devices. The chamber is equipped with two He-3 neutron detectors (EG&G Ortec: RS-P4-0803-235), a NaI scintillation counter (Bicron: 2M2/2) for gamma-ray spectroscopy, a silicon surface barrier detector (EG&G Ortec: CU-020-450-300) for charged particle spectroscopy and a high-resolution quadrupole mass spectrometer (Ulvac: HIRESOM-2SM) for gas analysis.
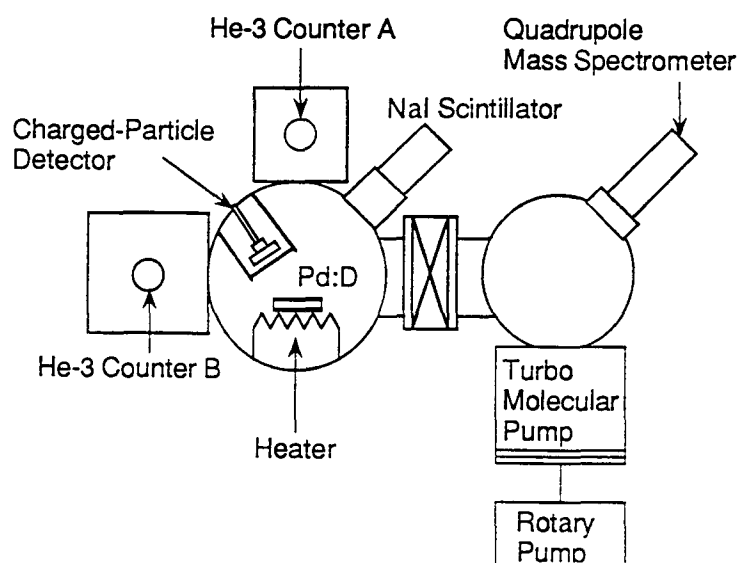
Figure 1 Schematic view of experimental devices

Neutron detectors surrounded with polyethylene modulators are used only for neutron counting. Counting system consists of preamplifiers (EG&G

Ortec : 142PC), amplifier and single channel analyzers (EG&G Ortec : 590A) and counters (EG&G Ortec : 996) which are connected to a personal computer by GPIB interface. As to gamma-ray spectroscopy system, we use a preamplifier (EG&G Ortec : 276), an amplifier (EG&G Ortec : 575A) and a multi-channel analyzer (SEIKO EG&G : MCA4100, 4200). Charged particle spectroscopy system consists of a preamplifier (EG&G Ortec : 142B), an amplifier (EG&G Ortec : 570) and a multi-channel analyzer (SEIKO EG&G : MCA4100, 4200).

All these devices are located in a clean-room where temperature and humidity are always controlled at constant levels (23°C±1°C, 40%±5%) in order to prevent contamination and false counts induced by humidity in the air. We always monitor electrical signals from these detectors by digital storage oscilloscopes to confirm that the signals originate from true nuclear events.

2-3 Experimental procedure

As a way to induce anomalous nuclear effects, we heat the sample and make deuterium in the palladium metal released out. The reason is that the authors consider that anomalous nuclear effects occur in deuterium diffusion process or recombination process on the surface. If we heat the deuterated palladium sample kept at room temperature up to about 400K, deuterium atoms contained in the palladium metal move toward the gold or aluminum thin-film surfaces of the sample and then release out as deuterium gas. We observed neutron, tritium and charged particle emissions several times during deuterium gas desorption from the samples by heating.

Experimental procedure is as follows.
(1) Pre-treatment of a palladium sample (washing and annealing)
(2) Loading
(3) Calculation of D/Pd ratio
(4) Surface modification (gold or aluminum vapor deposition)
(5) Set the deuterated sample into the vacuum chamber.
(6) Evacuating the chamber (~10^{-6} Torr)
(7) Begin to measure neutron, gamma-ray, charged particle, pressure in the chamber, temperature of the heater and start up the quadrupole mass spectrometer
(8) Heating the sample up to 400K
(9) Observation
(10) Heater off

3. Results and Discussion

3-1 Neutron emission

Figure 2 shows an example of experimental results on neutron emission. This sample has gold thin film on it, and D/Pd is 0.66. In this
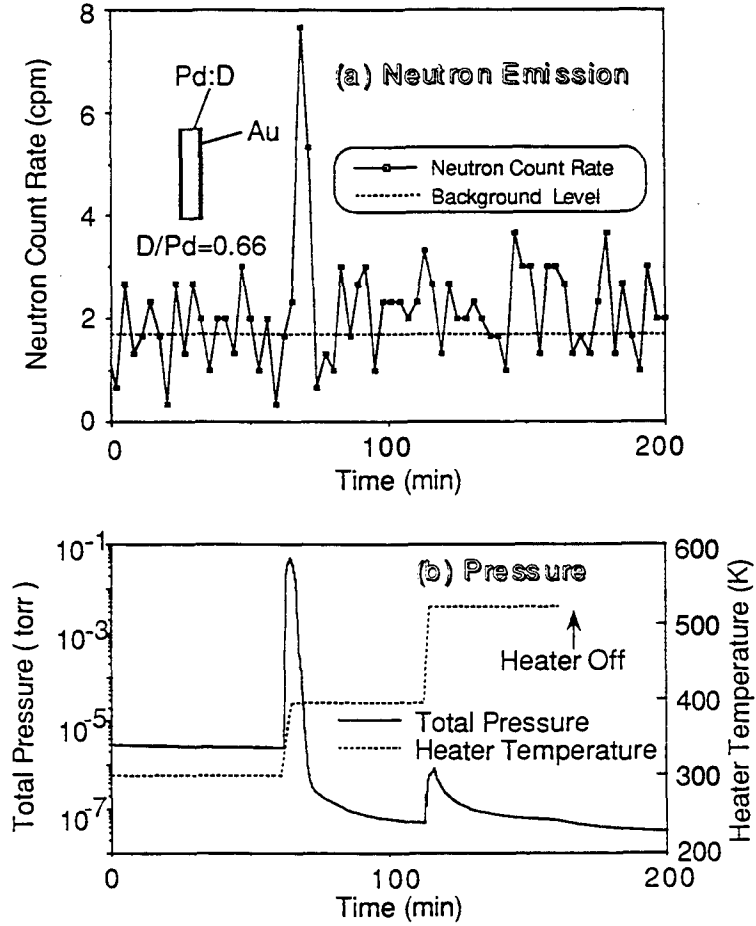
Figure 2 Neutron emission

experiment, we had only a single neutron counting line. At the beginning, heater temperature equals to room temperature, then we can see only background neutron counting. With heating the sample up to 400K, we can see in Fig.(b) that total pressure in the vacuum chamber increases and decreases rapidly. Simultaneously a clear and prominent neutron emission peak is observed as shown in Fig.(a). After heating up to 520K, we cannot see any peak in Fig.(b). It is considered that in the case of heating up to 520K, the release rate of deuterium gas, which is closely related with diffusion process of deuterium atom in palladium lattice and recombination process on the sample surface, is not adequate to induce neutron emission. However, the reason why neutron emission occurs is not clear. The emission rate is estimated 4.0×10^2 (neutron/sec) by using a Cf-252 calibration source, and that corresponds to the rate of 3.0×10^{-20} (event/sec/d-d pair).

3-2 Tritium production

An experimental result of mass spectrometric analysis of released gas from a sample is shown in Fig.3. D/Pd of this sample with gold thin film is 0.65. Since the resolution (M/ΔM) of this measurement is low (M/ΔM=60M), both signals shown in this figure are composed of DT(5.030 amu) and DDH(5.036 amu). The signal for mass number 5 (DT+DDH) after heating reaches about 6 times as large as loading D2 gas.
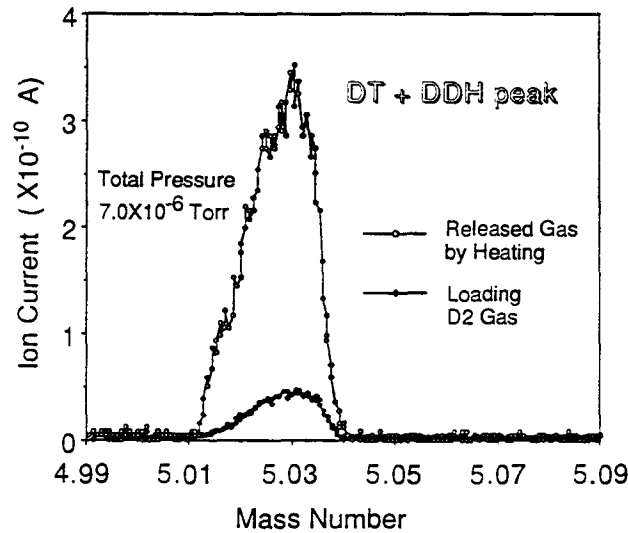
Figure 3 Mass spectrum for released gas
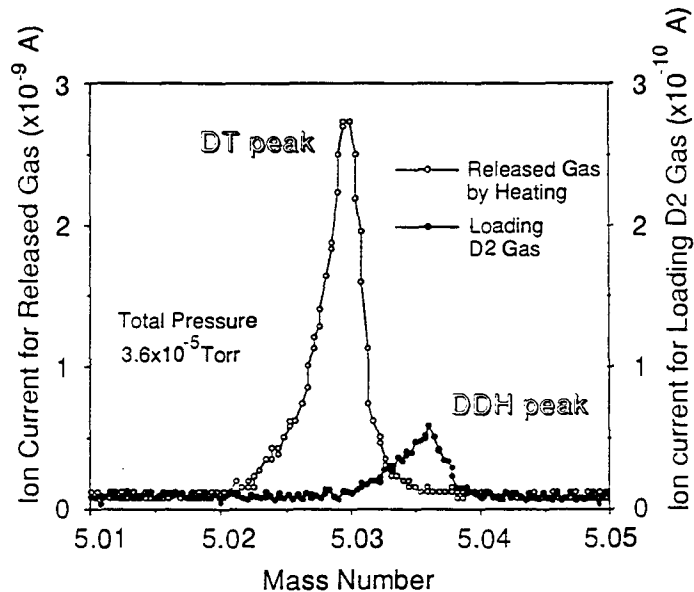
Figure 4 Separation of DT and DDH

12-5

In order to distinguish DT signal from DDH, the released gas from the sample and D_2 gas used for loading were analyzed with high resolution($M/\Delta M$=250M). Figure 4 shows a result of the high resolution measurement. Mass difference between the peak for released gas and the peak for loading gas is 0.006 amu. These peaks for released and loading gas correspond to DT and DDH, respectively. We can see that DT signal was about 50 times as large as DDH signal. Therefore it demonstrates that DT is dominant in the released gas around mass number 5. We can say that certain tritium production mechanism exits in our experimental process.

It is possible to consider that signal of mass number 5 after heating in Fig.3 is also attributed to DT. Although we can distinguish DT from DDH by high resolution operation, there is a demerit that we lose sensitivity instead of obtaining high resolution. Therefore we chose to monitor mass number 5 with low resolution and high sensitivity, since the sensitivity was important for measurement of time evolution of DT.

3-3 Neutron and tritium production

An experimental result on neutron and tritium production with time evolution of total pressure in the vacuum chamber is shown in Fig.5. The atomic ratio D/Pd of this sample, which has aluminum thin film, is 0.66. Two independent He-3 counters are used to improve neutron counting reliability. Concerning tritium production, we measured only peak value of the signal for mass number 5 detected by the mass spectrometer. We define DT+DDH breeding ratio as shown in the figure, and it is normalized by the measured value of loading D_2 gas. If DT+DDH breeding ratio is larger than 1.0, it means that the released gas from the sample contains more DT and DDH than D2 gas used for loading. Furthermore, it is considered that most of the released gas consists of DT as we described before.

After heating the sample up to 400K, we can see sudden increases of total pressure, neutron count rate and DT+DDH breeding ratio simultaneously. It shows that both neutron and tritium are generated with deuterium gas release from the sample. Coincidence of neutron and tritium production with deuterium gas release has been observed several times.

A larger neutron emission peak can be seen after about 40 minutes of the first neutron emission. We also experienced to observe similar phenomena in the other samples. The authors consider that these phenomena are related with the diffusion process of deuterium atom, since the time for diffusion through 1mm thick palladium metal at 400K is about several ten minutes[5-6] and it corresponds to the delay time of the second neutron emission.
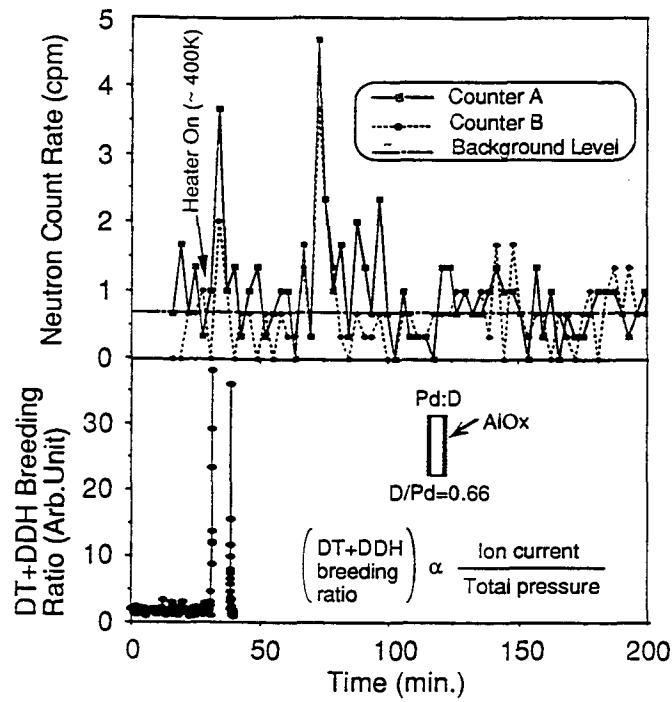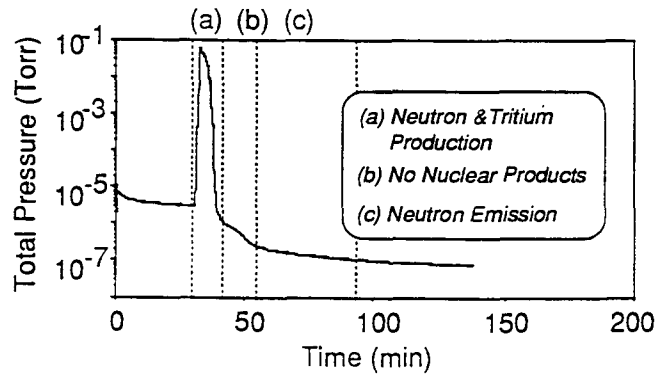
Figure 5 Neutron and tritium production

3-4 The other nuclear products

Up to the present, gamma-rays which would emitted from deuterated palladium samples have never been detected. However, we observed charged particle spectra several times during deuterium gas release from some quenched samples covered with aluminum thin film. Mass number of charged particles can not be specified at present, since only one detector for charged particle is available. Therefore the authors will show the spectra after specifying what type of charged particles are produced in the samples.

3-5 Reproducibility

Reproducibility on neutron emission and tritium production is summarized in the table 1. The number-of total samples is about 50. Criteria for neutron emission and tritium production are also shown in the table. We experienced that some deuterated palladium samples did not show any nuclear effects with the same experimental procedure. It suggests that the nuclear effects we observed depend on the hidden condition of the sample.

Table 1 Reproducibility

	Neutron	Tritium
A	6%	3%
B	9%	60%
C	85%	37%

Criteria	Neutron emission statistical significance	DT+DDH Breeding Ratio
A	$> 5\sigma$	$> 10^2$
B	$3\sigma - 5\sigma$	$10 \sim 10^2$
C	$< 3\sigma$	< 10

With regard to neutron emission, only 15% of total samples emitted statistically significant neutrons if we choose the criteria shown in the table. Reproducibility of tritium production is better than neutron emission, however, it is desirable to measure DT gas only by β-ray counting to decide quantitative tritium production rate. It is a next work to be done.

Reproducibility of our experiments is not good as it is shown in the table. Since the nature of cold fusion phenomena is still unclear, we cannot

control macroscopic experimental factors in order to cause anomalous nuclear effects that must be dominated by uncertain microscopic factors. It is necessary to investigate much more about cold fusion phenomena to establish this new field of science.

4. Conclusion

We heated deuterated palladium metals in the vacuum chamber and made deuterium gas in the samples released out, assuming that anomalous nuclear effects occur in deuterium diffusion process or recombination process on the surface. As a result of it, neutron emission and tritium production induced by deuterium gas release have been observed several times. Coincident neutron emission with tritium production has been also observed. However, reproducibility of our experiments is not good at present. It is considered that these anomalous nuclear effects in D_2-Pd system are attributed to cold fusion phenomena reported in many papers.

References

1. M. Fleishmann and S. Pons, J.Electroanal. Chem., 261 (1989) 301
2. A. Takahashi et al., Int. J. Appl. Electromag. Materials, 106 (1992) 1
3. J. Kasagi et al., Proc. of ICCF-3, Nagoya, (1993) 209
4. E. Yamaguchi and T. Nishioka, Proc. of ICCF-3, Nagoya, (1993) 179
5. F. A. Lewis, *The Palladium Hydrogen System*, Academic Press, 1967
6. Y. Fukai, *The Metal-Hydrogen System*, Springer-Verlag, 1993

.

Deuteron Fusion Experiment with Ti and Pd Foils Implanted with Deuteron Beams II

Toshiyuki Iida, Morio Fukuhara, Sunarno, Hiroyuki Miyamaru
and Akito Takahashi

Department of Nuclear Engineering, Faculty of Engineering,
Osaka University, Yamada-oka, Suita, Osaka 565, Japan

Abstract

Deuteron implantation experiments on Ti and Pd foils have been made for the examination of the "cold" deuteron fusion reaction. In the center of a target chamber fitted to a 300 keV deuteron accelerator, a Ti or Pd foil sample was set to face toward 3 nsec pulsed deuteron beams collimated with a 3 mmϕ aperture. A Si-SSD was placed behind the foil to detect high energy charged particles emitted from the foil by the supposed deuteron fusion reactions.

In the 243 keV deuteron implantation experiments for 3-20 μm Ti and 5-22 μm Pd foils, unusual counts and peaks were measured in the energy region higher than the proton peak due to the well-known D-D reaction. And from the energy loss measurement with the screen foil in front of the Si-SSD, some of the unusual high energy peaks were found to be helium, though the original reactions are not identified. These helium peaks and unnatural counts are difficult to be explained and might have something to do with the multibody fusion reactions proposed by A. Takahashi. More elaborate experiments with more detailed measurement such as correlated particle measurement should be necessary for confirmation of the multibody fusion reaction.

1. Introduction

Since Akito Takahashi, the leader of our group, proposed the very unique multibody fusion model [1][2] for explaining the large excess-heat produced in the D_2O/Pd electrolysis experiments[3][4][5], we have performed deuteron beam implantation experiments[6] with Ti and Pd foils. The goal of the deuteron beam experiments is to find out nuclear particles (energetic charged particles) which mean the evidence of the multibody fusion reaction. Vacuum environment in the beam implantation experiments is suited for the identification of nuclear reactions in a foil sample, i.e. for the exact measurement of the type and energy of the charged particles emitted from the foil. At first this paper describes the experimental method and some preliminary results obtained for Ti and Pd foil samples and then proposes a further research plan for more elaborate implantation experiments to confirm the multibody fusion reaction.

2. Experiment

It is supposed that fairly high energy charged particles are produced in the Takahashi's multibody fusion reactions. And such particles are possibly identified with energy analysis.

A 20 cmϕ x 24 cm cylinder-type vacuum chamber was installed to a 300 keV deuteron accelerator OKTAVIAN[7]. In the center of the chamber, a Ti or Pd sample foil was set to face toward the deuteron beam collimated with a 3mmϕ aperture. The configuration of the experimental apparatus is shown in Fig.1. A platform with a standard vacuum flange was made, and all components such as a sample foil, a silicon semiconductor detector (Si-SSD) and others were fastened to the platform with the same stand. The central portion of a foil sample was implanted with 3 nsec pulsed deuteron beams, whose repetition frequency was 2 MHz. The average beam current was 2-10 μA. To examine the nuclear charged particles from the foil, the Si-SSD was set behind the foil, which was for the avoidance of the disturbance of the deuteron beams. The Si-SSD was commercially available, had the effective window area of about 35 mm^2 and the depletion layer depth of about 150 μm and analyzed energy up to about 15 MeV for α-particles and about 4 MeV for protons. The distance between the foil sample and the Si-SSD was 15-30 mm. Another foil (Al or Ti) was occasionally placed in front of the Si-SSD for the examination of the types of particles emitted from the sample foil. The type of particles can be identified from their energy loss in the screen foil.

Sample foils had the thickness of 3-20 μm (Ti) and 5-22μm (Pd) and were penetrated by not 300 keV deuteron beams but ~ MeV charged particles due to nuclear reactions. Inside a sample foil, deuteron beams slow down and many deuteriums could come to exist in lattice atoms excited by repeated pulsed beams, which might lead to the opening of the multibody cold fusion reactions. As for some of the same sample foils, moreover, we formed about 0.1 μm thick Al layer on their surface by an evaporation process. The Al layer was oxygenated in the air. Such a thin metal oxide layer has influence on the deuterium trapping in the foil and is expected to be possibly effective in enhancing the cold fusion reactions [8][9][10][11]. A series of the deuteron implantation experiments was carried out under almost the same conditions of deuteron beams, the measuring system and others.
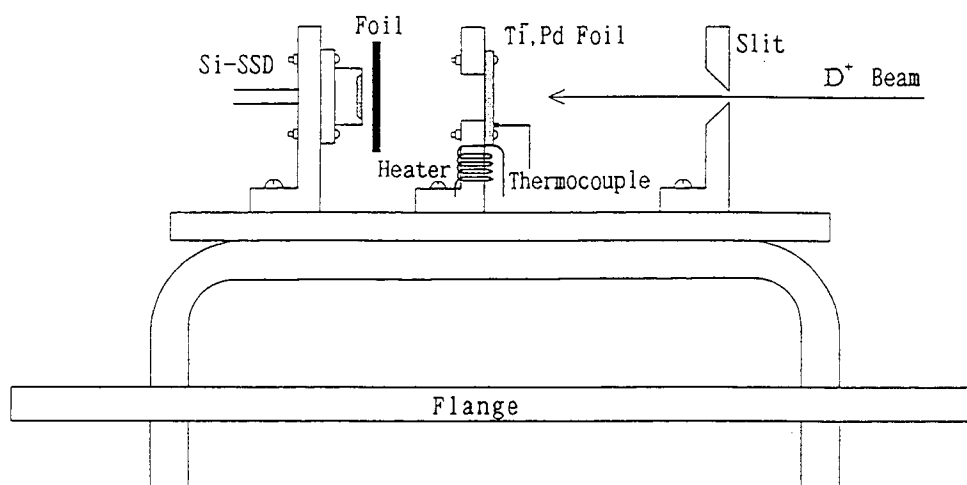
Fig.1 Configuration of experimental apparatus

3. Result and Discussion

Figure 2 shows an example of unusual energy spectra of charged particles measured for 20 μm Ti foil with aluminum-oxide layer bombarded by 243 keV deuteron beams. Besides the normal proton peak from the well-known D-D reaction, some counts (3 ~ 5 MeV) and a group of counts (8 ~ 9 MeV) were measured in the energy region higher than the proton peak, though statistics of the counts were low. And in the similar measurement with the screen foil in front of the Si-SSD, we observed that the 8-9 MeV counts were completely removed by a 40 μm Ti foil. From this, the 8-9 MeV counts are considered to be helium. Eight MeV hydrogen can easily penetrate the 40 μm Ti foil. These helium counts might have something to do with the 3D fusion reaction; 3D → D (15.9 MeV) ÷ ^{4}He (7.9 MeV). The 15.9 MeV D correlated with 7.9 MeV ^{4}He can not be analyzed with the Si-SSD because its depletion layer is too thin (150 μm). As for the 3-5 MeV counts, the type of the particles could not be identified because of the low statistics and the disturbance of the large proton peak.

Figure 3 shows a typical energy spectrum of charged particles emitted from a 5 μm Ti foil bombarded with 243 keV deuteron beams. This spectrum has a small sharp peak around 7 MeV and seems to be apparently different from that shown in Fig.2 in the higher energy region, though we do not see the reason. The similar energy loss measurement with screen foils was made especially for the four clear peaks (1.2, 2.7, 3.6 and 6.6 MeV peaks in Fig.3). Figure 4 summarizes results of the relation between the particle energy and the foil thickness. The range of 243 keV deuterons is about 1.5 μm and we assumed that above reactions all took place
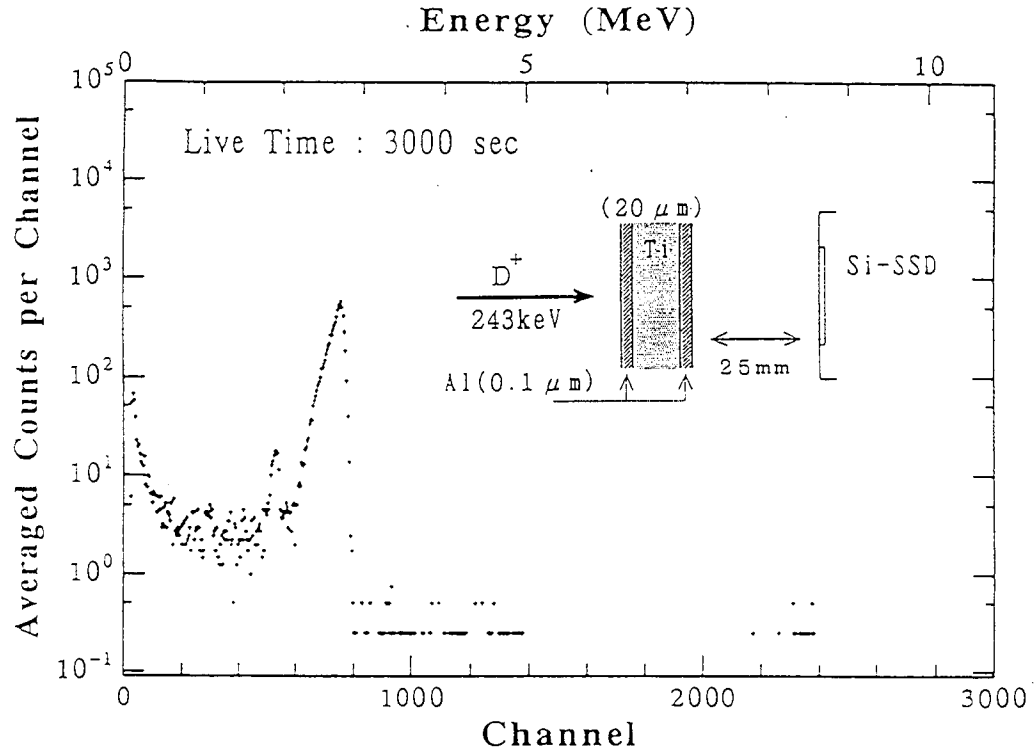
Fig.2   Unusual energy spectrum of charged particles measured for 20 μm Ti foil
with aluminum-oxide layer bombarded with 243 keV deuteron beams.

around 1 μm from the foil surface.   The energy loss curve for the 2.7 MeV peak (black circle) has close resemblance to that for the 3.6 MeV proton peak (white circle) due to the normal D-D reaction.   Therefore the 2.7 MeV peak is considered to be proton and seems to come from ^{12}C $(d,p)^{13}$C reaction in point of energy.   The case for the 6.6 MeV peak (triangle) has a larger decline in the energy loss than that for the triton peak (cross) due to the D-D reaction, and the 6.6 MeV peak is considered to be helium though its original reaction is not identified.

Table 1 summarizes unusual peaks and counts in the energy spectra measured in the present experiments.   Although these peaks and counts are unnatural and difficult of explanation, more significant data are needed for the discussion of the relation to the multibody fusion reactions.   At least data on correlated particles emitted in opposite direction should be necessary at least.

13-4
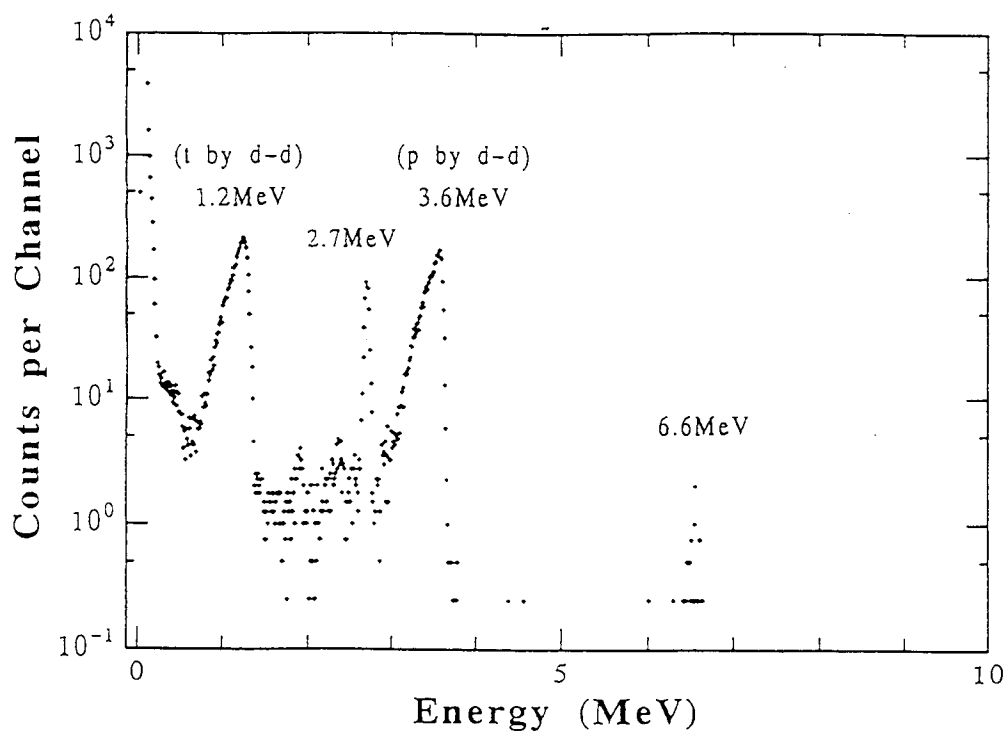
Fig.3. Unusual energy spctrum of charged particles emitted from a 5 mm Ti foil
bombarded with 243 keV deuteron beams

Table 1. Unusual peaks and counts of charged particles emitted from sample foils bombarded
with 243 keV deuteron beams.

Foil Sample (Thickness: μm)	Energy Range		
	3 ~ 5 MeV	5 ~ 8 MeV	8 ~ 12 MeV
Ti (3~20)	Some counts	peak (He)	None
Pd (5~22)	None	None	None
Ti (10~20) + Al (0.1)	Some counts	Some counts (He)	Peak (He)
Pd (12.5~22) + Al (0.1)	Some counts	Some counts	Some counts (He)
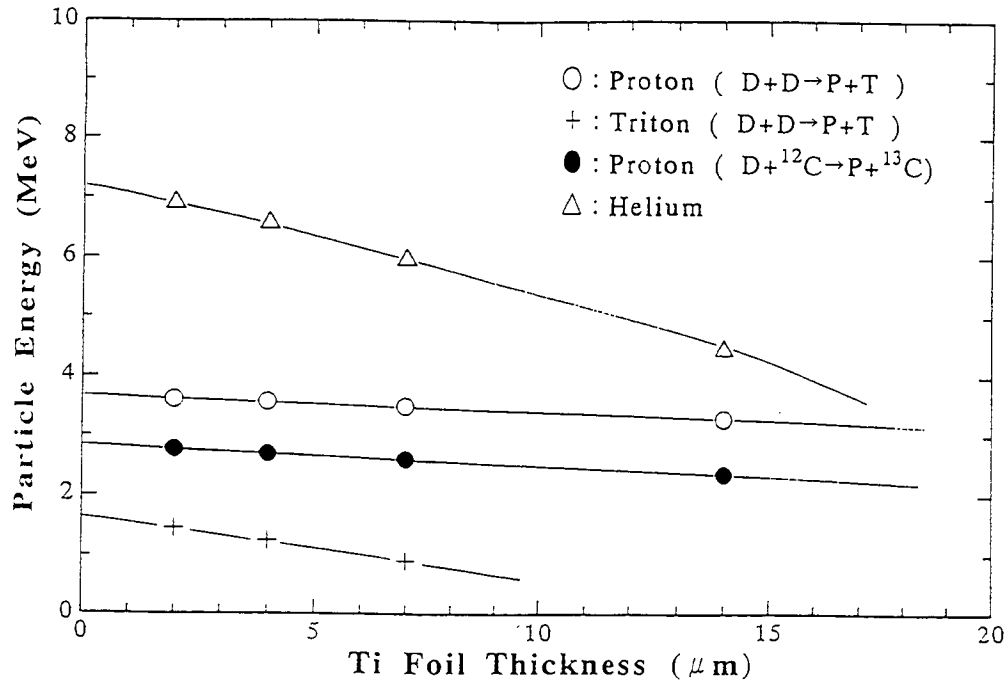
Fig.4 Relation between particle energy and Ti foil thickness

Figure 5 shows a schematic drawing of the experimental arrangement which is now in preparation. A pair of Si-SSDs with thick depletion layer depth and ΔE counters analyze the energy and types of the correlated particles emitted in opposite direction. Also an angle θ between the deuteron beam line and the detector is changed by a manipulator. This angle-dependent measurement should be also essential to the confirmation of the cold fusion reaction. If the reaction is caused by the direct impingement of deuteron beams, the energy of emitted particles must be determined from the kinematics, in other words, must vary exactly with the angle θ . The cold fusion reaction should not have such angle-dependent energy characteristics. Another Si-SSD or a microchannel plate (MCP) with time of flight (TOF) technique analyzes the energy of deuterons scattered by the sample foil. The energy spectrum of scattered deuterons gives the information on deuterium in the surface of the foil. The measurement of the deuteron-induced nuclear reaction and the deuterium profile analysis are to be made simultaneously.

300keV Pulsed D⁺

Aperture (3~5mmΦ)

$\left(\begin{array}{c}\text{Nuclear Reaction Measurement}\\ \text{—Correlated Particles—}\end{array}\right)$

Vacuum Level : 1×10^{-9} Torr

E Si–SSD

ΔE Si–SSD

Pd, Ti Sample Foil

Heater
(Temperature Control)

θ

Deflector
(Selecting Particles)

Screen Foil

P, D, T, He

ΔE Si–SSD
≦100 μm

E Si–SSD
~2mm

MCP (TOF)
Si–SSD

V

A

Thermocouple

$\left(\begin{array}{c}\text{Nuclear Reaction Measurement}\\ \text{—Correlated Particles—}\end{array}\right)$

(Deuterium Profile Measurement)

D

Pd

3MeV P

Fig. 5 Schematic drawing of new experimental arrangement

4. Conclusion

In order to examine the cold fusion reaction, 3-20 μm Ti and 5-22 μm Pd foils were implanted with 243 keV, 3 nsec pulsed deuteron beams. The energetic charged particles from the foils were measured with the Si-SSD which was placed behind the foil.

In the implantation experiments, unsual peaks and counts were measured in the energy region higher than the proton peak due to the well-known D-D reaction. And from the energy oss measurement with the screen foil in front of the Si-SSD, some of the unusual high energy peaks were found to be helium, though their original reactions are not identified. These helium peaks and unnatural counts are difficult of explanation and might have something to do with the multibody fusion reactions proposed by A. Takahashi, for example, $3D \rightarrow {}^4He$ (7.9 MeV)+D(15.9 MeV). However, the confirmation of the multibody fusion reaction requires more significant data at least about the correlated particles and the angle-dependent energy characteristics. More elaborate experiments with more detailed measurements should be necessary for further cold fusion research.

References|

1) Takahashi, A., 1989, J. Nucl. Sci. Tecnol., 26 [5], 558.
2) Takahashi, A. et al., 1991, Fusion Technology, 19, 380.
3) Fleishmann, M, and Pons, S., 1989, J. Electroanal. Chem. 261, 301.
4) Takahashi, A., 1992, Proc. Int. Symp. Nonlinear Phenomena in Electromagnetic Fields, Nagoya, 5.
5) Takahashi, A. et al., 1992, Int. J. Appl. Electromag. Materials, 3, 221.
6) Iida, T. et al., 1992, Frontiers of Cold Fusion, Proc. 3rd ICCF, 201.
7) Sumita, K. et al., 1990, Nucl. Sci. Eng., 106, 249.
8) Yamaguchi, E. and Nishioka, T., 1990, Jpn. J. Appl. Phys., 29, 2666.
9) Yamaguchi, E. and Nishioka, T., 1990, Proc. Anomalous Nuclear Effects in Metal/Deuterium Systems, 354.
10) Yamaguchi, E. and Nishioka, T., 1992, Frontiers of Cold Fusion, Proc. 3rd ICCF, 179.
11) Takahashi, A. et al., 1992, Frontiers of Cold Fusion, Proc. 3rd ICCF, 79.

Behavior of Key Elements in Pd for the Solid State Nuclear Phenomena Occurred in Heavy Water Electrolysis

M. Okamoto, H. Ogawa, Y. Yoshinaga, T. Kusunoki[*], and O. Odawara[**]
Research Laboratory for Nuclear Reactors
Interdischiplinary Graduate School of Science & Engineering [**]
Tokyo Institute of Technology
Ookayama, Meguro-city, Tokyo 152 Japan

Present address:Japan Atomic Power Co.Ltd.Tsuruga-city,Japan[*]

Abstract

The behaviors of some key elements in Pd cathodes used for study of solid state nuclear phenomena have been studied by means of a SIMS analysis of Li, D, Pd, Si, Na, and Al. The mechanism of the anomalous accumulation of deuterium in the surface of Pd electrodes is discussed based on the depth profiles of these elements obtained from the Pd cathodes which gave no nuclear effect, neutron emission, and neutron and excess heat, respectively.

Introduction

The behaviors of the key elements in Pd cathode have been discussed with respect to the occurrence of the solid state nuclear phanomena. As discussed in our previous report, (1)the anomalous accumulation of deuterium is the most significant process to realize the solid state nuclear phenomena. Lithium has been used as the most relevant electrolyte for the electrolysis method, but there is only one discussion on the role of the lithium for the occurrence of the solid state nuclear phenomena.(1) In this discussion, we proposed a hypothetical process for the anomalous accumulation of deuterium based on the intermetallic compounds of Li-Pd, and showed the clear correlation between the anomalous accumulation of deuterium in the surface region of Pd electrode and the neutorn emission. In the present work, we provided a set of Pd electrodes which can be classified into three categories:(1)Pd with no nuclear effects, (2)Pd with neutron emission , and (3)Pd with neutron emission and excess heat generation. The SIMS analysis has been carried out on the above Pd samples to clarify the process of the anomalous accumulation of deuterium and to discuss the excess heat evaluation method.

Experiment

The Pd samples were obtained by a High/Low pulse mode electrolysis described elsewhere in this proceedings by the present authors. The analysis of

the key elements was performed on a secondary ion mass spectrometer(Model IMS-4S, CAMECA/France). The primary ion used was oxygen(O_2^+) and its accelerated velocity was 15.1keV, and the resolution power (M/ Δ M)is more than 15,000.

Results and Discussion
SIMS results

The examples of the depth profiles of D, Li, Pd, Si, and Al are illustrated in Fig.1 and Fig.2. The profiles with bold line represent the depth profiles of each elements obtained from the Pd sample with the nuclear effect of neutron emission and excess heat generation, the medium line for Pd sample with only neutron emission, and the chain-line for Pd sample with no nuclear effect. The curves shown in these figures are normarized to the secondary ion intensity of Pd obtained in each analysis run to carry out the discussion on the concentrations on the same elements. Evidently from the figures, the depth profiles of the elements with no nuclear effects are monotonous as expected from the electrochemical point of view. (2)While, the depth profiles with some nuclear effects have some of irregular structures, especially in the surface within 2 μ m for every element. The depth profiles of lithium and deuterium are very similar in each. This fact indicates that there is a very strong chemical relation between the lithium behavior and the deuterium behavior as discussed in the previous paper.
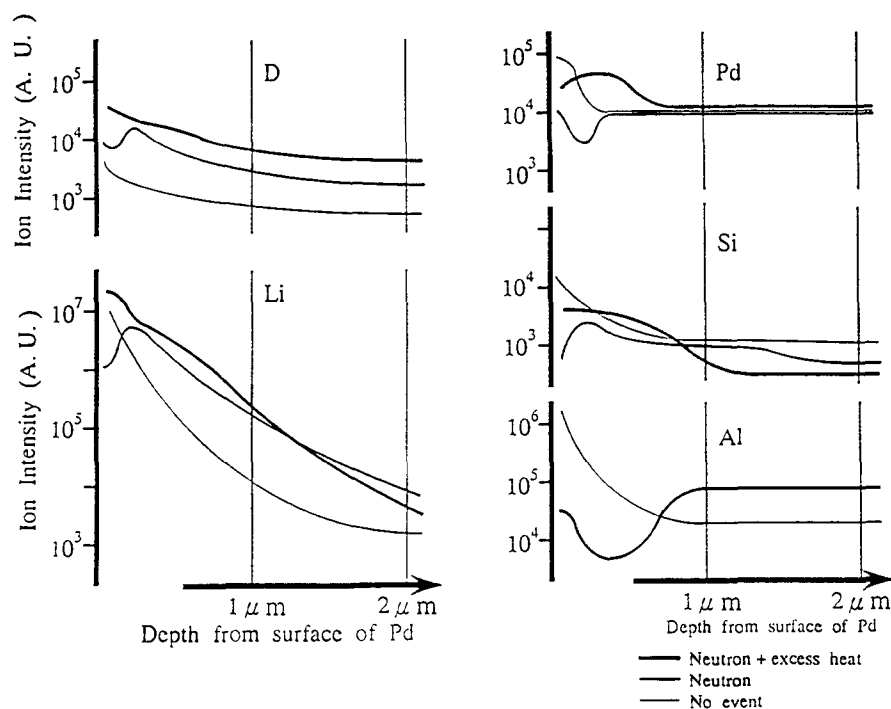
Fig.1 Examples of Depth Profiles for Each Element

14-2

The depth profiles of the deuterium are very interesting not only in the structures but also in the concentrations. The deuterium absorbed into the Pd by the electric force releases easily to the solution phase when the force is off. The sample Pd plates were stocked for more than one week or for three months till the element analysis by SIMS, in the present study. The SIMS analysis gave us only the traces of deuterium accumulation like an archeology. Even so, the significantly large amount of deuterium remained in the surface area of the sample Pd. From this consideration, it can be concluded that the more deuterium had been accumulated when the electrolysis was carried on. The anomalous accumulation of the deuterium should be recognized to have an important correlation to the occurrence of the nuclear effects.

Accumulation process of deuterium

As shown schematically in Fig.3, the cell voltage increased with the increase of the H/L pulse cycle in the present constant current operation. This indicates that the electric resistance of the Pd electrode increased in the way of the electrolysis. We have a hypothesis based on the chemistry of Pd-Li intermetallic compounds and Pd-Li-D compound reported by O.Loebich and J. Raub, and by B.Nacken and W. Bronger, respectively.(3,4) The hypothesis is that by the electrolysis of the D_2O-LiOD solution lithium also migrates into tne metallic Pd and formes the very stable intermetallic compounds, so the electric resistance of Pd surface increases, resulting the increase of the cell voltage. As illustrated in Fig.4, the intermetallic compound layer works as the barrier for the back migration of the deuterium when the current density is reduced from the high mode to the low mode. The depth profiles at the equilibrium state of the high mode operation and low mode operation can be illustrated as shown in the lefthand side of Fig.5. When the operation mode changed from the high mode to the low mode, the equilibrium depth plofile of the high mode should be changed to the low mode operation by the back migration of the deuterium. However, the intermetallic compound layer works as the barrier the amount of the deuterium corresponded to the shaded area in the high mode operation retaines at the righthand side of the intermetallic compound layer as illustrated in Fig.5. The next high mode operation starts with this depth profile. The repeating of the high mode and the low mode operations, the layer of the intermetallic compound becomes thicker and the concentration of the deuterium increases with increase of the cycle number of the high and low mode operation. The concentraitons observed [archeologically] in the above Pd electrodes with the nuclear effects are higher almost one order than that of no nuclear effect. It can be concluded that the present high and low mode operation enables us to provide an
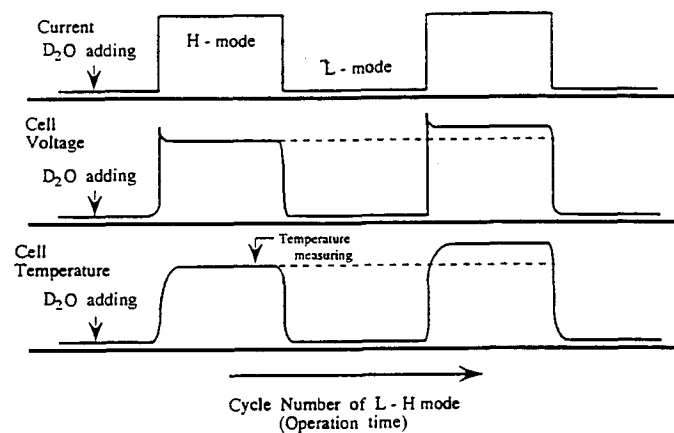
Fig.3 Schemes of Electrolysis
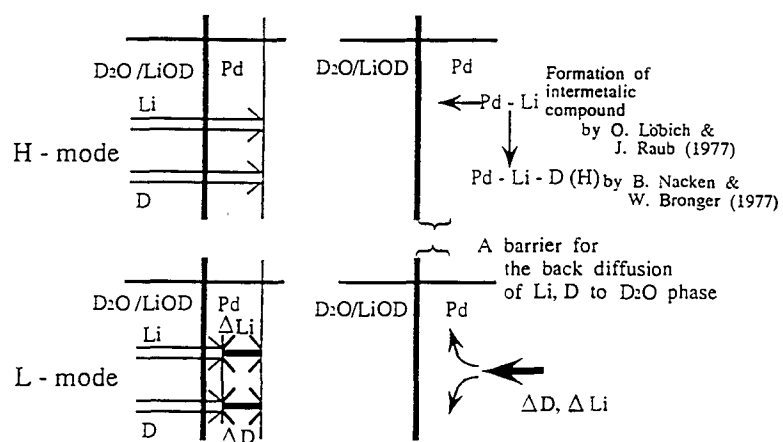
Fig.4 Role of Metallic Layer
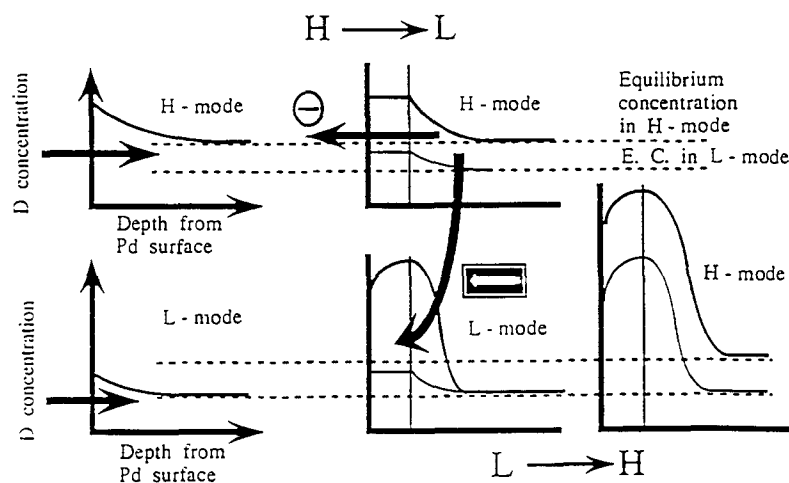
Fig.5 Model of D Accumulation Process

14-4

anomalously high density zone of the deuterium in Pd electrode occasionally. The depth profiles of Si and Al have the irregular structures but just reversal each other. When these elements coexist, Al can be excluded by Si which formes more stable intermetallic compound with Pd. The profiles are the trace of the above chemistry.

The irregular structures of Si and Al were observed only in the Pd electrode with the neutron emission and the excess heat generation(Run No.3). These two elements seems to have some key roles to the occurrence of the nuclear effects in D_2O electrolysis through the anomalous accumulation of deuterium.

The excess heat evaluation

In the present high and low mode operation, the electrical resistance of the Pd electrode increases with the increase of the number of the pulse mode cycles. The calibration of the cell temperature as a function of the input power should be changed along with the electrolysis operation, unlikely discussed by Mizuno and Takahashi et al.(5,6) The excess heat has been evaluated from the upper deviation of the cell temperatures from the calibration curve obtained before the full-operation of the electrolysis or by use of inert metal electrodes. When the cell temperature depends on the cycle number of the high and low mode operation as mentioned above, the calibration should not be the same before and after the full-operation of the electrolysis. A typical example of the dependency is illustrated in Fig.6 along with the cell voltage dependency on the input power. The calibration curve obtained after the full-operation should deviate upward because of the increase of the electrical resistance of the Pd electrode in the high and low mode of electrolysis . We have confirmed this in our electrolysis cell equipped an excess heat monitoring system. In Fig.7, a couple of typical examples of calibration curves before and after the operation are shown as a function of the input power. An upward diviation is observed in the calibration curve after the electrolysis as expected above. In this case, the upward deviation of the cell temperature of $\sim 0.2°C$ from the calibration curve before the full-electrolysis can not be concluded as the excess heat generation. Based on the fact, for the evaluation of the excess heat in the present open system, the calibration curves should be obtained at least two times, before and after the full operation. In the excess heat evaluation from the present cell temperature measurement, a linear function was introduced as a corrected calibration curve by connecting the last point of the calibration curve after the full-operation and the first point of the calibration curve before the full-operation. The plots of the cell temperature are shown in Fig.8. These cell temperatures are average values obtained from the three thermocouples placed around the electrodes as described in other paper by

the present authors in this proceedings. In this electrolysis, it can be said that we detected the excess heat clearly, but the feature of the excess heat generation is not continuous unlikely to the previous report.
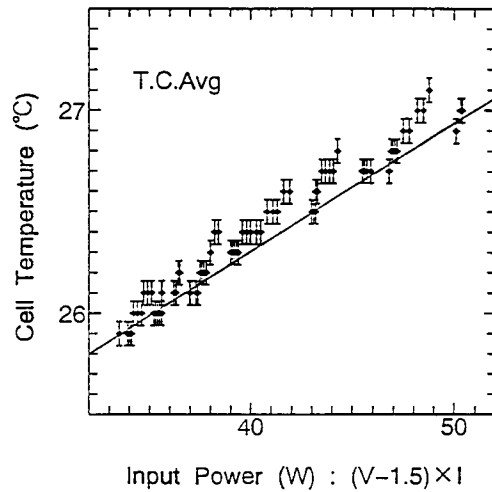
Fig.6   Typical Example Plots of
Excess Heat Evaluation
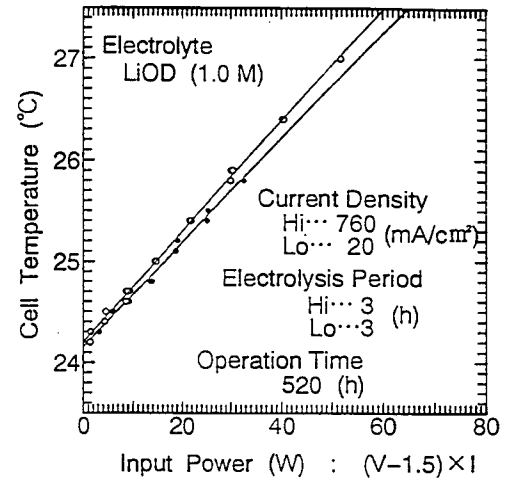
● : Calibration line measured before electrolysis
○ : Calibration line measured after electrolysis

Fig.7   A Couple of Calibration Curves
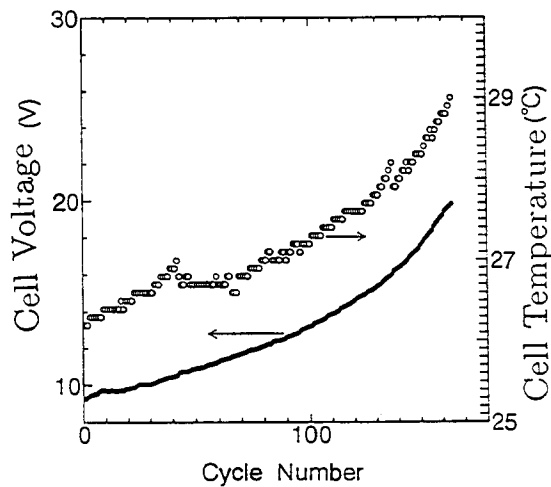
Fig.8   Cell Voltage and Cell Temperature vs. Input Power

Conclusion

Based on the SIMS analysis data, the anomalous deuterium accumulation in the surface area of the Pd electrodes which gave the nuclear effects including the excess heat generation has been confirmed and the deuterium concentration was

14-6

found to be in the sequence of

Pd with the excess neutron emission with the excess heat generation
V
Pd with the excess neutron emission
V
Pd with no nuclear effect.

The process of the anomalous accumulation of deuterium was discussed based on the formation of the Pd-Li intermerallic compound in the surface area of Pd electrode. According to the formation of the intermetallic compound, the electric resistance of the Pd electrode increases, the calibration curve for the evaluation of the excess heat in the open cell system should be obtained not only before the full-operation but also after the full operation. The calibration curves obtained by use of inert metals as the electrodes give an over estimation of the excess heat, because, even if they form some intermatallic commpounds, the electric resistance by the formation may be smaller than the case of Pd. For further quantitative discussion of deuterium based on nuclear phenomane in the solid state, the absolute concetration of the deuterium should be determined in real time and the evidences attributed to the nuclear phenomena also should be detected in real time with the excess heat monitoring.

References
(1)Mutsuhiro Nakada, Takehiro Kusunoki, Makoto Okamoto and Osamu Odawara. A Role of Lithium for the Neutron Emission in Heavy Water Electrolysis, Frontiers of Cold Fusion, Tokyo : Universal Academy Press, 1992. pp.581-586. [book]
(2)Kenichirou Ota, Hideaki Yoshitake, Osamu Yamazaki, Masaaki Kuratsuka, Kazuhiro Yamaki, Kotoji Ando, Yoshihiro Iida and Nobuyuki Kamiya. Heat Measurement of Water Electrolysis and the Electrochemistry, Abstract of ICCF-IV, Hawaii Dec. 1993. pp.C-2.7.
(3)J.H.N.Van Vucht and K.H.J. Buschow. Note on the Occurrence of Intermerallic Compounds in the Lithium-Palladium System. J.Less-Common Metals, 1976. pp.345-347.
(4)O.Loebich, Jr. und Ch.J.Raub. Das Zustandsdiagram Lithium Palladium und Die Magnetischen Eihgenschaften Der Li-Pd-Legierungen, J.Less-Common Metals, 1977. pp.67-76.
(5)Tadashi Mizuno, Tadashi Akimoto and Kazuhisa Azumi. Cold Fusion Reaction Products and Behavior of Deuterium Absorption in Pd Electrode, ibid.

pp.373-380.

(6)Akito Takahashi, Akimasa Mega, Takayuki Takeuchi, Hiroyuki Miyamaru and Toshiyuki Iida.   Anomalous Excess Heat by D_2O/Pd Cell under L-H Mode Electrolysis, Fronties of Cold Fusion, Tokyo : Universal Academy Press 1992 pp.79-91. [book]

REPRODUCIBILITY OF TRITIUM GENERATION FROM NUCLEAR REACTIONS IN CONDENSED MEDIA

V.A.Romodanov, V.I.Savin, V.V.Elksnin

142100 Podolsk, Moscow Region, Zheleznodorozhnaya 24,
SRI of SPA LUTCH
Tel.: 095-137-9258
Fax: 095-137-9384

Ya.B.Skuratnik

SRPCI named after Karpov, Obukha 10, Moscow

ABSTRACT

In this work on the basis of the proposed model and the results
of practical activity in the nuclear reactions in condensed
media (NRCM) field we try to discuss the limits of the main
parameters of the ion bombardment by using a glow discharge as
an example and to specify the requirements to them and to the
used materials for the purpose of obtaining some reproducible
results on tritium generation.

We have formulated some practical recommendations for the ion
bombardment systems to obtain 100% reproducibility of tritium
generation at a level of 10^6 - 10^7 atom/s by means of NRCM.

We have been discussing the methods of the bombardment system
modification to improve their efficiency when potentially
using NRCM for practical purposes.

1. INTRODUCTION

The nuclear reactions in condensed media (NRCM) have been
still studied rather in breadth than deep into. As a result,
at present reliable results of investigations of practically
all types don't exceed the background noise level much. To our

mind, that can be explained both by poor reproducibility of the basis investigation method (electrolysis) and seeming simplicity of obtaining different nuclear reactions when interpreting the results close to the background noise ones. The former caused a great number of negative results and made one doubt as to existence of the above-mentioned nuclear effects. The latter caused the fact that some investigators ignored Coulomb barrier and tried to attribute the results of the experiments which were not rather correct to the reactions which were hardly propable even at higher energies.

The experiments made by E.Yamaguchi, when some heat was released and a great number of ^{4}He was registered /1/, and those made by R.Bush, when some heat and X-radiation were correlated /2/, are very convincing, but one shouldn't consider them to be the final solution of the problem yet. In the experiments made by Jamaguchi the heat was released when desorbing both protium and deuterium and ^{4}He was released only when desorbing deuterium. The helium and deuterium peaks are comparable in their values, that is difficult to achieve by nuclear reactions. In the experiments made by Bush the heat and the X-radiation were close to the background noise values. This fact doesn't give ground for drawing simple conclusions.

We think that the works by the scientists from Japan /3, 4/, China /5, 6/, India /7/ and the USA /8/, which were performed at higher energies of interacting particles, are the most important experiments of the last years, in which some results helping us understand the character of the phenomena under investigation were obtained. In these experiments one has less doubt about the result correctness due to the considerable emission of the nuclear reaction products and a better reproducibility.

The powerful glow discharge that we have used for the similar NRCM investigation for the first time allowed to obtain some reliable data on tritium and neutron generation and element transmutation /9/. One of the main features of our glow dischar-

ge system is usage of higher-plasma-generating gas pressures allowing relatively easily to obtain high densities of the flux of deuterium ions bombarding the studied target sample which is a cathode.

The article seeks to detect the conditions of obtaining a reliable NRCM reproducibility when bombarding the targets by accelerated deuterium ions and when using tritium generation for checking purpose.

2. EXPERIMENTAL PROCEDURE

The design of the discharge unit and the experimental procedure on tritium detection are similar to those described in /9/. The deuterium ions from the glow discharge plasma of direct current bombarded the target-sample when supplying the negative potential to the sample.

Plates, pipes having the wall of 0.2-5 mm thick and rods having 2-20 mm in diameter were used as samples. The samples were mainl made of tungsten and niobium.

Deuterium having a protium content up to 5% and a tritium content up to $(6-8) \cdot 10^{-10}\%$ (in atomic fractions) was used as a plasma-generating gas. The pressure of this gas was kept within $10^3 - 1.5 \cdot 10^5$ Pa. At these pressures the ion energy was within 0.1-0.01 of the discharge voltage varying from 200 up to 2000 V. The current density was $5 \cdot 10^2 - 10^5$ A$\cdot$m^{-2}. In the investigation process the sample temperature was given within 700-3600 K by varying both the applied power and the frequency of the pulses 0.01 s long.

The tritium analysis of the deuterium was made according to β-activity by the liquid scintillation method at the plant BETA-2 having three photomultipliers and recording the scintillation bursts according to the majoritic coincidence scheme. The error of measuring the tritium content in the probes didn't exceed $\pm$ 50%.

3. DISCHARGE PARAMETER EFFECT ON TRITIUM GENERATION

- Ion energy:

According to the correlative model /9/, when two deuterons collide, Coulomb barrier can be efficiently shielded near the excited matrix atom which can release not only its valence electrons, but also the electrons which are close to the nucleus into the shielding area. This phenomen occurs both when transferring a pulse from the deuterons to the matrix atom and when transferring a pulse from the matrix atom to the deuterons and can be rather probable.

According to the estimating calculations (Table 1, /9/) the optimal interaction energy depends on the matrix material, it accounts for about 30 eV for the deuterium medium and reaches 5 keV for the heavy elements of Mendeleev's periodic table. One should assume this energy range as a basis for obtaining reproducible NRCMs. The lower energy range is verified by fig. 4 /9/ and Table 2 given in this article. In Table 2 one can see that, when operating in the near-threshold energy range, the tritium generation efficiency (the nuclear inter-action coefficient) has decreased by about an order of magni-tude as a result of some ion energy decrease in spite of the fact that the current density has increased by a factor of 30. Perhaps, the quicker decrease in the tritium generation ef-ficiency, when the ion energy exceeds the model predictions (fig. 4, /9/), is connected with the fact that according to the experimental conditions the energy increase has been ac-companied with a current density decrease.

The total range of the interaction energy of the fast partic-les, which causes some abnormal nuclear phenomena in condensed media, is from $\mathcal{E}_0$ up to $\mathcal{E}_2$ according to our model /9/. That approximately corresponds to the range from 20 eV up to 30 keV. When the interaction energy is lower than 20 eV, the nuclear reaction rate isn't high and when the interaction energy exceeds 30 keV, the abnormal NRCM efficiency decreases as a result of increasing the nonelastic energy losses.

Table 1

NRCM efficiency versus discharge parameters

Material	Discharge parameters					Nuclear interaction coefficient, atom·ion^{-1}	Tritium flux, atom·s^{-1}
	Voltage, V	Current density, A·cm^{-2}	Temperature, K	Pressure, x10^3 Pa	Time, h		
Nb	1560	0.05	1070	20	22	$5.3 \cdot 10^{-13}$	$2.8 \cdot 10^6$
-"-	1900	0.1	1270	30	23	$5 \cdot 10^{-13}$	$2.7 \cdot 10^6$
-"-	750	0.1	1170	12	162	$3.8 \cdot 10^{-13}$	10^7
-"-	1800	0.2	1670	40	8	$2.5 \cdot 10^{-12}$	$1.7 \cdot 10^7$
-"-	2100	0.3	1770	50	6	$3.1 \cdot 10^{-12}$	$2.6 \cdot 10^7$
-"-	1080	2	1670	20	6	$7.1 \cdot 10^{-11}$	$0.6 \cdot 10^9$
-"-	1000	2	1670	40	8	$1.2 \cdot 10^{-10}$	$0.9 \cdot 10^9$
-"-**	820	10	1170	20	60	$6.8 \cdot 10^{-11}$	$1.7 \cdot 10^9$
W /III/	640	0.08	1470	10	20	$6.4 \cdot 10^{-14}$	$0.7 \cdot 10^6$
-"-	640	0.08	1270	10	18	$7.3 \cdot 10^{-14}$	$0.7 \cdot 10^6$
W *	1550	0.2	900	30	44	$1.1 \cdot 10^{-13}$	$1.5 \cdot 10^6$
-"-	1200	0.3	1670	40	42	$2.8 \cdot 10^{-13}$	$4.2 \cdot 10^6$
-"-	1080	1	3500	50	7	$4.8 \cdot 10^{-12}$	$4.5 \cdot 10^7$
-"-	800	1.5	3600	65	6	$8.1 \cdot 10^{-12}$	$8.4 \cdot 10^7$
-"-**	720	10	1500	21	115	$9.1 \cdot 10^{-12}$	$2.5 \cdot 10^8$
-"-	880	1	1670	20	8	$3 \cdot 10^{-11}$	$2.5 \cdot 10^8$
-"-	1150	8	1670	40	20	$2.5 \cdot 10^{-11}$	$1.7 \cdot 10^8$

* - Pulsed discharge
** - Discharge in the magnetic field

Table 2

NRCM efficiency versus discharge parameters at higher pressure

Mate-rial	Discharge parameters					Nuclear interaction coefficient, $atom \cdot ion^{-1}$	Tritium flux, $atom \cdot s^{-1}$
	Voltage, V	Current density, $A \cdot cm^{-2}$	Temperature, K	Pressure, $\times 10^3$ Pa	Time, h		
W	900	0.2	1070	20	22	$9.4 \cdot 10^{-13}$	$1.1 \cdot 10^7$
-"- *	1300	0.6	1170	40	46	$3.2 \cdot 10^{-13}$	4.10^6
-"- *	2540	2	1170	80	115	1.10^{-13}	$1.5 \cdot 10^6$
-"- *	1380	6	1170	120	52	$1.6 \cdot 10^{-13}$	$2.5 \cdot 10^6$

* - Pulsed discharge

- Ion flux:

The nuclear interaction coefficient versus the current density at a slight deviation of the rest of the parameters can be determined from Table 1.

According to the Table the current density increase by two orders of magnitude resulted in the tritium generation efficiency increase by about three orders of magnitude. It is a slight higher than in the work by T.Claytor /10/ and the given dependence requires a further more precise definition.

The current density increase in the discharge can be optionally accompanied by the NRCM efficiency increase if it results in decreasing the energy of the deuterium ions bombarding the target, in particular, at higher pressures in the near-threshold energy range (Table 2).

According to Table 1 one can consider the current density about 500 $A \cdot m^{-2}$ to be the lower limit to detect the NRCM reliably.

The upper limit of the current density will be restricted to a considerable extent by the melting temperature of the surface due to a high-rate vapour generation resulting in a great decrease in the energy of the ions bombarding the target surface. Hence, one can estimate the maximum current density for different materials from Table 3. This current density was determined when solving the problem of generating the heat amount required for heating the sample surface up to the melting temperature by using the nonsteady heat conduction equation for half-space. The calculations were performed for the samples about 2 mm thick, provided that the surface was bombarded by the accelerated particles having the energy of 1 keV supplied by the pulses 0.01 s long. One should consider the above current density to be the upper limit, as before the surface achieves the melting temperature, the NRCM efficiency will start decreasing as a result of growth of the thermionic emission decreasing the voltage drop near the cathode and the ion energy in the discharge and also as a result of decreasing the hydrogen solubility in the target material for hydride-generating materials.

Pressure:

The plasma-generating gas pressure has an effect on the hydrogen solubility and the mean energy of the ions bombarding the surface. The pressure increase results in increasing the hydrogen concentration in the target and decreasing the mean ion energy. The normal current density in the discharge is proportional to $\sim p^2$ under normal and abnormal conditions close-to-normal. So under the specific pressure optimum it is difficult to obtain the required hydrogen atom concentration in the matrix and to provide a sufficient current density and at higher pressures the increase in the current density and concentration can't

.Table 3

The current density of the bombarding particles, required for achieving the melting temperature at the target surface

Material	Thermal flow required for the surface melting, τ=0.01 s, $J \cdot cm^{-2}$	Melting current density, τ=0.01 s, E = 1 keV, $A \cdot cm^{-2}$
Uranium	87	0.09
Thorium	108	0.11
Bismuth	8	0.01
Lead	20	0.02
Platinum	274	0.27
Rhenium	382	0.38
Tungsten	622	0.62
Tantalum	281	0.28
Hafnium	161	0.16
Erbium	90	0.09
Cerium	36	0.04
Lanthanum	51	0.05
Palladium	262	0.26
Molybdenum	420	0.42
Niobium	297	0.30
Zirconium	139	0.14
Yttrium	82	0.08
Nickel	288	0.29
Iron	286	0.29
Vanadium	172	0.17
Titanium	142	0.14

compensate for the NRCM efficiency decrease by decreasing the
energy of the ions bombarding the target (fig. 1). In fig. 1
one can see that for molybdenum, tantalum and tungsten the
pressure optimum according to the maximum value of the nuclear
interaction coefficients is within $(20-40) \cdot 10^3$ Pa. For niobium
the optimum is most probably shifted down to $(10-30) \cdot 10^3$ Pa.
This, if any additional methods of increasing the current den-
sity aren't used, one can consider the optimal plasma-genera-
ting gas pressure in the glow discharge to be equal to $20 \pm 10 \cdot 10^3$
Pa for reproducible tritium checking of the NRCMs.

- Target temperature:

As the target is bombarded by the deuterium ions having a mini-
mum energy of tens of electron-volts (hundreds of thousands of
Kelvins), the target temperature should have a slight direct
effect on the NRCM efficiency. However, the temperature has a
direct effect on the hydrogen concentration in the target.
Therefore, for the hydride-generating materials (niobium, zir-
conium, palladium, etc.) a temperature increase should result
in a tritium generation decrease and for the nonhydride-genera-
ting materials (nickel, molybdenum, tungsten, etc.) - in its
increase. As the temperature increase is accompanied by the
exponential thermionic emission increase, the nonhydride-
generating materials have the optimal temperature about
$0.5 \ T_{melt}$ (1300-1800 K for molybdenum and tungsten). The hydride
generating materials have the optimal temperature too. It should
be maximum for the given concentration because the diffusion
acceleration results in increasing the atom collision frequency
and the reaction product migration (see Table 1) e.g. this
temperature can be 1300-1500 K for the rare-earth lanthanides
of MD_2 - type and the pressures of $\sim 20 \cdot 10^3$ and it shouldn't
exceed 1100 K for zirconium and hafnium dihydrides.

- Target material and surface state
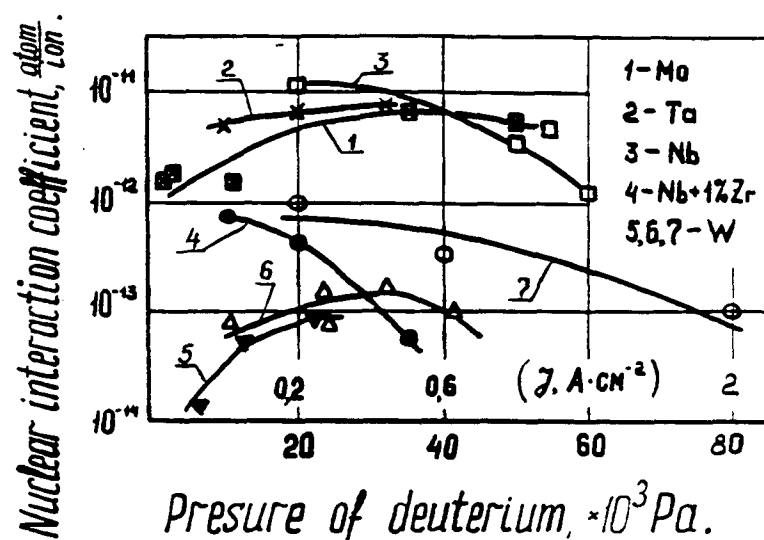
Fig. 1. The nuclear interaction coefficient versus the
plasma generating gas pressure when the deute-
rium ions from the glow discharge plasma bombard
different materials

1 - molybdenum; 2 - tantalum; 3 - niobium;
4 - niobium + 1% of zirconium; 5, 6, 7 - tungsten
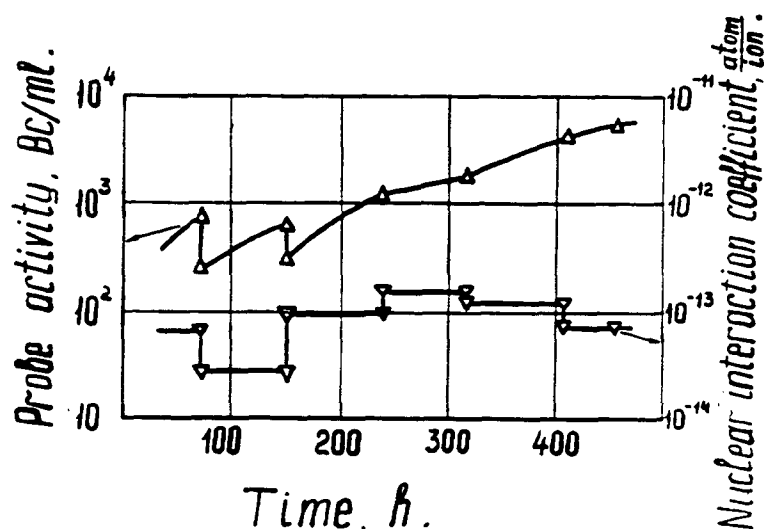
Fig. 2. The nuclear interaction coefficients and the
probe activity versus the time of the deuterium
ion bombardment of the tungsten-and-molybdenum
sample (U=620-800 V, J=0.05-0.6 A·cm^{-2},
T = 1500-1700 K)

According to our model /9/ two deuterons of Coulomb potential
are efficiently shielded by the excited atoms of the target
matrix most probably as a result of some additionally released
electrons which together with the deuterons can generate quasi-
plasma, e.g. in /11/. Therefore, one can come to two important
conclusions. Firstly, the heavy elements will have a higher
shielding efficiency because their atoms have more electrons at
a lower binding energy except for K-cladding. Secondly, the
NRCM area won't exceed the value of the projective ion path in
the condensed media (10-1 nm for the energies of about 1 keV).
In this case different surface compositions with lighter elements
e.g. carbides, nitrides or oxides, will considerably decrease
the NRCM efficiency both by decreasing the hydrogen solubility
in the near-surface layer and by decreasing the efficiency of
Coulomb potential shielding. It is verified by the experiment
where the reverse deuterium countercurrent flow through the wall
of the tight sample inhibited the foreigh film formation at the
surface facing the plasma (Table 4).

Table 4

NRCM efficiency versus deuterium flux through the sample wall

Mate-rial	Experi-ment type	Discharge parameters				Nuclear interac-tion co-efficient, $atom \cdot ion^{-1}$	Tritiur flux, $atom \cdot s^-$
		Vol-tage, V	Tempe-rature, K	Pres-sure, $x10^3 Pa$	Time, h		
Zirco-nium	Steady-state	820	1070	15	6	$1.7 \cdot 10^{-12}$	$1.1 \cdot 1($
Zirco-nium	Deuteri-um coun-tercur-rent flow, $\Delta P = 60 \cdot 10^3$ Pa	950	1270	30	5	$1.4 \cdot 10^{-11}$	$1.4 \cdot 1($

To our mind, a considerable number of unreproducible results
in the NRCM experiments is concerned with the foreigh film
evailability on the surface. The experiments, in wich the
noble metals (platinum, palladium) or molybdenum, tungsten,
rhenium are used as targets at temperatures exceeding 1000 K,
have no this disadvantage. Realization of the promising proper-
ties of zirconium, hafnium or the metals included in the lan-
thanide group is concerned with a careful purification of the
plasma-generating gas, lower temperatures and application of
some active methods to imhibit the foreigh film formation at
the surface, e.g. the ion bombardment sputtering.

4. DEDUCTIONS

Summing up the above-mentioned, one can conclude that selection
of procedures for efficient tritium generation when using the
NRCMs is rather limited. For this purpose one can't use electro-
lysis due to in low ion energy. Various plasma-generating
devices having a high current density and low energia can't be
used either. For obtaining efficient NRCMs one should use the
target bombardment by the dense ion fluxes by means of various
accelerators or the target bombardment directly by the ions
out of the plasma of the _dense_ glow discharge.

For the simplest reproducibility of the above-mentioned results
one can use the glow discharge of direct current at a deuterium
pressure of about $20 \cdot 10^3$ Pa. One can use either rods having
5-10 mm in diameter or plates 0.2-1 mm thick made of molybdenum,
tungsten or niobium as a target sample (cathode). The sample
temperature should be kept within 1100-1500 K at the expense
of the glow discharge power. In this case the forced cooling
isn't required. The discharge voltage within 600-1000 V can be
additionally controlled by the distance between the anode and
cathode. The current also depends on the sample demensions and
the cooling level and the value of 1-5 A will be sufficient.

We think that if one follows these recommendations, the tritium will be generated at a level of $10^6 - 10^7$ atom·s^{-1} when the efficiency is at least 10^{-14} atom·ion^{-1}. One can detect the above tritium generation when the experiment lasts 10-100 h. The long-term experiment, when using the bimetallic tungsten-molybdenum sample in a form of pipe having the outer diameter of 20 mm and the two-layer wall thickness of 1.5 mm is shown for illustration (fig. 2). One can see that even at the comparatively low nuclear interaction coefficients the tritium generation is continuous and the specific activity of the samples increases continuously and they don't depend on adding some deuterium into the system.

Following the above recommendation we have made over 60 experiments for the last year. In all the experiments the tritium fluxes were at a level of 10^6-10^7 atom·s^{-1}, when the nuclear interaction coefficients were at least 10^{-14} atom·ion^{-1} for such target materials as niobium, molybdenum, tungsten.

For achieving higher tritium generation rates and increasing the NRCM efficiency one should considerably increase the current density as compared with the normal one, that can be achieved by restricting the discharge combustion area by means of insulators, magnetic fields, etc. (see Table 1).

5. CONCLUSION

5.1. We proposed and tested the new method of obtaining the reproducible NRCMs, i.e. bombarment of the targets on condensed media base by the dense ion beams (J $>$ 0.05 A.cm^{-2}) having the optimal energy within 30 eV - 5 keV.

5.2. We described the simple procedure of the reproducible NRCMs on the base of the glow discharge having a higher density. This procedure allows to achieve the tritium generation rate at a level of 10^6-10^7 atom·s^{-1}.

5.3. It is shown that the reproducibility of the proposed method of obtaining the NRCMs by means of checking the tritium generation in over 60 recent experiments is approaching 100%.

REFERENCES

1. E.Yamaguchi and T.Nishioka. Direct Evidence for Nuclear Fusion Reactions in Deuterated Palladium. - Frontiers of Cold Fusion. Proceedings of the Third International Conference on Cold Fusion. October 21-25, 1992, Nagoya, Japan. Ed. by H.Ikegami. Universal Academy Press Inc., Tokyo, Japan, p. 179-188.

2. R.T.Bush and R.D.Eagleton. Experiment Studies Supporting the Transmission Resonance Model for Cold Fusion in Light Water: II Correlation of X-Ray Emission with Excess Power. - Ibidem //. p. 409-516.

3. T.Iida, M.Fukuhara, H.Miyazaki et al. Deuteron Fusion Experiment with Ti and Pd Foils Implanted with Deuteron Beams. - Ibidem //. p. 201-207.

4. J.Kasagi, K.Ishii, M.Hiraga and K.Yoshihara. Observation of High Energy Protons Emitted in the TiD+D Reaction at E_d=150 keV and Anomalous Concentration of ^{3}He. - Ibidem //. p. 209-215.

5. H.Q.Long, S.H.Sun, H.Q.Liu et al. Anomalous Effects in Deuterium/Metal Systems. - Ibidem //. p. 447-454.

6. H.Q.Long, R.S.Xie, S.H.Sun et al. The Anomalous Nuclear Effects Inducing by the Dynamic Low Pressure Gas Discharge in a Deuterium/Palladium System. - Ibidem //. p. 455-459.

7. R.K.Rout, M.Srinivasan, A.Shyam and V.Chitra. Detection of High Tritium Activity on the Central Titanium Electrode of a Plasma Focus Device. - Fusion Technology, 1991, v. 19, p. 391.

8. G.H.Miley, J.U.Patel, J.Javedani et al. Multilayer Thin Film Electrodes for Cold Fusion. - Frontiers of Cold Fusion. Proceedings of the Third International Conference on Cold Fusion. October 21-25, 1992, Nagoya, Japan. Ed. by H.Ikegami Universal Academy Press Inc., Tokyo, Japan, 1993, p. 659-662

9. V.Romodanov, V.Savin, Ya.Skuratnik and Yu.Timofeev. Nuclear Fusion in Condensed Matter. - Ibidem //. p. 307-319.

10. T.N.Claytor, D.G.Tuggle and S.F.Taylor. Evolution on Tritium from Deuterided Palladium Subject to High Electrical Currents. - Ibidem //. p. 217-229.

11. H.Hora, J.C.Kelly, J.U.Patel et al. Screening in Cold Fusion Derived from D-D Reactions. - Physics Letters A, 1993, v. 17 n. 2, p. 138-143.

Cathode Material Change after Deuterium Glow Discharge Experiments.

I.B. SAVVATIMOVA, Ya.R. KUCHEROV, A.B. KARABUT

Scientific Industrial Association "Luch"
24 Zhelesnodorozhnaya St., 142100 Podolsk, Moscow Region, Russian Federation

Abstract

Results of impurity concentration measurements in a palladium cathode by different methods before and after deuterium glow discharge experiments are presented. The concentration of some impurities increases up to 10^4 times. Elements appear which cannot be found in the discharge environment. Auto radiography of cathode samples shows that isotopes with different radiation energy exist in the cathode after experiment. The obtained results cannot be explained by the existence of a conventional fusion reaction, but may be explained by a more complex fusion-fission reaction.

Introduction

Our previous papers [1, 2] reported some results of deuterium glow discharge experiments. Neutron, charged particle, gamma and x-ray emission, changes in the cathode material composition including the appearance of elements undetectable before the experiments, and exposure of x-ray film in contact with the irradiated cathode samples were observed.

The present paper is devoted to more detailed consideration of cathode material investigations prior to and after irradiation by deuterium ions.

The cathode material study included investigations of
- surface topography by scanning electron microscopy,
- element composition and impurity distribution by x-ray microprobe analysis,
- element and isotopic composition by spark mass spectrometry, secondary ion mass spectrometry, and x-ray fluorescence,
- micro structure by transmitting electron microscopy,
- radioactive isotopes by auto radiography,
- thermodesorbtion of hydrogen and deuterium using a mass spectrometer.

Initial Cathode Composition

99.99 and 99,9 grade palladium was used as a cathode material. The bulk impurities content was defined by spark mass spectrometry for all the elements of the Periodic Table. The analyses were made in the mass spectrometry laboratory of the GIREDMET analytical center. The resolution of this method was 10^{-6} atomic percent, with a standard deviation of 0.15-0.30 for different elements.

For 99.9 grade the concentration of the following elements was greater than 10^{-4} atomic percent: Mg – 7, Ca – 6, Fe – 10, Rh – 4, Ag – 7, Ta – 10, Pt – 30, Au – 9 ($\cdot 10^{-4}$). The content of other impurities was 1-3 orders less. The total amount of impurities did not exceed $9.5 \cdot 10^{-3}$ atomic percent.

Surface Topography

A significant change of the surface topography is observed in the irradiated zone of the cathode samples including formation of various spikes, more pronounced on the border between irradiated and shielded zones. Under certain discharge conditions, spikes having a predominantly conical shape are formed on a large scale (Fig. 1). They initiate at sites having damaged structure.

Change in Elemental and Isotopic Composition of Cathode Material.

The elemental and isotopic composition of cathode material was analyzed by various methods in more than ten laboratories. Impurities in the discharge environment were also investigated, because of the possibility of mass transport to the cathode from the molybdenum anode or insulators (silica or alumina)
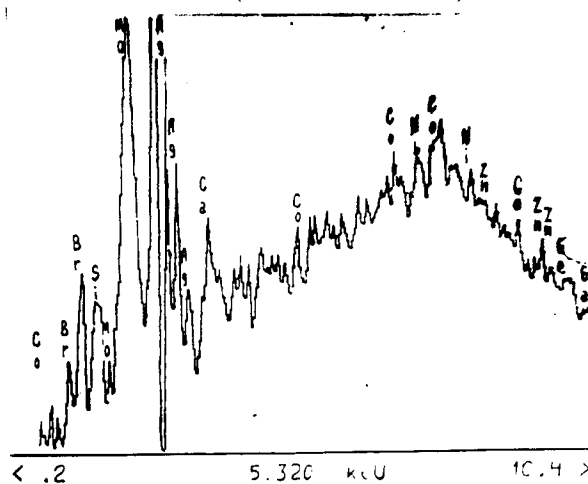
Fig.1 X-ray characteristic spectrum of an irradiated palladium sample without initial.

Fig. 2 Surface of Pd after irradiation .Fig. 3 Impurity distribution over Pd surface

X-ray microprobe analysis of representative areas on the front of the sample (irradiated and shielded), on the backside and in the section perpendicular to the front side was made before and after experiments. The spatial resolution was about 1 micron.. The thickness of analyzed layer was 1 micron. The Pd cathode samples after experiments show that the content of the some elements increases from tens to hundreds of times . In the analyzed layer the content of elements, undetectable by microprobe analysis before experiments, increases

16-2

up to 0.5 atomic percent. The results of the microprobe analyses for two cathodes are presented in the Table 1. These elements did not found in the initial sample by the microprobe analysis. The content of the impurities in Pd cathodes varies after other experiments.

<div align="right">TABLE 1</div>

IMPURITIES IN THE PD AFTER EXPERIMENTS OF DIFFERENT DURATION
(X-ray microprobe analysis , A. Senchucov "Luch")

Element	Atomic number	Impurity content, 10^{-2} at %.	
		after 4 hours exp.	after 40 hours exp
Na	11	7±0.3	3±0.3
Mg	12	1±0.3	2±0.3
Al	13	4±0.3	2±0.3
Si	14	1.5±0.3	<0.3
Ca	20	4±0.3	3±0.3
Ti	22	1±0.3	1.5±0.3
Br	35	3±0.6	2±0.6
Sr	38	7±0.6	6±0.6
Y	39	40±1	20±1
Mo	42	15±1	40±1
Tc	43	20±1	10±1

The characteristic x-ray spectrum of sample 1550 is shown in Fig. 2 as an example. Both irradiated and shielded areas of this sample show clear maximum corresponding to Zn, Br, Ca, for which initial concentrations measured by spark mass spectrometry were 10^{-4}, 10^{-3} and 10^{-6} atomic percent respectively.

The impurity distribution over cathode surface measured by microprobe analysis appeared non uniform. The comparison of the distribution (Fig.3) with SEM photos (Fig.1) shows that impurities are localized along crystalline subgrain boundaries . An example of the distribution for an individual element and for a set of elements is shown in Fig. 3 .

The impurity segregation point density is about $(1-10)10^{10}$ m^{-2} (for example (1-2)10^{10} m^{-2} for Zn and (2-4)·10^{10} m^{-2} for Br). Density of the all segregation points containing Mg, Co, Zn, Br is about 10^{11} m^{-2} (Fig. 3a). With changing experimental conditions and initial content the set of the observed elements also changes.

A significant increase in Mo and Nb impurity content was registered by x-ray fluorescence (B.M. Kudinov's group, GIREDMET). The detection threshold of the method was (2-5)·10^{16} atom/cm^2. The upper 20-25 μ layer was analyzed. Assuming that Nb and Mo impurities are distributed uniformly in 100 μ sample, their content would amount up to 0.07 and 0.08 mass percent respectively. Real quantity of the Mo and Nb was observed 1.5·10^{17} and 1·10^{17} at/cm^2, responsibility. But they were not found on the back side of the sample. Thus, assuming that Mo and Nb impurities exist only in upper 1 μ layer their content would amount to about 0.5 mass per cent. Mo is present in the discharge environment, but Nb is not.

For the first time, deviations from natural isotope ratios for impurities in the palladium cathode after our experiments were found by **secondary ion mass**

spectrometry in I.P.Chernov's group (Tomsk Polytechnic Institute). Changes in the isotopic ratio for some elements are presented in Table 2.

CHANGE OF ISOTOPIC COMPOSITION OF PD CATHODE AFTER DEUTERIUM GLOW
DISCHARGE EXPERIMENTS

(secondary ion mass-spectrometry; on a per unit basis)

Mass	6	7	10	11	51	53	54	56	57
Element	Li	Li	B	B	V	Cr	Fe	Fe	Fe
Initial	0.02	0.02	0.01	0.1	0.3	0.6	2.2	22.2	11.0
Front side	1.00	9.00	0.01	7.00	10.0	30.0	15.0	55.0	45.0
Back side	0.15	0.28	0.01	0.05	0.2	1.0	2.0	20.0	12.5

Mass	60	61	63	87	88	90	91		
Element	Ni	Ni	Cu	Sr	Sr	Zr	Zr		
Initial	0.1	0.2	1.4	0.1	0.5	0.0	0.1		
Front side	3.0	10	60	1.0	0.1	57.0	34.0		
Back side	0.2	0.2	1.0	0.1	0.2	0.0	0.1		

The change of elemental composition was also observed by **spark mass spectrometry** in the Testing Analytical Center GIREDMET(G.G. Glavin's laboratory). The upper layer with thickness of tens of microns was analyzed. It has been found that the increase of individual element content ranges from 10 to 10^4 times.

Results of this analysis for two experiments of different duration are presented in Table 3. In these experiments cathode consisted of two palladium foils: the irradiated foil at the top and the underlain foil. The content of Ti, Zr, Nb, Ag, Rb, Y increases from tens to thousands of times. A significant change in the impurity content is also observed for the underlain sample. In a four hour experiment, the density of deuteron flux was higher. Possibly for that reason, the impurity content increase was greater (for Nb—by 20 times, Rb—$\sim$1000, Zr— 50). It can also be seen that the isotopic ratio changes for some elements. The isotope ratio increases for $^{41}K/^{39}K$ by $\sim$2 times, $^{44}Ca/^{40}Ca$ —$\sim$4-2 times, $^{90}Zr/^{91}Zr$ — by more than 20 times, $^7Li/^6Li$ — $\sim$3 times.

After experiments in hydrogen it was also registered some increase in the content of impurity elements, but in the case of deuterium the increase is much greater: the elements with mass numbers 24, 25 (Mg), 27 (Al), 29, 30 (Si), 59 (Co), 70 (Ge), 90,91 (Zr) — by 10 times; 10,11 (B) — by 5 times; 107,109 (Ag) — 3-4 times, 31 (P) — 2 times.

Usually x-ray microprobe analysis (1 m analyzed layer) gives greater or equal values of the impurity content than spark mass spectrometry (10-100 m). The results, obtained by these methods for the same sample, are presented in Table 4. The comparison of the results gives ground to the suggestion that possible nuclear reactions, producing impurity elements, occur in the narrow near surface layer.

Table 3

Impurities in the Pd after Experiments of Different duraion Discharge Experiments
(by spark mass-spectrometry)

Mass	Ele-ment	Initial content ppm	Impurity content increase, times			
			after 40 h eperiment		after 4 h experiment	
			irradiated (upper). sample	underlain sampie	irradiated (upper). sample	underlain sampie
6	Li	0.06	2.5			
7	Li	0.08	6.5	4.5	11	5
10	B	0.07		2		
11	B	0.07	4	3	3	2-10
23	Na	0.44	10	2.5	7	13
27	Al	6	15	1.5	25 -50	4
28	Si	9	2	1		0.3
29	Si	7	3	1.5		1.5
30	Si	6	3	1.5	3-4	11
32	S	7	0.5-2	0.3	0.5	0.3
39	K	3	3		4	1.5
41	K	3	4	0.3	5	3
47	Ti	1.2		1.5	43-60	
48	Ti	1.4	370	1.5	-	2.5
49	Ti	1.3	357	2.5	100	2
50	Ti	1.7		2	65	
78	Se	0.23	<1	<1	<0.9	16
80	Se	0.3	0.7	0.7	<0.5	11
85	Rb	<0.03	<0.13	1.7	3000	1700
90	Zr	<0.05	500	<0.1	1200	<4.4
91	Zr	<0.05	1000	<0.5	1220	-
93	Nb	<2	20	1	360	2
98	Mo	0.4				7.5
100	Mo	1,8	2500	1	1600	
103	Rh	7	<2-4	<2-4	5-2.3	1
107	Ag	1	63	3	1	3.2
109	Ag	1	50	1.5		2.5
115	In	<0.04	12	1	20	4

TABLE 4
COMPARISON OF IMPURITY CONTENT IN THE PD CATHODE MEASURED BY TWO DIFFERENT METHODS

Element	Impurity content, ppm	
	Spark mass spectrometry	X-ray microprobe analysis
Na	5.8±1	700±30
Mg	35±1	100±30
Al	500±300	400±30
Ca	35±8	400±30
Si	30±5	150±30
Ti	100±50	100±30
Br	<0.5	300±60
Sr	<2.5	700±60
Y	0.2	4000±100
Mo	3000	1500±100
Tc	not detected	2000±100

Auto radiography Investigations

Radioactive isotopes appearing in cathode materials after deuteron bombardment in our experiments were registered by auto radiography. For registration auto radiographic film RT-1V was used. Two-three films were placed by each side of irradiated sample and fixed with rubber spacers in a box to prevent from sample and film displacement. Then the box was hold isothermally in a refrigerator for a time from 2 up to 250 hours. After some experiments the films were replaced and developed every 2-8 hour interval during 48 hours.

Considerable film exposure occurs from contact with irradiated samples. Light spots on positive images (Fig. 4,5) resulted from exposure by radioactive isotopes. All six 100 μ palladium foils, placed in cathode holder, cause film exposure, though only upper foil was bombarded (Fig.5 a-c). This fact can possibly be explained by tritium diffusion from the initial gas (tritium content in the initial gas $\sim 10^{-12}$).

The degree of exposure substantially depends on experimental conditions such as deuteron flux, irradiation temperature and site at the cathode sample. The degree of exposure increases with increasing run time and deuteron fluxes. This dependence breaks down at higher fluxes.nder low density fluxes, exposure in the irradiated zone is greater than that in the shielded zone. Under high density of deuteron fluxes sputtering of cathode upper layers occur due to intense ion bombardment and the discharge zone exposes the film to a lesser extent than the shielded zone does. It can be supposed that isotopes formed during the experiment diffuse from the discharge (irradiated) zone to the cooler (shielded by cathode holder) zone.
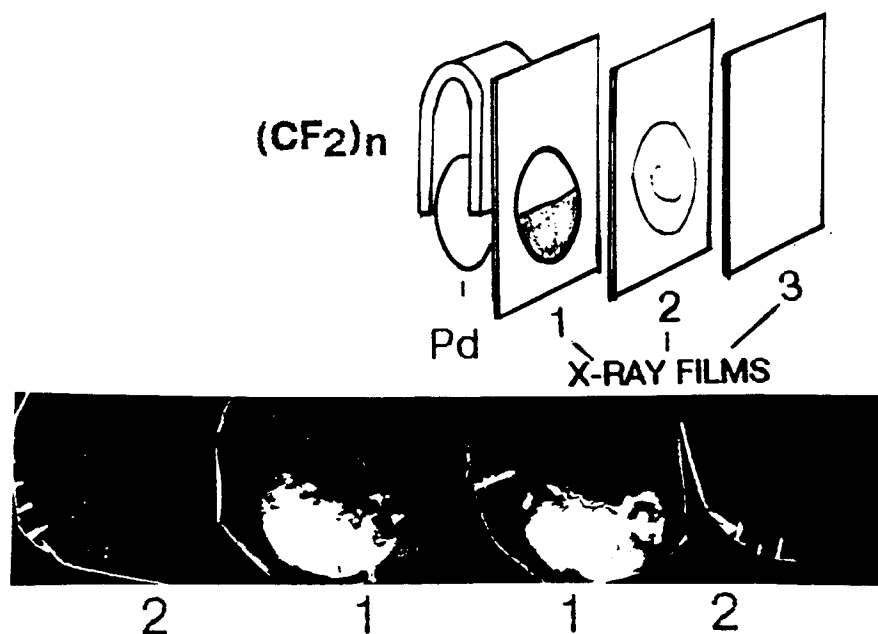
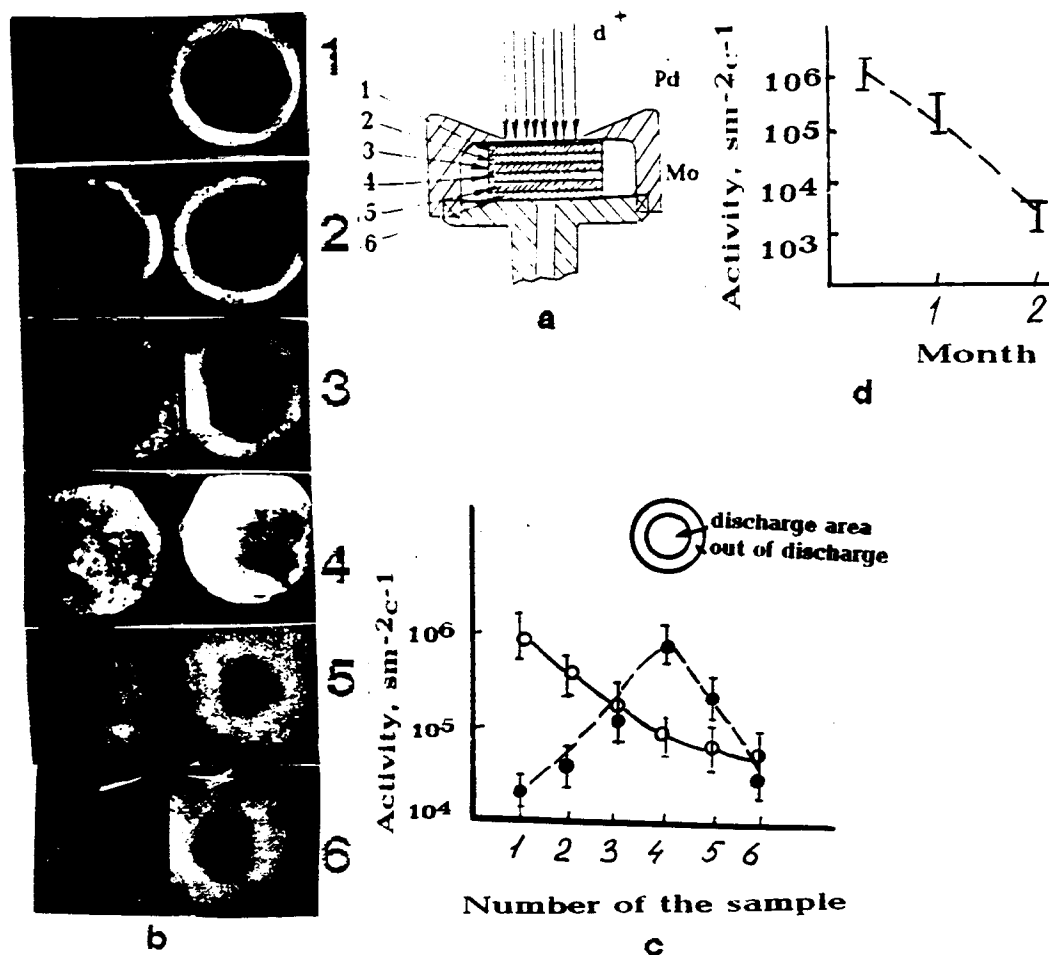Fig. 5 A scheme of auto radiographic energy measurements.

Fig. 6 Results of activity measurements (b, c) for the cathode, consisting of six palladium foils (a), and time dependence of tritium type activity (d).

The formation of isotopes with different radiation energies is observed. The energy of radiation has been evaluated using attenuating screens. Fig. 5a shows a scheme of energy measurements.

A twenty micron film of $(CF_2)_n$ was placed between a sample and two auto radiographic films so that it shielded half of the sample. The first film (next to the sample) demonstrates that the $(CF_2)_n$ screen stops a considerable part of radiation. The second film exhibits weak but uniform exposure all over the sample surface including outside the discharge areas. Thus, soft and hard components of radiation are observed. Soft components can be betas from tritium with energy <20 keV. Particles penetrating through $(CF_2)_n$ film and 200 μ auto radiographic film are equivalent to 0.1-0.5 MeV betas.

A semiquantitative estimate of beta activity of the samples was made. The film was calibrated against reference tritium beta source with activity of $4.1 \cdot 10^9$ β/s (Ti implanted with tritium). The films were placed into the vacuum chamber at 100 mm from the source and exposed for a time from 5 minutes to 5 hours. The exposure doses ranged from 10^9 to 10^{11} β/cm^2. The blackening degree of the film was measured using a densitometer (MF-4) and the blackening was plotted as a function of the exposure dose. The film was also calibrated against ^{90}Sr source with $E_\beta \sim 546$ keV using the same routine.

Assuming the low energy components to be tritium betas, the activity of palladium samples from different experiments is estimated as $5 \cdot 10^5$-$5 \cdot 10^6$ β/(cm$^2 \cdot$s) within 2-20 hours after discharge termination. The activity decreases to 10^3 β/(cm$^2 \cdot$s) after 200-2000 hours (Fig. 6d). It should be noted that the activity depends on cathode materials, combination of cathode materials, and experimental conditions.

The high energy radiation was compared with ^{90}Sr radiation ($E_\beta \sim 546$ keV). Within $\sim 10^3$ s after discharge termination the second film exposure corresponds to equivalent dose of $(1.5-4.5) \cdot 10^{10}$ β/cm^2 from ^{90}Sr. Activity of the isotope(s) with high radiation energy is estimated as corresponding to ^{90}Sr activity of $\sim(2-5) \cdot 10^4$ β/(cm$^2 \cdot$s).

Structure Changes

The micro structure of the palladium cathode before and after experiments was analyzed by transmitting electron microscope (ES-120). Fine palladium structure is shown in Fig. 6. After hydrogen ion irradiation, the bulk material structure remains unchanged and second phase precipitates appear on the surface. This phase appears to be hydride judging by electron diffraction.

A diffraction pattern from an area of 30 μ diameter shows that the sample is a single crystal.

After deuteron bombardment at 200 C, the dislocation density increases and cellular dislocation structure with lesser cells is formed. The fragmented structure is supplemented with void formation mainly along fragment subgrains. The void density in the surface layer with the thickness ~ 10000 angstroms is 10^{20} m^{-3}. Cellular structure with voids at the depth of 1000 angstroms is shown in Fig. 6. Voids sizes are to 1000-1500 angstroms. Isolated second phase inclusions with size up to 1500 angstroms can also be seen.

Void structure formation under ion bombardment is usually observed at higher homological temperatures, corresponding to much larger ion flux and fluence. This can be circumstantial evidence of nuclear reaction.

^{3}He and ^{4}He Content

Some of the irradiated cathode foils together with reference samples were analyzed by mass spectrometer of Rockwell International (Oliver's group). The

16-8

helium content was determined both in irradiated and in shielded zones of cathode. Results of the study are summarized in Table 3 (in the form as we received them). A small increase in the ^{3}He concentration and a large increase in the ^{4}He (4-100 times) concentration was found in the irradiated areas.

^{3}He AND ^{4}He CONTENT BEFORE AND AFTER DEUTERON BOMBARDMENT
(ROCKWELL INTERNATIONAL LABORATORY)

Sample number	Analyzed area	Sample mass, g	^{3}He, ×10^{9}a/s	$\dfrac{^3He_{after}}{^3He_{before}}$	^{4}He, ×10^9 a/s	$\dfrac{^4He_{after}}{^4He_{before}}$
Initial material		8.42	0.1±0.6		0.3±0.3	
		10.31	0.2±0.6		0.6±0.3	
		9.77	0.2±0.6		0.2±0.5	
		9.82	0.0±0.6		0.1±0.5	
1497	irradiated	1.90	0.2±0.3	1-10	1.8±0.2	9-100
		2.12	1.2±0.5	>2	1.3±0.6	4-90
1497	shielded	11.11	0.0-0.6	—	0.2±0.3	—
		12.25	0.2-0.3	—	0.8±0.8	—
1504	irradiated	16.5	0.4-1.3	1-2	7.1±0.2	5-35
		18.5	1.0-0.5	1-2	7.7±0.6	4-30
1504.	shielded	14.4	0.3±0.6	—	0.3±0.3	—
		16.4	0.0±0.2	—	0.1±0.8	—

Hydrogen and Deuterium Thermodesorbtion from Cathodes

The deuterium and hydrogen content in irradiated cathode samples was measured by mass spectrometry.

The amount of desorbing hydrogen, deuterium and HD depends on cathode material and irradiation conditions. The temperature of maximum gas release is 425±25 K (Fig. 7a) under low density ion flux, and 1000±25 K under high density ion flux (Fig. 7b). The temperatures of maximum release for deuterium and HD are close. When ion flux and fluence increase the maximum are shifted and amount of the desorbing gas increases by 4-5 times .
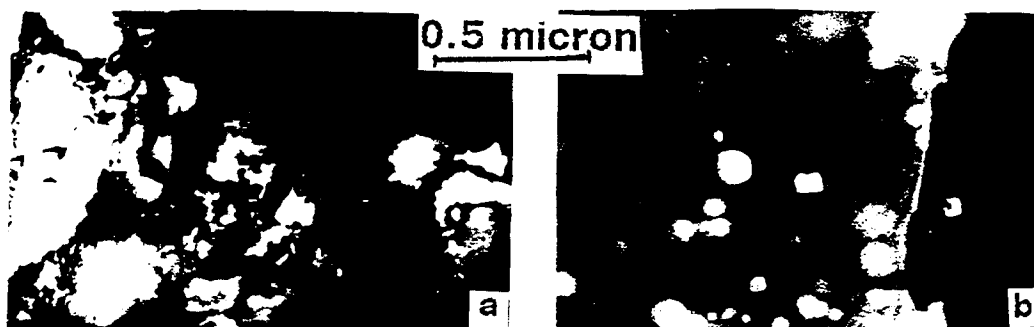
Fig.7   Transmissing electron microscope photos of irradiated cathode sample at a distance of~1000 angstroms from the surface

Figure 7

Hydrogen and Deuterium Thermodesorbtion from Pd after Experiments

a) after 2 minute irradiation
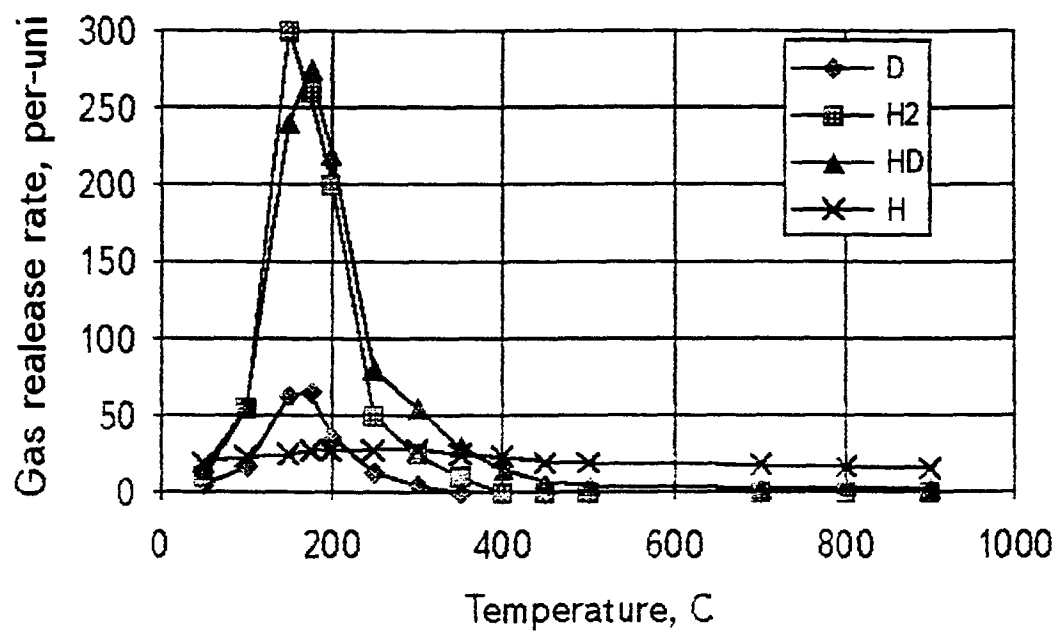
b) after 40 minute irradiation
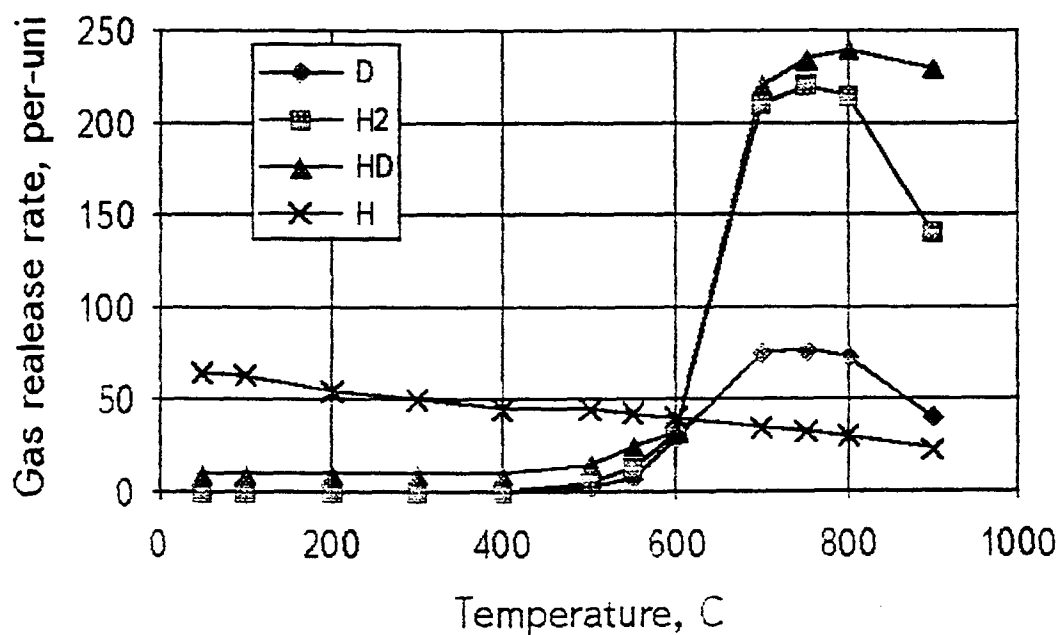
Conclusion

The following observations can be made after deuterium bombardment of Pd cathode in a glow discharge:

1. Increase of individual elements in the Pd cathodes up to 2-10000 times, depending on the experimental conditions. Greater changes in the element composition have been observed after more intense ion bombardment.

2. Change of the isotope ratio for individual elements up to 2-20 times for the following elements. The quantity of the each isotope may be different in different analyses zones. The difference may be about 75%.

3. Increase of the ^{4}He content by 10-100 times.

4. Formation of the radioactive isotopes with low and high radiation energy (<20 keV and ~0.5 MeV) occurs in the irradiated cathode after deuterium glow discharge experiments.

5. Formation of the void structures in or near the surface of the palladium cathode.

Weak radioactivity of the sample and large impurity concentration may be a result of "cold" nuclear products.

The results of the element and isotopic change in cathode material do not contradict to the earlier suggestion [3] that the reason for the appearance of elements undetectable before the experiments is fusion-fission nuclear reactions in the cathode.

References

1. Karabut A.B., Kucherov Ya.R., Sawatimova I.B. The Investigation of Deuterium Nuclear Fusion at Glow Discharge cathode. Fusion Technology, December, 1991, v.20, #4, part 2, p. 924.

2. Karabut AB, Kucherov Ya.R., Sawatimova I.B. Nuclear Product Ratio for Glow Discharge in Deuterium. 1992. Physics Letters A, 170, 265.

3. Karabut A.B., Kucherov Ya.R., Sawatimova I.B. Possible Nuclear Reactions Mechanisms at Glow Discharge in Deuterium. Frontiers of Cold Fusion, Proc. of the third International Conf. on the Cold Fusion, October 21-25,1992, Nagoya, Japan, University Academy Press, Inc., Tokyo, Japan, p.165

SEARCH FOR NEUTRONS FROM DEUTERIDED PALLADIUM

SUBJECT TO HIGH ELECTRICAL CURRENTS

Stuart F. Taylor*, Thomas N. Claytor, Dale G. Tuggle
Los Alamos National Laboratory
Los Alamos, New Mexico 87545

Steven E. Jones
Department of Physics and Astronomy
Brigham Young University
Provo, Utah 84602

*Also with Brigham Young University

Abstract

Tritium has been detected evolving from samples of deuterided palladium wires and powders subject to pulsed high voltage at Los Alamos[1]. We wanted to measure whether these samples were emitting neutrons. The idea of pulsing current through the wires and powders was to drive the deuterium in and out by rapid electrical heating. With promising tritium results in hand, the experiments were prepared at Los Alamos, and then taken to BYU and run in our neutron detector located in a tunnel in Provo canyon under 35 m of rock and dirt overburden. The neutron detector and sample setup are described. Results including total neutron counts, time distributions, and an indication of the energy distributions are discussed. The results do not provide compelling evidence of neutron production, but are not inconsistent with earlier measurements of neutrons and tritium[2]. Difficulties in explaining the difference in tritium and neutron measurements are also discussed. Plans for further work are presented.

Experimental Setup

Neutron Detector

The neutron detector at BYU is referred to as a "**modified Jomar detector**" because it is a helium-3 tube detector designed at Los Alamos and produced by the Jomar corporation with a plastic scintillator placed in the cylindrical cavity of the Jomar detector (Figure 1). This detector is described in detail in this volume by S. E. Jones et. al.[3]; a brief summary will be provided here.

The efficiency of the Jomar helium-3 detector alone is 34%, and the efficiency of the plastic scintillator is 48%, for a combined efficiency of 16%. Three plastic scintillator veto counters around the detector greatly reduce the cosmic ray background; with the veto counters in place, the efficiency of the modified Jomar detector is near 15%. In this tunnel, the background rate in the helium-3 detector alone is about 85 counts per hour.

To be considered valid, a detection "event" must pass software cuts, to be described. A pulse from the plastic followed by a helium-3 tube pulse within a 160 microsecond window is considered a candidate for a valid "single" neutron detection event. A single event is only
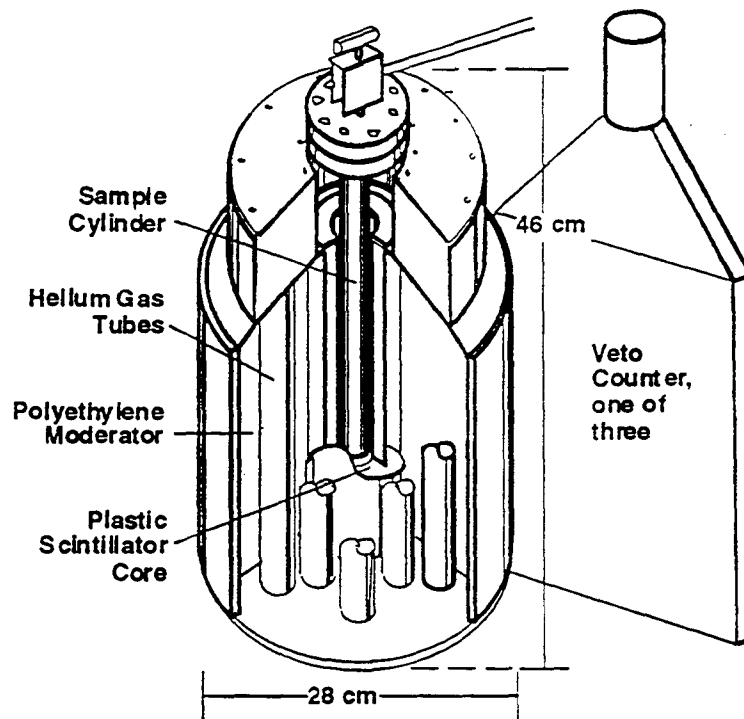
Figure 1: The BYU modified Jomar detector in a tunnel in Provo Canyon, Utah. A sample cylinder built at Los Alamos is shown inside. Not shown are two of the three large veto counters which allow removal of counts from charged particles traveling in all three directions.

considered a valid single if the area of the plastic pulse (referred to as a "**start**") is within certain ranges, and only if after the plastic start pulse the helium 3 tubes count a "**stop**" within a certain time bounds. The **area** of a plastic pulse is not quite a linear function of the energy the neutron deposits in the scintillator. The total energy of the neutron is not determined because not all of its energy is deposited into the scintillator. Any signal from the veto counters in these bounds invalidates the signal. The start areas are given in arbitrary units; the cut ranges are decided after a calibration study of events from neutron sources. The optimal cut accepts the most neutrons while rejecting other particles and electronic noise. A tight "cut 1" refers to a cut that considers valid only those counts with a plastic pulse "start" area of 200 to 1500 and time bounds of 0.6 to 80 microseconds; the medium "cut 2" has an area of 200 to 1500 and time bounds of 30 to 8000 microseconds. An event is considered a "**double**" if the helium 3 detector detects a second neutron in the following 160 microsecond window. It is considered a "triple" if a third neutron is detected within this same time window from the second, etc. All these events of more than one neutron detection are referred to as "**multiple**" events. Multiple counts must be within the same time bounds, but because of their rarity, in all cuts multiples are accepted in the wider plastic area bounds of 55 to 10000.

When combined with the plastic scintillator, the modified Jomar detector has a background count rate of 0.45 detected neutrons per hour when we require tight time correlation and narrow plastic scintillator pulse area range of cut 1. We feel that this cut may remove too many actual neutron events; therefore, in this paper we primarily use the medium cut 2 for which we have measured a background rate of 0.7 counts per hour. Using cut 2, approximately once every 30 hours we record a multiple count.

Setup of Samples

Earlier [1,2], when neutrons around cells were measured in a tunnel in Los Alamos using a standard Jomar detector, it appeared that the cells were producing neutrons. Because the background neutron count is about 55 per hour in the Los Alamos "Ice House" tunnel vs. near 0.7 per hour at the BYU detector, we prepared experiments at Los Alamos and took the experimental cells to the BYU lower background detector to measure neutrons from the cells.

The "**compact**" type of cell used in Los Alamos, with alternating layers of silicon and pressed palladium powder, had regularly evolved just under 0.1 nCi per hour tritium. Based on three previous experiments that evolved high levels of tritium and also appeared to emit neutrons at an average rate of 3×10^{-9} neutrons per triton, our expected maximum neutron production was up to 6 source neutrons per hour, or with the BYU neutron detector's ~15% efficiency, we expected to detect up to ~0.9 neutron counts per hour above background at BYU.
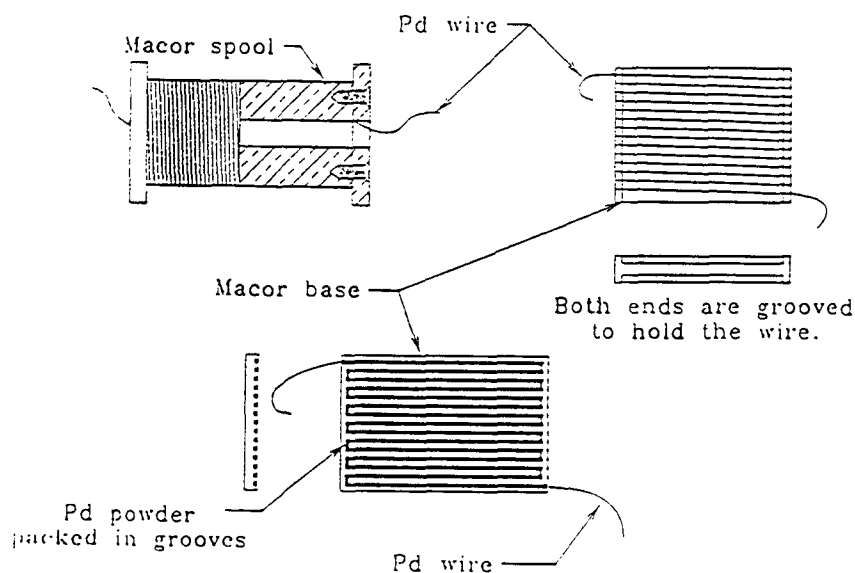
Figure 2: Schematic drawings of the three types of experimental samples used: compacted palladium powder layered with silicon, wire, and palladium powder pressed into long grooves.

A difficulty in running the compact cells is that they evolve more tritium when close to a "breakdown" voltage, that is when the voltage is nearly high enough to cause mild arcing through the layers of silicon and palladium. Operating near this limit is problematic in that if catastrophic arcing does occur, the resistance of that sample is permanently greatly decreased, and no longer shows tritium evolution. Therefore, other methods were sought that would allow faster turn around time between experiments. We therefore tried two alternate experiments where we tried to reproduce the same conditions of high current density in the palladium to see if they would evolve

tritium and emit neutrons. The first alternate "wire" experiment was to use high purity palladium wire with a diameter on the order of 0.1 mm. Subsequent analysis of the wires showed that the commercially available "high purity" wire in fact often contained both metallic impurities and non-metallic impurities (i.e. carbon), most likely from the process of drawing the wire. The second alternate method was to press palladium powder into a narrow track, or "groove", and run current through the palladium in the track. These three types of samples are shown in Figure 2.

BYU cell 51 and control
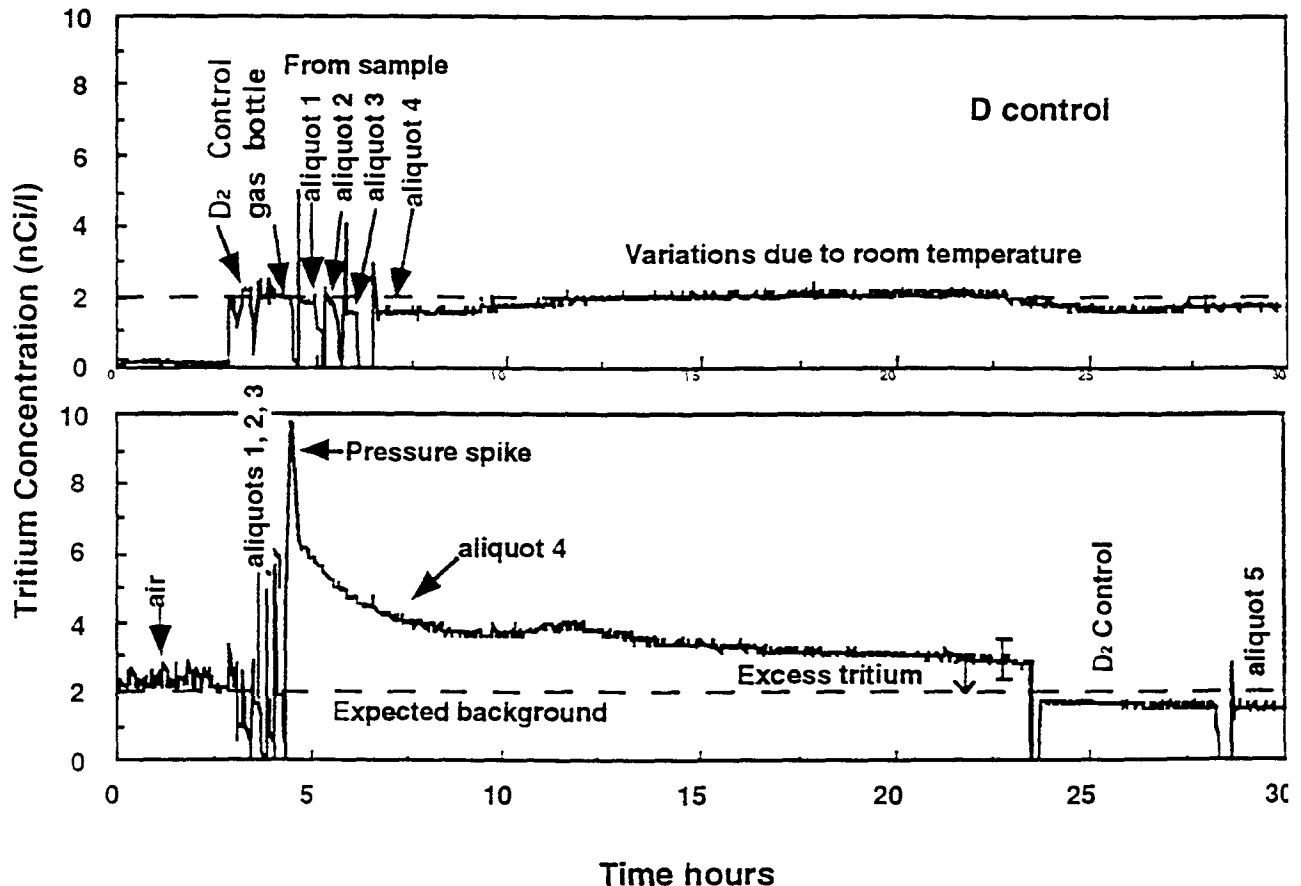
Figure 3: Tritium measurements for compact cell 51 and a background, where the ionization current has been converted into tritium concentration. The sample gases are put into the Femtotech ionization gauge in four aliquots (shots). The background level on this ionization gauge is 2 ± 0.2 nCi/litre due to fixed tritium contamination in the system. Before being used in the experiments, the low tritium deuterium gas contains 2 nCi/litre tritium (dashed line). To obtain the total amount of tritium, multiple the concentration by the total volume of the measurement system of 3 litres.

Experiments Run

The first experiment, "Wire 01", was a test of the "wire" method. Because the cell was taken to vacuum to rapidly remove deuterium absorbed in the palladium, the gas evolved was not available for tritium analysis. In this run, the neutron counts were separated into three groups of times: (1)

17-4

When the palladium was placed in a deuterium atmosphere and therefore the deuterium was being absorbed, and current was run through the wire (an "in" run), (2) when no current was being sent through the wire, and the palladium remained in the deuterium atmosphere (a "stable" run), and (3) when current was sent through the palladium wire while it was placed under vacuum to rapidly drive deuterium out of the sample (an "out" run). Because the out runs appeared to have higher neutron outputs than the stable runs, with the in runs in between, we were encouraged to repeat the wire type of experiments. Three more wire runs were then done in a chamber prepared in Los Alamos; in these runs the wire was not put into vacuum in order that the gas could be saved for subsequent tritium analysis. Two compact experiments were run, and three groove experiments were run.
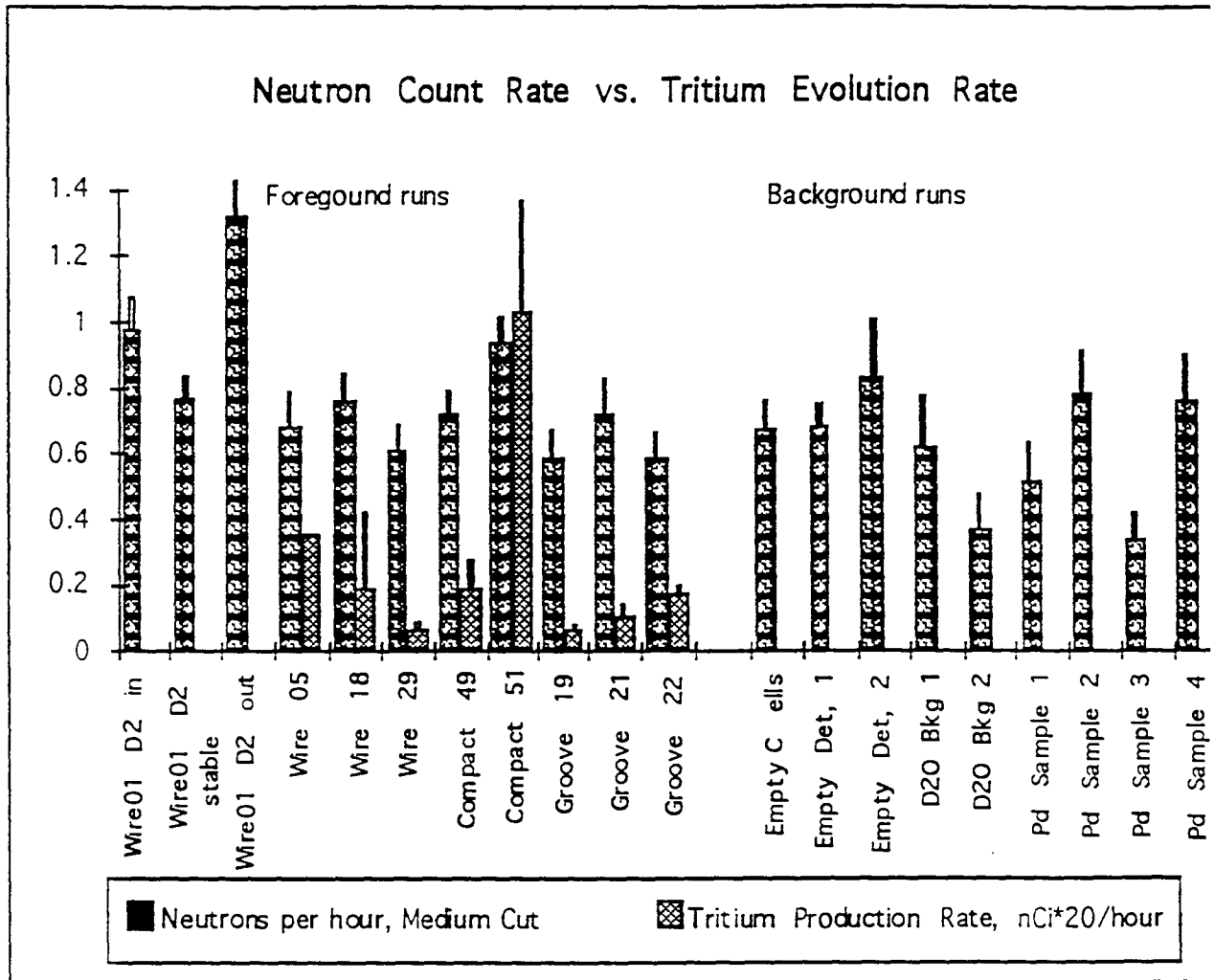
Figure 4. Neutron counts for runs done at BYU, with tritium measurements (multiplied by 20 to fit graph) shown for comparison.

Total Counts Results

Figure 3 shows the measurement of tritium for sample compact 51. This sample showed the highest tritium evolution of any sample reported here (Figure 4). The method of measurement is described in this volume[6]. We regret that the sample was not measured until the ionization current

17-5

stabilized, as we now have a larger uncertainty in this tritium measurement than if the measurement were continued for another 10 to 20 hours.

Shown on figure 4 is a compilation of the neutrons detected during the wire run done in the BYU chamber (Wire 01), the eight experimental runs using the Los Alamos chamber (three wire runs, two compacts, and three groove runs), followed by background runs in the detector. For the runs done in the Los Alamos chamber, the quantity of tritium measured following the runs divided by the time of the run to obtain a tritium evolution rate is shown; the unit used for the tritium is nanocuries multiplied by 20 to fit on the same graph. There appears to be a higher neutron rate above background from the sample (Compact 51) from which more tritium was measured, and also a higher neutron rate in the first wire sample during the times that the deuterium is either being absorbed into or driven out from the palladium. The significance of this, however, is very uncertain due to the possibility of systematic effects; in any case, the higher neutron rates are within a few sigma of background.

Neutron Capture Time for Bursts

Legend:
- Pu, 1310 seconds
- D2 out, 268.8 hours
- D2 in, 174.3 hours
- D2 stable, 288.5 hours
- H2, 394 hours

Y-axis: Counts
X-axis: Time (Microseconds)
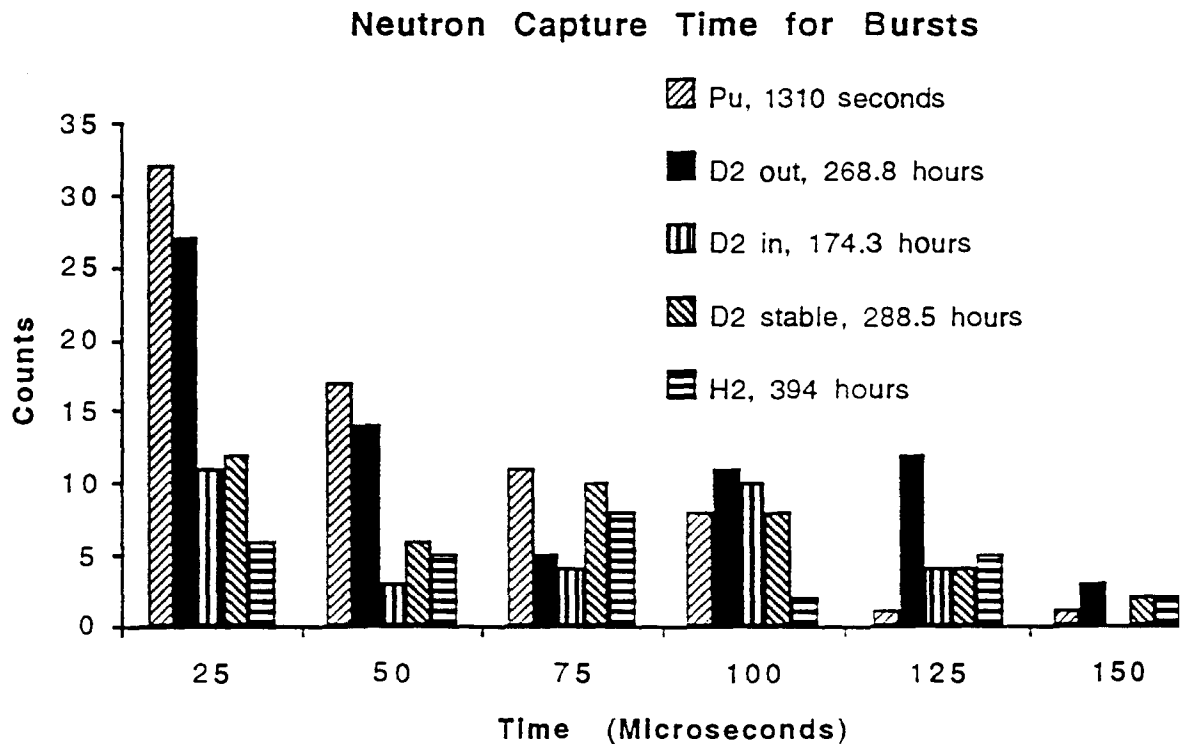
Figure 5: The time distribution of each count from multiple events shows an exponential decrease for a plutonium source where the neutrons in multiple events are "correlated" (produced simultaneously, but taking an exponentially decreasing time distribution to thermalize in the polyethelyne before being detected by the helium-3 tubes) However, in a hydrogen background where multiple events are uncorrelated this distribution randomly varies around close to the same value . The appearance of a decrease in the counts from multiples from runs in which D_2 is being driven out suggest a posible admixture of correlated counts in these runs.

It should be noted that the background runs vary more than the one sigma error bars, which only show the statistical error associated with the number of counts. Work is underway to determine the level of systematic error, and to understand if the occasional low background runs are a result of a problem in the equipment or analysis.

Time distribution of multiples

We refer to the time from the plastic pulse to when the helium-3 counter detects the neutron as Δt. When the time distribution of Δt are histogrammed for a plutonium source, the result is an exponential decrease with a 55 microsecond die away time. The plutonium is used for comparison because it is a good source of bursts of simultaneous neutrons -- the exponential time distribution of the detection of the neutrons is a result of the time it takes for the neutrons to thermalize in the polyethylene moderator. In other words, a 55 microsecond exponential die away time in the time distribution of the detected neutrons is indicative of the neutrons being emitted simultaneously. In contrast, when this time distribution is histogrammed for the counts from a hydrogen background, the distribution is closer to being flat, indicating less or no correlation between the plastic and the helium-3 signals. Figure 5 shows the multiple counts plotted for the runs where deuterium was being forced out of the palladium. It appears that perhaps the distribution is a mix of a flat distribution and an exponential decrease, indicating a possible source component to this signal; however, at the available level of data this conclusion is not conclusive.

Energy determination

A rough idea of the energy bounds of the neutrons that produced a start pulse in the plastic scintillator can be obtained. The total amount of scintillation of the pulse produced by the neutron, called the area of the pulse, is nearly proportional to the amount of energy deposited by the neutron in the scintillator, which is a fraction of the neutron's energy. Thus neutrons of a single energy would produce a characteristic distribution of areas. The distribution of the foreground and background runs are plotted and compared in figures 6 and 7. The small number of neutrons detected do not yet produce a very smooth distribution of the areas in either the foreground or the background: when the events in which a single neutron is detected in the helium 3 tubes are plotted it is not apparent whether there is a significant difference between the two distributions. The number of multiple events, where two neutrons are detected in the helium 3 tubes, is 18 doubles plus 1 triple in the 260 hours of foreground and 7 doubles plus one triple in the 260 hours of background. In 130 hours with a cell containing deuterium but not subject to current (called a "stable" cell) there were 3 doubles. Perhaps most significant is that all 8 multiples in the background have a plastic pulse area less than 800, but 8 of the 19 multiples in the foreground have plastic pulse areas greater than 800. In the stable cells, there were 2 multiples with area below 800, and 1 count above. Greater plastic pulse areas could indicate neutrons of higher energies, or could be produced by more than one of the neutrons of a multiple event scintillating the plastic at the same time. Therefore, these multiple event results may indicate that more energetic neutrons are being emitted from foreground samples than from background, or that the neutrons in the foreground multiple events are more correlated. However, such a low number of multiple events cannot give a conclusive difference between the foreground and background. As this neutron detector is not optimized for energy spectroscopy, these results suggest more use of another BYU detector that is optimized for energy spectroscopy. A possible source of error is that the plastic scintillator is heated by the current sent through the samples in the foreground experiments: whether this results in it giving larger or spurious pulses has not yet been determined.
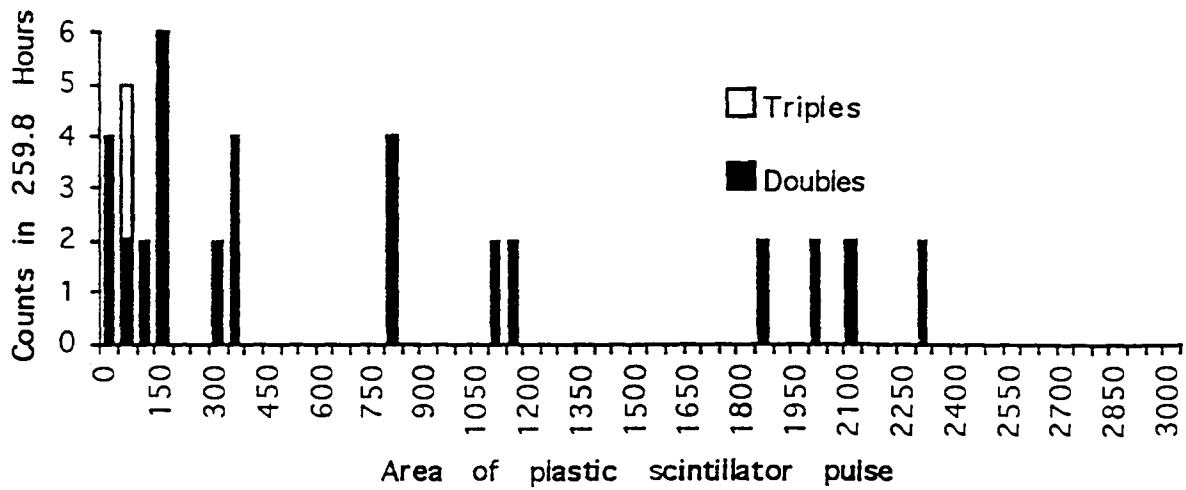
Neutron Multiples Counts, D2 Being Driven Out

Figure 6: Number of multiples counts as a function of pulse area, plotted for 259.8 hours where deuterium was being driven out of the palladium. This can be compared with background in Figure 7.
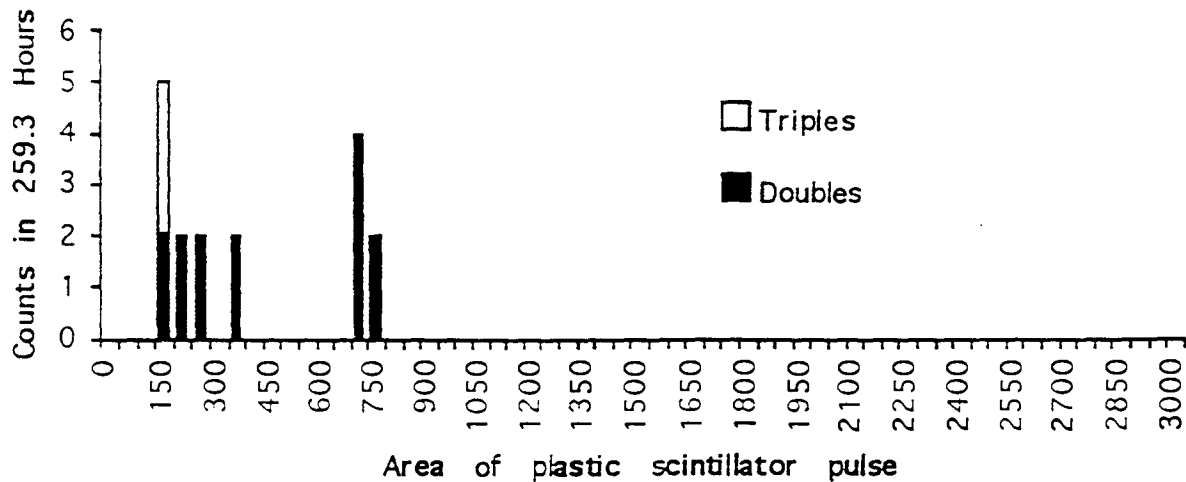
Background Multiples Counts

Figure 7: Number of multiple counts as a function of pulse area, plotted for 259.3 hours of background runs.

Conclusions

The data obtained do not present a clear picture that neutrons are being produced in these experiments. What is clear is that the source neutron production rate would be much less than the roughly 1000 fusions per hour estimated as being produced in electrolytic cells run by the BYU team in 1988 [3]; since that time, the newer detectors have much improved detection efficiency and greatly reduced background, and one would expect such a signal to now stand out clearly against the lower background. That the above indications of neutron detection are similarly close to background leads our group to be suspicious that systematic effects rather than neutrons may be producing the signals, and we are searching for these effects. There is a possibility that these data indicate a low level production of neutrons -- the evidence warrants further search, but no verified detection of neutrons is claimed at this time. It should be pointed out that the previously seen rate of 10^{-9} neutron/triton[1] was unfortunately not well tested by the rates of tritium seen in these experiments. While tritium is being evolved fairly reproducibly in "compact" cells at Los Alamo; not every compact cell evolves significant levels of tritium (15 nCi or more), and the level of tritium seen in the two compact runs at BYU is consistent with marginal levels of tritium evolutioi In retrospect, it may have been better to run more compact cells than wire cells, but we were encouraged by possible neutron signals detected in the first wire experiment to run more of the wire experiments. The wire experiments were also chosen because they were easier to build and were not prone to the compact cell's problem of arcing and premature failure. We conclude that t] neutron rates seen were consistent with the postulated 10^{-9} neutron emitted per triton evolved rat but were too close to background to be considered a confirmation.

The question of whether it is possible to have as few as only one neutron produced for every $\sim 10^9$ energetic tritons produced must be considered. The problem is that energetic tritium ions (**tritons** produced in nuclear reactions are of the order of MeV's of energy. The reaction triton + deuteron $\rightarrow$ neutron + alpha has a resonance near 150 KeV[4]. Any triton with an energy not less than this 150 KeV energy resonance will produce significant numbers of "secondary" neutrons from this reaction, as the triton's energy will pass through this resonance as the triton loses energy and thermalizes. The reaction $d + d \rightarrow p + t$ produces tritons of 1 MeV; the mass differences of the reactants and products in any other energetically favorable tritium producing reaction would certainly impart much more energy to the triton than 150 KeV. It has been estimated that there should be at least 10^{-6} as many neutrons as tritons when the tritons lose their energy in a deuteriu rich environment[5], but this experiment indicates a ratio of less than 10^{-8}. The cross sections for the $t + d \rightarrow n + \alpha$ reaction have been obtained along with code for the stopping of a triton in deuterium and palladium; this will allow a calculation of the minimum n/t value for a given energ of the triton. Experimental results of this value are being sought. The lack of detection of large numbers of secondary neutrons remains the biggest challenge to the findings of tritium actually being produced in experiments where tritium had evolved.

Alternative sources of the tritium signal are being considered in this volume[6]. The tritium level measured in the sample Compact 51, 5 nCi, corresponds to 5.4×10^9 atoms tritium per gram of palladium. The concentration of the tritium decay product ^{3}He in the palladium powder used in t] compact cells was found to be 1.6×10^7 atoms ^{3}He per g Pd powder by Jane Potts of Los Alamos National Laboratory. Because the powder used was at least 6 years old and tritium decays into ^{3}H with a 12 year half life, the amount of tritium contamination in the palladium powder could not have been very many factors greater than this concentration of ^{3}He (unless the contamination occured shortly before the experiments and occured only in the foreground samples). If contamination was responsible for the tritium signal, this would require an anomalous capture. storage, and release of tritium. Another source of error is that some process other than tritium

decay may produce ionization current in the Femtotech detector. This would also be unlikely as the tritium has been measured by scintillation. The possibility of false detection such as from internal leakage current is also considered in detail in reference 6.

Gamma ray measurements of palladium samples run in experiments have been made by Jack Parker at Los Alamos, and have shown nothing above background, including from samples from experiments where tritium was detected.

Further Work

More experiments are planned at BYU with the expectation that we will obtain a run that produces more tritium, similar to more significant levels seen at Los Alamos, and thus a better test of whether the detection ratio of 10^{-9} neutrons per triton is valid.

The possible energy difference of neutrons in the foreground and background deserves more attention. The Jomar/plastic scintillator neutron detector described in this paper is optimized for high efficiency and discrimination against other particles, not for energy spectrometry of the neutrons as was the neutron detector used in the initial BYU report of evidence for neutron detection from deuterided solid systems[7]. These experiments have not used the spectrometer due to its low efficiency relative to the modified Jomar detector; however, an energy determination would best be done in the spectrometer.

The amount of data produced by having the time information is huge, and work is progressing to improve the analysis software's ability to obtain the time and energy distributions of the helium-3 tube signals relative to the plastic scintillator signals. Also, a more flexible histogramming of the neutron signals as a function of the time during the run is being developed.

It is important that the tritium be looked for as it is being evolved in order to determine the energie of the tritons at their source. This would provide evidence that the tritium seen is actually being produced rather than merely being contamination being driven out. We plan to use a surface barrier detector to look for energetic tritons. Because the neutron to tritium detection ratio is so low, tritons of energies less than 40 KeV should be searched for. For this, we plan on using an ion implanted surface barrier detector made for being more sensitive to lower energy tritons.

Alternative sources of the apparent neutron signal can be evaluated. The experiments do heat the detector which may generate spurious signals from causes such as cracking of the plastic scintillator. This adds another uncertainty as to whether the higher neutron signal is due to actual neutron production. We plan to reduce this problem by wrapping the cell in copper foil, and cool the foil on top. This would reduce the heat on the detector sufficiently that background runs could be done with the detector heated to the same level as the sample runs with the fear of damaging the detector.

Acknowledgments

1. T. N. Claytor, D. G. Tuggle, S. F. Taylor. "Evolution of Tritium from Deuterided Palladium Subject to High Electrical Currents," Frontiers Science Series No. 4, Proceedings of the Third International Conference on Cold Fusion, Frontiers of Cold Fusion, H. Ikegami (Ed), Nagoya, Japan, October 1992, pp. 217-229.

   Another paper that reports detection of tritium and neutrons: V. Romodanov, V. Savin, Ya. Skuratnik, Yu. Timofeev. "Nuclear Fusion in Condensed Matter," Frontiers Science Series No. 4, Proceedings of the Third International Conference on Cold Fusion, Frontiers of Cold Fusion, H. Ikegami (Ed), Nagoya, Japan, October 1992, pp. 307-319.

2. T. N. Claytor, D. G. Tuggle, H.O. Menlove, P.A. Seeger, W.R. Doty, and R.K. Rohwer. "Tritium and Neutron Measurements From Deuterated Pd-Si," AIP Conference Proceedings, Anomalous Nuclear Effects in Deuterium/Solid Systems. S.E. Jones, F. Scaramuzzi, and D. Worledge (Eds) Provo Utah, 1990, p 467.

3. Steven. E. Jones, David E. Jones, David S. Shelton. and Stuart F. Taylor. "Search For Neutron, Gamma, and X-ray Emissions From Pd/LiOD Electrolytic Cells: A Null Result," this volume.

4. G. M. Hale, R. E. Brown, N. Jarmie. "Pole Structure of the $J^{\pi} = \frac{3}{2}^{+}$ Resonance in ^{5}He," Physical Review Letters 59 (1987) 763.

5. J. Rafelski, personal communication.

6. D. G. Tuggle, T.N. Claytor and S.F. Taylor, "Tritium Evolution From Various Morphologies of Palladium," this volume.

7. S. E. Jones, E.P. Palmer, J.B. Czirr, D.L. Decker, G.L. Jensen, J.M. Thorne, S.F. Taylor and J. Rafelski, Nature, 338 (1989) 737-740.

CHARACTERISTIC PEAK STRUCTURES ON CHARGED PARTICLE SPECTRA DURING ELECTROLYSIS EXPERIMENT

R. Taniguchi

Research Institute for Advanced Science and Technology,

University of Osaka Prefecture

Gakuen-cho, Sakai-shi, Osaka 593, Japan

Abstract

Origins of strange peak structures, which appeared frequently on charged particle spectra during electrolysis experiments, were studied. A charged particle detector, Si-SSD, was placed close to the thin- foil palladium cathode of an electrolysis cell. The total counting rate of the "strange peak region" showed a possible correlation with experimental conditions, i.e., electrolysis, electrolyte, and materials surrounding the detector. The peak patterns of the strange structure corresponded neither to that of any background sources nor to that of the ordinary D-D reaction. It is probable that some unknown nuclear reactions contributed to the appearance of the peaks.

1. Introduction

In recent experiments on cold nuclear fusion, strange charged-partile emissions have been reproted [1]-[4]. These experiments had the following common features.

- Bombardment of titanium deuteride with accelerated deutrons.
- Observation of mono-energetic charged particles emitted with energies above several MeV.
- Inexplicablity from the reaction products of ther ordinary D-D reaction.

These strange data should be interesting in relation to the mechanism of the cold fusion phenomenon. However, there still remains a tiny suspicion that the disturbance reactions, accompanied with accelerater experiments, might have had some effect upon these data.

In this study, similar strange spectra of charged particles were measured with the electrolysis experiment. The method used were free from background and competitive

reactions possibly contained in the accelerater experiments. They were also superior in the signal-to noise ratio in spite of extremely low counting rate.

In this paper we first describe the experimental data, and then discuss the spectra with comparison to some natural background radiations.
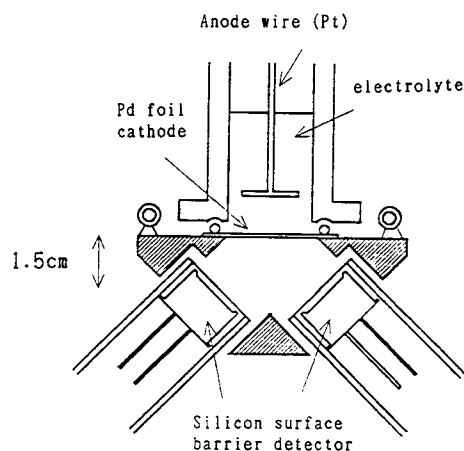
Fig.1 Experimental setup for the charged particle measurement.
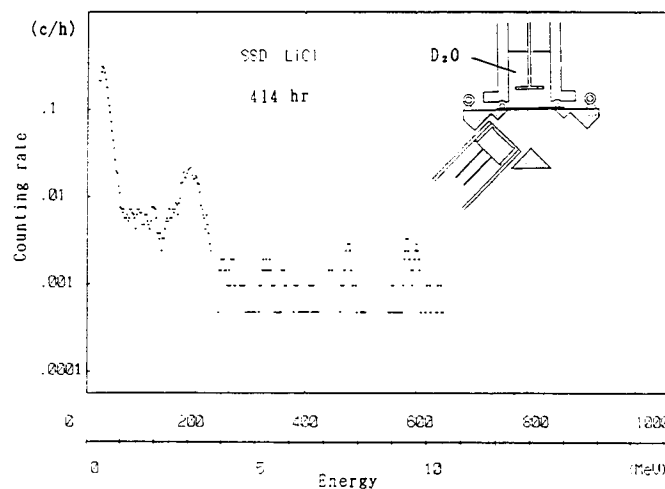
Fig.2 An expample of the strange structures in the charged particle spectrum measured during D_2O electrolysis. The most significant peak at 3 MeV was caused by the penetration of high energy protons.
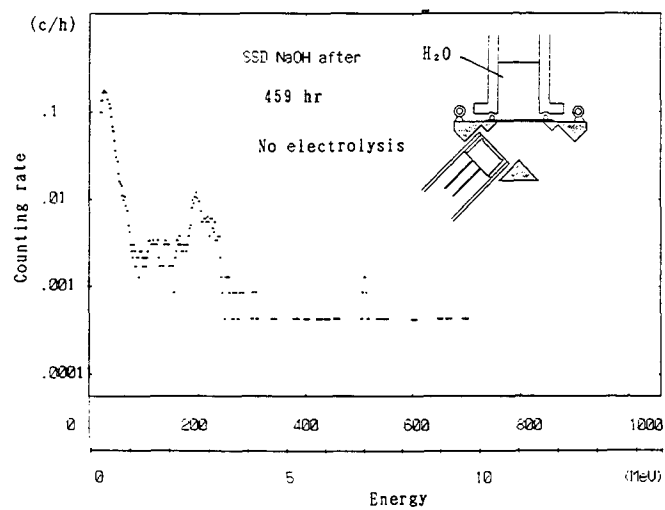
Fig.3 The charged particle spectrum measured without electrolysis.(background type [1])
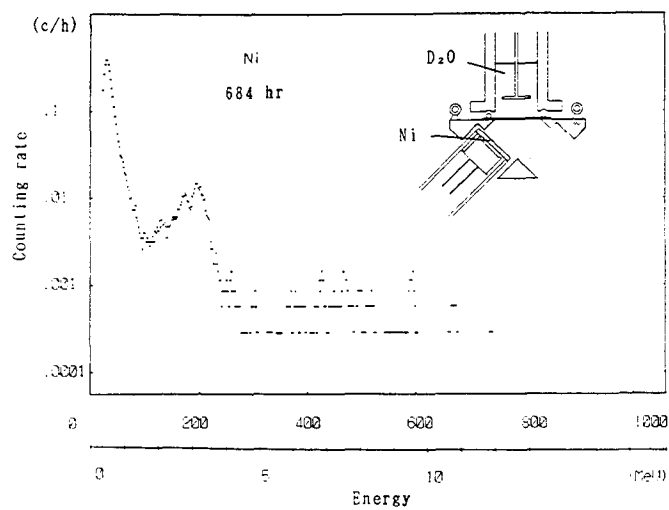
Fig.4 The charged particle spectrum measured with the Si-SSD covered with a Ni plate of 1-mm thickness. during the D_2O electrolysis.(background type [2])
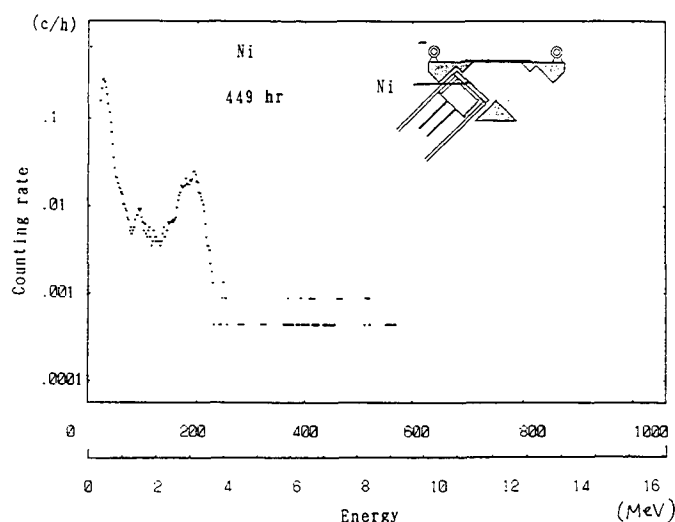
Fig.5 The background charged particle spectrum without electrolysis cell and with the covered Si-SSD (background type [3]).

2. Experimental
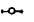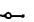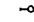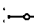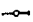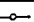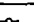
Figure 1 shows the experimental setup. The charged particles were detected by a Si-SSD attached to a thin-foil palladium cathode, which formed the bottom of an electrolysis cell. The palladium foil cathode, 20-μm thick and 15 mm in diameter, was covered by a deposited 0.1 μm Ag layer on the air side for the purpose of forming a hydrogenous diffusion barrier. The electrolyte was 0.1 molar LiOD. Electrolysis current of 30 mA was applied for six hours repeatedly with an intermittent pause of six hours.

The following three types of runs were tried for background measurements.

[1] Zero-current electrolysis run.

[2] Electrolysis run in the condition that the Si-SSD was covered by some metal plate for the purpose of stopping the charged particles.

[3] Pure background run with the covered Si-SSD and without electrolysis cell.

Figure 2 shows an example of the charged particle spectra during D_2O electrolysis. Weak peaks were distributed in the energy region from 2 MeV to 10 MeV. In contrast, Fig.3 shows a result of the background run of type [1], which was the light water data without electrolysis. Figure 4 shows the background data of type [2]. The charged-particle spectrum was measured with the Si-SSD, which was covered by a Ni plate of 1mm thick. The pure background (type [3]) is shown in Fig.5.

Table 1 Relation between the total counting rate of the "proton penetration peak" and experimental conditions.

Counting rate

		0	0.5	1.0 (c/h)
back ground	H_2O no electr.	—o—		
	Ni without cell		—o—	
D_2O electrolysis	No.1	—o—		
	No.2		—o—	
	No.3		—o—	
	No.4		—o—	
	covered with Ni	—o—		
H_2O electrolysis	No.5		—o—	
	No.6		—o—	

From these above results, we can point out the followings.

- In Fig.2, two types of peak structure are seen in the energy regions around 0.5 MeV and around 3MeV. From the comparison with the background spectra in Figs.3-5, they were presumed to be ordinary background responses.

- Small peaks appeared in the high-energy region in Fig.2. This strange peaks disappeared in background runs, Figs. 3 and 5, but a slight bump structure seems to have remained.

3. Discussion

The two groups of spectrum structures metioned above would be discussed in this section respectively. Focussing the view point on the comparison of the back ground response and the correlation to electrolysis, the origins of the strange structures were considered in detail.

(1) Large peaks at 0.5 MeV and 3 MeV.

Both of the structures are considered to have been caused by background phenomena. Origins of the peak in the energy region around 0.5 MeV are rather complicated. Various factors, electrically induced noises, penetration of high-energy electrons and muons, incomplete operation of the lower-level discrimination (LLD) etc., were possibly intermingled because of the lower signal level. For the 3 MeV peak, interpretation

is simpler. The energy of the peak was decreased to a half when the applied voltage on the SSD was decreased to a quarter. The thickness of the detection layer of the SSD is proportional to the square root of the applied voltage. The detection depth of the Si-SSD used was about 130 μm, which corresponded to the range of 3.5 MeV protons. These facts indicate that the peak was caused by the penetration of high energy-protons contained in cosmic rays.

Table 1 shows the total counting rates of the "proton peak" for different experimental conditions. No definite correlation is seen between the counting rate and the electrolysis.

(2) Tiny strange peaks in the energy region above 4 MeV.

Table 2 shows relations between the total counting rate in the energy region from 4 MeV to 10 MeV and the experimental conditions. The counting rate during electrolysis was remarkably higher compared with that of the background runs. This fact indicates that some parts of the structure have correlation with electrolysis and the cold fusion phenomenon.

Next, we will consider the fine structure of the strange peaks. The following three types of background source would be possible to generate mono-energetic charged particles.

- *α emitter*

    Because of their short lives, high-energy alpha emitters cannot exist stably in natural environment except radon (^{222}Rn) and thoron (^{220}Rn).

- *Neutron reaction*

    Mono-energetic neutron sources could not be found in the natural background radiations except thermal neutrons.

- *Giant resonance*

    The giant electric-dipole resonance reactions,$(\gamma,p),(\gamma,\alpha)$ of Si and the elements surrounding the detector, induced by high-energy gamma-rays contained in cosmic rays are possible to generate characteristic peak structures.

Figure 6 shows a summary of the above discussions. In the upper part of the figure, three of the experimental data, corresponding to Figs.2, 3 and 4, are shown. In the second part, the peak energy of alpha particles, emitted from radon, thoron and their daughters, are indicated. The third part shows the peak positions of alpha particles emitted by the reactions of thermal neutrons in the materials surrounding the detector. In the bottom part of this figure, the cross section curve of the giant resonance recation, $(\gamma,p),(\gamma,\alpha)$ of Si, is shown.

The structures of the spectra measured do not fit well to the peak patterns expected from the background radiations. Especially, the sharp peaks of 10 MeV in D_2O electrolysis data did not correspond with any peaks from the background sources. A slight

similarity between the outline of the spectrum structure and the cross section curve of the giant resonance is to be noted in this figure.

4. Concluding Remarks

The following remarks can be made from the above discussions.
- The peak structure in the energy region about 3 MeV was formed by high-energy protons penetrating the detection layer of the Si-SSD.
- The strange peak structures, which appeared during electrolysis, could not be explained by background radiations, i.e., radon, thoron and neutron reactions.
- The spectrum pattern seems to have some correlation with experimental conditions. The counting rate of the "strange peak region" (4-10 MeV) during electrolysis was remarkably higher compared with that of background runs.

These phenomena could not be explained by the ordinary D-D reaction occurring in the palladium cathode. An accurate determination of the peak energies of the strange structures would be a key to resolve the unknown nuclear reaction lying behind the anomalous phenomena.

Acknowlegement

References

1) T.Iida,M.Fukuhara,H.Miyazaki.Y.Sueyoshi,J.Datemichi and A.Takahashi, Proc. 3rd Int.Conf.on Cold Fusion 201,Nagoya,Japan(Oct.1992)

2) F.E.Cecil,H.Liu,D.Beddingfield and C.S.Galovich, Proc.Anomalous Nuclear Effects in Metal/Deuterium systems 375,Provo. UT(Oct.1990)

3) G.P.Chambers,G.K.Hubler and K.S.Grabowski, Proc.Anomalous Nuclear Effects in Metal/Deuterium systems 383.Provo. UT(Oct.1990)

4) Y.R.Kucherov,A.B.Karabut and I.B.Savvatimova, this Conf..Maui (Dec.1993)

5) J.F.Ziegler, Nucl.Instr.& Meth..191.p.419(1981)

Table 2 Relation between the total counting rate of the "strange peak region" and experimental conditions. The broken line shows the calculated value [5] of the cosmic-ray.

Counting rate

		cosmic ray 0.1 0.2 (c/h)
back ground	H_2O no electr.	
	Ni. without cell	
	B. without ceil	
D_2O electrolysis	No. 1	
	No. 2	
	No. 3	
	No. 4	
	covered with Ni	
	covered with B	
	covered with Ti	
H_2O electrolysis	No. 5	
	No. 6	
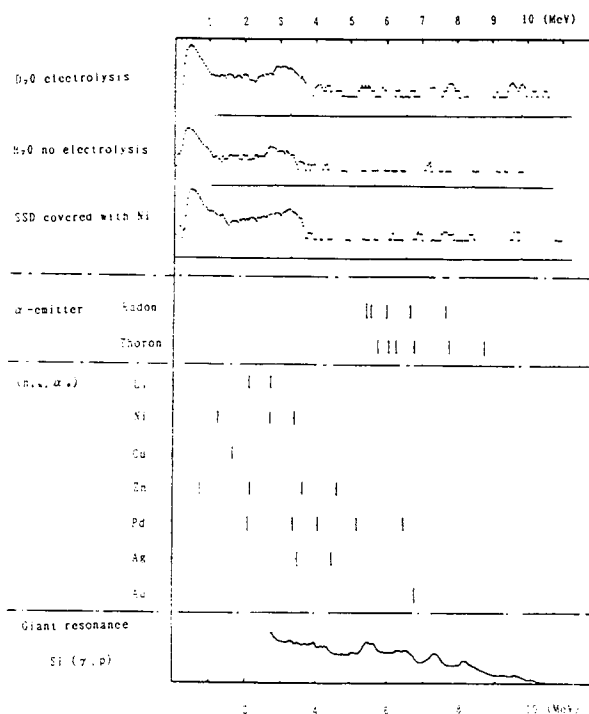
Fig.6 Comparison between the charged particle spectra and peak energies attributed to some background sources.

Observations of Cold Fusion Neutrons from Condensed Matter

Shigeyasū SAKAMOTO
Department of Nuclear Engineering, Tokai University
1117 Kitakaname, Hiratuka-shi, Kanagawa, Japan

Abstract

This paper reports the results of our experimental studies on neutron measurements of palladium hydride cathodes under conditions similar to those in the study of Jones, on electrochemically induced nuclear fusion of deuterons. Electrolysis was carried out in small cells containing 99.8% pure heavy water with alkaline. A BF_3 counter and/or ^3He counters were employed forthe neutron detection. Excess neutrons were observed in only one cell.

Introduction

Since the announcements of electro-chemically induced cold fusion[1],[2], many confirmatory experiments have been carried out. However, no clear evidence has been obtained yet.

The present paper concerns the results which we obtained on the neutron emission following the electrolysis of heavy water utilizing palladium cathodes. The electrolysis was performed in small cells, containing 99.8% pure heavy water with alkaline. The neutron detectors used were Bonner counter type which is proportional counters for thermal neutron with a moderator.

Experimental apparatus and procedure

In the preliminary experiments[3], electrolysis was performed in a 2 ml glass cell containing 99.8% pure D_2O with NaOH. The cathode was a palladium wire of 99.9% purity with the dimension of 0.1 mm in diameter and 25 mm in length. The anode was a platinume wire of the same size as the cathode. The electrolytic cell is surrounded by thermal insulating materials as shown in Fig.1.

Figure 2 shows the arrangements for the experiments. The neutron detector consists of a cylindrical BF_3 proportional counter, 250 mm in length and 25 mm in diameter, filled with 400 mm torr of BF_3 gas, and the outer moderator which is 5 cm-thick paraffin wax. The cell and the neutron detector are shielded by layers of borated and ordinary polyethylene with the total thickness of 10 cm. The counting efficiency of the neutron detector was estimated 1.4×10^{-3} using a Californium-252 neutron source.

BLISTERED POLYSTYRENE

COTTON

BLISTERED
POLYSTYRENE

TEST
TUBE

D₂O

THERMOCOUPLE

CATHODE
(Pd)

ANODE (Pt)

THERMAL RADIATION
SHIELD

30mm

10mm
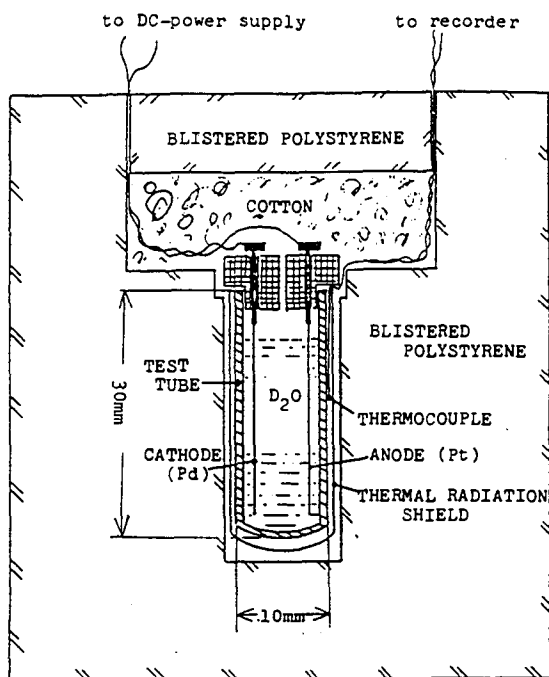
Figure 1. Electrolyte cell and thermal insulator
in preliminaly experiments

NEUTRON SHIELD

DETECTOR
BIAS

MCA/MCS

NEUTRON
DETECTOR

PRE-AMP.

MAIN-AMP.

DISCRI.

CALORIMETER

γ-ray
detector

SCALER

THERMOCOUPLE

AMPLIFIER

DISCRI.

PRINTER

RECORDER
(temperature)

DETECTOR
BIAS

SCALER

A

RECORDER
(current)

DC-POWER
SUPPLY

REM COUNTER

SCALER

PRINTER
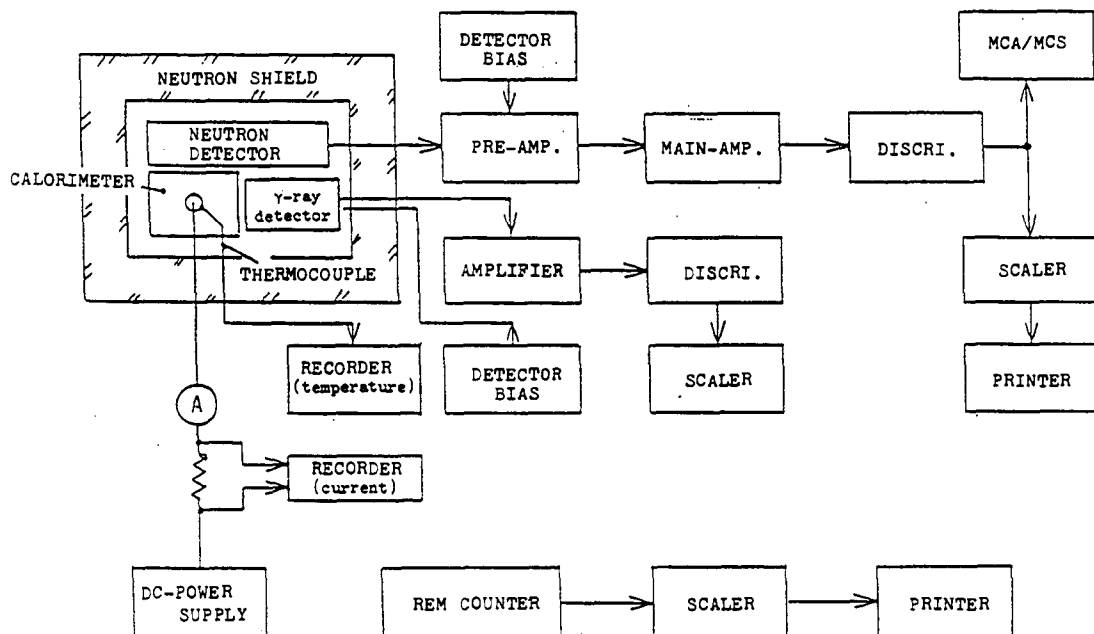
Figure 2. Experimental setup in preliminary studies

The background measurement was carried out over 30 hours before starting electrolysis, while heavy water was inserted in a cell and the current for electrolysis was stopped.

A regulated direct-current power supply provided 4 to 25 Volts across the electrodes at the current of 10 to 30 mA. Electrolysis continued being carried out for 19 days at the current density of 140 to 320 mA/cm^{-2} on the palladium cathode. additional background runs were made for 86 hours, while the electric current was turned off. Electrolysis was resumed after the background runs for 58 hours. Neutron counting were executed every 90 min. during of the experiment.

Subsequently to the preliminary experiments, we designed and constructed a new measuring system, which has high detection efficiency for source neutrons, low counting efficiency for background radiations, noise-resistant for external electromagnetic noises, high stability for long term operation, and high reliability.

The electrolytic cell was a polypropilene test tube of 1 cm diameter and 7 cm high, with electrodes inside. The cathode was a palladium wire of 99.9% purity with dimensions of 0.1 mm in diameter and 20 mm in effective length. The anode was platinum wire with dimensions of 0.3 mm in diameter and the same effective length as the cathode. The configuration of the new electrolysis cell is drawn in Fig.3. Teflon-sheathes were attached to the electrodes for the purpose of the stabilization of electrolysis in long term.
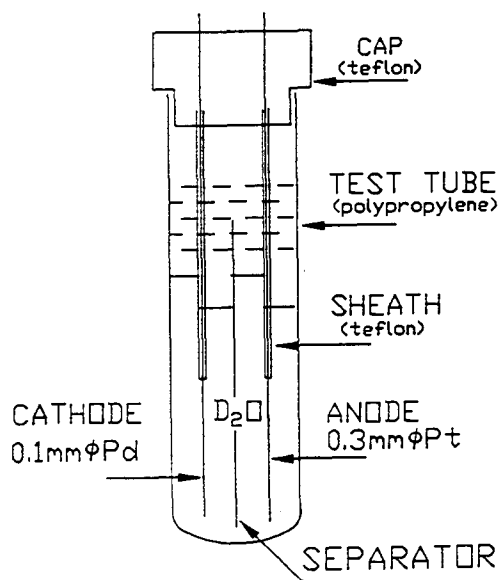
Figure 3. Electrolyte cell for new experiment system

Six cylindrical proportional counters, 25 mm in diameter and 250 mm in length filled with 5 atm ^{3}He gas, are positioned along the circumference of the cell. The arrangement of the cell, ^{3}He counter banks, and the shielding materials, is shown in Fig.4. For the purpose of cross checking, two counter banks were employed. The paraffin wax serves to enhance the detection efficiency of the ^{3}He counters by moderating fast neutrons emitted from the cell. External background neutrons are slowed down and captured in the 20 cm-thick layers of borated and ordinary polyethylene shield with Cd sheets.
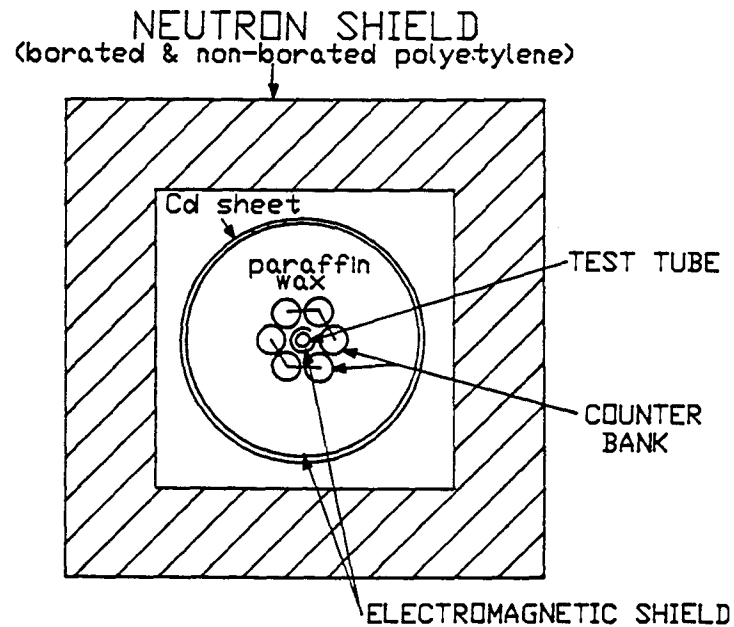
Figure 4. Arrangements of cell and detector

The block diagram of the direct-current source and measuring system is shown in Fig.5. Electrolysis was carried out with constant voltage method and the current constantly was monitored by the pen-recorder. Electromag neticshields were attached on a cell and direct-current feeder cables, to prevent the noise associated with electrolysis from entering the counters. Additionally, for the purpose of preventing electric noises from the AC power supply line, Bin & Power Supply of the NIM system was connected to the AC power line through a noise-filter and an insulation transformer. Signal from the two counter banks are processed by individual circuits and counting. Detector biass of the two counter banks were supplied from the common one power supply. Electrical noises can be detected by using a coincidence circuit because many of them occur simultaneously in both channels.

We observed the time-variation of neutron counts corresponding to the full energy peak for ^{3}He(n.p)T reaction area on the pulse height spectrum, using Timing Single Channel Analyzers(TSCA) and preset counters with 100 min. time steps. The pulse height spectrum from the counters are constantly monitored by a 512 channels pulse height analyzer in parallel with the preset counter. The spectrum data were transfered to a personal computer every hundred-thousand seconds and stored there.

The neutron detection efficiency, including the geometrical acceptance and pulse height discrimination effect, was measured using the ^{252}Cf neutron source to be 6.4% for the source neutrons. The background neutron counting rate of the system was 0.02 cps, this value is equivalent to 0.3 sec^{-1} source neutron.

Experiments on the new apparatus started at end of the August in 1993. The background measurement and stability test were carried out over 30 days before the start of electrolysis while the heavy water is inserted in a cell and the electric current for electrolysis is stopped. After that, electrolysis continued being carried out for 3 months at the current density of 400 to 600 mA/cm^{-2} on the palladium cathode.
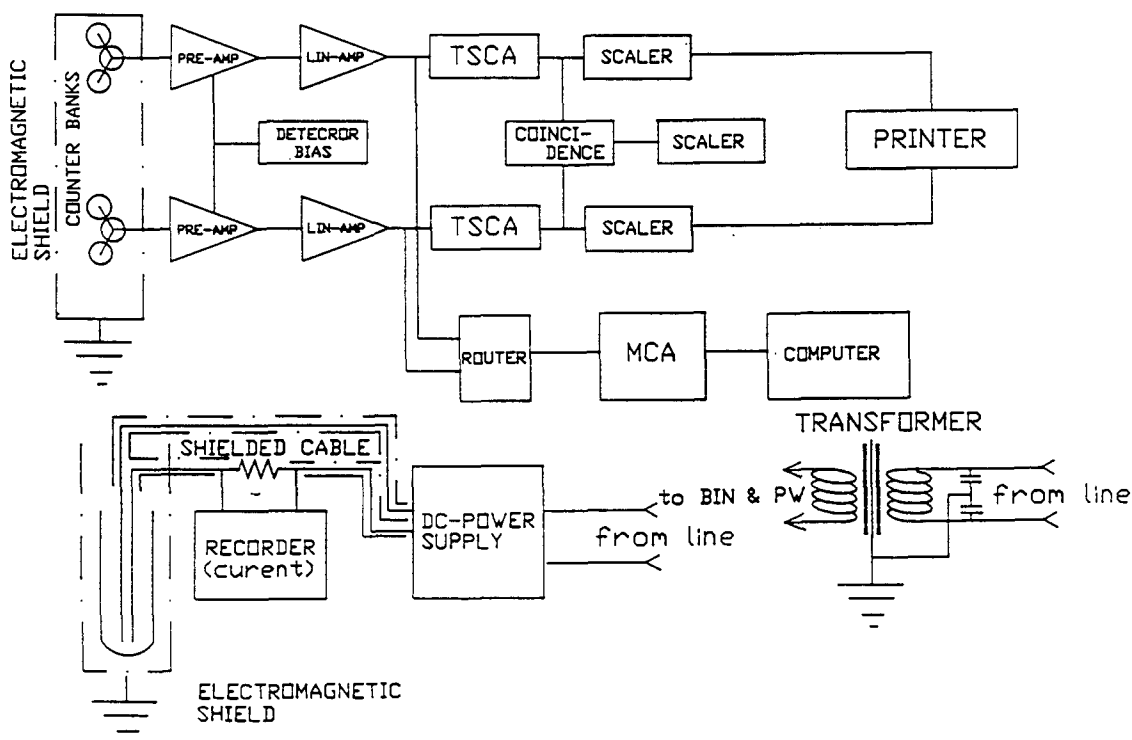
Figure 5. Experimental arrangement for recent experiments

Results of experiment

Figure 6 shows the change of the neutron count-rates for all the runs of the foreground and the background in the preliminary experiments. This results indicate weak evidence for excess neutron emission from electrolytic cell with electrolysis. The excess neutron counts are in the level of 2 or 3 times of the background. Figures 7 and 8 show frequency distributions of the neutron counting rate for the runs of foreground and background.
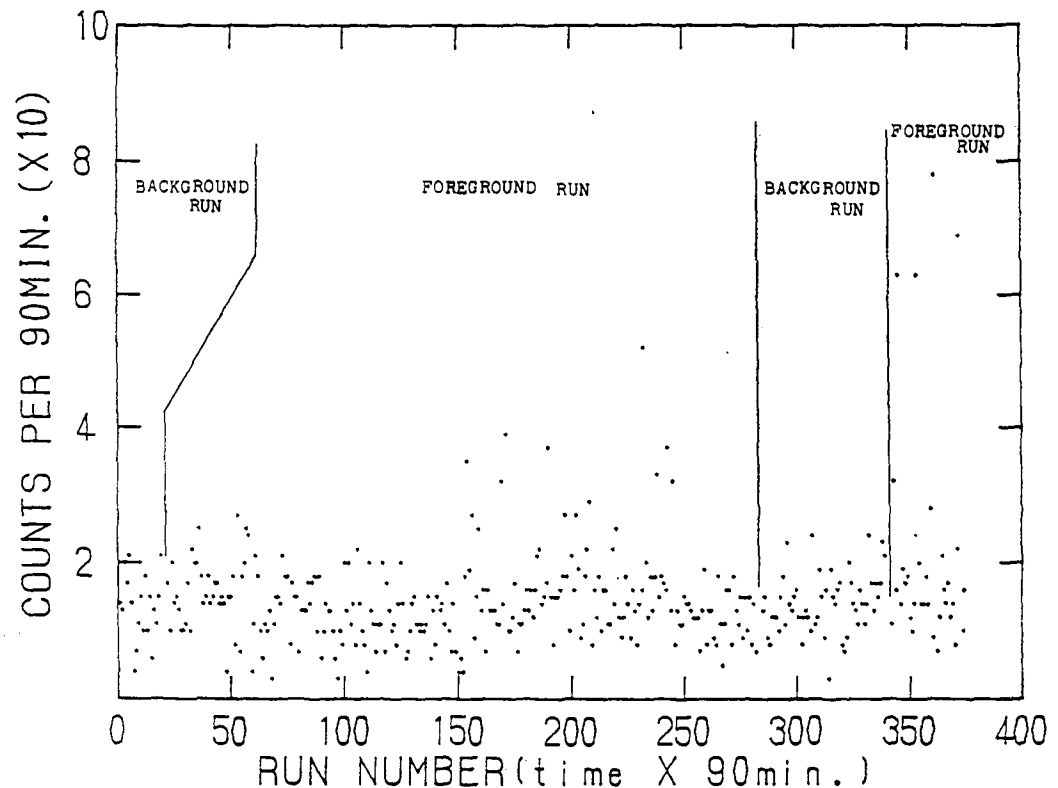
Figure 6. Neutron count-rate as a function of electrolysis time

Figure 9 shows a typical pulse height distribution of the ^{3}He counters during electrolysis indicate with the window levels of the TSCA. The change of the neutron count-rate as a function of electrolysis time about the two months after electrolysis started is shown in Fig.10, compared with the background level.

Conclusions

Excess neutrons were observed in the preliminary experiments, while our recent experiment did not show any excess neutrons. However, this result does not deny the possibility cold fusion. The difference between the two experiments is due to the change of the palladium wire during the
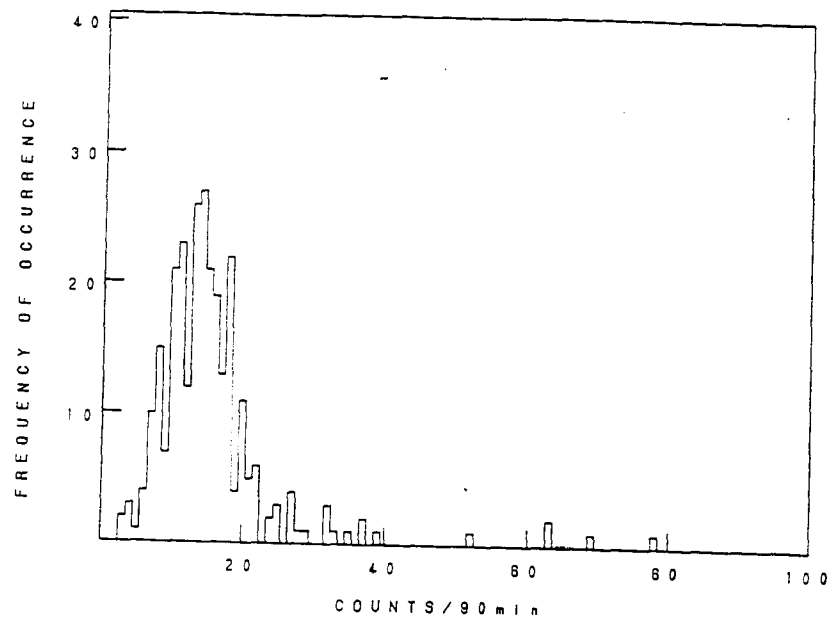
Figure 7. Frequency distribution of neutron count-rate for foreground run
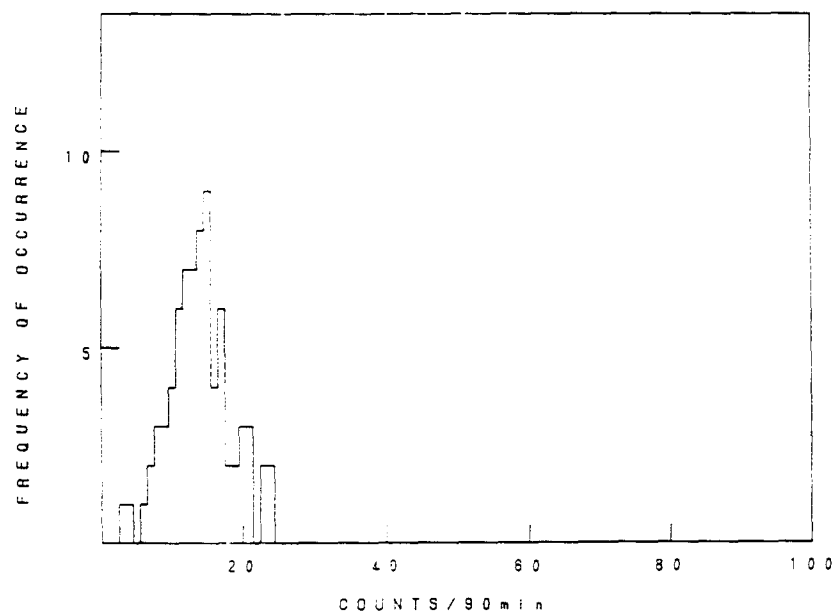
Figure 8. Frequency distribution of neutron count-rate for background run
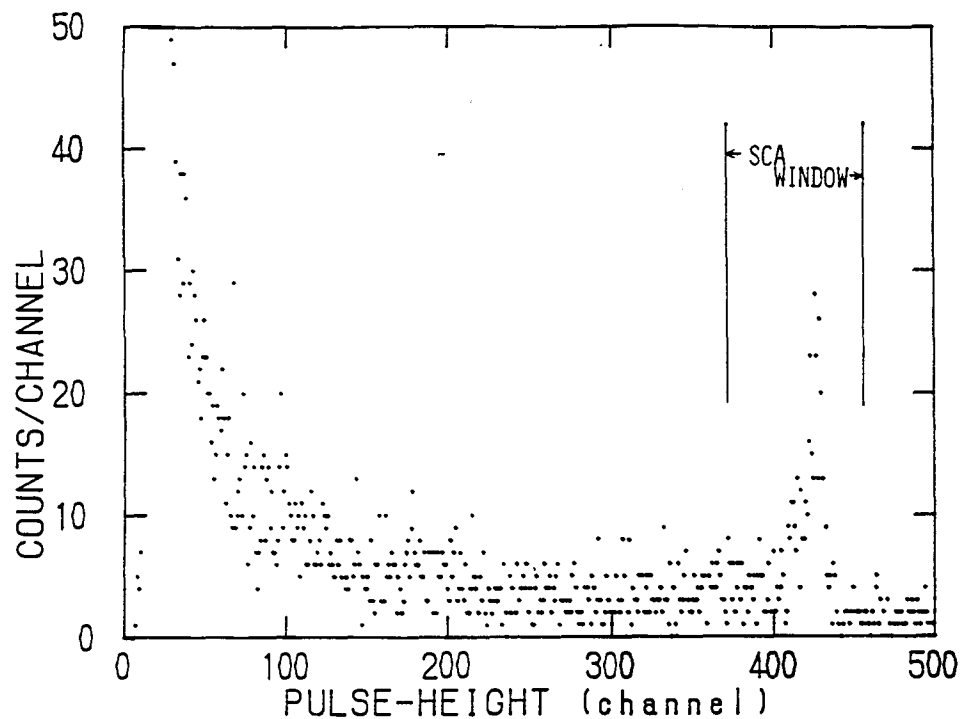
Figure 9. Typical pulse height distribution of ^{3}He
counter bank
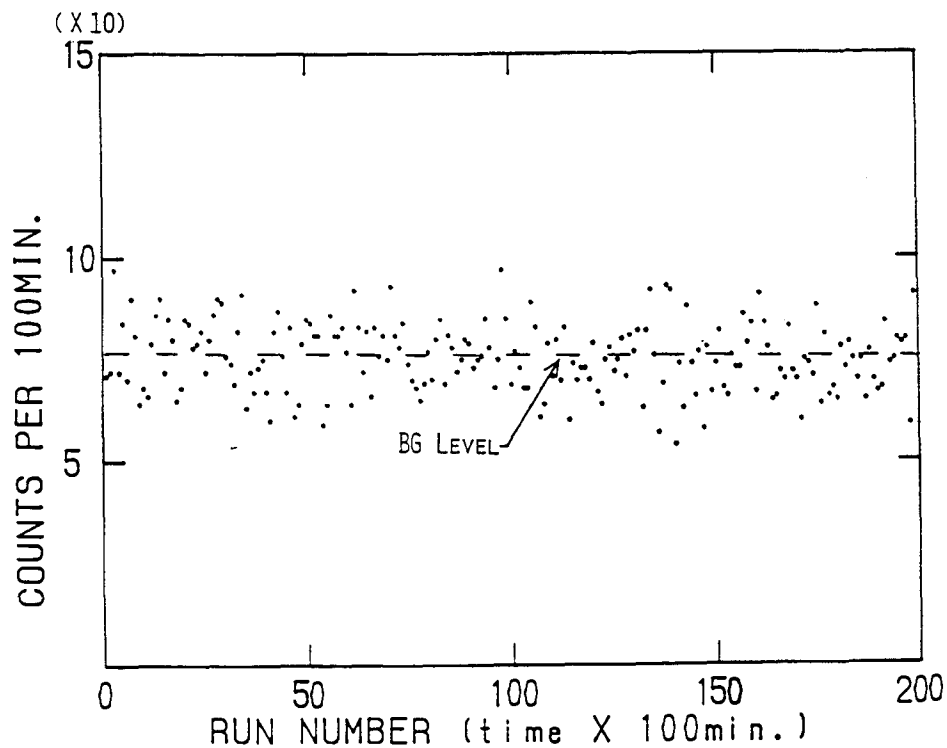
Figure 10. Neutron count-rate as a function of electrolysis
time, for recent experiment, comppared with
background level

electrolysis.

While the palladium electrode was considerably fragile after the preliminary experiments there was only a minor change in the resent experiments. It is conceivable that a difference is due to the density of the deuterium inside the palladium electrode with some unknown experimental conditions.

References
1. M.Fleischmann, and S.Pons. "Electrochemically Induced Nuclear Fusion of Deuterium." J. Electroanal Chem., Vol.261,p.301(1989).
2. S.E.Jones, et al., "Observation of Cold Nuclear Fusion in Condensed Matter." Nature, Vol.338,p.737(1989).
3. S.Sakamoto, "Follow-up Experiments on Room Temperature Nuclear Fusion" Proceedings of the 13th Joint Symposium, Tokai University-technical University, Budapest, Kanagawa, Japan (Sep.1989)

INVESTIGATION OF THE ERZION-NUCLEAR
TRANSMUTATION BY ION BEAMS

D.S.Baranov,Yu.N.Bazhutov, V.P.Koretsky
Scientific Research Center of
Physical Technical Problems "Erzion"
P.O.Box 134, 119633 Moscow, Russia

Yu.M.Plets,G.P.Pohil,E.M.Sakharov
Nuclear Physics Institute, Moscow State University,
110899 Moscow,Russia

Abstract

The studies of nuclear transmutation were conducted in the copper-beryllium target. This target was irradiated by xenon nuclei (E=120keV). According to Erzion Model xenon nucleus can carry heavy neutral hadron (enion) wich must catalyse nuclear transmutation. Expected gamma-rays were mesuared during the experiment with NaJ cristal material. Beta-activity decay of target was mesuared after the accelerator runs.

1.Introduction

It was demonstrated [1] that some nuclei may hold heavy neutral hadrons, named "enions", near the nucleus. The bonding energy of nucleus and enion is about 100eV. Such elements may serve as donors to enions for transmutation in the Erzion model. The released enion may provide energy allowed reactions with some elements. Thus elements may serve as fuel for transmutation.In the present work it is proposed to intiate such reaction by the accelerated ions-donors (in this case-xenon) with irradiation the target containing elements-fuel (in this experiment - copper and beryllium). It was suggested that the transmutation will be registrated with the help of gamma-activity and beta-activity measuraments of turning out isotopes.

2.Experimental

The target was made from six alternating layers of two elements Cu and Be. The depth of copper layers - 1mm and berillium layers - 0.01mm. The column of the layers was surrounded with berillium plate so that construction makes the "glass" form.

The electrostatic ion accelerator was used as a source of enions. Ion beam was directed into botton of the target's glass. The energy of accelerated xenon ions was equal to 120 keV. Such energy may be sufficient to "shake-off" the enion from xenon nucleus. Average beam current was iqual to 50 microamper, beam diameter – 4 mm. Total flux irradiation was about 10^{20} ions (with 20% accuracy) for beta spectroscopy and $2x10^{19}$ ions for gamma spectroscopy.

Gamma-activity was measured during the irradiation with NaJ crystall (diameter 15 cm, height 20 cm) and photoelectric multiplier (type ФЭУ-49). Beta-activity was measured after the accelrator runs by plastic scintillator.

3.Model Prediction

From the model predictions it was concived that the radioactive isotopes Cu-64, Cu-66 and Ni-65 can be turned out after appearing enion in target material. Their half-lifes are moderately low (12.7 hour; 5.1 minute and 2.5 hour respectively) resulting in high intensity of gamma-lines. The energies of gamma-lines for Copper isotopes are 511 keV, 1340 keV and 1030 keV. In the dacay scheme of Ni-65 the cascade of two gamma-quants are presented with the energies 378 keV and 1115 keV. During the process of our test the gamma-radiation with above energies were recorded.

4.Result and Discussion

The gamma-activity and beta-activity measurements don't show any statistically considerable counts (more than three root-mean errors) for the gamma and beta source. Some reasons one might expect an absence of well-defined results. Firstly, as expected from the model [2], the relative concentration of enions on xenon nucleus may be located in interval $10^{-16} - 10^{-21}$. It is follows that the probability that the enion will appear in the target may be mutch less than 1. Secondly, the radioactive isotopes production may be less then $2x10^{5}$ for Cu-64 and for Cu-66, 10^{5} for Ni-65, 10^{12} for Be-9 and the more homogeneous and pure target may be necessary to reduce losses of enions.

References

1. Yu.N.Bazhutov, G.M.Vereshkov. "New Stable Hadrons in Cosmic Rays, their Theoretical Interpretation and Possible Role in Cold Nuclear Fusion Catalysis". Preprint, CSRIMash, N1, 1990.
2. Yu.N.Bazhutov, A.B.Kuznetsov."Erzion-Nuclear Spectroscopy of Stable Isotopes", Preprint, CSRIMash, N4, 1992.

THE INITIATION OF REPRODUCIBLE NUCLEAR REACTIONS
IN THE STRUCTURES OF THE OXIDE TUNGSTEN BRONZE

K. Kaliev, N. Svedlov, Yu. Istomin, E. Golikov, V. Butrimov,
D. Babaeva, G. Vasnin, V. Fyodorov

The Institute of High-Temperature Electrochemistry
620219 Ekatherinburg, Russia

Abstract

The possibility of control emission of neutrons at interaction deuterium with oxide tungsten bronzes by electrolysis in the electrolyte based on heavy water is shown.

Introduction

At last year during the Third International Conference on Cold Fusion in Nagoya, We reported about our method of realization of reproducible nuclear reactions by deuterium interaction into oxide cubic tungsten bronze. The concentration and interaction of the deuterium gas we carried out in the channels of the (100) facet of cubic monocrystal sodium tungsten bronze. The forming of the channels was carried out by extraction of sodium ions from crystal lattice of oxide bronze by electrochemical and vacuum methods /1-3/.

We continue work on study of interaction deuterium with oxide tungsten bronzes. To our mind the hexagonal structures are the most suitable because it is known that cation's mobility in particular hydrogen's mobility increases on some levels.

In this paper we presented the results of experiments on interaction of gas deuterium with special treatmented surface of hexagonal kalium oxide tungsten bronze ($K_{0.3}WO_3$) and the results of investigation on electrolytic saturation of surface of such crystal by electrolysis of solution on a base of heavy water (carried out by the known method /4/).

2

The methodic of carring out of the first type experiment was the same as presented in previous paper one /2/. However temperature of vacuum treatment for hexagonal structure kalium tungsten oxide bronze crystal was lowel (550-580 °C) than for a cubic sodium tungsten bronze. The type of cell, in which we realized cation's extraction, are shown on the fig. 1. The cell represents "sandwich" structure, which consists of monocrystals kalium tungsten and sodium-tungsten bronze in the first variant, and of pills, textured by monocrystal needles hexagonal kalium tungsten bronze in the second variant. In this case the surface of the pills represents regular located planes.

Texture of the pills reached by electrolytic method, by growing of the priming-needle through the regular located quartz capillaries. The electrolytic cell for growing was made from quartz tube with 10 mm in side. We used the melt 40 mol. % K_2WO_4 - 60 mol. % WO_3, temperature 850 °C. After its cooling, the cell was cut into disks with the thickness 5 mm. These disks had to be grind and polish.

The electrolysis of heavy water was carried out both in equilibrium conditions, and in conditions, which are far from it. The last was reached by putting the electric field. As it was shown earlier, superpolarization of the surface between electrode-electrolyte is reached by the electric field, to our mind because of the oversaturation of the segnetoelectric nature's phase, which is formed on oxide bronze. The electrolysis current of heavy water was 100+300 mA (in dependence of the structure kalium-tungsten bronze). The experiments were carried out at room temperature. Chrome-aluminium thermocouple fixed the change of the temperature. The thermocouple is situated directly on the work surface of the crystal. Two independent   ways from two meter's blocks (type SNM-42 with paraffin) measured the emission of neutrons.

The signals were summed up by the numeral voltmeter, and taken out independently. Summary effectiveness was about 1.4 %.

Results

The main results of the experiments, which were carried out on the cells of the first type (vacuum) are shown on the picture 2. They were received in accordance to the method /1/.

21-2

The typical course of change of the temperature of the monocrys-
tal's surface of the hexagonal structure in the moment of con-
tact with deuterium in the working tube after the extraction of
the kalium ions is the same, that for cubic oxide bronzes. For
the short time (0.1-0.3 sec) there temperature was achieved
5-30 °C. Typical observed neutron production during electrolysis
for the hexagonal kalium oxide bronzes in a cell (fig. 1) is
showed in fig. 3. The last result was received during changing ·
the polerity of the electrodes in the cell of the second type.

Discussion

As the previous works this work confirms the main result, that
is going out on the level of reproduction of experimental data,
which prove proceeding of nuclear reactions in surface phase of
oxide tungsten bronze, correlated from the moment of deuterium's
overlapping into their structures. The main result of our inves-
tigation is a result received in the cell of the second type. The
histogram of these events during 40 minutes – on the fig. 3.
The fact, that realization of nuclear reactions in the second
type of cells first of all increases neutron emissions speed on
several levels, and in the second place makes this process diri-
gable is evident. This effect (that is considerable exceeding of
neutrons going out, and also it dependence on polarity of ten-
sion) connects with phenomenon of "superpolarization" of the elec-
trodes from oxide tungsten bronze./5/.

Conclusion

                 exchange of the
It is shown that direction of nuclear reactions in condensed me-
diums is possible for hexagonal structures of oxide tungsten
bronze.

References

1. K. Kaliev, A. Baraboshkin, A. Samgin, E. Golikov, A. Shaly-
apin, A. Andreev, P. Golubnichiy. Frontiers of Cold Fusion
Edited by H. Ikegami October 21-25, 1992, p. 241-244.

2. K. Kaliev, A. Baraboshkin, A. Samgin and et al. Physics
Letters A 172 N 4 (1993) 199-202. North-Holland.

3. A. Aksentyev, K. Kaliev, A.Baraboshkin. Electrochemistry,
1982, v. 18, p. 563-568.

4. Fleischmenn M., and Pons S. 1989. Electroanal. chem., 261,
301.

5. The phenomen of tungsten improvement in polytungsten melts.
Electrochemistry, 1992, issue 12, 1855-1856.

6. S.E. Jones et al., 1989, Nature, 338, 737.

"goldEN behavior"

ICCF-4-93

Isolation *(tos)*   1   membrana

Electrolyte

+   −

< 0001 >

Oxide bronzes

Channels
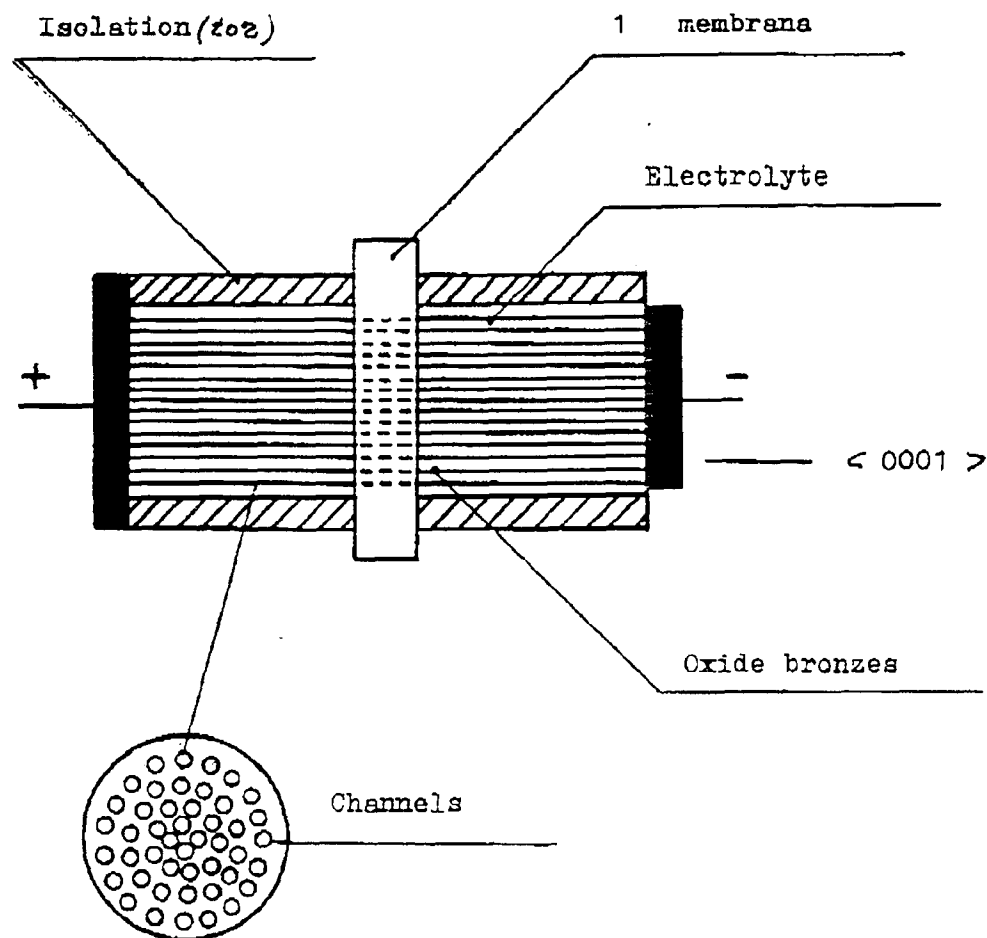
Fig. 1 Experimental sell for the initiation of the
reactions Cold Fusion in a system D_2O $(Li_2SO_4)-K_xWO_3$

Fig. 2   Typical observed neutron flux
after interaction D_2 – gas
with $K_{0.3}WO_3$

Infusion D_2

Pumping
out D_2

Observed count

16
14
12
10
8
6
4
2

Average
background

60   120   180   240   300   360   420   460   540   600   sec

5000

4100   4300

3000
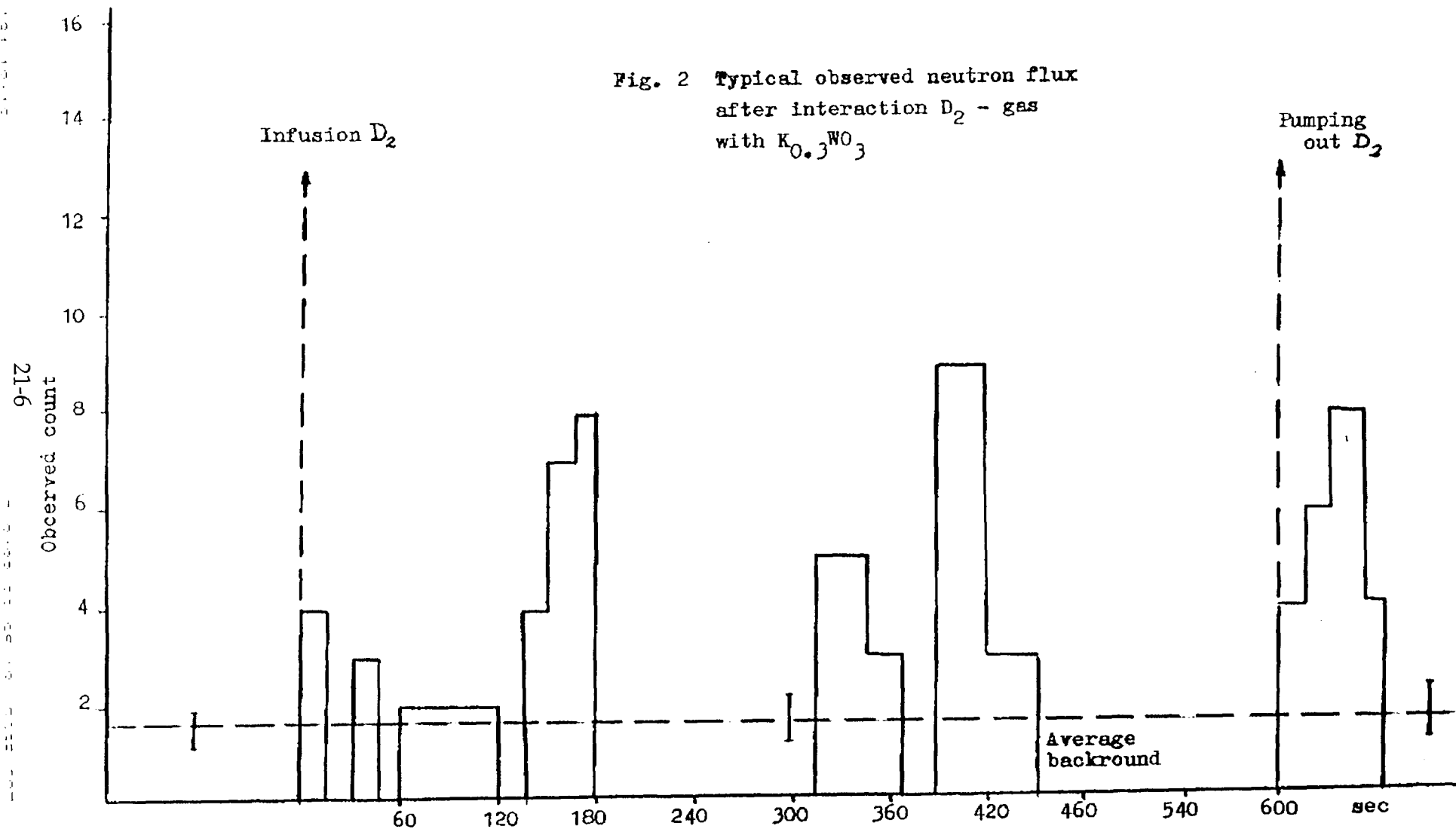
Fig. 3 Neutron flow intensity
        at electrolysis heave water
        with $K_{0.3}WO_3$ electrodes.
        $\Delta U = 0.5 \rightarrow 2.5$ kV.

2500

Observed count

2000

21-7

1500

1000

500

Average background

min   5   10   15   20   25   30   35   40   45   50

time (min)
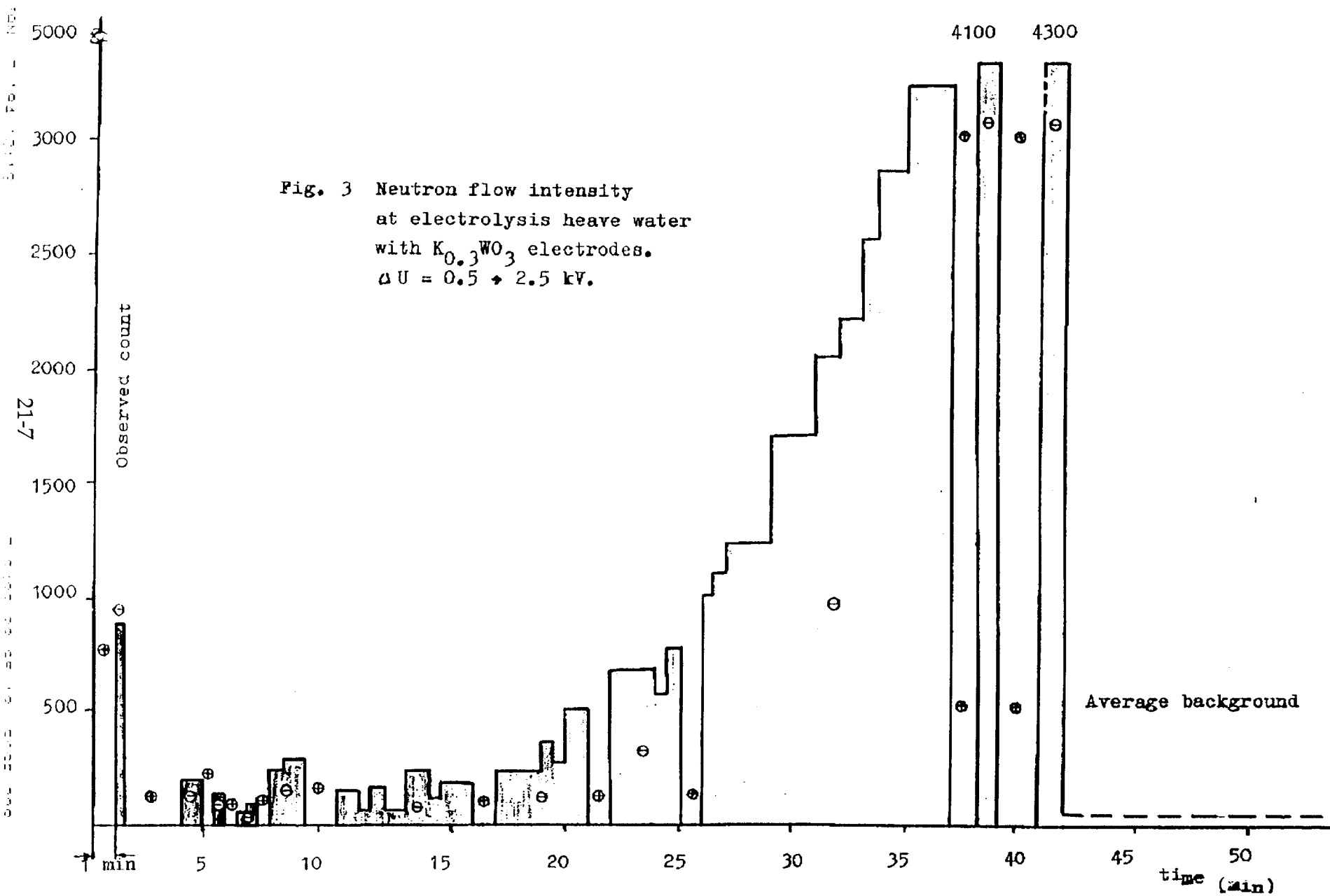
CONCEPT OF TARGET MATERIAL CHOICE FOR NUCLEAR REACTIONS IN CONDENSED MEDIA

V.A.Romodanov, V.I.Savin, S.G.Korneev

142100 Podolsk, Moscow Region, Zheleznodorozhnaya 24,
SRI of SPA LUTCH
Tel. 095-137-9258
Fax: 095-137-9384

Ya.B.Skuratnik

SRPCI named after Karpov, Obukha 10, Moscow

ABSTRACT

On the basis good and reproducibility tritium generation results which gett in condition of the high densities glow discharge to begin studying the influence of different parameters of the deuteron and the base atom interaction process on the nuclear reactions in condensed media (NRCM) efficiency.

The possibility of choosing the most efficient materials is discussed on the basis of the model proposed before.

The heaviest elements of Mendeleev's periodic system are shown to be the most promising materials for NRCM.

The practical results obtained when using a powerful glow discharge have been considered. They verify the above-mentioned hypothesis and the features of realizing the promising properties of the materials for NRCM.

1. INTRODUCTION

Most of the experiments on nuclear reactions in condensed

media (NRCM) are made when using pallasium, titanium or nickel
as base materials and their reproducibility isn't high. When
usinf other materials, the results are more contradictory and
the required number of the models, where the NRCM rate depen-
dence on the base material type is discussed, isn't available.

The "swimming" electron model by H.Hora supposes that the maxi-
mum shielding effect of Coulomb potential for the interacting
deuterons is achieved as a result of the electron accumulation
either on the solid surface or at the joint of the material
surfaces having different Fermi energy levels /1/. The composi-
tions of nickel-cerium, iron-cerium and titanium-cerium layers
10-30 nm thick are considered the most efficient. However, to
verify this concept at rather low energies the layers should
be very thin, perhaps, due to this fact the first experiments
were performed when using the plasma focus where the energy
level of the bombarding ions could be rather high.

The material efficiency in Bazhutov-Vereshkov model is under
discussion. The existence of heavy "erzion" particles which
can be used as nuclear reaction catalysts is supposed in this
model /2/. This model verifies the prospects of such materials
as palladium and nickel and proposes the compositions of the
materials in which one of them deliver the catalyst particles
and the others consume them. Copper and iron aren't considered
promising materials for the NRCMs within this model. One hasn't
enough experimental data for verifying this model yet.

A.S.Davydov in his work proposed the method where Coulomb
potential of two deuterons is shielded by the bound bipolar
electrons having the total zero spin and twice the charge /3/.
The PdD-crystal goes to the superconducting state at the tem-
perature of 11 K. That is indicative of the possibility of a
considerable reorganization of the electron shell structure
in the process of hydrogenation. The shielding like that should

be especially considerable for superconductors and within the lower temperature range.

M.Rabinovich in his work notes the connection between super-conductivity and "cold fusion" too /4/. He affirms that the low - temperature superconductivity can be the proper condition for resonant overcoming of Coulomb barrier.

In the article by J.Waber he proposed to use superconducting materials too but their property caused by the third type of boson state, i.e. the deuteron superfluidity caused by their position in Boson-Bloch-Condensate, was considered to be the main cause responsible for overcoming of Coulomb barrier in the NRCMs. The deuteron superfluidity is supposed to exist at 300 K too /5/.

At present the available experimental results on the supercon-ducting materials and low temperatures haven't detected any particular advantages of these materials as for the nuclear reaction efficiency /6, 7/.

E.Ragland in his work affirms that as a result of the a parti-cular deuteron structure and its high mobility in the lattices of some metals it is possible to overcome Coulomb barrier at their high concentrations and low energies /8/. The periodic elements from titanium to nickel, from zirconium to palladium and from hafnium to platinum can be these metals. On the whole, many experimental results verify this hypothesis.

G.V.Fedorovich showed that the deuterons energy could be con-centrated in so-called E-elements of the crystal lattice and it could achieve the level enough for the nuclear reaction proceeding. That is verified for piezo- and ferroelectric mate-rials when their temperature changes in the proximity of Curie point /9/.

In spite of the great scepticism concerning the high results
on tritium generation, which were obtained by some groups,
this problem is becoming the leading one for under-standing
the NRCM mechanism because the most reliable results on neut-
ron, γ- and X-radiation, charged particle, ^{3}He and ^{4}He, measu-
rement element transmutation and heat excess don't exceed the
background noise level very much. For some methods of tritium
generation on gas discharge base one has obtained the reliable
results exceeding the background noise level by 2-5 orders of
magnitude /10, 11/, that allows to start studying the effect
of different parameters of the deuteron and target atom inter-
action process on the NRCM efficiency. We've already proposed
the model of two nuclei interaction in close proximity to the
excited atom of the condensed medium matrix /11/.

This work seeks to consider the conclusions of the proposed
model, which show up the matrix material importance for the
NRCMs at low energies.

2. MODEL CONCEPT

In the above-mentioned model we supposed that the nuclei col-
lisions correlated with those of the atoms and at low energies
the nuclear reactions most probably took place when most of the
bombarding particle energy was spent on the elastic atom col-
lision,but it wasn't dissipated by the electron system /11/.
In view of the matrix material effect the range of the optimal
energies $\mathcal{E}_1$ for the deuteron ions is from 30 eV up to 5 keV.
In view of the energies from $\mathcal{E}_0$ up to $\mathcal{E}_2$ this range is
within $20\text{-}3 \cdot 10^4$ eV. The further discussion of the NRCM pos-
sibility concerns this energy range.

We think that the shielding of Coulomb potential of two nuclei
will be more efficient of their collision takes place in close
proximity to the excited (at least one) matrix atom. In this

case it is possible to shield-Coulomb potential not only by
valence electrons, but also by those ones which are closer
to the matrix atom nucleus. That can take place at the moment
when the atom shifts from its equilibrium position and a num-
ber of electrons leave the stationary orbits. The electrons
and ions move in condensed media rather fast and the energy
relaxation time for the electrons is $\sim 10^{-13}$ s and that one
for the ions $\sim 10^{-14}$ s. At the same time the nuclear reaction
rate is much higher ($10^{-16} - 10^{-19}$ s), i.e. while the deu-
teron and matrix atom collisions caused, for example, by the
ion bombardment take place, the collisions resulting in such
a Coulomb potential shielding, that some nuclear reactions can
proceed, are possible to take place in this mixture. The simi-
lar collisions take place when the accelerated ions having the
energy exceeding the target matrix atom shift threshold bombard
the target which consists of the atoms of the matrix having
some atoms dissolved in it before or introduced in it during
the ion bombardment by the atoms which can undergo the nuclear
reactions with each other or with the matrix atoms. The simplest
variants of such collisions take place according to the follow-
ing type: D —▶D —▶matrix atom or matrix atom —▶D —▶D
(fig. 1). The probability of such collisions increases when
increasing the reacting nuclei concentration in the matrix
volume and when increasing the bombarding ion flux.

The conclusions concerning the choice of the target matrix
materials and the elements undergoing the nuclear reactions
are a matter of interest. Firstly, one should choose the ligh-
test elements, such as hydrogen, lithium, beryllium, having
the minimum Coulomb barrier when closing in, as the elements
which can ungergo the nuclear reactions most readily. Secondly,
the heaviest atoms from periods VI and VII in Mendeleev's
periodic table are the best matrix elements which can release
the greatest number of electrons into the area of shielding
Coulomb potential of the reacting nuclei when they are excited.

In this case one should highlight the elements from the lant-
hanide and actinoid groups, having not only the maximum number
of electron shells, but also the maximum hydrogen solubility.
One should note that the heavy elements practically don't
undergo the nuclear reactions at the above-mentioned energies
and they are unconsumed catalysts for the lighter elements
undergoing the nuclear reactions.

The supposed comparative efficiency of the elements from Men-
deleev's periodic table, taken as a matrix material playing
the part of catalyst for the reactions proceeding on the deu-
terium nuclei in view of the solubility is shown in fig. 2.
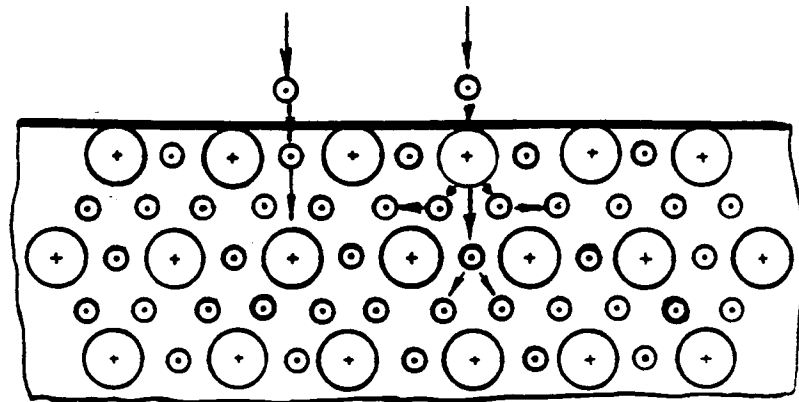
Fig. 1. The diagram of possible triple collisions of the
        light and heavy atoms when bombarding the targets
        by accelerated particles

The arrows (see fig. 2) show the directions of the nuclear
reaction efficiency growth when using different elements as
a matrix material. One can see that the most efficient cata-
lysts of the nuclear reactions can be the elements from the
actinoid group, which have both the maximum hydrogen solubi-
lity and the maximum number of electrons which can take part
in Coulomb potential shielding.

	I	II	III	IV	V	VI	VII		VIII		
1	H 1										2 He
2	Li 3	4	5	6	7	8	9				10 Ne
3	Na 11	12	13	14	15	16	17				18 Ar
4	K 19	20	21	22	23	24	25	26	27	28	
4	29 Cu	30	31	32	33	34	35				36 Kr
5	Rb 37	38	39	40	41	42	43	44	45	46	
5	47 Ag	48	49	50	51	52	53				54 Xe
6	Cs 55	56	57-58	59	60	61	62				
6		63	64	65	66	67	68	69			
6		70	71	72	73	74	75	76	77	78	
6	79 Au	80	81	82	83	84	85				86 Rn
7	Fr 87	88	89	90	91	92	93	94			
7		95	96	97	98	99	100	101			
7		102	103	104	105	106	107	108	109	110	

Fig. 2. The proposed methods of the efficiency increase when using the elements from Mendeleev's periodic table as the target components for catalyzing the NRCMs on the deuterium nuclei

One should note that within the proposed model the target has
the optimal catalyst atom-to-reacting nuclei atom ratio which
can be both calculated and experimentally measured. This ratio
unit obligatory to agree with the maximum possible concentra-
tions of the reacting nuclei in the target matrix, but it can
be one of the criteria of the proposed model realibility.
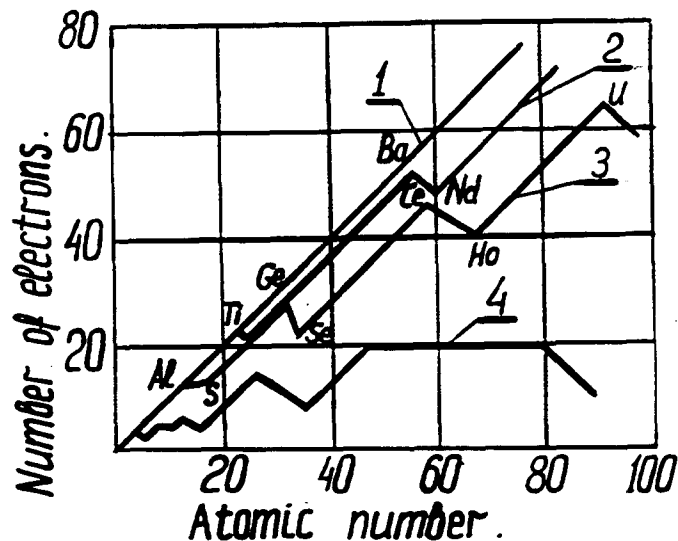
Fig. 3. The dependence of the electron number which can
leave their orbits on the atomic number of the
target elements for different ionization energies
I - total number of electrons.
The ionization energy is:
2 - 6 keV; 3 - 1,4 keV; 4 - 0,1 keV

No doubt, hydrogen is the best light element for the nuclear
reactions because of the lowest Coulomb potential arising bet-
ween its nuclei when they collide, but when considering the
possibility of the nuclear reaction proceeding at low energies,
one should take into account some additional limitations as
compared with the high-energy range. If one supposes that the
neutron-to-tritium generation rate ratio experimentally obtained
for the NRCMs at a level of 10^{-7}-10^{-9} is attributed to the

behaviour of the model of Oppengheimer-Phillips type /12/, it becomes clear that deuterium is practically the only isotope applicable to the nuclear reactions at low energies. It is caused by the fact that the reactions with a proton addition are forbidden (the probability concerning the channel with a neutron addition is 10^{-7}-10^{-9}). Therefore, the direct new element generation providing any proton addition to the nucleus in these reactions at the above-mentioned energies is impossible.

By way of exception, the NRCM can go when protium takes part in it, however, unlike Bush model /13/, it is possible only if one finds any materials, besides deuterium, which can release neutrons for the NRCMs. It is possible by using the low binding energy of the last neutron in beryllium:

$$P + {}^9Be \longrightarrow D + {}^8Be + 0.6 \text{ MeV}$$
$$\searrow 2\ {}^4He + 0.09 \text{MeV}$$
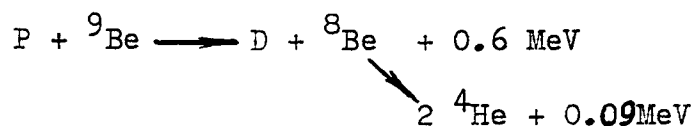
The other merit of this reaction is the fact that the toxic beryllium converts into the typical helium.

It is interesting to note that if the electron throw-off from the matrix atoms into the light nuclei interacting area is considered to be the main cause of Coulomb potential shielding, the maximum energy which the bombarding ion requires for throuing off all the electrons (up to L-shell, except for K-shell) is about $\mathcal{E}_1$ (Table 1).

It is seen in Table 1 that the difference between the total ionization energies and $\mathcal{E}_1$ is getting more considerable for the heavy elements (lanthanides and heavier ones) with their atomic number growth. This fact can be taken into account to revise by experiment the shielding effect on the possibility of Coulomb barrier overcoming.

Table 1

Comparison of ionization energies and maximum nuclear losses
for different target materials during deuterium ion bombard-
ment

Target material	Energy $\mathcal{E}_1$, eV	L-shell ioniza- tion energy, eV
Magnesium	350	270
Titanium	740	460
Vanadium	780	520
Yttrium	1530	2400
Zirconium	1580	2500
Niobium	1630	2700
Lanthanum	2410	6300
Erbium	3130	9800
Thorium	4520	20000

Due to the periodic law in the structure of the electron shells
of an atom, at the same energy the number of electrons which
are thrown off when these interact with the other atoms and,
therefore, the shielding efficiency, aren't a simple function
of the atomic number (fig. 3). Verification of the nonmonoto-
nicity of the NRCM efficiency function for different target
materials at the same energy also given an opportunity to
revise the shielding significance in the nuclear reaction
mechanism at low energies.

3. DISCUSSION

According to the tritium generation efficiency results which
we obtained before the series in increasing order can be writ-
ten as follows: molybdenum, tantalum, hafnium, tangsten, nio-
bium. The highest position of niobium in this series is natural
because of its rather high hydrogen solubility and the consider-

able tungsten efficiency is caused by its high atomic number.
To our mind, the lower values of the NRCM efficiency for
tantalum and hafnium are caused by the fact that it is neces-
sary to revise the discharge parameters for these materials,
in the first place, the temperature and energy level.

In work /14/ one gives the series of materials arranged ac-
cording to the neutron generation efficiency increase, which
partly agrees with our results, i.e. iron, molybdenum, copper,
silver, palladium, tungsten, niobium, platinum. These results
were obtained at energies about 20 keV in the glow discharge
and are reliable. On the whole, this series agrees with our
model, except molybdenum which should be placed before copper
and palladium which should be placed before niobium.

The estimation of the yttrium transmutation rate /11/ which
proved to be lower by six orders of magnitude than the rate
of D-D reaction with tritium generation, which was going at
the same time, verifies the fact that if the nuclear reactions
between the hydrogen and matrix atoms go, the NRCM rate for
the elements having a high atomic number product will be lower
than that one for the elements having a lower product.

4. CONCLUSIONS

4.1. On the basis of the proposed model it has been shown that
the most efficient materials for the NRCMs are the targets
consisting of the heaviest atoms mainly playing the part of
catalysts and the lightest elements mainly undergoing the
nuclear reactions when the targets are bombarded by accelerated
particles.

4.2. The metals from the lanthanide and actinoid groups have
been proposed as heavy target elements which are the most ef-
ficient NRCM catalysts.

4.3. The particular significance of deuterium and beryllium for the NRCM proceeding at low energies has been noted.

REFERENCES

1. H.Hora, J.C.Kelly, J.U.Patel et al. Screening in Cold Fusion Derived from D-D Reactions. - Physics Letters A, 1993, v. 175, n. 2, p. 138-143.

2. Yu.N.Bazhutov, G.M.Vereshkov. The Model of Cold Nuclear Fusion by Ersions Catalysis. Cold Nuclear Fusion. The Assembly of Science Proceedings. Kaliningrad. M.r.: TsNIImash, 1992, p. 22-28.

3. A.S.Davydov. The Possible Explanation of Cold Nuclear Fusion. - Ukrainskiy Fizicheskiy Zhurnal, 1989, v. 34, No 9, p. 1295-1297 (in Russian).

4. M.Rabinovitz. Modern Physics Letters, 1990, v. 4, No. 4, p. 233-247.

5. J.T.Waber. Solid State Boson Condensation Model of Cold Fusion. - Frontiers of Cold Fusion. Proceedings of the Third International Conference on Cold Fusion. October 21-25, 1992, Nagoya, Japan. Ed. by H.Ikegami. Universal Academy Press Inc., Tokyo, Japan, p. 627-632.

6. K.Watanabe, Y.Fukai, N.Niimura et al. A Search for Fracture-Induced Nuclear Fusion in Some Deuterium-Loaded Materials. - Ibidem // p. 473-476.

7. M.Fujii, M.Chiba, K.Fukushima et al. Measurement of Neutrons in Electrolysis at Low Temperature Range. - Ibidem //. p. 481-484.

8. E.Ragland. A Physical Description of Cold Fusion. - Ibidem // p. 649-658.

9. G.V.Fedorovich. Physics Letters A, 1992, v. 164, No. 2, p. 1∠

10. T.N.Claytor, D.G.Tuggle and S.F.Taylor. Evolution on Tritiur from Deuterided Palladium Subject to High Electrical Currents. - Frontiers of Cold Fusion. Proceedings of the Third International Conference on Cold Fusion. October 21-25, 1992, Nagoya, Japan. Ed. by H.Ikegami. Universal Academy Press Inc., Tokyo, Japan, p. 217-229.

11. V.Romodanov, V.Savin, Ya. Skuratnik and Yu.Timofeev. Nuclea: Fusion in Condensed Matter. - Ibidem //. p. 307-319.

12. I.R.Oppengheimer, M.Phillips. Note on the Transmutation Function for Deuterons. - Phys. Rev., 1935, v. 48, p. 500.

13. R.T.Bush. A Light Water Excess Heat Reaction Suggests that "Cold Fusion" may be "Alcaly-Hydrogen Fusion". - Fusion Technology, 1992, v. 22, p. 301-306.

14. S.Sihai, L.Heqing, L.Hongquan et al. Anomalous Effects in Deuterium/Metal Systems. - Frontiers of Cold Fusion. Proceedings of the Third International Conference on Cold Fusion. October 21-25, 1992, Nagoya, Japan. Ed. by H.Ikegami. Universal Academy Press Inc., Tokyo, Japan, p. 447-454.

A NEW DEVICE FOR MEASURING NEUTRON BURST IN COLD FUSION EXPERIMENT

Wang Xiaozhong, Tang Peijia, Zhang Wenliang, Liu Hengjun, Lu Feng,
Chen Guoan, Liu Jiangang, Chen Zhonglin and Zhu Rongbao

China Institute of Atomic Energy P.O.Box 275-48, Beijing 102413,
People's Republic of China

Abstract

A new neutron detection system has been set up and used in measuring neutron burst from thermal cycling of metal(Ti)-deuterium system. The equipment is composed of the HLNCC-II device and another special data acquisition system with an AST-386 computer. The experiment is performed to measure the electronic noise from spikes and the neutron burst signals in thermal cycle of metal(Ti) absorbed deuterium in pressurized deuterium. The die away time derived from time distribution of neutron counts in two neutron bursts generating in thermal cycling of Metal(Ti)-deuterium system is 52 μs, which is consistent with the 46 μs for ^{252}Cf source declared by HLNCC-II developer. Such a Consistency enlightens us on the probability of anomalous nuclear events in the system.

Introduction

Since "cold fusion" phenomenon was argued in 1989. The thermal cycling experiment of Metal absorbed deuterium in pressurized deuterium was studied by some labs., [1,2,3] The neutron burst signal from this kind of experiment using High Level Neutron Coincidence Counter (HLNCC) has been measured on stringent temperature, humidity condition in our lab. also. Most experiments have been based on D-C power condition. Some experiments have been carried out at deep-mine(500m) location at Mentou Valley in Beijing. The results of these measurements show that the neutron burst signals have been observed in many times. One of them was shown as Fig. 1[4]. For getting clearer in physics interpretation. we have improved these devices in 1992, a system for measuring the die away time during neutron burst period in HLNCC was developed. Some information about anomalous nuclear phenomennon from the experiment of metal(Ti) absorbed deuterium in pressurized deuterium gas have been gotten. It unveils a probability about the existence of anomalous phenomena.

Experiment scheme

In general, one of the methods about studying neutron burst signals from metal(Ti) absorbed deuterium in pressurized deuterium gas is that the coincidence counts in thermal cycle were measured with HLNCC. Some labs. have measured the maximum counts of neutron signal coincidence counts which is about 10^4 counts during a burst period.(measurement gate period : 128 μs, in fact , the period of original neutron signal burst to be measured is much less than 128 μs.), It is difficult to measure the time distribution of original neutron signals during 128 μs or less, Besides, the neutron burst take place in lower repeat rate, so even if the neutron time of flight (T-O-F) spectrometer with ns pulse technique can't be used to resolve such problem, because the period , 10μs, had to be taken for a conversion of TAC (time of amplitude converter) in T-O-F spectrometer. Another reason is that the detector efficiency for fast neutron in T-O-F spectrometer is lower, it's total efficiency (include the detector volume etc.) is much less than HLNCC. Perhaps it can be estimated that the total counts measured is less than 5 counts for such a neutron burst event. But the measurement with HLNCC is just for thermal neutron or near-thermal neutron coming from slowing down of the fast neutron in polythene, it can't be obtained the original time distribution of the neutron burst also. The die away time in HLNCC (mainly in polythene) can be obtained from measuring the time distribution of thermalized neutron during the burst period. Based on these consideration ,we planed to take the high speed counting property of HLNCC for thermal neutron ,and increase a data acquisition plate designed specially. While the coincidence counts of neutron burst signals were measured, at the same time, the signal was fed to the data acquisition plate and transitory in register with a parameter ,time scale, for every neutron burst signal. After the neutron burst ending, all signals were taken from register and fed to computer for data treatment. Obviously, the slowing down situation of the neutron burst in HLNCC can be obtained in this way. For such measurement principle, it should have a fast neutron detector or γ detector (suppose γ excised) as the start signal of the measurement period . The best reasonable device would be like an arrange as Fig. 2. Unfortunately, due to the existence of the fast neutron or γ detector , the total efficiency will be decreased too much. i.e. the many chance of catching neutron burst signals will be lost. For getting high efficiency, we have to abandon the fast neutron detector (or γ detector) and let the data acquisition plate and computer always set up at a waiting state , the cycle of measurement period would be formed, as soon as any signal(include random noise) arrived. So that the situation of the slowing down neutron would be included in a measuring period. According to these idea, we have improved our device(included design of the data acquisition plate and the interface , improvement of AST-386 computer) and developed a soft program. The experiment with these device was set up and used in practical measurement.

Experimental set up
Sample preparation

The 25 batches of sample is prepared by drilling, latheing Ti alloy bar or pure Ti plate. The thickness of chips is in the range of 0.2-0.6mm with width of 1.5-4.0mm and length of 5-8mm. The chips underwent a pretreatment procedure as follows:

a. procedure I: Samples were cleaned with chloroform and methylachol and washed promptly with large volume of distilled water and dried with acetone.

b. procedure II: degas in vacuum by heating to about $60°c$ for about 2 hours and filled with 2 atm. D_2 gas for several times to clean the system.

c. procedure III: hated to about $600°$ c in a sealed sample bottle with 9-20 atm. D_2 gas and formed a larger of TiO_2 at the surface of Ti chips. after the pressure of D_2 gas dropped to 0.1 atm., let the Ti chips cold down to room temperature.

d. procedure IV: filled with D_2 gas to a pressure of 60-80 atm..

Experiment measuring

The device used in practice measuring was shown as Fig. 3. The HLNCC-II made by Jomar Company was consisted of 18 ^{3}He proportional counters which was divided into 6 groups, the each counter is 50cm long and filled by ^{3}He with 4 atm., They were buried into a central cavity and concentric column polythene with dia. 17.5cm and 34 cm separately, such design is for slowing down the neutron and getting the best detector efficiency. The signal from the ^{3}He tubes was fed to the fast preamplifier and discriminator made by Amptek company. The pulse was formed into a logic pulse with 0.5μs wide and divided into two pulses by pulse divider. One of them was fed into JSR-11 coincidence counter based on shift register principle and printed output by HP-97 calculator. The output scale quantity includes the measurement period ,total counts, accident coincidence counts and real plus accidence coincidence counts. Another signal was fed into the special data acquisition plate for measuring the die away time. After primarily data treatment, the count density distribution of the thermal neutron signal on time scale would be shown on AST-386 computer. An experiment lasts about 3 months was performed to measure the electronics noise from spikes occurring in high voltage conjunction box forced cooling down period of HLNCC-II by increasing the humidity or sample bottle number. The thermal neutron time distribution of the typical fake pulse group or background pulse were shown as Fig. 4. Then on stringent temperature and humidity condition , the experiment was performed continually for another 3 months. 25 batches sample were tested. 75 thermal cycles were performed. For every measurement, 3 sample bottles were used only, The neutron burst signal groups detected is 7% of total cycle number. The two typical result measured were shown as Fig. 5. Obviously, it is possible that the different count density distribution on the time scale between real and fake pulse group was observed from Fig. 5, the density of real pulse group on time scale decrease while time increasing . One of them in Fig. 5 shows out a possibility of two bursts.

Data treatment and conclusion

The fact. the count density decreases while time increasing, shows a possibility of a burst decay event. Because the coincidence counts measured with HLNCC -II were the thermalized neutron generating from nuclear events , it would be existent that an innate die away time of the instrument , which can be compare with thermal cycle experiment data, some information can be obtained. From the typical time distribution of burst event signal in Fig. 5., even if the statistic error is larger, it is proper to make the relation between the counts density in unit time period and time into a decay

with $e^{-\alpha t}$ rule. If taking this relation, $y=e^{-\alpha t}$, to fit the counts per time unit, it will be :

$\alpha 1=0.019043/\mu s=1/\tau$

$\alpha 2=0.019131/\mu s=1/\tau$

(i.e. $\tau 1=1/\alpha 1=52.5\mu s$ and $\tau 2=1/\alpha 2=52.3 \mu s$)

If it is coming from a real neutron burst signal, then the time $(\tau 1,\tau 2)$ will be the die away time of HLNCC-II. According to the data provided by factory , the die away time of HLNCC-II in practice can be measured by using a spontaneous fission neutron source also. The every fission event is relative to be a burst neutron source , the decay rule is also according to the $e^{-\alpha t}$ relation. After the gate period of HLNCC-II was determined. the whole measurement counts during 0-t period can be shown as follow approximately:

$R(t)=R(total)(1-e^{-t/\tau})$

if two differential gate period ,for example 32µs and 64µs ,were selected, the counts can be shown as follows:

$R(32)=R(total)(1-e^{-32/\tau})$

$R(64)=R(total)(1-e^{-64/\tau})$

The τ can be obtained from two formula above. The τ of HLNCC -II on using in our experiment is 43 µs provided by manufactory, the τ value measured by developer using a ^{252}Cf neutron source is 46µs. The data of die away time on some conditions were shown in table 1.

Table 1: The comparision of the die away time experiment data

provided by factory	measured with ^{252}Cf	measured in cold fusion	
43µs	46µs	52.5µs	52.3µs

According to the table 1, even if the statistic error in our measurement is larger, the die away time is consistency with other's. This fact give us a clue, i. e. it is a possible that a decay behavior of burst anomalous nuclear phenomena in the bottle really took place .

we should give the fact that the repeat rate of experiment is much less than before, One of the main reason is the different sample used in our experiment. For getting good repeated experiment , it is very important that a proper sample was selected.

Acknowledgments

References

[1] S.E.Jones. et al.. "In Quest of Trigger Mechanism for Neutron Emission from Deuterium Solid/Systems". Proceeding of Anomalous Nuclear Effects in Deuterium/solid Systems. (American Institute of Physics. 1991) pp. 206-235

[2] H.O.Menlove, et al ., "Low Background of Neutron Emission From Ti Metal in Pressuized Deuterium Gas" Proceeding of the II Annual Conference on cold fusion. Como(Italy), 1991, p.385

[3] H.O.Menlove et al., "Neutron burst Detectors for cold fusion Experiments", Nuclear Instruments and Methods in Physics Research A299, 10-16(1990)

[4] Rangbao Zhu et al., Fusion Technology 20,263 (1991)

Measuring background in 3 days
(No any neutron burst took place)

1370

LN Cycle1   536

LN Cycle2   LN Cycle3

LN Cycle4   LN Cycle5

LN Cycle6   LN Cycle7

LN Cycle8

500
400
300
200
100
0

24   48   72   96   120   144   168   172

9/18   9/19   9/20   9/21   9/22   9/23   9/24   9/25

Time/hour   Mon./day
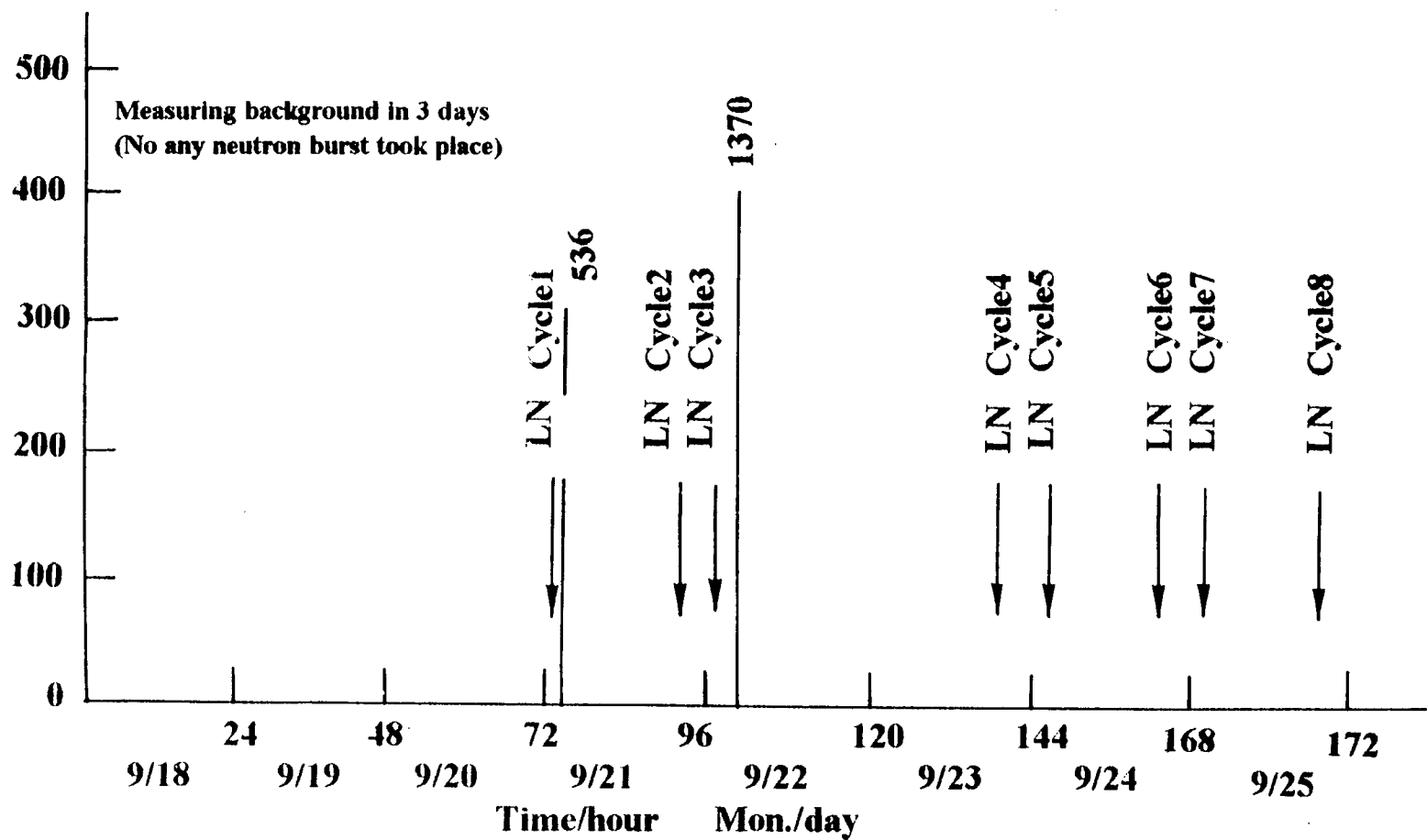
Fig. 1   Demonstration of neutron burst occurring during
the operation of 8th sample batch with median
positive effect

LN-Liquid Nitrogen
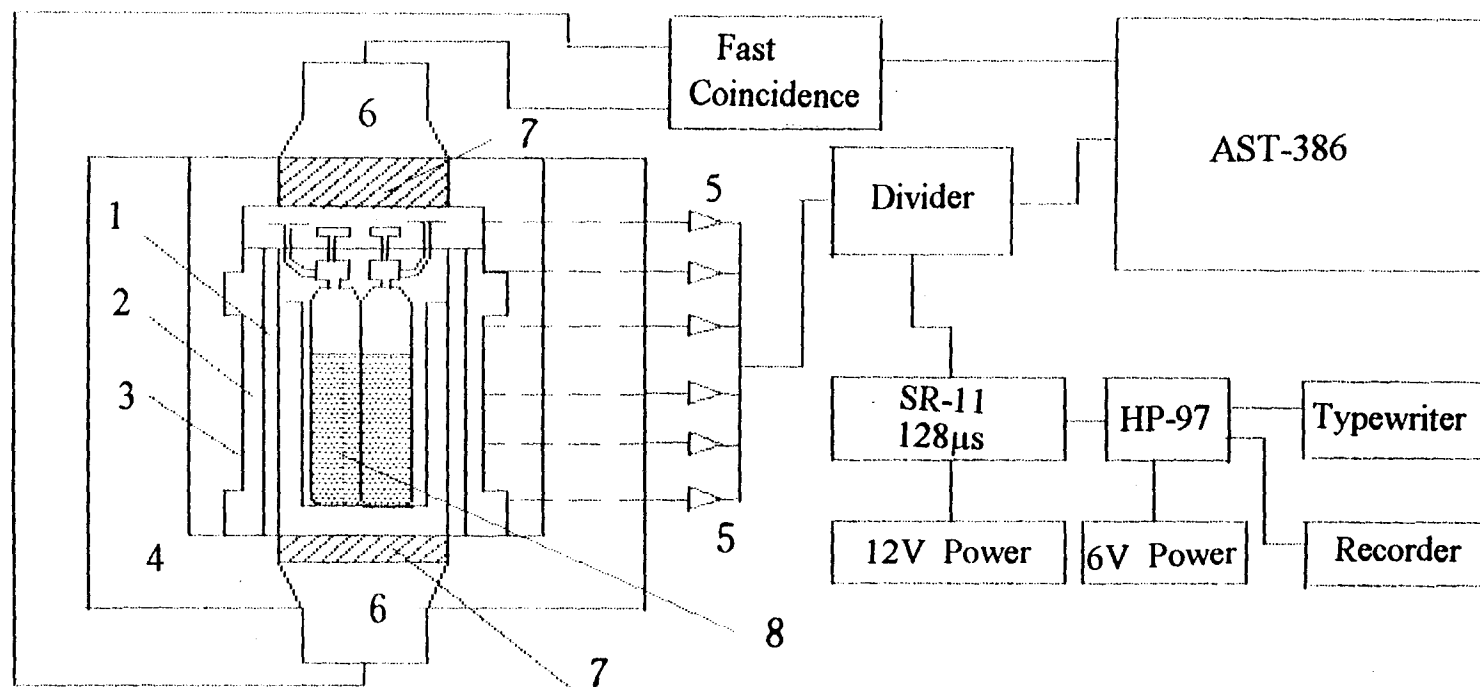
Fig. 2 The scheme of experiment setup for thermal cycle
experiment with fast neutron detectors
1) Counters: 2) Polythene: 3) Cadmium: 4) Paraffin:
5) Fast Preamplifier and Discriminator:
6) Fast Photomultiplier: 7) Scintillator: 8) Sample
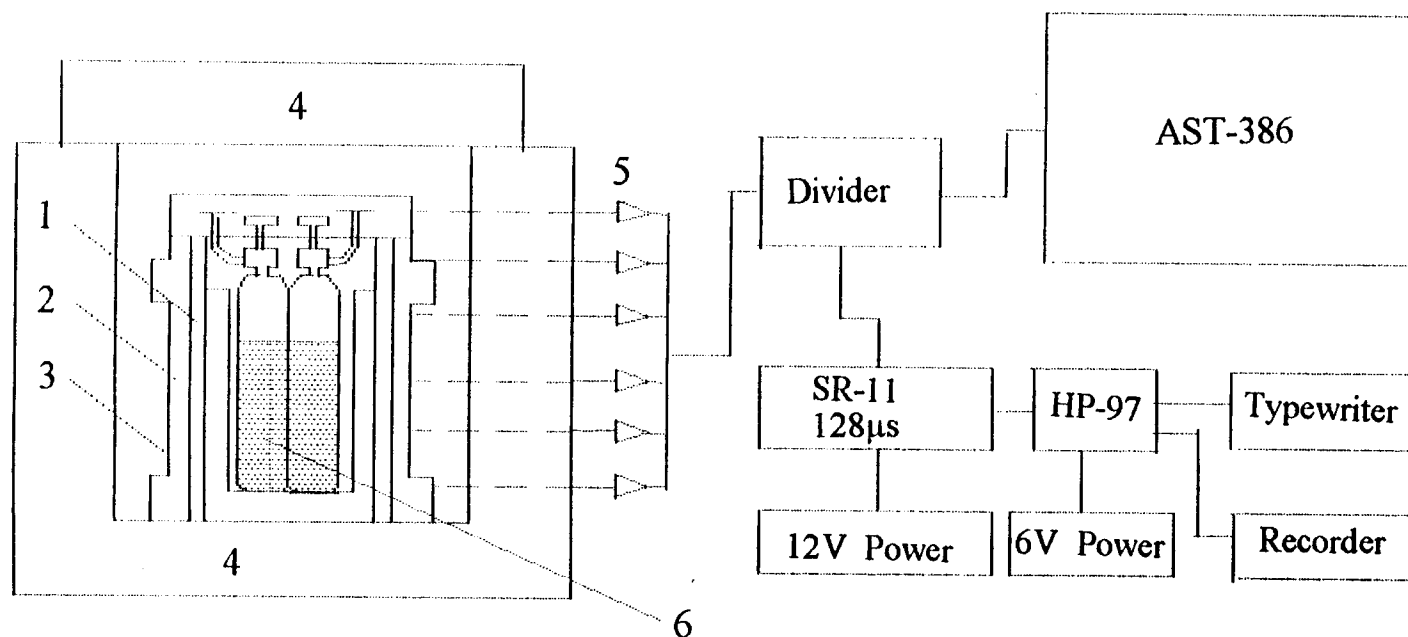
Fig.3 The schematic diagram of experiment setup
for thermal cycle experiments
1) Counters; 2) Polythene; 3) Cadmium; 4) Paraffin;
5) Fast Preamplifier and discriminator;   6) Sample
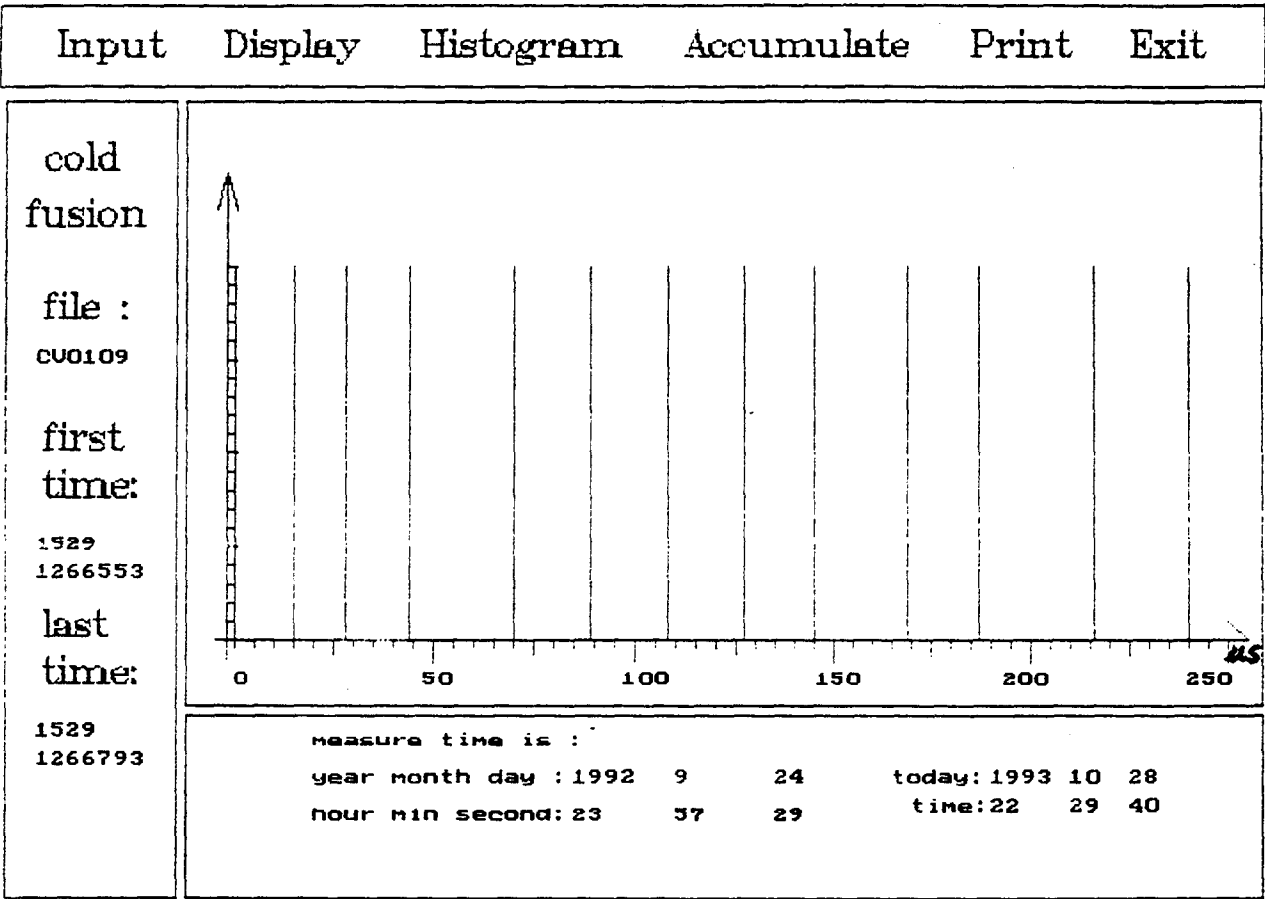
Fig. 4-1 One count density distribution of two fake pulses
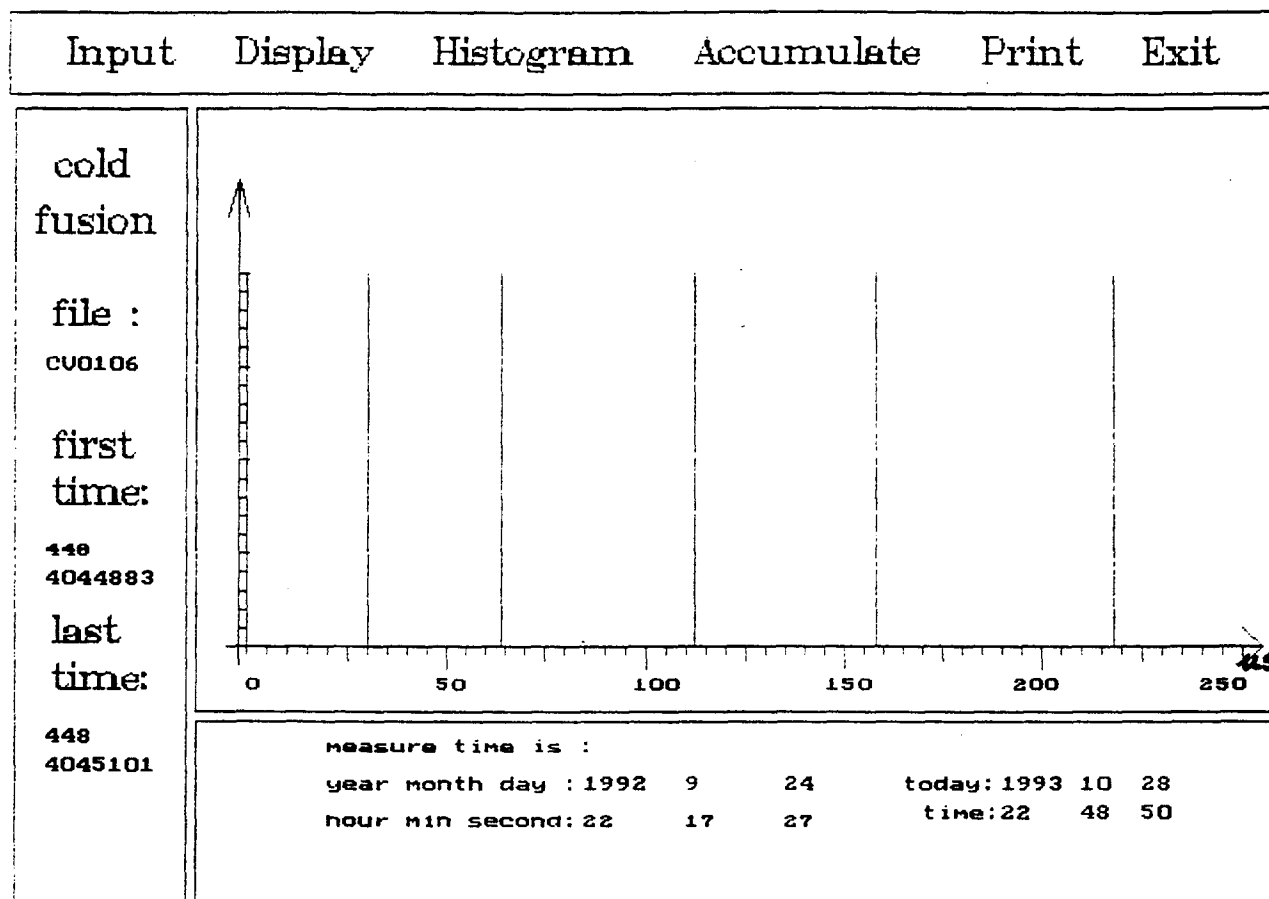
Fig. 4-2 One count density distribution of two fake pulses
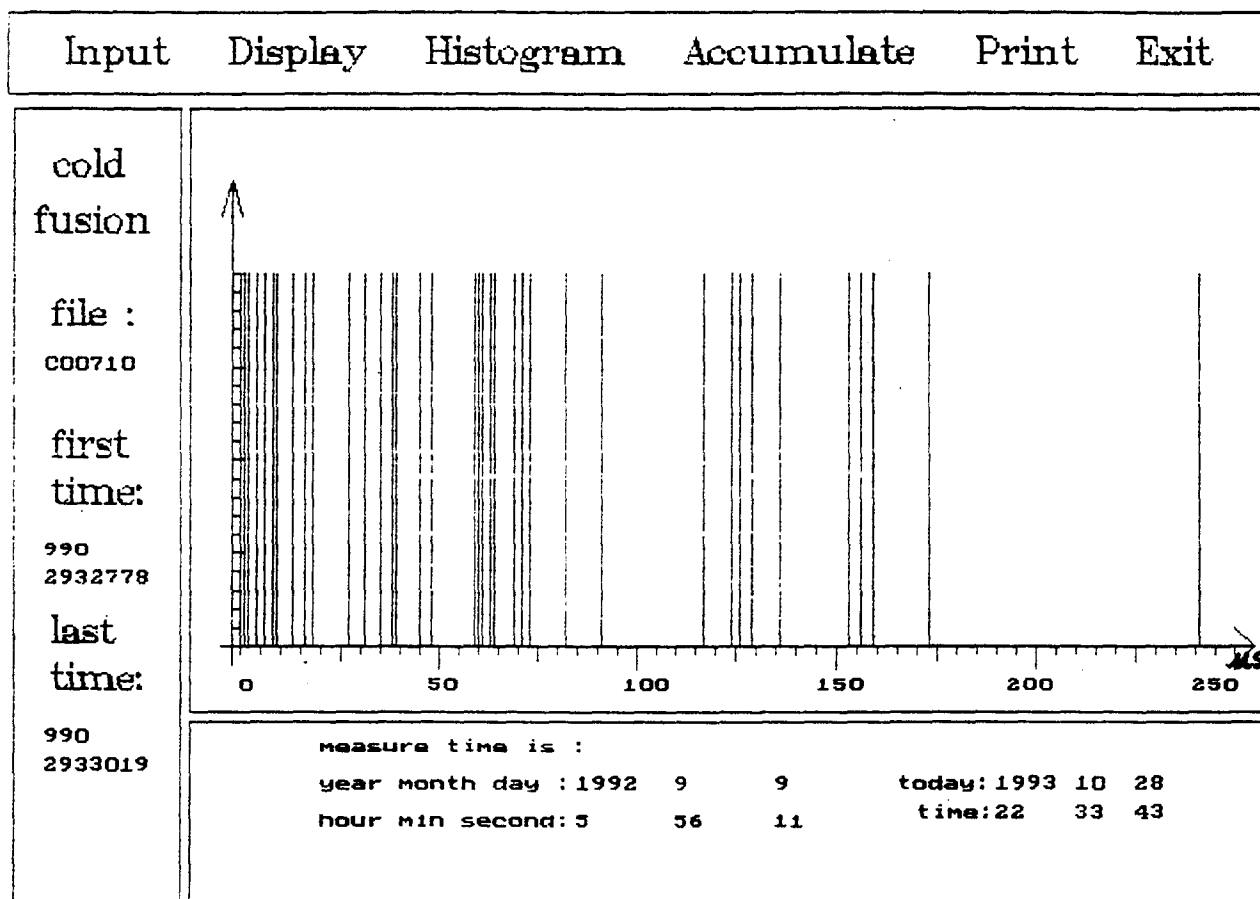
Input   Display   Histogram   Accumulate   Print   Exit

cold
fusion

file :

C00710

first
time:

990
2932778

last
time:

990
2933019

```
measure time is :
year month day :1992    9      9        today:1993  10   28
hour min second:3       56     11        time:22     33   43
```

0   50   100   150   200   250   MS

**Fig. 5-1   One count density distribution of two typical neutron
burst signals**

Input	Display	Histogram	Accumulate	Print	Exit

cold
fusion

file :

CHO305

first
time:

613
2606096

last
time:

613
2606339

measure time is :

year month day : 1992   8   18   today: 1993 10   28

hour min second: 3   32   16   time: 22   38   40
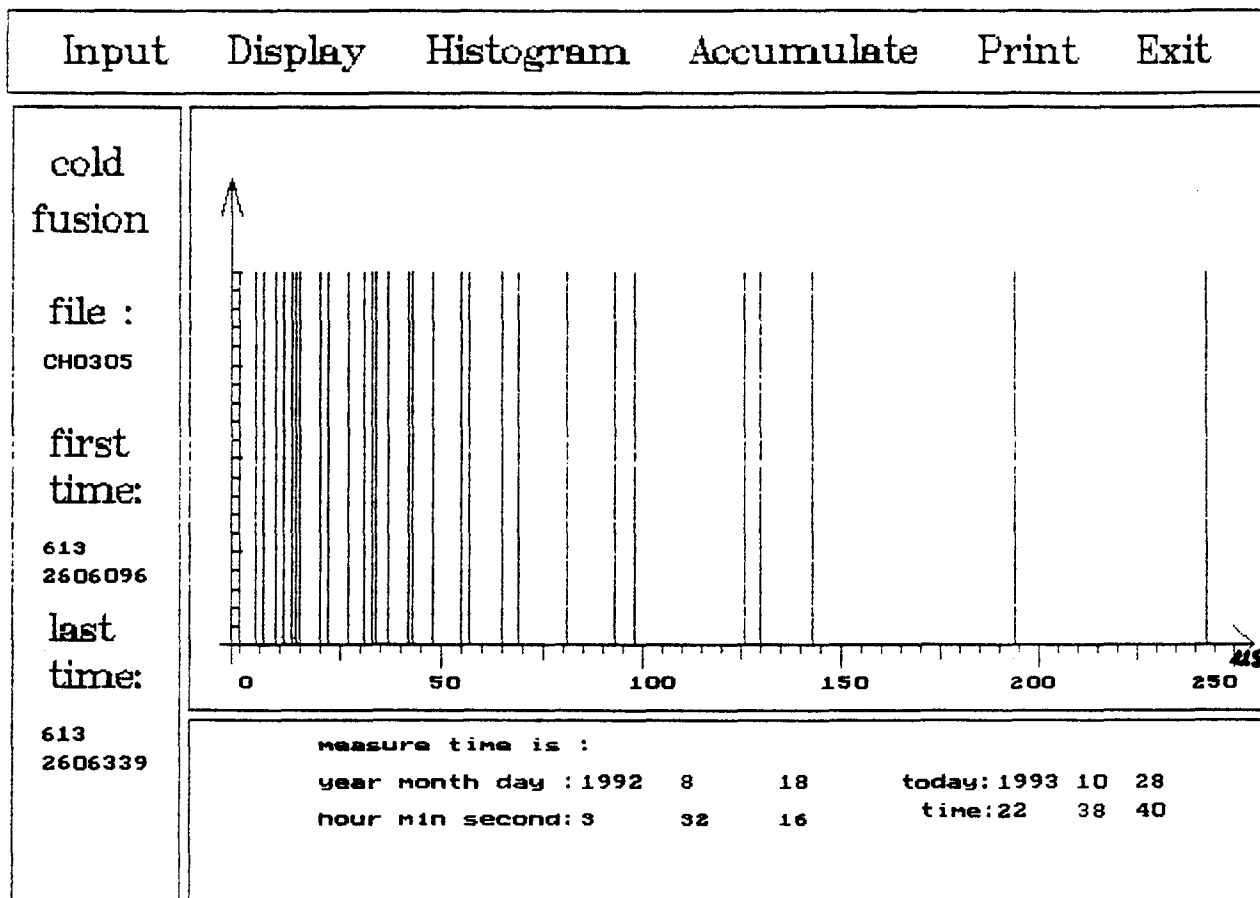
**Fig. 5-2   One count density distribution of two typical neutron
burst signals**

New experimental results of anomalous nuclear effect in Deuterium / Metal Systems

Long He−Qing, Yin Wen

Institute of Sichuan Material and Technology,PRC

Zhang Xin−Wei, Wu Jun, Zhang Wu−Shou

Institute of Applied Physics and Computational Mathematics

P.O. Box 8009 Beijing 100088, PRC

Tang Hong−Qing, Li Ze, Shen Quan−Ren

Zhou Zu−ying, Qi Bu−Jia, Liu Yong−Hui,

Wang Xiao−Zhong, Yang Yi

China Institute of Atomic Energy, P.O. Box 275, Beijing 102413, PRC

Abstract

Counts and energy spectrum of anomalous neutron and probable anomalous X−ray have been detected in Deuterium / Metal gas discharge Systems. Electrodes were made of Pt,Nb,Ta,WTh_x,W,Pd,Cu,Mo,Ag,Fe or other metals and were fixed to both ends of a glass reaction bulb, the effective value of applied alternating voltage was 2.7−18 KV (50Hz). 2.45 MeV neutrons have been measured on condition of dynamic low pressure($<$100Pa) deuterium gas glow discharge, neutrons of other energy over background have not detected. The ratio of experimental neutron yield to theoretical yield was much greater than 1 when low voltage applied; the ratio >8 in D / WTh_x system when U = 4.7KV; the ratio >46 in D / Ta system when U = 4.1KV; the ratio >170 in D / Nb system when U = 2.7 KV. The neutron emission was stable, reproducible and controlled.

Comparing with air discharge, there were indications that anomalous X−ray had produced in D / Pd system. The X−ray spectrum (Ex $<$20KeV) detected were similar to the Bremsstrublung spectrum but not any normal spectrum of which low energy X−ray was absorbed mostly by the glass wall of reaction bulb (about 2mm thick).

— 1 —

Key words

Deuterium / Metal system, Gas discharge, Neutron spectrum, X—ray spectrum, Cold fusion

1. Introduction

Since the annoucement of the cold fusion by Fleishmann and Pons[1] and Jones etal[2], a lot of experiments have been carried out in the field. Most of the researches are concentrated on the low energy process such as the electrolysis of the heavy water, absorbing and degassing the deuterium gas. The luckwarm fusion on the charged $(D_2O)_n^+$ molecules cluster ($E = 200 - 325Kev$, $n = 10 - 100$) impinging on the deuterium targets has been reported by Beuhler etal[3].There have been few results of conditions between the cold fusion and the luckwarm fusion in the world[4-6]. The gas discharge method which will be introduced below is the very situation.

The apparatus used for the fusion studies was discribed in the preceding publications[5,6]. The values of the voltage mentioned below are the effective ones.

2. Neutron Measurements

The neutron detector is composed of a liquid scintillator (ST—451, 10.5 cm in diamter and 5 cm thick) and a photo multiplier tube XP—2041. To reduce γ—ray background, an n—γ pulseshape discriminator modular (CANBERRA 2160A) was used. The detector efficiency was calibrated with n—p scattering experiments and Monte—Carlo calculation[7].

The detector is calibrated by 2.5 MeV neutrons releasing in a standard neutron source.The electrodes used in the neutron measurements are rods of Ta, Nb, Ni,WTh$_x$, Pd....

Neutron spectrum are obtained with different metals at various voltage, the recoil—proton spectra of D / Ta system at 7.1 KV is shown in Fig.1. Neutron spectra correspond to Fig.1 is shown in Fig.2,there are 2.45 MeV neutrons and the $D(d,n)^3He$ reactions taking place in the gas discharge process can be deduced from it.

The recoil—proton spectrum of three different D / M systems at 9.1 KV are shown in Fig.3, the energy of nertrons is 2.45 MeV as well.

Last year, we reported that we had measured lower and higher energy neutrons[5,6], but we have not detected them in the present experiment. We think there were too high

— 2 —

errors in the detectors used before, so we had obtained wrong informations.

For the gas discharge method there would be a problem whether the neutrons are normal beam—target neutrons or not. For distinguishing them, we compare the experimental results with the theory.

Experimental and theoretical works of high—voltage / low—pressure discharge had been established by McClure[8,9]. As a result of calculation, we found that the beam—target neutrons are produced major in the cathod fall region between the electrodes instead of the cathod targets, the gas pressure and distance of electrodes have few efforts on the neutron yields. The neutron yields are inversely proportional to the secondary emmission coefficients γ (number of secondary electrons rleased from the cathode by positive ion and fast neutral atom impact), i.e. neutron yields $\propto \dfrac{1}{\gamma(\gamma + 1)}$.

There are different γ values for different materials, various configurations and surface conditions of cathodes. The γ tends to a constant when the energy of impinging particles (D_2, D_2^+, D, D^+) is high. Therefore, the ratios of the neutron yields for different cathodes at a fixed voltage are constants. In Fig.4, there are ratios of experimental neutron yields for three kinds of electrodes to the theoretical neutron yields for a reference conditions taken from ref.[8], experimental results corresponding to Fig.4 are listed in Table 1. From Fig.4, we found that when $U > 7 - 9$ KV, the ratios are roughly constants in 4 times, but when $U < 7 - 9$ KV, the experimental results are much greater than that of theories.the maximum discrepancy reaches 10^2 fold. When $U = 11 - 15$KV, there are small peaks which are very lower than those of low voltage, it is difficult to understand. We have regulated theoretical parameters but the considerable discrepancy at low voltage ($5 - 7$ KeV) and small discrepany at $11 - 15$ couldn't be eliminated. We can draw a conclusion that there are anomalous neutrons at low voltages at least in D / M discharge systems.

It seems that the neutron yields depend on the gas pressure.

3. X—ray Measurements

The measurement system is composed of a Ge(Li) detector (GMX200) made in ORTEC company of U.S.A.; a pulse shape analyser (CANBERRA,2160A) and a IBM—PC / XT computer.

The detector sensitive volume is 102 cm^3, the measuring range is 5 KeV to 1.64 MeV, the relative efficiency is 20%. The Ge(Li) detector is placed in a lead shielded

— 3 —

cabin so that the background is 11 counts / sec with in 20 to 1024 channels (the background is decreased to 1 / 20, compared to the ones before shielded).

The electrodes used for X—ray measurements are in shape of Pd plate. The thickness of the glass wall of the reaction bulb is 2.0 ± 0.2mm.

The theoretical spectrum of X—ray are calculated with calssical Bremsstrablung formula[10]:

$$\frac{dN}{dE_r} = N_0 \frac{1}{E_r} \int_{E_r / eV_0}^{1} ln\left[\frac{(\sqrt{x} + \sqrt{x - E_r / eV_0})^2}{E_r / eV_0}\right] \frac{dx}{\sqrt{1 - x^2}}$$

and empirical formula

$$\int E_r dN = 1.1 \times 10^{-9} Z V(IV)$$

Where E_r is energy of X—ray, Z is atom number of target metal, e is magnitude of electron charge, V_0 and V are the maximum and effective voltage in a period respectively. The glass wall and absorbing plates of Al, Cu etc. are considered at the same time.

In Fig.5, the experimental and theoretical spectrum of air discharge at 11.8 KV are shown, they are consistent very well.

The Fig.6 shows the spectrum of D / Pd and air / Pd system under the glow discharge condition of 8.0 KV voltage and 0.05 cm absorbing plate (Cu). We can see that the spectra of air discharge is close to the background due to the thick absorbing plates, and the spectra of deuterium discharge is similar to the emission spectra of Bremsstrablung instead of a spectra through the absorbing plate. That means the measured X—rays of D / Pd system are formed at the outside of the reaction bulb instead of the inside.

When the reaction bulb and the detector are coaxial, we think the X—ray spectra of D / Pd system is close to the background due to the thick plate electrode absorbing, but there is still emission spectra and which is shown in Fig.7.

In Fig.8, there are spectrum of D / Pd system when the collimator hole of the detector aims at the reaction bulb or diverges it. It seems that the emission spectra is not caused by the electromagnetic interference.

The photons causd by neutrons are less than 10^2 / sec under this condition in the theory, but we have measured about 10^4 photons / sec. It could not be interpreted by the ordinary theory.

— 4 —

4. Conclusion

(1) 2.45 MeV neutrons are produced in D $/$ M discharge system if the voltage greater than 2.7KV;

(2) when the applied voltages are less than 7 to 9 KV, the neutron yields are much greater than the theoretical results, the discrepancy reaches 10^2 at 2.7 KV;

(3) the anomalous X−rays have been measured, they should be produced at the outside of the reaction bulb, it seems secondary X−rays;

(4) the anomalous X−ray phenomena should be detected further in the future.

Reference

[1] M.Fleishmann etal., J. Electronal. Chem. 261,301,1989

[2] S.E.Jones etal., Nature, 338,737,1989

[3] R.J.Beuhler etal., J.Phys.Chem. 94,7665,1990

[4] A.B.Karabut etal., Physics Lett.A 170,265,1992

[5] Long Heqing etal.,ICCF3 Nagoya,1992

[6] Long Heqing etal.,ICCF3 Nagoya,1992

[7] G.Dietze and H. Klein,PTB−Report ND−22, Braunschweig, Oct.,1982

[8] G.W.McClure, Phys.Rev.124,969,1961

[9] G.W.McClure etal.,Phys.Rev. 125,1792,1962

[10] J.D.Jackson, Classical Electrodynamics, Jon Wiley & Sons,Inc.,1976

Table 1   Results of neutron measurements

D / Nb		D / Ta		D / WTh$_x$	
Voltage (KV)	*	Voltage (KV)	*	Voltage (KV)	*
2.7	0.199	4.1	3.145	4.71	1.323
3.6	0.7416	4.6	3.204	5.48	0.789
4.7	1.558	5.66	4.538	6.48	2.971
5.6	5.921	6.8	11.65	6.97	4.99
6.4	4.315	7.1	11.85	7.28	6.89
7.0	12.04	7.3	16.11	8.07	13.2
8.6	40.6	8.44	53.06	8.15	14.9
9.6	83.5	8.7	63.96	9.07	25.78
10.6	164.17	9.63	122.66	9.25	30.69
11.9	371.69	10.04	239.15	10.01	56.09
12.8	636.83	10.9	511.22	10.22	63.9
13.2	946.03	12.3	887.2	11.52	179.9
13.3	788	13.7	1369.3	12	202.89
14.04	1029.51	14.9	1556.7		
14.5	1397.9	15.65	2462.5		
15	1712.83	16	2437		
15.6	1841.67	17	3307.9		
16.8	2003.8	18	3988.2		
17.6	2209.4	19	4266.37		
18	2496.96	20	4993.5		
21	3034.5				

*   neutron yields (I = 10mA, n / s)
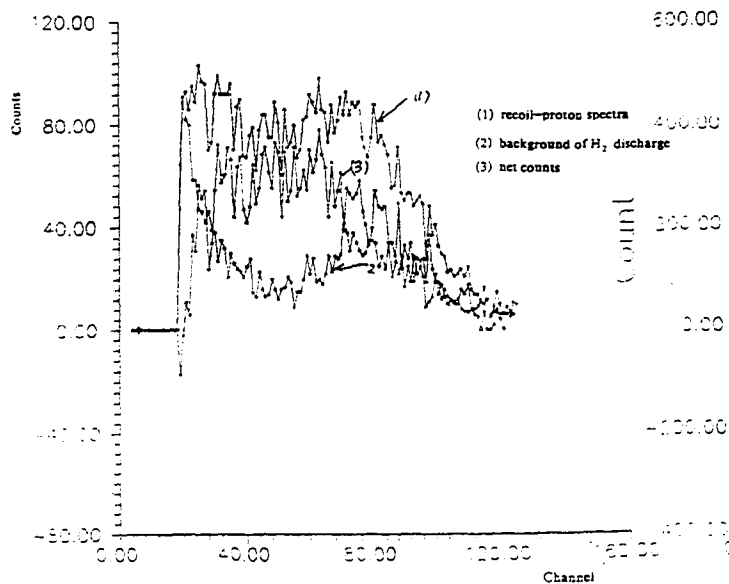
Fig.1   Recoil–proton spectra of D / Ta, 7.1KV, 22mA

(1) recoil–proton spectra
(2) background of H_2 discharge
(3) net counts
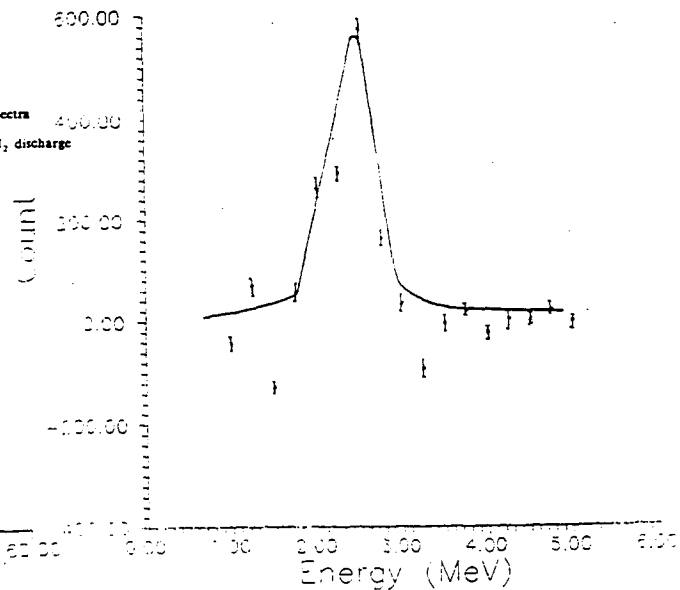
Fig. 2   Neutron spectra corresponding to Fig. 1
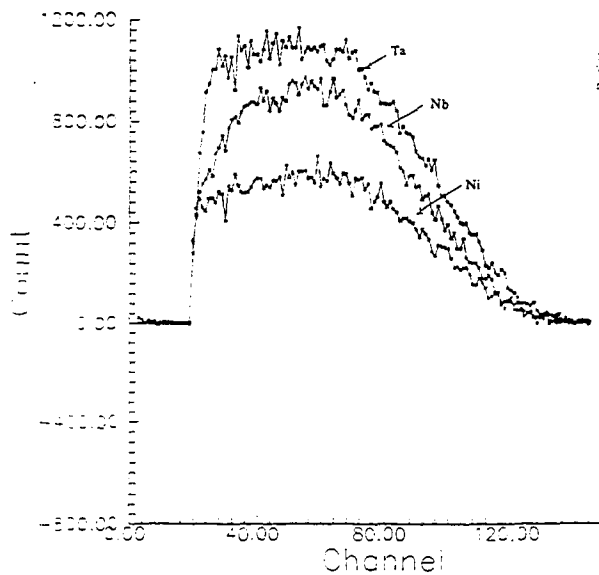
Fig.3   Recoil–proton spectrum of different electrodes.   9.1KV,   10mA
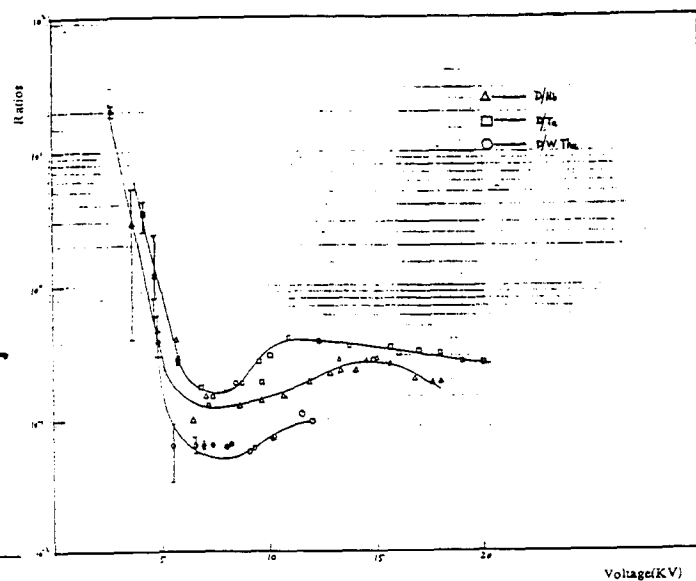
Fig.4   Ratios of experimental neutron yields for three kinds of electrodes to theoretical neutron yields for a reference condition.

24-7
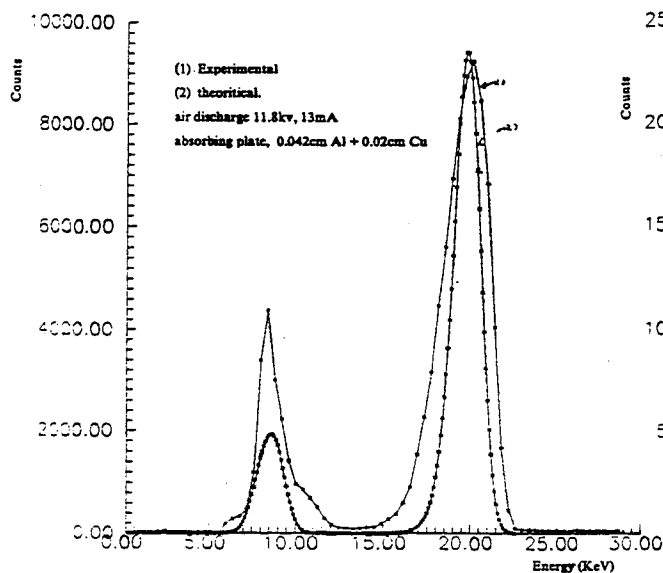
Fig.5 Results of X-ray spectra of experiment and theories

(1) Experimental
(2) theoritical.
air discharge 11.8kv, 13mA
absorbing plate, 0.042cm Al + 0.02cm Cu
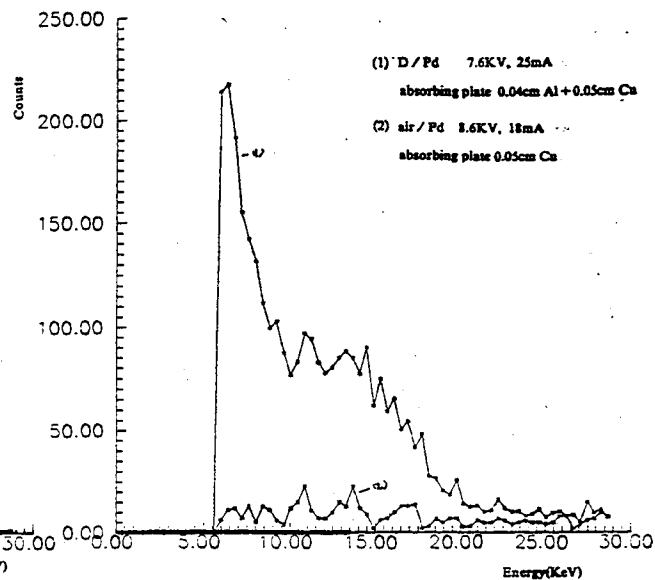
Fig.6 Comparing the X-ray Spectra of D / Pd with air / Pd

(1) D / Pd   7.6KV, 25mA
    absorbing plate 0.04cm Al + 0.05cm Cu
(2) air / Pd   8.6KV, 18mA
    absorbing plate 0.05cm Cu

Fig.7   X-ray spectra of D / Pd.   reaction bulb and detector are coaxial.
7.25KV,   24.5mA.
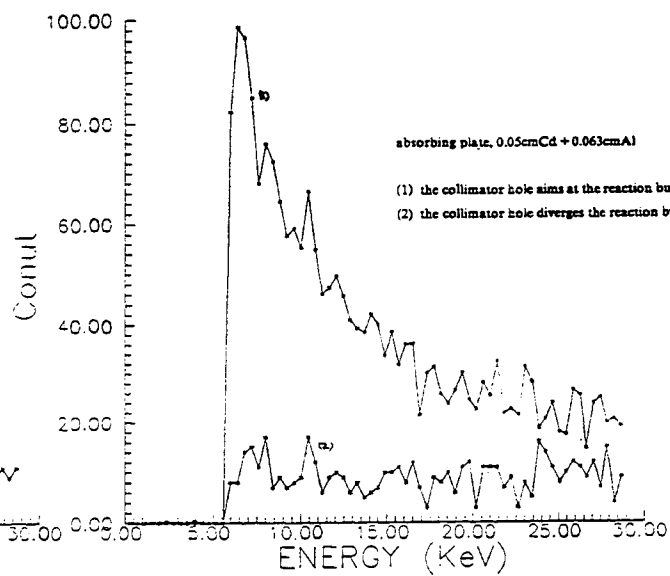
Fig.8   X-ray spectra of D / Pd   8.9-11.5KV,   26-35mA

absorbing plate, 0.05cmCd + 0.063cmAl

(1) the collimator hole aims at the reaction bulb
(2) the collimator hole diverges the reaction bulb

24-8

ON THE SUBSISTANCE OF ANOMALOUS NUCLEAR EFFECTS AFTER INTERRUPTING THE ELECTROLYSIS IN F-P TYPE EXPERIMENTS WITH DEUTERATED Ti CATHODES

M. Alqueró, F. Fernández, F. Cuevas and C. Sánchez
Dpto. Física de Materiales C-IV, Universidad Autónoma
de Madrid, Cantoblanco, 28049 Madrid, Spain

Abstract

Subsistance of neutron emission after interrupting the electrolysis has been reported in F-P type experiments with deuterated Ti cathodes [1,2]. An explanation is proposed of the neutron emission decay transients observed after interrupting the electrolysis. The transients are related to the reduction of TiD_x cathode bulk of D concentration (D/Ti) over a threshold due to diffusion ph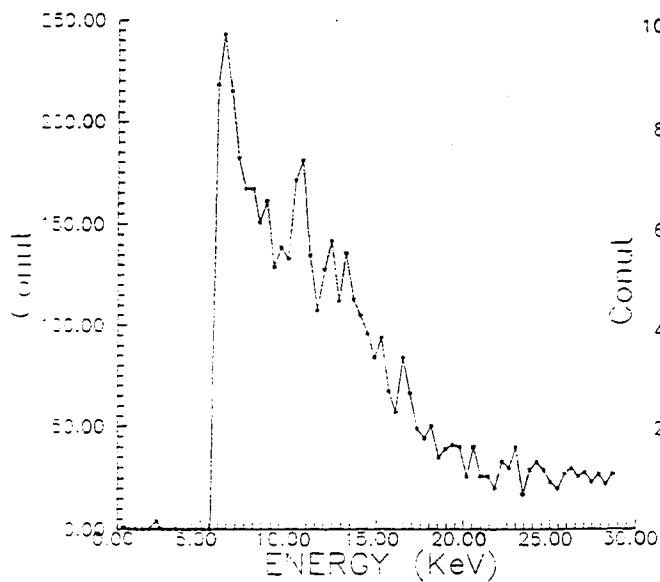enomena. The hypothesis assumes fusion reactions to go on in the TiD_x sample bulk of D concentration over a threshold whatever the previous triggering agent is.

Experimental data on neutron emission

Figure 1 shows neutron data recorded in an experiment labelled ETi6 carried out in our laboratory in 1989 [1,2]. Neutron emission lasted near 100 minutes in absence of polarization current. The count rate given by the detector remained constant for 40-50 minutes before starting a smooth decay. Neutrons coming from the electrolytical cell were detected with a BF_3 proportional counter (mod. 2202D from Alnor, Finland) placed at 20 cm far from the Ti cathode. The signal from the detector was sent directly to a recorder and to an electronic pulse counter.

The Wagner model

D-diffusion properties in Ti are well described by the Wagner model [3] as it has been shown by Mizuno et al [4] and Fernández et al [5]. The Wagner model treats the diffusion mechanism in polyphasic systems. Electrochemical loading of Ti with D usually implies temperatures near RT so α and δ phases of the D-Ti system are involved in the diffusion problem as the phase diagram shows.

The Wagner model assumes that the growing phase (FCC δ phase) nucleates fast enough so its growth is ruled by the deuterium flow through the α-δ interface due to diffusion phenomena (Equation 1).

$$(C_{\delta\alpha} - C_{\alpha\delta}) \frac{\partial \xi}{\partial t} = -D_\delta \frac{\partial C}{\partial z}\bigg|_{\xi_-} + D_\alpha \frac{\partial C}{\partial z}\bigg|_{\xi_+} \tag{1}$$

D-Concentration profiles during the electrolysis

D-loading of a Ti cathode is mathematically described by the diffusion equation plus the Wagner equation with the adequate boundary condition.

$$\frac{\partial C}{\partial t} = D_\delta \frac{\partial^2 C}{\partial z^2} \quad [0, \xi] \tag{2}$$

$$(C_{\delta\alpha} - C_{\alpha\delta}) \frac{\partial \xi}{\partial t} = -D_\delta \frac{\partial C}{\partial z}\bigg|_{\xi_-} + D_\alpha \frac{\partial C}{\partial z}\bigg|_{\xi_+} \tag{3}$$

$$C(0, t) = C_S \tag{4}$$

C_S stands for the surface coverage. It is determinated by kinetics of Volmer and Tafel processes at the metal electrolyte interface i.e. by the electrochemical conditions and the surface morphology.

D-loading process can be understood as a deuteride growth governed by deuterium diffusion from the Ti surface. The D profile in the cathode tends to a constant value of C_S as the α-δ interface progresses in the Ti sample.

The problem has analytical solution. Fig 2 shows D-profiles in the cathode at different times after starting the electrolysis. Fig 3 shows how the different parameters relevant to the problem affect to the deuteration process.

This solution assumes the diffusion step to be the slowest one involved in the absortion kinetics. Different profiles and absortion rates appear if the δ-phase nucleation or the D-adsorbed to D-absorbed step are not fast enough.

D-Concentration profiles after the electrolysis

The post-electrolysis evolution of D-profiles across Ti cathodes is also described by the Wagner model. The mathematical problem to be solved is:

$$\frac{\partial C}{\partial t} = D_\delta \frac{\partial^2 C}{\partial z^2} \qquad [0, \xi] \qquad\qquad (5)$$

$$(C_{\delta\alpha} - C_{\alpha\delta}) \frac{\partial \xi}{\partial t} = -D_\delta \frac{\partial C}{\partial z}\bigg|_{\xi_-} + D_\alpha \frac{\partial C}{\partial z}\bigg|_{\xi_+} \qquad (6)$$

$$\frac{\partial C}{\partial z}(0, t)_+ = 0 \qquad\qquad (7)$$

No deuterium flow through the surface is allowed.

Equations have been solved by numerical methods. Fig 4a shows D profiles at different times after finishing the electrolysis. Fig 4b shows how the $\alpha-\delta$ interface goes on progressing through the Ti plate until a C$\delta\alpha$ concentration is reached in the whole deuterated layer. Values of the parameters refer to ETi6.

Numerical Calculus

The difference method has been used to solve the equations. The spatial variable has been discretized in subintervals of 0.1 μm. This discretization has been chosen to take into account the violent initial deuterium lost observed in ETi6 just after switching the current off by assigning a zero concentration to the first point of the grid. The time has been subdivided in subintervals of 0.01 minutes in order to ensure the stability of the method.

The initial profile used is the analytical solution of the electrolysis problem described before.

The hypothesis of an active bulk

Nuclear phenomena in absence of polarization current is related to the post-electrolysis evolution of D-profiles in the Ti cathode.

Neutron emissions are assumed to go on in the bulk portion of loading ratio over a threshold whatever the previous triggering agent is.

The hypothesis is tested by comparing ETi6 data to numerical calculations of the post-electrolysis active bulk decay transients in ETi6 (see Fig 5).

Discussion

A good qualitative agreement is reached between active bulk and neutron curves.

An estimation is made of the loading ratio threshold by fitting neutron data to the active bulk transients. The constant portion of the curves is chosen. The whole transients duration does not fit although the constant portions does. This apparent contradiction is solved by taking into account the BF_3 proportional counter sensitivity which limits the monitored decay time. The fusion rates estimated in [1,2] must be reviewed taking into account that only a small portion of the cathode is involved in the nuclear phenomena. New rates between $10^{-14}-10^{-15}$ f/ppd.s are stablished for ETi6.

Active bulk transients in palladium

Although the diffusion characteristics of the D-Pd system are well described by the Wagner model time involved in a diffusion dominated kinetics are really shorter than the D-Ti ones. A complete deuteration of the Pd cathode is easily reached in hours although a D/Pd=1 is not so easy to reach.

Defined a D/Pd threshold the postelectrolysis active bulk transients would last only a few minutes unless the process is dominated by deuterium flow across the surface.

Conclusions

Numerically calculated active bulk transients do not contradict the hypothesis.

The loading ratio threshold is estimated to be between 1.91-1.92.

References

(1) C. Sánchez, J. Sevilla, B. Escarpizo, F.J. Fernández and J. Cañizares, Solid State Communications, 71, 1039-1043 (1989).

(2) C. Sánchez, J. Sevilla, B. Escarpizo, F.J. Fernández and J. Cañizares, "Cold Fusion During Electrolysis of Heavy Water with Ti and Pt electrodes" published in "Understanding Cold Fusion Phenomena", p 29 Ed. R. Ricci, F. de Marco and E. Sindoni, Varena, Sep. (1989).

(3) C. Wagner, quoted by W. Jost, "Diffusion in Solids, Liquids and Gases", Academic Press, Inc. New York, (1952).

(4) T. Mizuno, T. Shindo and T. Morozumi, Anti-corrosion Techniques, 26, 185-193 (1977).

(5) J.F. Fernández, F. Cuevas and C. Sánchez, to be published in J. Alloys and Compounds.
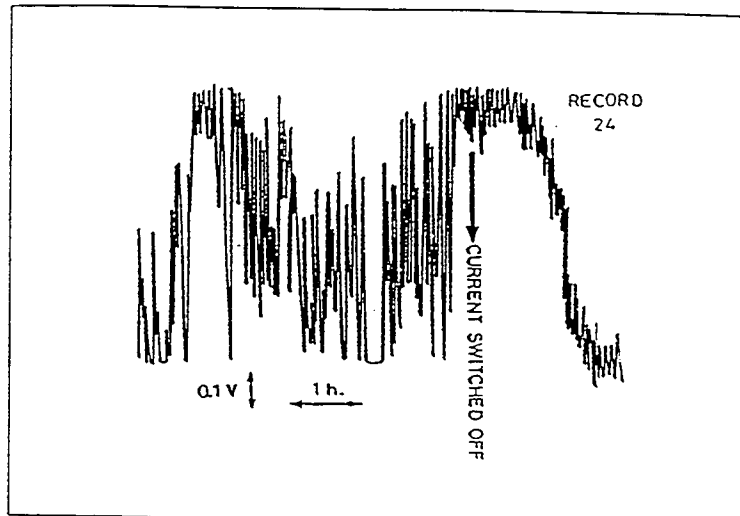
FIG 1: ETi6 neutron emission data without polarization current.
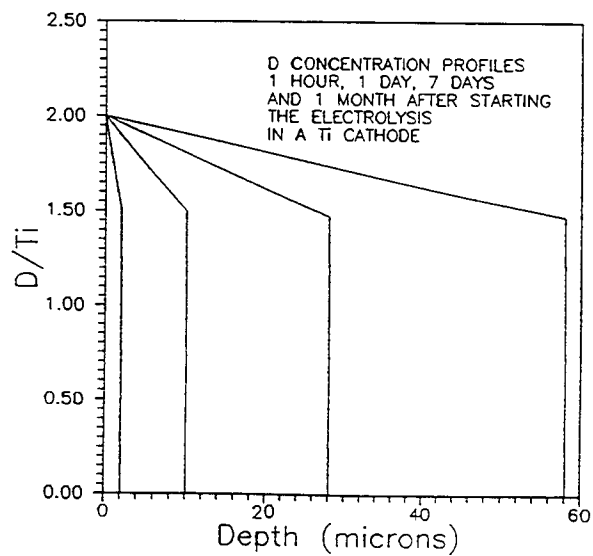
FIG 2: D-Profiles in a Ti cathode during its electrochemical loading at 30°C and its surface saturated ($C_S=2$).
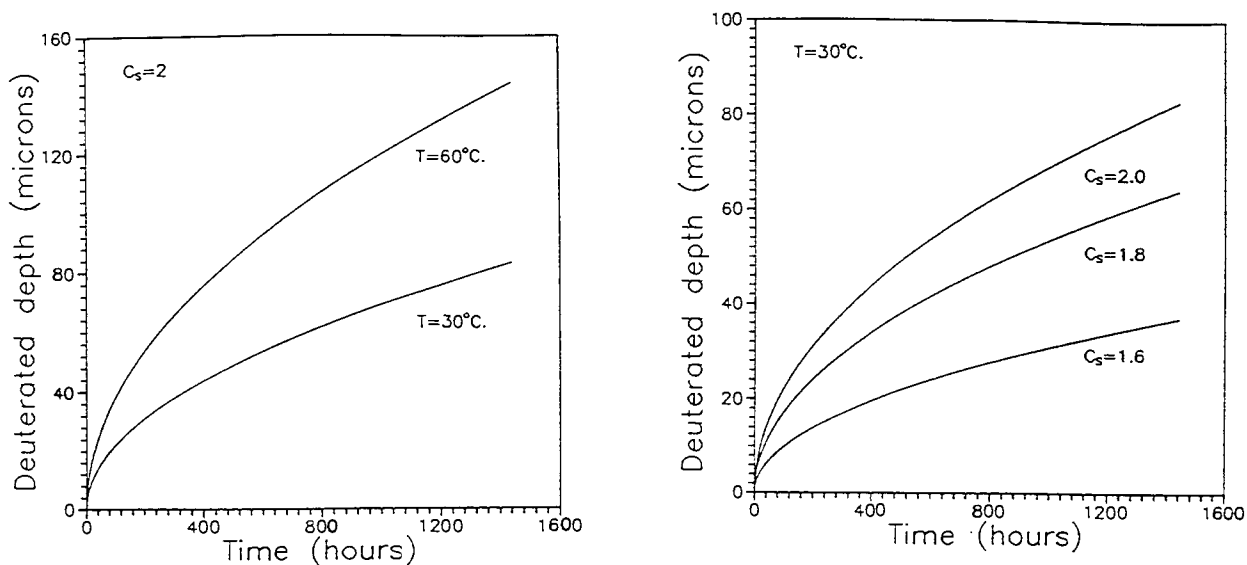
FIG 3: (a)Temperature dependence of the electrochemical D-
loading process of a Ti cathode with its surface saturated. (b)
Surface coverage dependence of the electrochemical D-loading
process of a Ti cathode at 30°C.
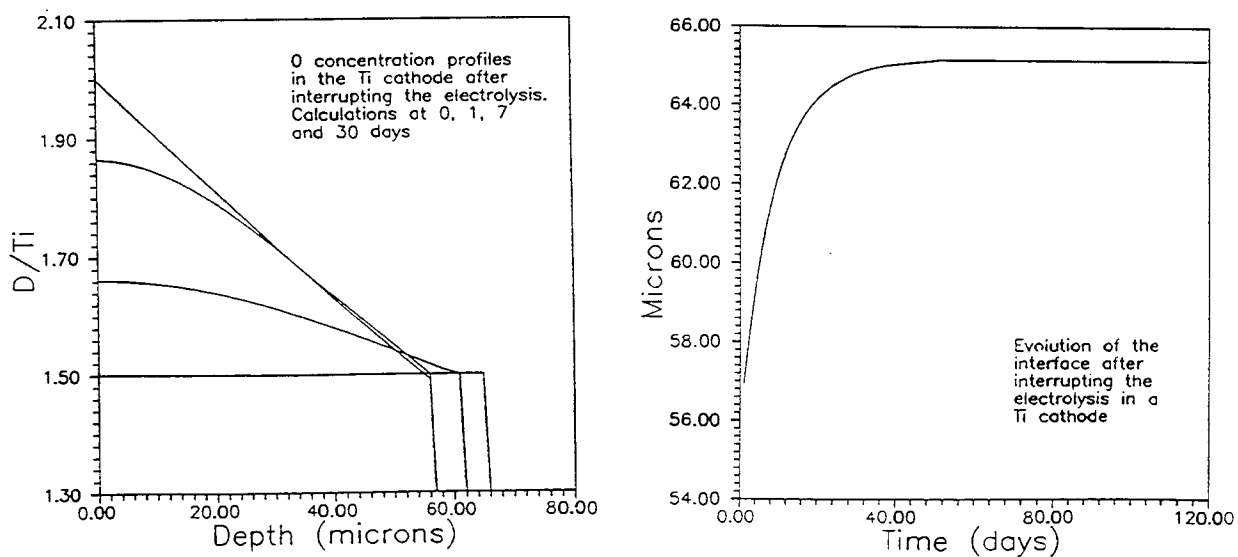
FIG 4: (a)Numerical calculations of the post-electrolysis D-
profiles in ETi6 Ti cathode. (b)Numerical calculations of the
postelectrolysis deuteride growth in ETi6 Ti cathode.
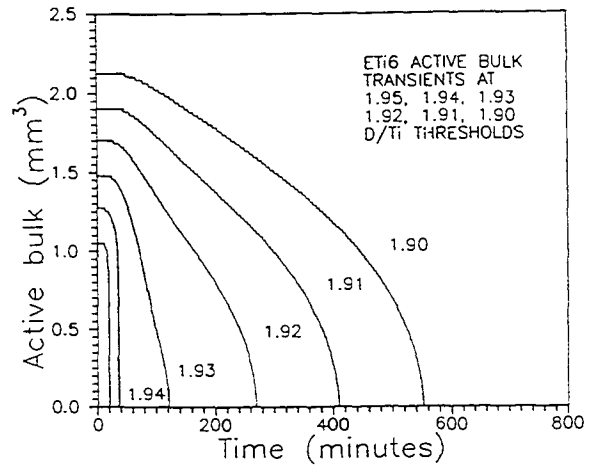
FIG 5: Numerical calculations of active bulk transients at differents loading ratio thresholds in ETi6.

SEARCH FOR NEUTRON, GAMMA AND X-RAY EMISSIONS FROM Pd/LiOD ELECTROLYTIC CELLS: A NULL RESULT

Steven E. Jones, David E. Jones, David S. Shelton,
and Stuart F. Taylor
Departments of Physics and Chemistry
Brigham Young University
Provo, Utah 84602

Abstract

We have conducted a series of experiments using state-of-the-art neutron, gamma and x-ray detectors to search for evidence for nuclear reactions occurring in Pd/LiOD electrolytic cells. No evidence for primary or secondary emissions from nuclear reactions was obtained in extended experiments.

Introduction

Since the announcement by M. Fleischmann and B. S. Pons of excess heat production via nuclear reactions in Pd/LiOD electrolytic cells [1], we have stressed the need for state-of-the-art detectors to scrutinize these claims. Here we present results from our most sensitive detectors. We also caution that compelling results can only be obtained with state-of-the-art systems, which we describe.

Overview of Detector Systems

Our primary detector for low-level neutron emissions consists of a combination of a large plastic scintillator core with a surrounding bank of sixteen 3He-filled proportional counter tubes (Figure 1), with all signals digitized at 50 Mhz and stored in computer memory. The central plastic scintillator is 35 cm in length and 8.9 cm in diameter. A central cavity of 4.8 cm diameter admits test cells. Fast neutrons from the sample can generate a recoil proton in the plastic generating scintillations (efficiency about 40%) which are viewed by a photomultiplier tube. Then the neutron slows further in polyethylene moderator 28 cm diam. X 30 cm long, and finally may be captured in one of 16 helium-3-filled proportional counter tubes embedded in the moderator (efficiency for 2.5 MeV neutrons is 34%). These tubes are arranged in four quadrants incorporating 4 proportional-counters in each.

The detector and experiments have the following special features:

1. All signals are digitized using a LeCroy fast-waveform digitizer operating 50 MHz, so that we retain pulse-shape
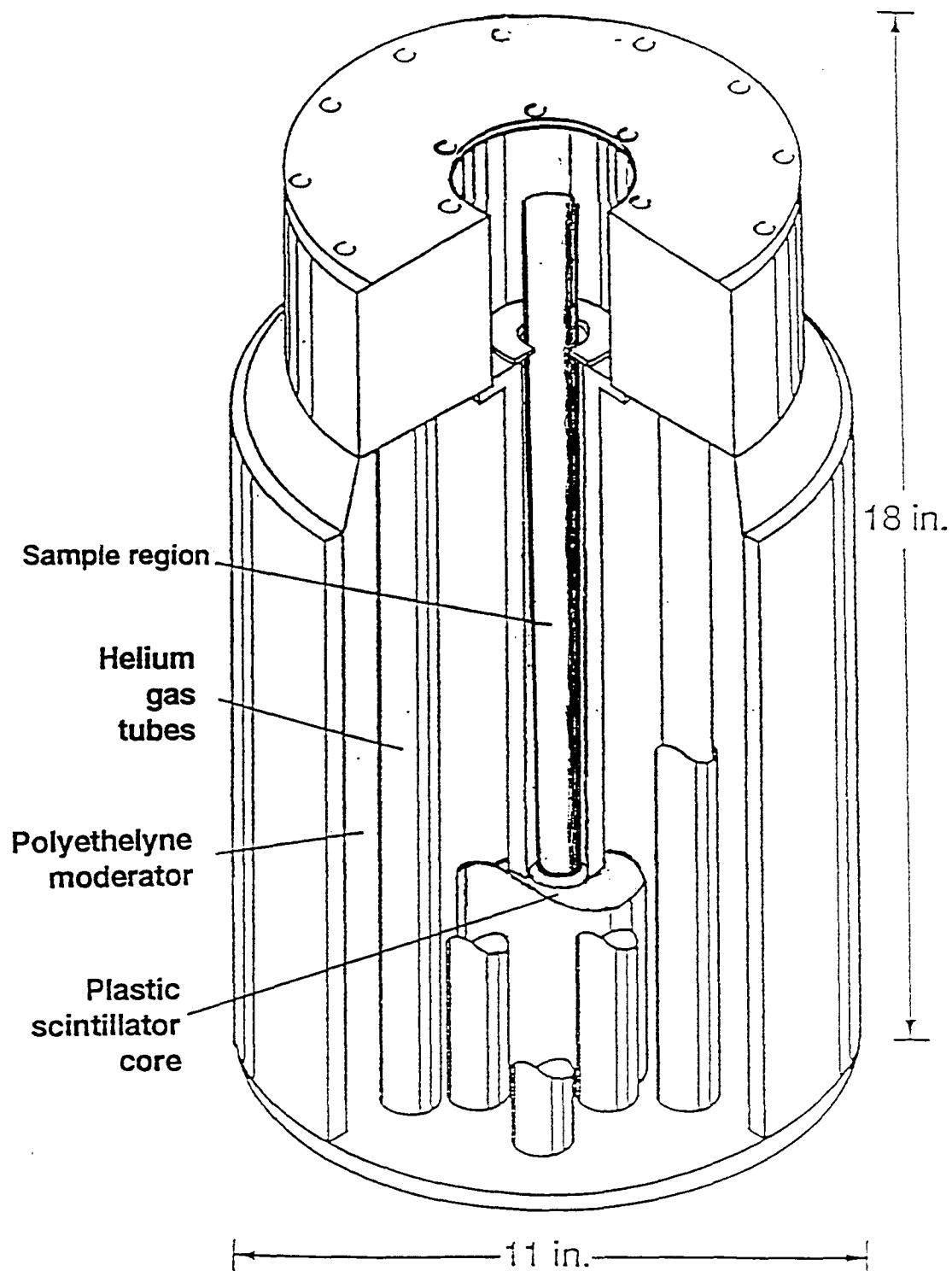
Figure 1. Cut-away drawing of neutron detector in Provo Canyon laboratory, showing plastic-scintillator core and 3-helium-filled proportional counter tubes. Not shown: three large cosmic-ray veto paddles covering X-, Y-, and Z-planes, and shielding.

information as well as timing between pulses. Pulse-shape analysis permits excellent noise rejection, along with giving some neutron-energy information (from the prompt plastic scintillator pulse). By rejecting (in software) events having small or no plastic pulses, we strongly discriminate against slow (especially thermal) neutrons. This background-reducing feature is not available to many detectors including those using BF3, 3He and even the Kamiokande detector in Japan [2]. By studying neutron-capture time distributions based on prompt and capture-neutron pulses, we check whether observed distributions agree with those found using a plutonium source.

2. The PC-based data acquisition system records which of the four quadrants of the 3He-type counter showed neutron capture, allowing for checking that the quadrants are hit in equal proportions.

This detector segmentation has, for example, allowed us to throw out apparent large bursts of neutrons (over 60 "neutrons" in a 320-microsecond window) whose signals unrealistically came from just one quadrant. (Occasionaly two quadrants are involved, due to electronic cross-talk). Even if neutrons are somehow emitted in one or two directions, the polyethylene moderator has the effect of spreading out the neutrons as they slow down, so that detected neutrons of sufficient statistics will necessarily appear in all four quadrants.

We have seen several cases of such large bursts in the past year of running (see for example Figure 2); but all bursts of over five detected neutrons have proven to be spurious. Dr. Howard Menlove of Los Alamos National Laboratory also reports large multiplicity "events" that have proven to be spurious, correlated with moisture condensation in the standard electronics of his detector. He agrees that earlier claims of high-multiplicity time-correlated-neutron events, notably those which appeared to correlate with sample cooling using liquid nitrogen, are doubtful. [3] Compelling data for large neutron bursts would require detector segmentation and pulse digitization (allowing signal visualization) as we have done, or other reliable methods of noise elimination.

3. Three large cosmic-ray veto counters show the passage of cosmic rays, which events are rejected off-line. Passive shielding of at least 35 m of rock (12,000 g/cm2) also greatly reduces cosmic ray-induced events and removes dependence of cosmic-ray rates on fluctuations in atmospheric pressure. After cosmic-ray rejection, the event rate is approximately 0.6 neutron-like singles per hour with an efficiency of 14% for 2.5 MeV neutrons, and 0.07 burst-events per hour with a detection efficiency exceeding 20% (increasing with neutron-burst multiplicity) [4].

4. Two additional highly-sensitive neutron detectors are available in the same deep-underground facility based on a

Figure 2. Example of large "neutron-burst" event seen in Jomar/Canberra (3-helium-type) counter only. With shift-register electronics in normal use with such detectors, this event would register as having multiplicity > 100 neutrons. However, since 1) all pulses come from just one segment of the 3-helium-type counter, 2) there is no pulse in the core scintillator, and 3) pulses in the Jomar counter are spaced rather regularly, we are forced to conclude that such events are spurious. No valid "neutron-burst" events of multiplicity > 5 detected neutrons have been observed in any of the BYU detectors in over four years of searching, and we no longer claim that such large bursts are real.

different neutron-capture scheme (capture in lithium-doped glass), to permit checking of any positive results found in the primary detector [4].

Results Obtained with Pd/LiOD Electrolytic Cells

The neutron data presented below represent 1,054.6 hours (6.3 weeks) of observation of Pd/LiOD cells and backgrounds in our most sensitive neutron detector, described above. Experimental protocols follow those provided by Dr. Thomas Passell [5], evidently based on methods used by Prof. Kevin Wolf [6], namely:

1. Pd cathodes (6mm diam. expect 4mm diam rod described in 2 below) were used in a 0.1 M LiOD solution (in D2O). Electrode spacing of the Pd rods relative to Ni-gauze which formed the cylindrical anode is approximately 2 mm, with a septum used to prevent electrical contacts.

2. Three cells were polarized in series at 40 mA from Sept. 24, 1993 to October 25, 1993, then at 80 mA until October 29, 1993.

3. Following a suggestion of Prof. K. Wolf [6], a fourth Pd/LiOD cell was operated at high altitude (8,500') for three weeks at 20mA/cm2, then added in series connection with the other three cells on October 25, 1993.

4. The palladium cathode rods were scraped/sanded approximately every seven days, and replaced in the cells within a period of about fifteen minutes to minimize deuterium loss from the cathodes during the cleaning procedure. We noticed that the cell potential slowly increased over days of (constant-current) operation, then decreased after the cathodes were cleaned, showing that a resistive surface coating had built up during cell operation. We also observed a gradual rise in electrolytic cell temperature, using a platinum-resistance probe, consistent with increased resistance and joule heating as the resistive surface coating developed.

5. A 12-hour cooling treatment was applied to the three primary cells on day 17. The fourth cell (described in 2 above) was subjected to diurnal cooling and heating due to its exposure to a mountain environment; the electrolyte was found to be frozen on two occasions.

6. Boron and aluminum (about 0.001 molar) were added to the LiOD electrolyte on the 18th day.

Search for Neutron Burst Events. A neutron burst event is defined as having a hit in the plastic scintillator core followed by two or more signals in the 3He-filled proportional-counter tubes within 320 microseconds. Since the die-away time for neutrons in the outer detector/polyethylene moderator is 55 microseconds, there is a possibility to see multiple distinct

neutron hits there. In effect, the outer detector "de-multiplexes" neutrons should an instantaneous burst occur, as first reported by H. Menlove et al. [3]. A burst is then defined as two or more neutrons captured in 3He within 320 microseconds of a start pulse in the plastic scintillator. The background rate for bursts is (0.07 +- 0.01) n/hr, all from multiplicity = 2 events, established using Pd loaded with hydrogen in 394 hours of separate runs.

We also scrutinize the time spectra of 3He-captured neutrons relative to the start pulse in the plastic scintillator to determine whether the time distribution corresponds to the 55-microsecond die-away time for neutrons in the 3He-portion of the counter, as seen with a plutonium neutron source.

The Pd/LiOD cells described above were polarized for 708.8 hours. During this time, 24 neutron-like burst events were seen, all having multiplicity = 2. (This represents approximately one burst candidate per 30 hours, a very low rate indeed.) Thus, the neutron-like rate for these events was 48/708.8h = (0.07 +- 0.01) n/hr. These numbers are in complete agreement with those found with hydrogen controls discussed above. There was no significant change in rate for neutron-like burst events between background and runs with electrical currents in the Pd/LiOD cells. There is therefore no indication of a neutron burst signal above a very low background.
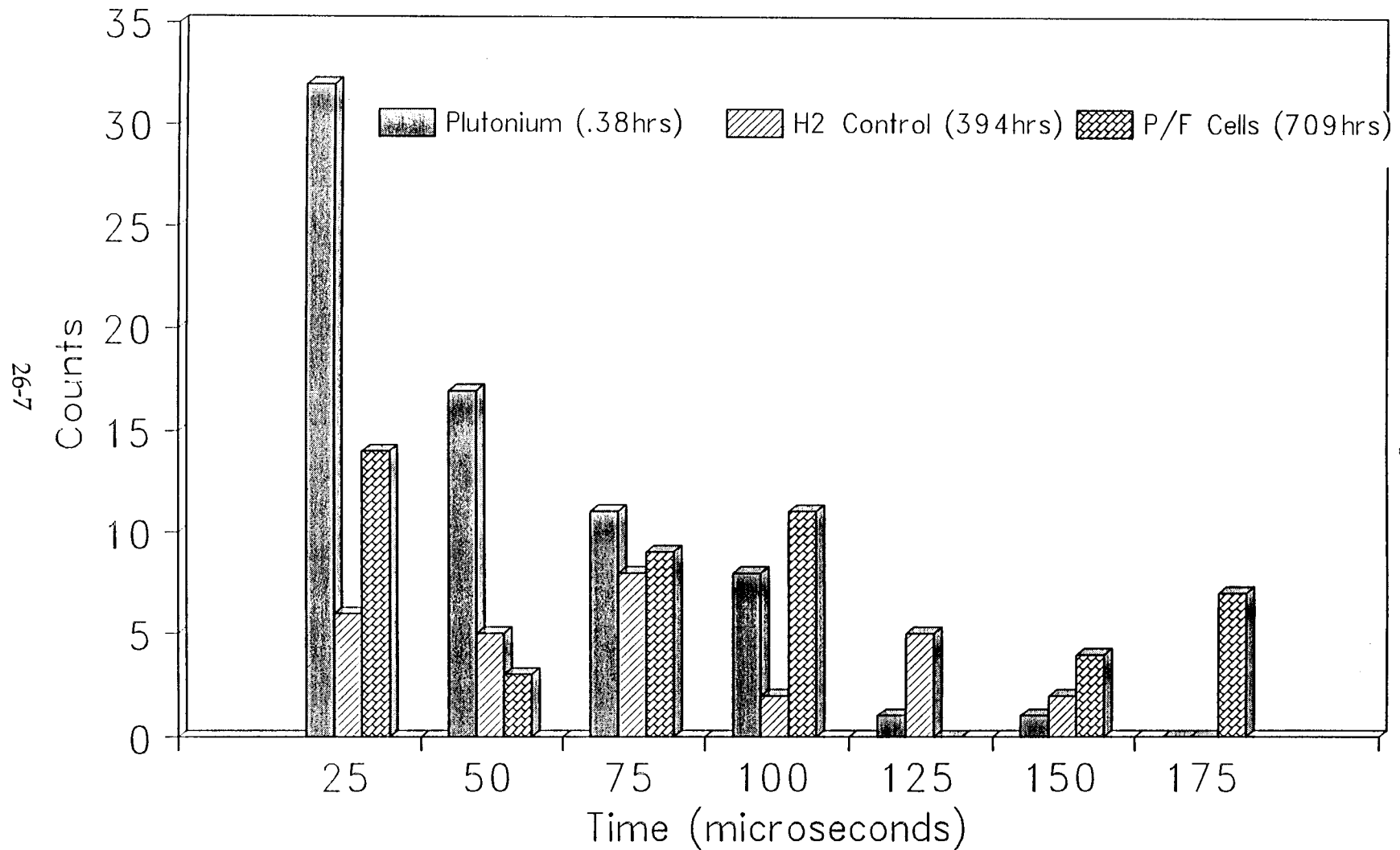
To complete the scrutiny for burst-like events, we compare time spectra from these Pd/LiOD electrolytic cell runs with those obtained from H2-control runs and from Pu-source runs. Figure 3 shows the time between each start pulse in the plastic scintillator detector and each stop pulse from the 3He-type outer detector.

The neutrons from the plutonium source follow a pattern consistent with the 55-microsecond die-away time for neutrons in the counter, but neither the controls nor the Pd/LiOD cells show such a distribution (the latter two spectra being consistent with backgrounds.) We conclude that there is no evidence for neutron-burst activity in the electrolytic cells. The upper limit on excess power from nuclear, neutron-generating reactions in the electrolytic cells is at the picowatt level.

Total neutron-like count rate. Even though there is no neutron-burst signal, there may still be neutron counts above background which we consider "singles." The background rate for such events has been established as (0.7 +- 0.1) counts/hour using Pd loaded with hydrogen. Figure 4 displays results from each run of the electrolytic cells, showing 1-sigma error bars (statistical only). The observed rates are entirely consistent with background levels of 0.7 h^{-1}. This exercise has as its conclusion that no neutrons were seen above very low background levels, in a high-efficiency detector. The most important

Figure 3.

Neutron Capture Time

Legend: Plutonium (.38 hrs), H2 Control (394 hrs), P/F Cells (709 hrs)

Y-axis: Counts (0 to 35)
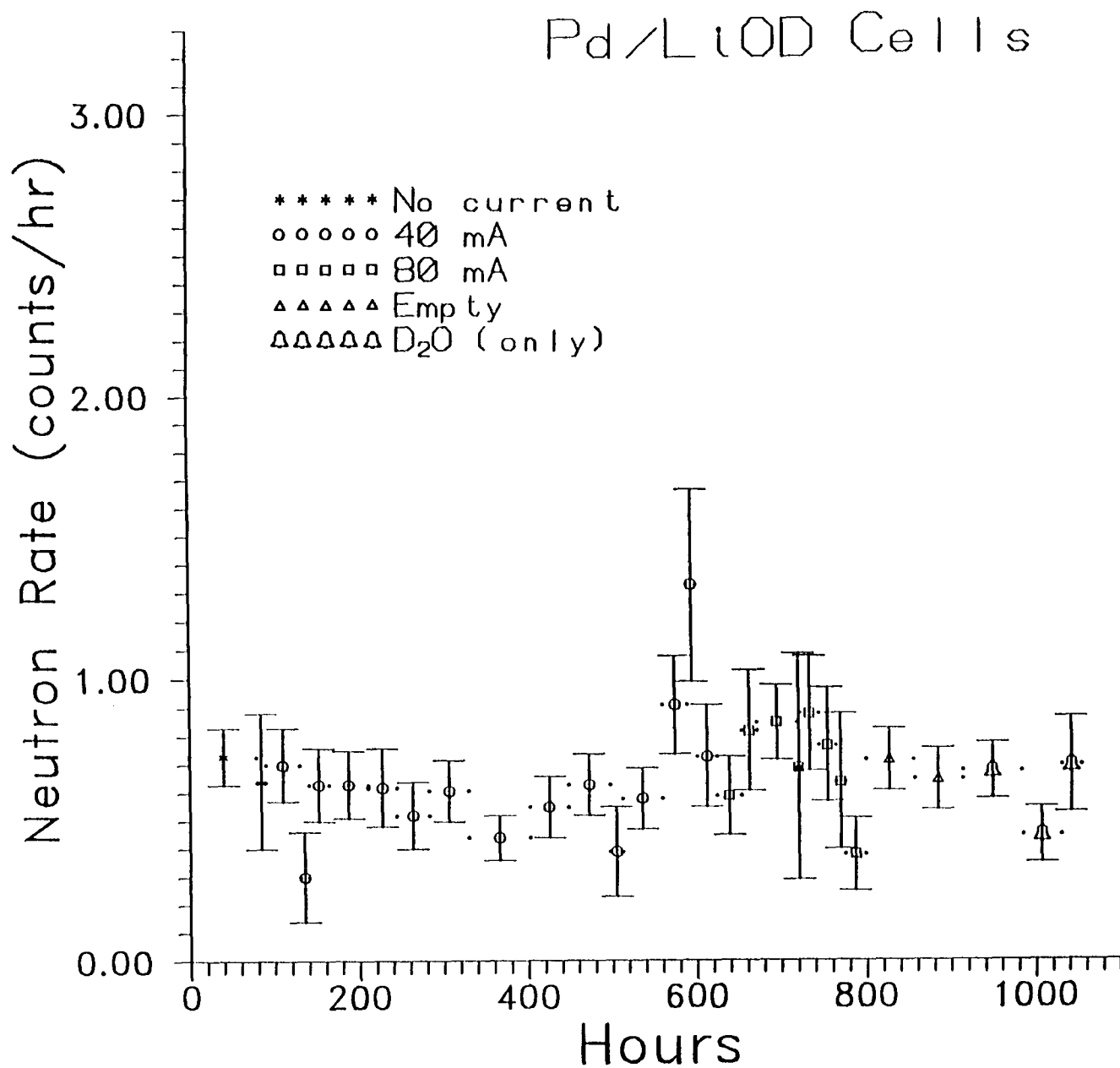X-axis: Time (microseconds) (25, 50, 75, 100, 125, 150, 175)

26-7

Figure 4. Signal rate in Pd/LiOD cells compared with rates seen for background conditions. Background rates are only 0.7 counts per hour, and there is no evidence of neutron production (above background) in the Pd/LiOD cells.

observation may be that state-of-the-art neutron detectors are now available for studies requiring high-sensitivity instruments.

Gamma and X-ray Spectroscopy

Immediately following the neutron search, all palladium rods were taken to Los Alamos for gamma-ray spectroscopic analysis. The purpose of this search was to determine whether radioactive isotopes of palladium, rhodium, ruthenium and silver might have been generated during the electrolytic runs, pursuant to claims of Y. Kucherov and others of such transmutations in deuterium-loaded palladium [7]. All four Pd rods were placed in a low-background germanium detector operated by Dr. J. Parker and counted for 75,000 seconds. No gamma lines above background were seen, except for a weak 59.5 keV line which represents americium-241. The americium contamination was traced to the nickel gauze used for anodes. The migration of americium from anode to Pd cathode during operation of the electrolytic cells demonstrates that radioisotopes can be picked up by the cathode originating from either the electrolyte or the anode. Therefore, any claims of nuclear transmutation in such cells must first show that the claimed radioisotopes were not originally present in the electrolyte or the anode. These checks must supplement checks for contamination of the cathode.

Further gamma-spectrographic analysis of essentially all of the palladium cathodes used in experiments at BYU and Kamiokande over the past five years have been undertaken: we found absolutely no evidence for radioisotope formation in any palladium cathodes. Careful scrutiny should therefore be applied to any claims that nuclear reactions produce transmutations in electrolytic cells. In particular, claims that radioisotopes are formed far off the line of nuclear stability should immediately arouse suspicion that materials used in the electrodes or electrolyte could have been contaminated or subjected to irradiation by an energetic particle beam. For example, if palladium-100 is found by gamma spectroscopy, then beam irradiation is likely since negative-Q reactions are implicated.

We have also followed our own challenge [8] of searching for x-rays as would be expected if nuclear reactions are indeed producing measureable heat in electrolytic cells. Nuclear reactions are characterized by release of MeV-scale energies, hence their importance to power-production schemes. Energy release at the nuclear level implies that secondary x-rays will be produced in the environment of a metal lattice, where only tens of keV are required to generate x-rays. That is, if nuclear reactions are indeed producing heat at the levels claimed (>1 mW), then sufficient x-rays should be produced to be detectable, since x-rays arise from ionizing effects of nuclear products on the materials in which the purported heat develops. Thus, x-ray measurements provide a crucial test for the presence of heat-generating nuclear reactions.

Characteristic x-rays of Pd (K-alpha of 21.1 keV) or Ni (K-alpha of 7.5 keV) which result from K shell vacancies produced by nuclear products are readily detected. We have searched for such lines using two x-ray spectrometers, a 10mmX10mm silicon detector having high sensitivity down to about 4 keV [8] and a lithium-drifted silicon detector with high sensitivity down to approximately 1 keV. We used a Pd/D2O electrolytic cell in which 25 micron Pd foil formed both cathode and external wall; no x-ray production was seen with this electrolytic cell. Similarly, a search for x-rays was conducted using a Ni/H2O cell in which the Ni cathode was placed against a very thin plastic window. Again, no x-ray production was in evidence in the electrolytic cell (see Figure 5). Using a montecarlo calculation to determine the overall x-ray detection efficiency from electrolytic cells [8], we set an upper limit of 10 microwatts of excess power from these cells, from any nuclear reactions which produce secondary x-rays.

In a "search for cold fusion using x-ray detection" [9], M.R. Deakin et al. found, as we have, that no x-rays above background were produced by Pd-LiOD electrolytic cells. An important caveat is provided in that paper: "Room background radiation fluoresces the cathode and Pd K x-rays are therefore present as an artifact of background." [9] Thus, the presence of x-rays alone (including fogging of x-ray film) is insufficient to demonstrate the presence of heat-generating nuclear reactions.

No "cold fusion" experiment anywhere has shown the presence of characteristic secondary x-rays lines (using an x-ray spectrometer) which would characterize fusion or any other nuclear reaction in a metal lattice to the best of our knowledge [10]. There are some experiments that show fogging of x-ray dental film, but such experiments are too crude to provide quantitative information regarding x-ray energies and intensities, and are subject to artifacts.

Thus, we find no compelling evidence to link nuclear reactions to excess-heat production claims. Instead, the lack of significant (primary or secondary) x-rays, gammas and neutrons after five years of searching argues convincingly against claims of excess heat production via nuclear reactions in electrolytic cells (or equivalent). This conclusion is supported by related experiments at BYU which show up to 700% "excess heat", but which apparent "excess heat" is in fact due to hydrogen-oxygen recombination in the cells coupled with commonly-used (but misleading) analysis techniques for excess-power production in "cold fusion" experiments [11].

Conclusions

In order to find compelling evidence for cold-fusion effects, state-of-the-art calorimeters and nuclear detectors are requisite. Table 1 juxtaposes such systems with other systems which are still more generally in use. It is disquieting that
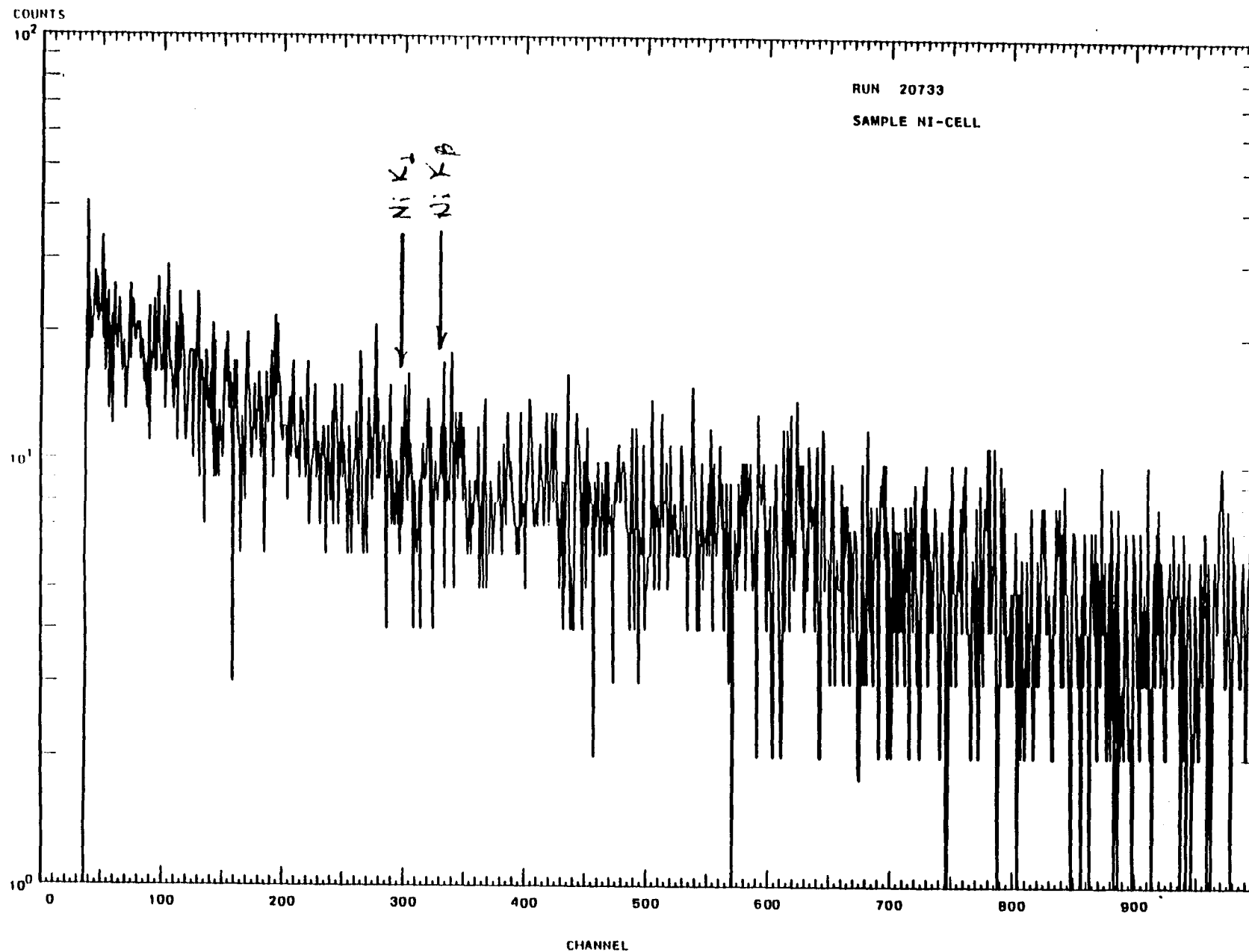
Figure 5.   X-ray spectrum obtained with lithium-drifted silicon
spectrometer, showing no features indicative of any
nuclear reactions in electrolytic cell.

TABLE 1. COMPARISON OF COLD-FUSION RESEARCH METHODS

It is evident that much of the present confusion surround "cold fusion" stems from the continued use of inadequate detectors. This list juxtaposes crude, better and state-of-the-art systems to promote the quest for compelling data, one way or the other. Use of the best available methods is clearly the path-of-logical science.

Crude (simply add to the confusion)	Better (but not good enough)	State-of-the-art (can provide compelling evidence)
Neutron survey meters, BF3	Segmented 3He, Plastic scintillators	Segmented 3He or Li-doped glass *plus* scint. with digitizing
Helium gas detection, Tritium gas detection	Charged-particle det. (Si surface barrier) (requires thin foil)	Thin dE/dx detector plus Si spectrometer (particle ID & energy)
X-ray film	X-ray film with foil energy-filters	X-ray spectrometer (Si, HgI2, CdTe,etc.)
Geiger-Mueller counter	see detectors listed above; Ge detector	
Infrequent I*V(t) sampling (e.g., every 300 s)		Integral I*V(t) correct via frequent, redundant sampling
Open cell calorimetry, no H2/D2 +O2 monitoring, during experiment	Measure H2/D2 + O2 simultaneous w/heat	Recombiner inside separate calorimeter
Metal of unknown source, quality or purity		Alloyed with known purity and properties
D2O of unknown source	D2O from known source, not exposed to reactor	Highly distilled D2O, known H,O isotopes
Visual techniques	Computer-logging, several probes	Redundant probes with fast data acquisition
Theories which disregard P, E conservation or light-cone constraints (e.g., "heating lattice"); or discount known branching ratios from muon-catalyzed cold fusion (e.g. 4He or 3H but no neutrons); or which use incorrect wavefunctions	Fractofusion ignoring e- vs. d+ acceleration	???

some researchers select open electrolytic cells over closed cells, and very long sampling intervals (e.g., 5-minute sampling intervals for input voltage used by Pons and Fleischmann in recent boiling-cell experiments [12]). Some researchers continue to use x-ray films instead of x-ray spectrometers, helium or tritium gas sampling instead of charged-particle spectrometers, Geiger counters rather than silicon or germanium detectors, and neutron survey meters instead of sensitive neutron detectors as described above. It is time to strongly question claims of cold fusion based on crude techniques and to demand tests at a rigorous scientific-proof level. Compelling evidence requires use of the best instruments available, incorporating fast data-sampling and digitization methods, the use of different detectors whose signals agree quantitatively, and presence of signals well above background levels. A real signal should be capable of scaling, and should not shrink as background levels are reduced. However, as we have proceeded to better detectors, cold-fusion data surety has diminished.

With these criteria for state-of-the-art detectors, we find that no compelling evidence for neutron, gamma or x-ray production from deuterided materials currently exists in any cold-fusion experiment, including our own. The only verified form of cold nuclear fusion to date is muon-catalyzed fusion. Nevertheless, having an obligation to resolve a few remaining issues [13], we will continue our search for several more months. We invite those with evidence for neutron production to accept our invitation to test their systems in the deep-underground neutron detection facility in Provo Canyon in order to confirm results. Gamma and x-ray spectrometers are also available on request.

Acknowledgments

References

1.   M. Fleischmann, B.S. Pons, {and M. Hawkins}, J. Electroanal.
      Chem. 261 (1989) 301.

2.   T. Ishida, "Study of the Anomalous Nuclear Effects in Solid-
      Deuterium Systems," Masters Thesis, Feb. 1992, University of
      Tokyo, ICRR-Report-277-92-15.

3.   H.O. Menlove, M.M. Fowler, E. Garcia, A. Mayer, M.C. Miller,
      R.R. Ryan, S.E. Jones, J. Fusion Energy 9 (1990) 495-506;
      and priv. comm. from H. Menlove.

4.   J. B. Czirr, G.L. Jensen, and J.C. Wang, "High efficiency
      neutron and charged particle spectrometers," in AIP Conf.
      Proceedings #228 (BYU, Provo, UT, October 1990), editors
      S.E. Jones, F. Scaramuzzi and D. Worledge (NY: American
      Institute of Physics), 1991.

5.   T. Passell, priv. comm., 16 July 1993.

6.   K. Wolf, priv. comm.; see also K.L. Wolf, J. Shoemaker, D.E.
      Coe, L. Whitesell, AIP Conf. Proc. #228 (NY: Am. Inst.
      Physics, 1991), p. 341-353.

7.   A.B. Karabut, Y.R. Kucherov, I.B. Savvatimova, "Possible
      nuclear reaction mechanisms at glow discharge in deuterium,"
      Proc. ICCF-3, editor H. Ikegami, Frontiers Science Series
      No. 4, pp. 165-168.

8.   D.B. Buehler, L.D. Hansen, S.E. Jones and L.B. Rees, "Is
      Reported 'Excess Heat' Due to Nuclear Reactions?", Frontiers
      of Cold Fusion, ed. H. Ikegami, 1993, p. 245.

9.   M.R. Deakin, et al., "Search for cold fusion using x-ray
      detection," Phys. Rev. C 40 (1989) 1851.

10.   See Proceedings of International Conferences on Cold Fusion.

11.   J.E. Jones, L.D. Hansen, S.E. Jones, D.S. Shelton, and J.M.
      Thorne, paper in preparation.

12.   M. Fleischmann and B.S. Pons, "Calorimetry of the Pd-D2O
      system: from simplicity via complications to simplicity,"
      Phys. Lett. A 176 (1993) 176; and "Fleischmann responds to
      Jones," 28 October 1993 e-mail posting on sci.physics.
      fusion.

13.   S.E. Jones, E.P. Palmer, J.B. Czirr, D.L. Decker, G.L.
      Jensen, J.M. Thorne, S.F. Taylor and J. Rafelski, Nature,
      338 (1989) 737-740.

ABOUT EPRI

The mission of the Electric Power Research Institute is to discover, develop, and deliver high value technological advances through networking and partnership with the electricity industry.

Funded through annual membership dues from some 700 member utilities, EPRI's work covers a wide range of technologies related to the generation, delivery, and use of electricity, with special attention paid to cost-effectiveness and environmental concerns.

At EPRI's headquarters in Palo Alto, California, more than 350 scientists and engineers manage some 1600 ongoing projects throughout the world. Benefits accrue in the form of products, services, and information for direct application by the electric utility industry and its customers.

EPRI—Leadership in Electrification through Global Collaboration